

**DEVELOPMENT AND CALIBRATION OF THE NORTH FLORIDA
SOUTHEAST GEORGIA GROUNDWATER MODEL**

(NFSEG V1.0)

By

Fatih Gordu, P.E.
Douglas Durden, P.E.
St. Johns River Water Management District

Trey Grubbs
Suwanee River Water Management District

St. Johns River Water Management District

Palatka, Florida

2016

CONTENTS

Contents	iii
List of Tables	v
List of Figures	vi
1.0 INTRODUCTION	1
2.0 NFSEG MODEL CONFIGURATION	2
Model Code Selection	3
NFSEG Model Grid	3
Model Layers	5
Model Layer 1	5
Model Layer 2	6
Model Layer 3	6
Model Layer 4	8
Model Layer 5	9
Model Layer 6	9
Model Layer 7	9
Model Lateral Boundary Conditions	28
Model Layers 1 and 2	28
Model Layer 3	28
Model Layer 4	30
Model Layer 5	31
Model Layer 6	32
Model Layer 7	32

Model Internal Boundary Conditions	38
River-Package Implementation.....	38
General-Head-Boundary-Package Implementation	43
Drain-Package Implementation	43
Recharge-Package Implementation	44
Evapotranspiration-Package Implementation	44
Well-Package and MNW2-Package Implementations.....	45
Time-Variant Specified Head Package Implementation.....	46
3.0 NFSEG STEADY-STATE MODEL CALIBRATION	64
Preliminary Model Testing and Sensitivity Analysis	64
PEST Calibration	64
Observation Data Groups.....	65
Calibration-Parameter Data Groups.....	69
Calibration Results.....	92
Calibration Statistics	92
Parameter Sensitivity and Predictive Uncertainty Analysis	94
Model Capabilities and Limitations.....	96
4.0 References.....	132

LIST OF TABLES

Table 2-1. Principal Representation of NFSEG Model Layers2

Table 2-2. NFSEG Model Layer Properties6

Table 3-1. NFSEG Layer-Wide Ratios of Modeled Anisotropy Ratios71

Table 3-2. Calibration Statistics.....93

Table 3-3. Simulated vs. Estimated Cumulative Baseflows, 2001 and 2009117

DRAFT

LIST OF FIGURES

Figure 2-1. NFSEG Active Model Domain and Grid Extent.....	4
Figure 2-2. Elevation, 10,000 mg/l Total-Dissolved-Solids (TDS)-Concentration Iso-Surface, Feet NAVD88 (after Williams and Kuniansky 2015)	10
Figure 2-3. Top Elevation, Layer 1 (Feet NAVD88; after Boniol and Davis, digital communication)	11
Figure 2-4. Bottom Elevation, Layer 1 (and Top Elevation, Layer 2; Feet NAVD88; after Boniol and Davis, digital communication)	12
Figure 2-5. Thickness, Layer 1 (Feet).....	13
Figure 2-6. Bottom Elevation, Layer 2 (and Top Elevation, Layer 3; Feet NAVD88; after Boniol and Davis, digital communication)	14
Figure 2-7. Thickness, Layer 2 (Feet).....	15
Figure 2-8. Bottom Elevation, Layer 3 (and Top Elevation, Layer 4; Feet NAVD88; after Boniol and Davis, digital communication)	16
Figure 2-9. Thickness, Layer 3 (Feet).....	17
Figure 2-10. Bottom Elevation, Layer 4 (and Top Elevation, Layer 5; Feet NAVD88; after Boniol and Davis, digital communication)	18
Figure 2-11. Thickness, Layer 4	19
Figure 2-12. Bottom Elevation, Layer 5 (Feet NAVD88; after Miller, written communication, Williams, digital communication, and Miller 1986).....	20
Figure 2-13. Thickness, Layer 5 (Feet).....	21
Figure 2-14. Top Elevation, Layer 6 (Feet NAVD88; after Miller, written communication)	22
Figure 2-15. Bottom Elevation, Layer 6 (Feet NAVD88; after Miller, written communication)	23
Figure 2-16. Thickness, Layer 6 (Feet).....	24
Figure 2-17. Top Elevation, Layer 7 (Feet NAVD88, after Miller, written communication, and Miller 1986)	25
Figure 2-18. Bottom Elevation, Layer 7 (Feet NAVD88; after Williams, digital communication, and Miller, 1986)	26

Figure 2-19. Thickness, Layer 7 (Feet).....	27
Figure 2-20. Model Lateral Boundaries, Layer 3	33
Figure 2-21. Model Lateral Boundaries, Layer 4	34
Figure 2-22. Model Lateral Boundaries, Layer 5	35
Figure 2-23. Model Lateral Boundaries, Layer 6	36
Figure 2-24. Model Lateral Boundaries, Layer 7	37
Figure 2-25. NHDPlusV2 Flow-Line Sub-Segments Used in River- and Drain-Package Implementations.....	41
Figure 2-26. Portions of NHD Flowlines for Which River Stages Were Obtained from Existing Surface-Water Models and Lake Sub-Polygons Represented in the NFSEG River Package	42
Figure 2-27. Gulf-of-Mexico Coastal Swamps Represented in the Drain Package	47
Figure 2-28. Assigned Recharge Rates, 2001	48
Figure 2-29. Assigned Recharge Rates, 2009.....	49
Figure 2-30. Assigned Maximum Saturated ET Rates, 2001	50
Figure 2-31. Assigned Maximum Saturated ET Rates, 2009	51
Figure 2-32. Assigned ET Extinction Depths	52
Figure 2-33. Distribution of Multi-Aquifer Wells	53
Figure 2-34. Distribution of Public-Supply, Commercial-Industrial, and Institutional Withdrawals, 2001	54
Figure 2-35. Distribution of Public-Supply, Commercial-Industrial, and Institutional Withdrawals, 2009	55
Figure 2-36. Distribution of DSS Withdrawals	56
Figure 2-37. Distribution of Agricultural Withdrawals	57
Figure 2-38. Distribution of Total Groundwater Withdrawals by County, 2001	58
Figure 2-39. Distribution of Total Groundwater Withdrawals by County, 2009	59

Figure 2-40. Groundwater Withdrawals by County and Use Type, 2001	60
Figure 2-41. Groundwater Withdrawals by County and Use Type, 2009	61
Figure 2-42. Location of Rapid Infiltration Basins, Injection Wells, and Sinks and Drainage Wells	62
Figure 2-43. Distribution of Specified-Heads.....	63
Figure 3-1. Location and Relative Magnitude of Springs 2001.....	75
Figure 3-2. Location and Relative Magnitude of Springs 2009.....	76
Figure 3-3. Estimated Cumulative Baseflows 2001	77
Figure 3-4. Estimated Cumulative Baseflows 2009	78
Figure 3-5. Vertical Head Differences, Surficial Aquifer vs. Upper Floridan 2001	79
Figure 3-6. Vertical Head Differences, Upper Floridan vs. Upper Zone of Lower Floridan 2001.....	80
Figure 3-7. Vertical Head Differences, Surficial Aquifer vs. Upper Floridan 2009	81
Figure 3-8. Vertical Head Differences, Upper Floridan vs. Upper Zone of Lower Floridan 2009.....	82
Figure 3-9. Horizontal Head Differences, Upper Floridan 2001	83
Figure 3-10. Horizontal Head Differences, Upper Floridan 2009	84
Figure 3-11. Distribution of Horizontal Hydraulic Conductivity Pilot Points, Model Layer 1	85
Figure 3-12. Distribution of Horizontal Hydraulic Conductivity Pilot Points, Model Layer 3	86
Figure 3-13. Distribution of Horizontal Hydraulic Conductivity Pilot Points, Model Layer 7.....	87
Figure 3-14. Distribution of Vertical Hydraulic Conductivity Pilot Points, Model Layer 6	88
Figure 3-15. Distribution of Vertical Hydraulic Conductivity Pilot Points and Vertical Hydraulic Conductivity Multiplier Pilot Points, Model Layer 2	89
Figure 3-16. Distribution of Vertical Hydraulic Conductivity Pilot Points and Vertical Hydraulic Conductivity Multiplier Pilot Points, Model Layer 4	90
Figure 3-17. Distribution of Vertical Hydraulic Conductivity Pilot Points and Vertical Hydraulic Conductivity Multiplier Pilot Points, Model Layer 5	91

Figure 3-18. Residuals of Hydraulic Head, Model Layer 1, 2001	98
Figure 3-19. Residuals of Hydraulic Head, Model Layer 1, 2009.....	99
Figure 3-20. Residuals of Hydraulic Head, Model Layer 3, 2001	100
Figure 3-21. Residuals of Hydraulic Head, Model Layer 3, 2009.....	101
Figure 3-22. Residuals of Hydraulic Head, Model Layer 5, 2001	102
Figure 3-23. Residuals of Hydraulic Head, Model Layer 5, 2009.....	103
Figure 3-24. Simulated vs. Observed Hydraulic Head (feet), Model Layer 1, 2001	104
Figure 3-25. Simulated vs. Observed Hydraulic Head (feet), Model Layer 1, 2009.....	104
Figure 3-26. Simulated vs. Observed Hydraulic Head (feet), Model Layer 3, 2001	105
Figure 3-27. Simulated vs. Observed Hydraulic Head (feet), Model Layer 3, 2009.....	105
Figure 3-28. Simulated vs. Observed Hydraulic Head (feet), Model Layer 5, 2001	106
Figure 3-29. Simulated vs. Observed Hydraulic Head (feet), Model Layer 5, 2009.....	106
Figure 3-30. Residuals of Vertical Head Differences Between Model Layers 1 and 3, 2001	107
Figure 3-31. Residuals of Vertical Head Differences Between Model Layers 1 and 3, 2009.....	108
Figure 3-32. Residuals of Vertical Head Differences Between Model Layers 3 and 5, 2001	109
Figure 3-33. Residuals of Vertical Head Differences Between Model Layers 3 and 5, 2009.....	110
Figure 3-34. Simulated vs. Observed Vertical Head Differences (feet), Model Layers 1 to 3.....	111
Figure 3-35. Simulated vs. Observed Vertical Head Differences (feet), Model Layers 3 to 5.....	111
Figure 3-36. Residuals of Horizontal Head Differences, Model Layer 3, 2001	112
Figure 3-37. Residuals of Horizontal Head Differences, Model Layer 3, 2009.....	113
Figure 3-38. Simulated vs. Observed Horizontal Head Differences (feet), 2001	114
Figure 3-39. Simulated vs. Observed Horizontal Head Differences (feet), 2009.....	114
Figure 3-40. Simulated vs. Observed Spring Discharges (cfs), 2001	115
Figure 3-41. Simulated vs. Observed Spring Discharges (cfs), 2009.....	115

Figure 3-42. Simulated Spring Discharge for Selected Springs with Flow Residuals, 2001116

Figure 3-43. Simulated Spring Discharge for Selected Springs with Flow Residuals, 2009116

Figure 3-44. Simulated vs. Estimated Baseflows (cfs), 2001118

Figure 3-45. Simulated vs. Estimated Baseflows (cfs), 2009118

Figure 3-46. Modeled Distribution of Horizontal Hydraulic Conductivity, Model Layer 1119

Figure 3-47. Modeled Distribution of Horizontal Hydraulic Conductivity, Model Layer 3120

Figure 3-48. Modeled Distribution of Horizontal Hydraulic Conductivity, Model Layer 5121

Figure 3-49. Modeled Distribution of Horizontal Hydraulic Conductivity, Model Layer 7122

Figure 3-50. Spatial Distribution of Transmissivity, Model Layer 3123

Figure 3-51. Spatial Distribution of Transmissivity, Model Layer 5124

Figure 3-52. Modeled Distribution of Vertical Hydraulic Conductivity, Model Layer 2125

Figure 3-53. Modeled Distribution of Vertical Hydraulic Conductivity, Model Layer 4126

Figure 3-54. Modeled Distribution of Vertical Hydraulic Conductivity, Model Layer 6127

Figure 3-55. Modeled Distribution of Leakance, Model Layer 2.....128

Figure 3-56. Modeled Distribution of Leakance, Model Layer 4.....129

Figure 3-57. Simulated Potentiometric Surface of Model Layer 3, 2001130

Figure 3-58. Simulated Potentiometric Surface of Model Layer 3, 2009.....131

1.0 INTRODUCTION

In 2009, a Groundwater Modeling group in response to a request by stakeholders was assembled to discuss issues regarding the development and application of the St. Johns River Water Management District (SJRWMD) Northeast Florida Groundwater Flow Model (SJRWMD NEF model). Application of the SJRWMD NEF model had indicated the potential for significant water resource related impacts in areas of both the Suwannee River Water Management District (SRWMD) and SJRWMD due to projected groundwater withdrawals within the model domain. The meetings of the Groundwater Modeling group, which were facilitated by the University of Florida Water Institute (FWI), occurred between August 2009 and February 2010 and enabled all stakeholders to come together for a series of meetings in which issues regarding the SJRWMD NEF model development and application were investigated. The stakeholders included a variety of groups, including water utilities, private industry, governmental organizations, and environment groups.

As a result of the facilitation process, a Summary Report on Groundwater Modeling was prepared by Dr. Wendy Graham and Lisette Staal of the FWI. Several recommendations for further groundwater model development were included as part of the report. One of the recommendations stated that: “More time should be spent ‘up-front’ with stakeholders providing input on methods and model evaluation criteria than on defending and/or critiquing the end product. Given the sensitive hydrologic and ecological conditions at the boundary between the SJRWMD and SRWMD, the two Districts should work toward developing a common North Florida model.” To that end, the SJRWMD and SRWMD undertook the joint creation of a regional groundwater flow model developed through a cooperative process that included all interested stakeholders.

A technical team comprised of a diverse group of scientists and engineers was formed to plan, develop, apply, and document the North Florida Southeast Georgia Ground-Water Flow Model (NFSEG model). The members of the technical team represent “stakeholder” groups from throughout the region of North Florida and South Georgia, including governmental organizations, water utilities, private industry, and environmental organizations. In addition to the technical team, an oversight committee or “steering committee” was also established. A project charter was developed. The purpose of the project charter was to outline the broad objectives of the project, the roles and responsibilities of the principle project participants, and the ground rules for their interaction. The project charter is available through NFSEG website located at <http://northfloridawater.com/groundwaterflowmodel.html>.

This document includes a detailed description of the model configuration and calibration of NFSEG version 1.0 (NFSEG v1.0). NFSEG v1.0 will be used to support development of the North Florida Regional Water Supply Plan (NFRWSP). The model will enable the assessment of the effects of withdrawals on groundwater levels, stream baseflows, and spring flows within the NFRWSP.

2.0 NFSEG MODEL CONFIGURATION

At its maximum extent, the active domain of the NFSEG groundwater flow model encompasses portions of three states—Florida, Georgia, and South Carolina, and portions of the Atlantic Ocean and the Gulf of Mexico, an area of approximately 60,000 square miles (Figure 2-1).

In its present form, the model is fully three-dimensional and steady-state and has been calibrated to hydrologic conditions of 2001 and 2009. The model consists of seven aquifer layers that represent, from top to bottom, the surficial aquifer system, the intermediate confining unit, the Upper Floridan aquifer, the middle semiconfining unit, the upper zone of the Lower Floridan aquifer, the lower semiconfining unit, and the Fernandina Permeable zone of the Lower Floridan aquifer, where these hydrogeologic units are present (Table 2-1)¹²³⁴.

Table 2-1. Principal Representation of NFSEG Model Layers

Downdip of Gulf Trough			Updip of Gulf Trough			
Series	Hydrogeologic Unit	Model Layer	Series	Hydrogeologic Unit	Model Layer	
Post-Miocene	Surficial Aquifer System	Layer 1 ¹	Post-Miocene	Surficial Aquifer System ¹	Layer 1	
Miocene	Intermediate Aquifer System/Intermediate Confining Unit	Layer 2 ²	Miocene	Intermediate Aquifer System/Intermediate Confining Unit ¹	Layer 2	
Oligocene	Floridan Aquifer System	Layer 3	Oligocene	Upper Floridan Aquifer	Layer 3	
Upper Eocene			Upper Floridan Aquifer	Upper Eocene	Pearl River Aquifer Confining Unit	Layer 4
Middle Eocene		Middle Semiconfining Unit	Layer 4 ³	Middle Eocene	Pearl River Aquifer	Layer 5
		Lower Floridan Aquifer (Upper Zone)	Layer 5			
Lower Eocene		Lower Semiconfining Unit	Layer 6	Lower Eocene		
Paleocene		Lower Floridan Aquifer (Fernandina Permeable Zone)	Layer 7	Paleocene	Chattahoochee River Aquifer Confining Unit	Layer 6 ⁴
Upper Cretaceous		Sub-Floridan Confining Unit	Inactive	Upper Cretaceous	Chattahoochee River Aquifer	Layer 7 ⁴

¹ Where the surficial aquifer system is not present, layer 1 represents a vertical segment of the intermediate confining unit and/or Floridan aquifer system.

² Where the intermediate confining unit is not present, layer 2 represents a vertical segment of the Floridan aquifer system.

³ Where the middle semiconfining unit is not present, layer 4 represents aquifer rather than semiconfining-unit material.

⁴ As with the sub-Floridan confining unit, the Chattahoochee river aquifer and confining unit are not represented in the model.

MODEL CODE SELECTION

The NFSEG groundwater model is an application of MODFLOW-NWT (Niswonger et al. 2011), a formulation of MODFLOW 2005 (Harbaugh 2005). MODFLOW-NWT is intended specifically for solving problems involving drying and rewetting nonlinearities of the unconfined groundwater flow equation. Unconfined aquifer conditions occur throughout the area corresponding to the NFSEG model domain in the surficial aquifer system or in outcrops of the intermediate confining unit or Floridan aquifer system. The ability of MODFLOW-NWT to represent drying and rewetting processes effectively was central to its selection for use in the model development. Other important considerations were the ability of MODFLOW-NWT to represent aquifer systems in a fully three-dimensional manner under both steady-state and transient conditions. In addition, as a product of the U.S. Geological Survey, MODFLOW-NWT is recognized worldwide, resides in the public domain, and is available for download as executable and source code at no cost to the user.

NFSEG MODEL GRID

The NFSEG model grid consists of 752 rows and 704 columns. The grid cells are uniformly 2,500 feet (ft) by 2,500 ft in dimension. The NFSEG model grid is nested within that of an early version of the grid of the U.S. Geological Survey system-wide groundwater flow model (<http://fl.water.usgs.gov/floridan/numerical-model.html>), (that grid has since been revised). (Figure 2-1). The size of the grid cells relative to the extent of the active model domain provides a high degree of resolution in the representation of the regional groundwater system. Grid uniformity lends towards simplicity of design (Figure 2-1). The NFSEG groundwater model is constructed in the NAD83 Albers, meters, horizontal coordinate system, as implemented in ESRI ARCMAP. The vertical datum is NAVD 1988 feet (feet NAVD88).

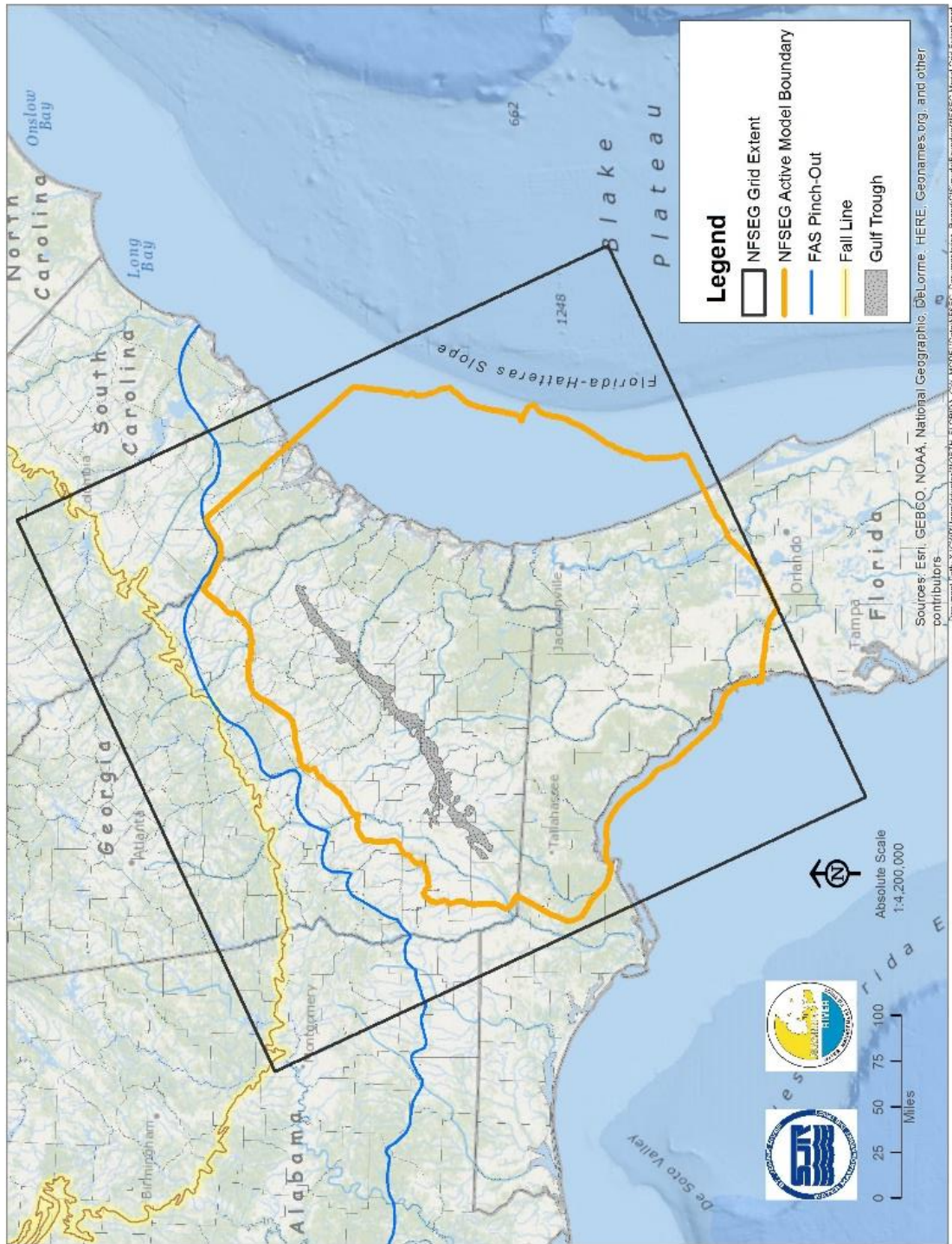


Figure 2-1. NFSEG Active Model Domain and Grid Extent

MODEL LAYERS

Each of the seven NFSEG model layers represents a single hydrogeologic unit (Table 2-1). However, these layers may be representative of portions of other hydrogeologic units, depending on local circumstances. This is by necessity due to the variability in hydrogeologic conditions across the model domain.

The active areal extent of each model layer is limited to that of fresh-water flow. In model layers 4 through 7, the extent of fresh-water flow was determined primarily by intersecting an estimated 10,000 milligram per liter (mg/l) total-dissolved-solids (TDS)-concentration iso-surface (Williams and Kuniandy 2015; Figure 2-2) with the estimated top elevations of the aquifers or confining units that comprise the Floridan aquifer system. Additional considerations were taken into account with respect to model layers 1 through 3, as discussed in greater detail in the section concerning model layer 3.

Model Layer 1

Minimum Layer Thickness of Model Layer 1

Model layer 1 is used primarily to represent the surficial aquifer system, where it is present (Table 2-1 and Table 2-2). In areas outside the extent of the surficial aquifer system, model layer 1 represents a vertical segment of the uppermost hydrogeologic unit or units present (i.e., either the intermediate confining unit, Floridan aquifer system, or a combination thereof).

This approach was implemented in the NFSEG groundwater flow model through use of assigned minimum thicknesses. In assigning minimum thicknesses, the estimated actual thickness distribution of the surficial aquifer system was determined first as the difference in the estimated top of the surficial aquifer system, i.e., land-surface elevation, and the estimated bottom of the surficial aquifer system, as determined by Davis and Boniol (digital communication). Where this difference was less than the minimum thickness, the minimum thickness was substituted in its place, and the bottom elevation of layer 1 was changed to reflect the substitution. If necessary, the thicknesses and corresponding bottom elevations of layers beneath layer 1 were also adjusted to reflect the change in thickness of layer 1 (Table 2-2). Respective minimum thicknesses were implemented in this manner for each model layer.

The approach of assigning minimum thickness to model layers is advantageous in that isolated patches of inactive and active grid cells are avoided. This provides greater numerical stability. This approach is also an acknowledgement that exact boundaries of hydrogeologic units such as the surficial aquifer and intermediate confining unit are not precisely known, either laterally or vertically, in many locations. In this approach, the calibration process becomes a guide as to the hydraulic properties of the uppermost 30 feet of material in areas of minimum thickness of aquifer layer 1, as the material may be representative of the surficial aquifer system, the intermediate confining unit, the Floridan aquifer system, or some combination thereof, depending on location (Figure 2-3, Figure 2-4, and Figure 2-5).

Table 2-2. NFSEG Model Layer Properties

NFSEG Model Layer	MODFLOW-NWT UPW Layer-Type Designation	Applied Minimum Thickness (Feet)
1	Unconfined	30
2	Confined	30
3	Confined	50
4	Confined	30
5	Confined	50
6	Confined	10
7	Confined	10

Determination of the Areal Extent of Model Layer 1

The areal extent of model layer 1 was made equivalent to that of model layer 3. Details regarding the determination of the areal extent of model layer 3 will be provided in the discussion of model layer 3.

Model Layer 2

Minimum Layer Thickness of Model Layer 2

Model layer 2 is used primarily to represent the intermediate confining unit where it is present (Table 2-1 and Table 2-2). Outside the extent of the intermediate confining unit, layer 2 represents a vertical segment of the Floridan aquifer system and/or surficial aquifer system. The minimum assigned thickness of model layer 2 is 30 feet (Table 2-1 and Table 2-2; Figure 2-4, Figure 2-6 and Figure 2-7).

Determination of the Areal Extent of Model Layer 2

The areal extent of model layer 2 was made equivalent to that of model layer 3. Details regarding the determination of the areal extent of model layer 3 will be provided in the discussion of model layer 3.

Model Layer 3

Minimum Layer Thickness of Model Layer 3

Model layer 3 is used primarily to represent the Upper Floridan aquifer where it exists as a separate aquifer unit within the overall Floridan aquifer system. Where the Upper Floridan

aquifer is not present as a separate hydrogeologic unit (i.e., where the middle semiconfining unit is absent), model layer 3 represents a vertical segment of the overall Floridan aquifer system. The assigned minimum layer thickness of model layer 3 is 50 feet (Table 2-2, Figure 2-6; Figure 2-8 and Figure 2-9).

Determination of the Areal Extent of Model Layer 3

The primary consideration in specifying the locations of the lateral boundaries of model layer 3 was to minimize or eliminate their influences on critical locations within the model domain. The approach for doing this was to place, where feasible, the lateral boundaries at locations that correspond approximately to the physical boundaries of the Upper Floridan aquifer or the boundaries of fresh-water flow within the Floridan aquifer system. Where placement at physical boundaries was not feasible, placement was made at locations that are as far as feasible from areas of critical concern.

The model domain of the NFSEG groundwater flow model is oriented along southwest-northeast and northwest-southeast alignments (Figure 2-1). Hence, the model is comprised of a northwest-facing lateral boundary, a northeast-facing lateral boundary, a southeast-facing lateral boundary, and a southwest-facing lateral boundary. For simplicity, these are referred to as the northern, eastern, southern, and western lateral boundaries, respectively.

As stated previously, the general approach in specifying the locations of the lateral boundaries was to place them at the physical boundaries or the limits of the fresh-water flow system, where feasible. In the course of the model development, however, some additional criteria were implemented to enhance numerical stability. These additional criteria resulted in changes in portions of the northern, eastern, and western boundaries and a corresponding reduction in the areal extent of model layer 3. These criteria are as follows: (1) the fresh-water thickness of the Upper Floridan aquifer was required to be at least 50 feet (prior to introduction of the minimum thickness); and (2) the height of the 2010 potentiometric surface as depicted by Kinnaman and Dixon (2011) was required to be at least 100 feet above the top of model layer 4. The purpose of these criteria was to reduce the tendency of grid cells located in proximity to the original northern and eastern lateral boundaries of model layers 3, 4, and 5 to desaturate as a result of numerical instability.

The physical boundary of the Upper Floridan aquifer north of the Gulf Trough in Georgia is its line of pinch-out, approximated by Williams and Kuniandy (2015; Figure 2-1). Accordingly, prior to implementation of the additional criteria described above, the northern boundary of model layer 3 was made coincident with this line.

The model domain that corresponds to areas beneath the Gulf of Mexico and the Atlantic Ocean extends to the approximate limits of fresh-water flow within the Floridan aquifer system. In the case of the Atlantic Ocean, the seaward limit of fresh-water flow in the Upper Floridan aquifer was assumed initially to be coincident with the onset of the Florida-Hatteras slope. Accordingly, the eastern seaward limit of model layer 3 was made to correspond in location to the onset of the Florida-Hatteras slope prior to implementation of the additional criteria discussed above. Along

portions of the Gulf of Mexico that fall within the active model domain, the Floridan aquifer system is unconfined, and hydraulic heads within it are generally near 0 feet NAVD88. Therefore, it was assumed that the limit of fresh-water flow within the Floridan aquifer system is within a relatively short distance seaward of the coast. Accordingly, the lateral boundary of model layer 3 was placed within approximately five to 10 miles of the Gulf Coast.

Placement of the southern lateral boundary was designed to position it at an adequate distance south of critical areas of the model domain, including the area of the Keystone Heights potentiometric high and the Lower Suwannee River basin. The Silver and Rainbow springs complexes are highly influential features of the Floridan aquifer system within their respective springsheds. The model grid was situated such that the respective basin areas of Rainbow and Silver Springs, as delineated by Faulkner (1973) and Knowles, Jr. (1996), are encompassed fully within the NFSEG active model domain. Their inclusion in the active model domain buffers critical areas to the north from influences of the southern lateral boundary.

The southern lateral boundary is delineated based on persistent features in the configuration of the potentiometric surface of the Upper Floridan aquifer (e.g., Kinnaman and Dixon (2011)). Additional details concerning the delineation of the southern lateral boundary are provided in the descriptions of the model lateral boundary conditions that follow.

The implementation of the additional criteria caused a small decrease in the size of the active portion of the model domain. The intersection of the estimated 10,000 mg/l TDS-concentration iso-surface (Figure 2-2) with the top of model layer 3 along the seaward-most portion of the eastern lateral boundary represents an improvement over the initial assumption for the location of this boundary, i.e., coincidence with the Florida-Hatteras slope. The southern lateral boundary was unaffected, and the western lateral boundary was affected minimally. The northern lateral boundary was affected the most. It now falls roughly along a line referred to by the U.S. Geological Survey as the “approximate up-dip limit of (the) productive part of Upper Floridan aquifer” (Williams and Kuniansky 2015).

Model Layer 4

Minimum Layer Thickness of Model Layer 4

The specified minimum thickness for model layer 4 is 30 feet (Table 2-2, Figure 2-8, Figure 2-10 and Figure 2-11).

Determination of the Areal Extent of Model Layer 4

The western and eastern lateral boundaries of model layer 4 were determined primarily by intersecting the estimated 10,000 mg/l TDS-concentration iso-surface with the estimated top of model layer 4 (Figure 2-2, Figure 2-8, Figure 2-10 and Figure 2-11). The northern boundary and the portions of the western and southern lateral boundaries within the fresh-water flow system coincide with the respective corresponding lateral boundaries of model layer 3.

Model Layer 5

Minimum Layer Thickness of Model Layer 5

The specified minimum thickness of model layer 5 is 50 feet (Table 2-2, Figure 2-10, Figure 2-12 and Figure 2-13).

Determination of the Areal Extent of Model Layer 5

The western and eastern lateral boundaries of model layer 5 were determined primarily by intersecting the estimated 10,000 mg/l TDS-concentration iso-surface with the estimated top of model layer 5 (Figure 2-2, Figure 2-10, Figure 2-12 and Figure 2-13). The northern boundary and portions of the western and southern lateral boundaries within the fresh-water flow system coincide with the respective corresponding lateral boundaries of model layer 3.

Model Layer 6

Minimum Layer Thickness of Model Layer 6

The specified minimum thickness of model layer 6 is 10 feet (Table 2-2, Figure 2-14, Figure 2-15, and Figure 2-16).

Determination of the Areal Extent of Model Layer 6

The areal extent of model layer 6 was determined primarily by intersecting the estimated 10,000 mg/l TDS-concentration iso-surface with the estimated top of model layer 6 (Figure 2-2, Figure 2-14, Figure 2-15, and Figure 2-16). The top of model layer 6 is based on data obtained from Miller (written communication). A portion of the western lateral boundary coincides with the approximate pinch-out of the lower-semiconfining unit, as discussed in more detail in the discussion of the model lateral boundary conditions.

Model Layer 7

Minimum Layer Thickness of Model Layer 7

The specified minimum thickness of model layer 7 is 10 feet (Table 2-2, Figure 2-17, Figure 2-18 and Figure 2-19).

Determination of the Areal Extent of Model Layer 7

The areal extent of model layer 7 was determined primarily by intersecting the estimated 10,000 mg/l TDS-concentration iso-surface with the estimated top of model layer 7 (Figure 2-17, Figure 2-18 and Figure 2-19). The top of model layer 7 was based on Miller 1986 and Miller (written communication). A portion of the western lateral boundary coincides with the approximate pinch-out of the Fernandina permeable zone, as discussed in more detail in the discussion of the model lateral boundary conditions.

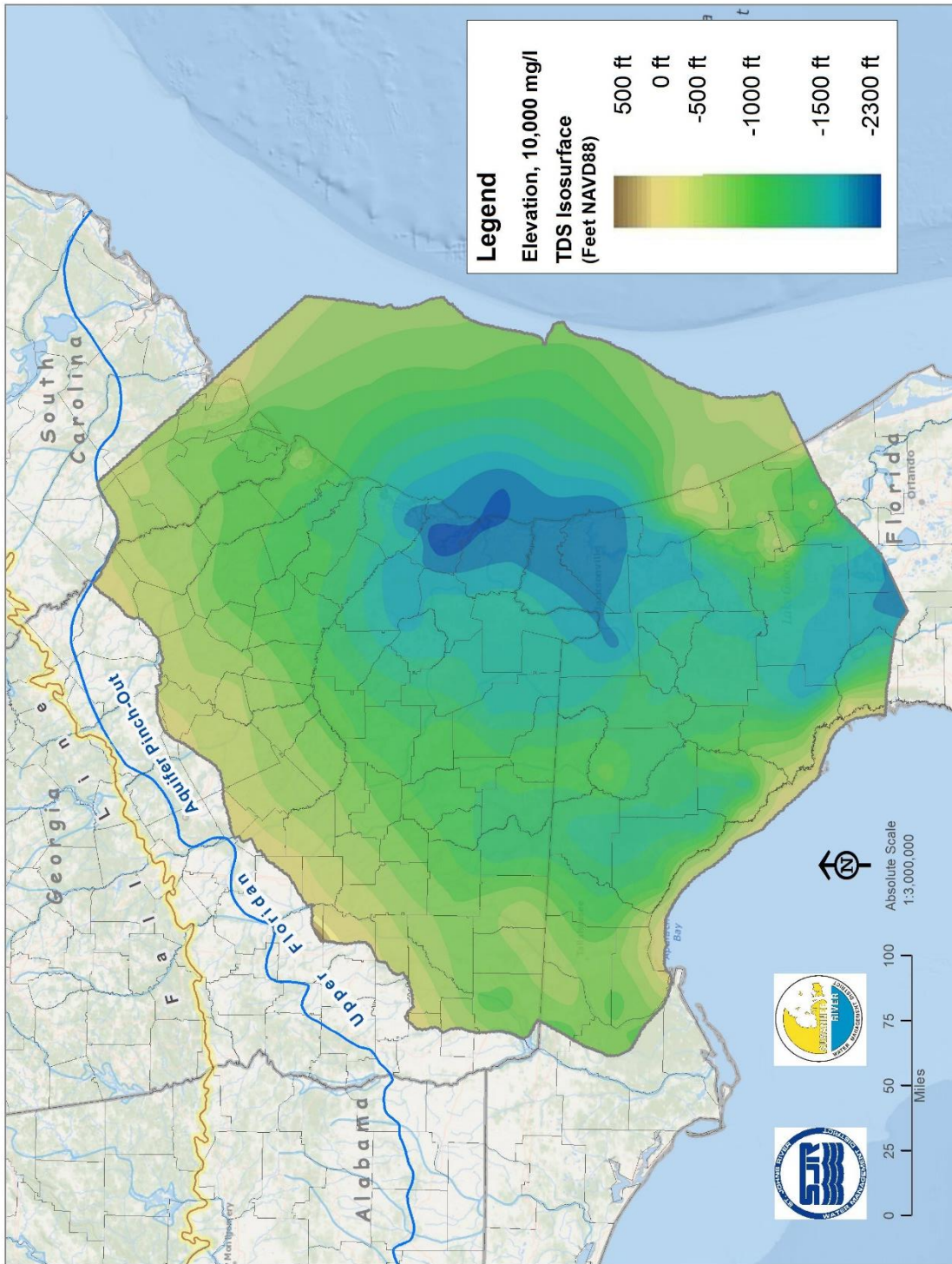


Figure 2-2. Elevation, 10,000 mg/l Total-Dissolved-Solids (TDS)-Concentration Iso-Surface, Feet NAVD88 (after Williams and Kuniansky 2015)

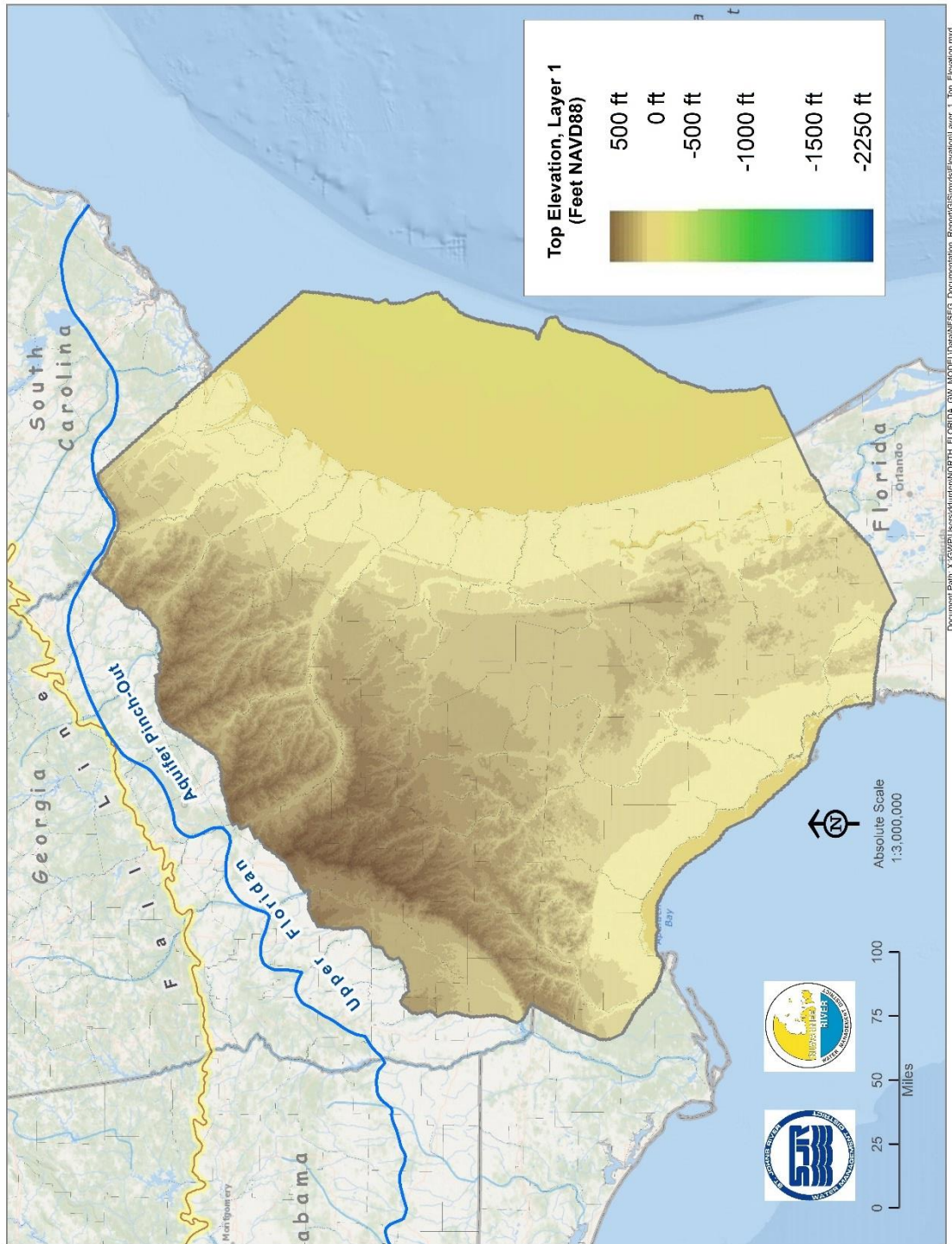


Figure 2-3. Top Elevation, Layer 1 (Feet NAVD88; after Boniol and Davis, digital communication)

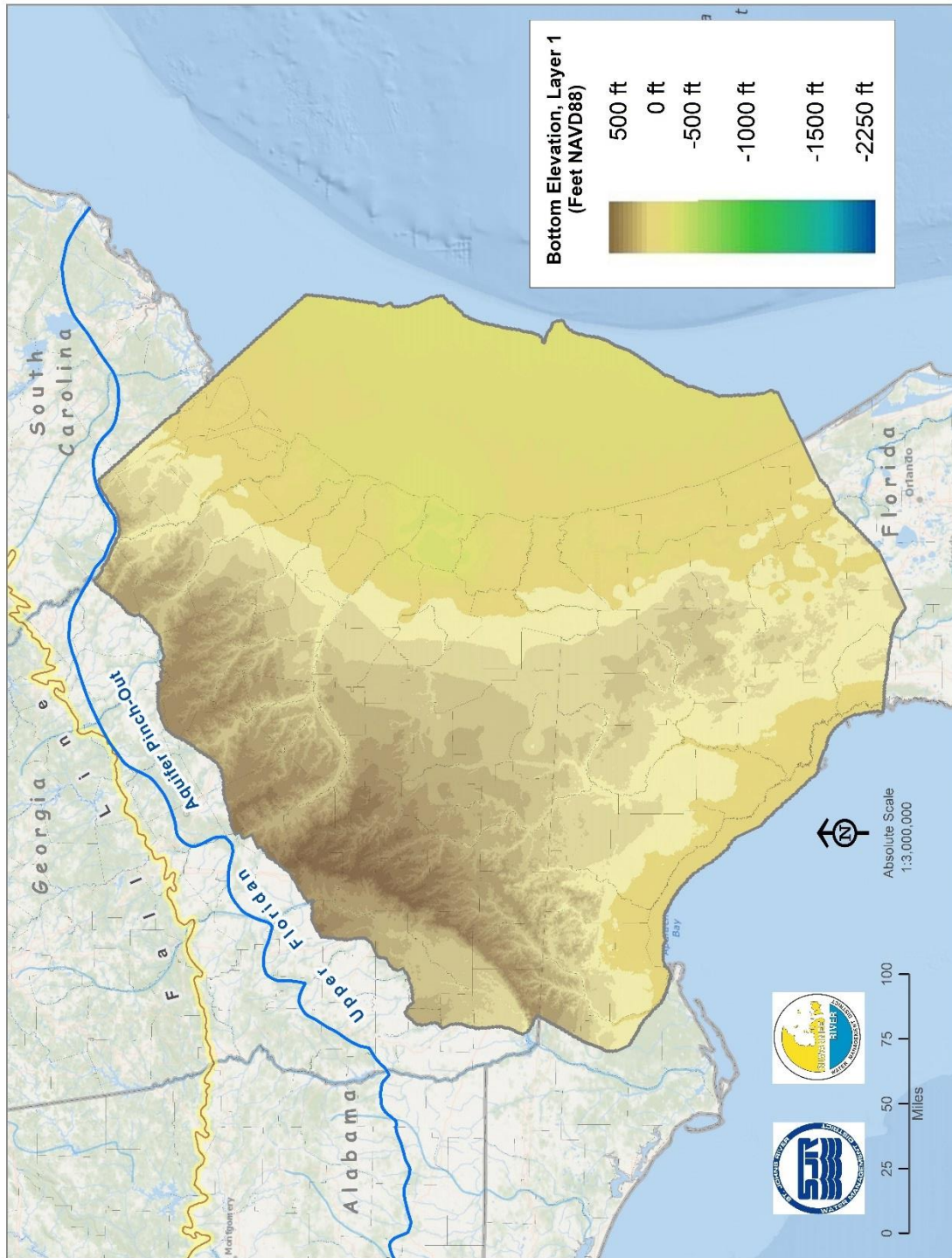


Figure 2-4. Bottom Elevation, Layer 1 (and Top Elevation, Layer 2; Feet NAVD88; after Boniol and Davis, digital communication)

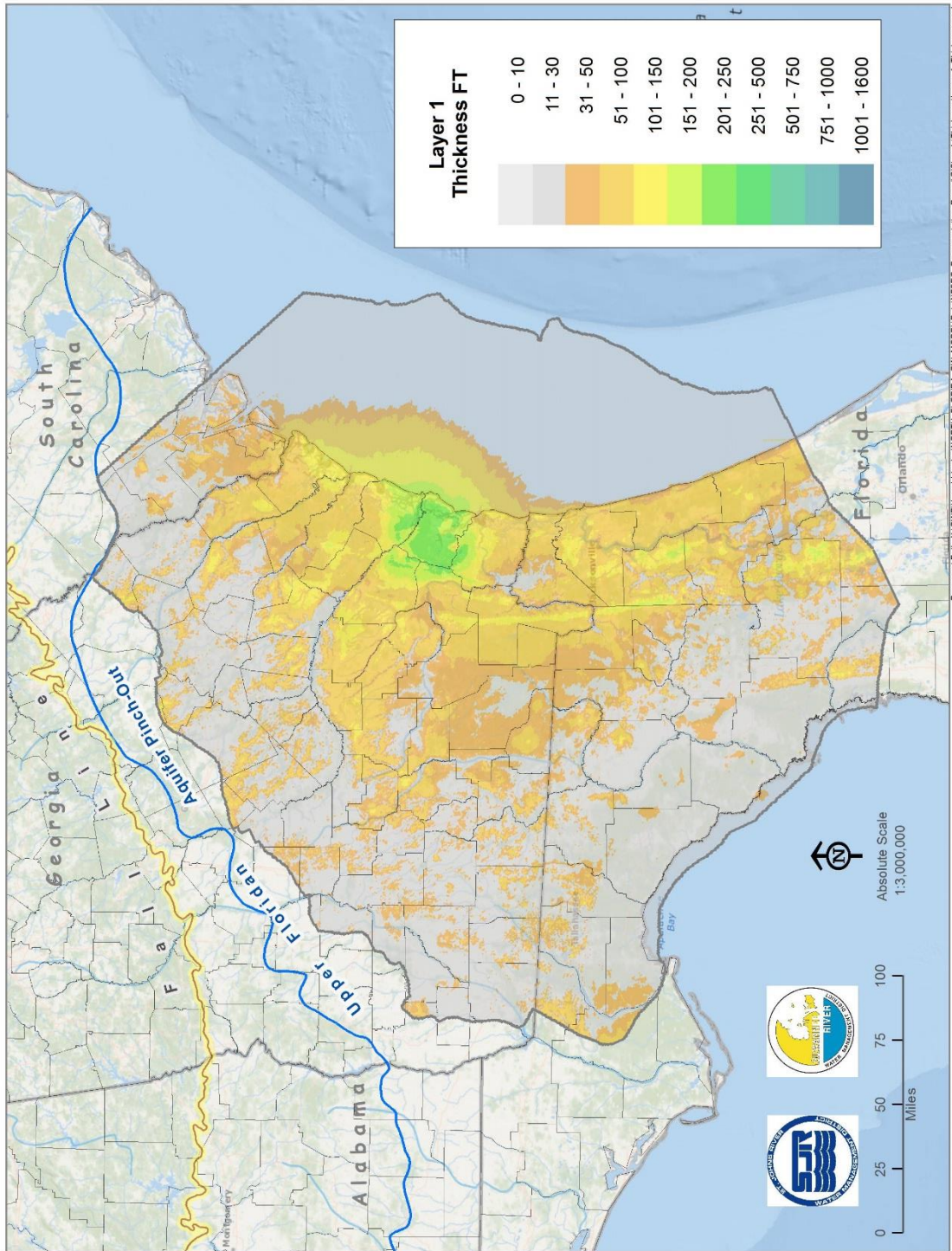


Figure 2-5. Thickness, Layer 1 (Feet)

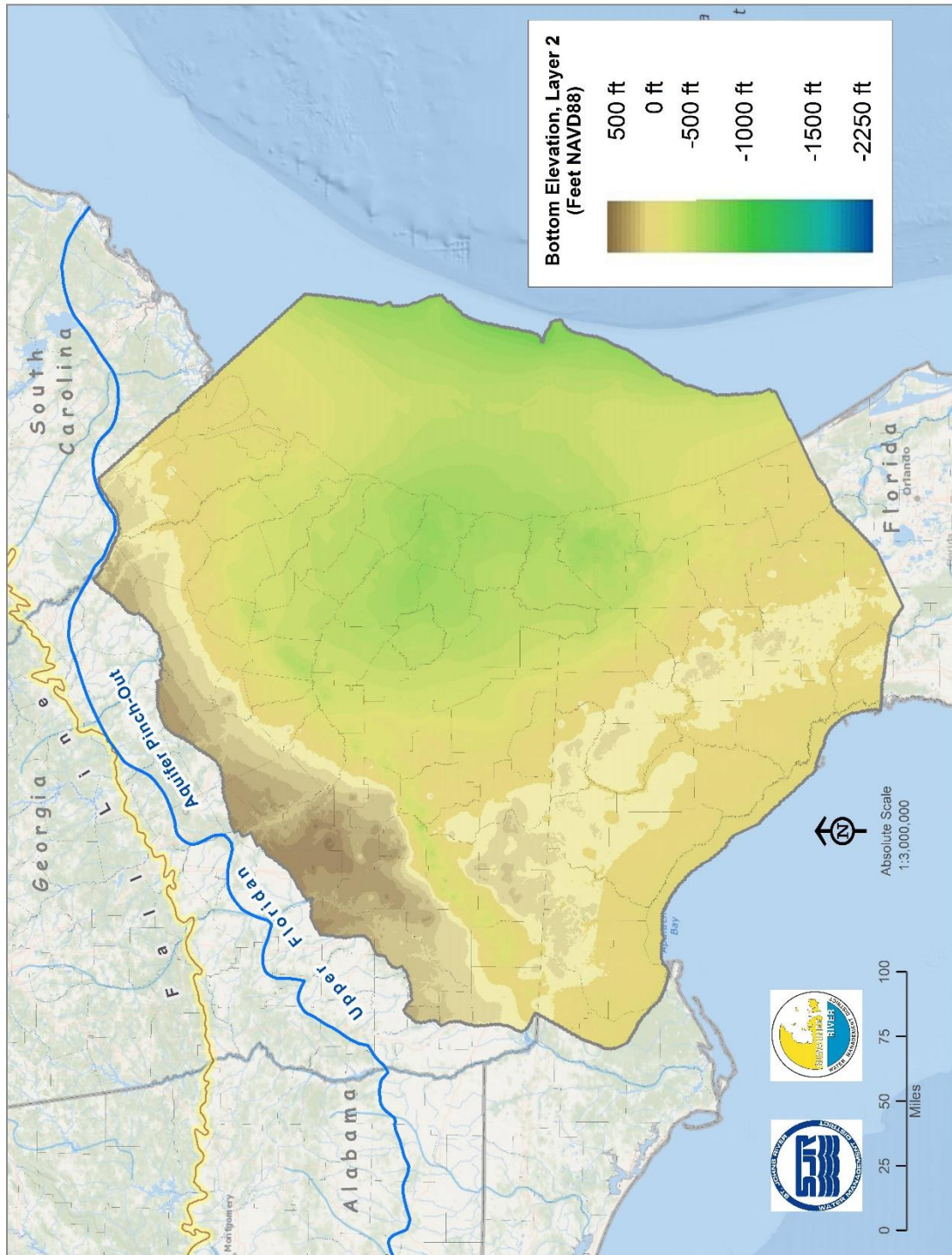


Figure 2-6. Bottom Elevation, Layer 2 (and Top Elevation, Layer 3; Feet NAVD88; after Boniol and Davis, digital communication)

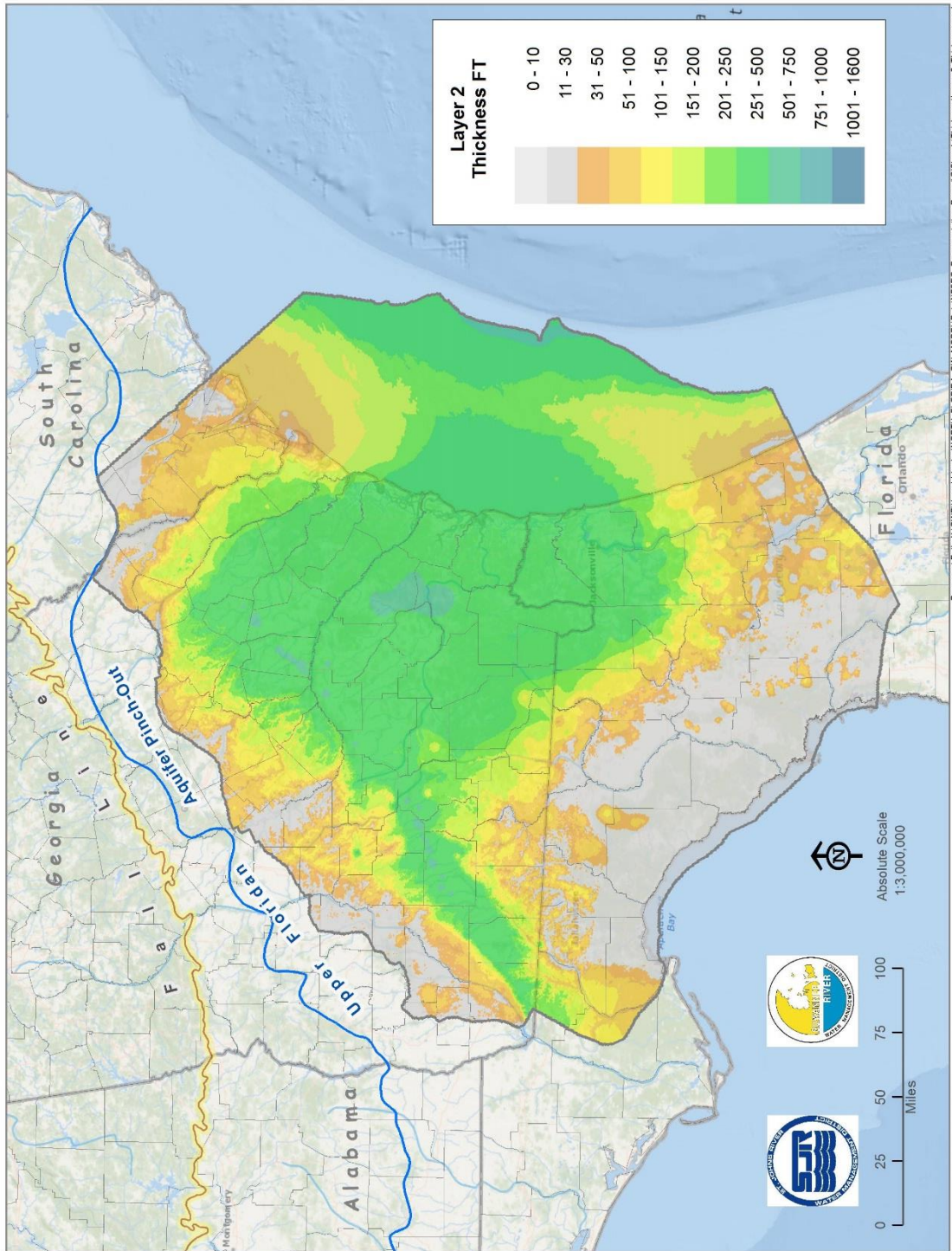


Figure 2-7. Thickness, Layer 2 (Feet)

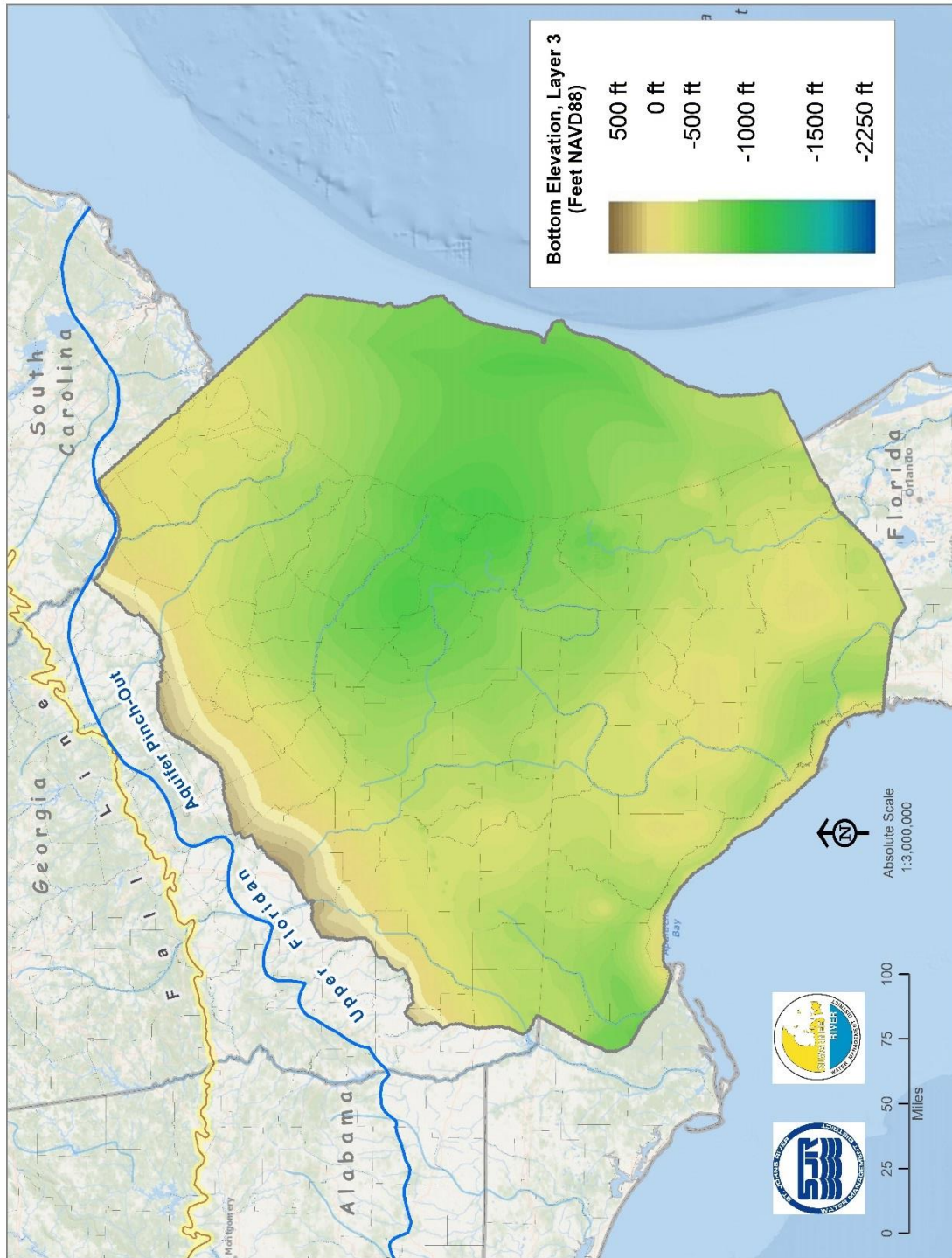


Figure 2-8. Bottom Elevation, Layer 3 (and Top Elevation, Layer 4; Feet NAVD88; after Boniol and Davis, digital communication)

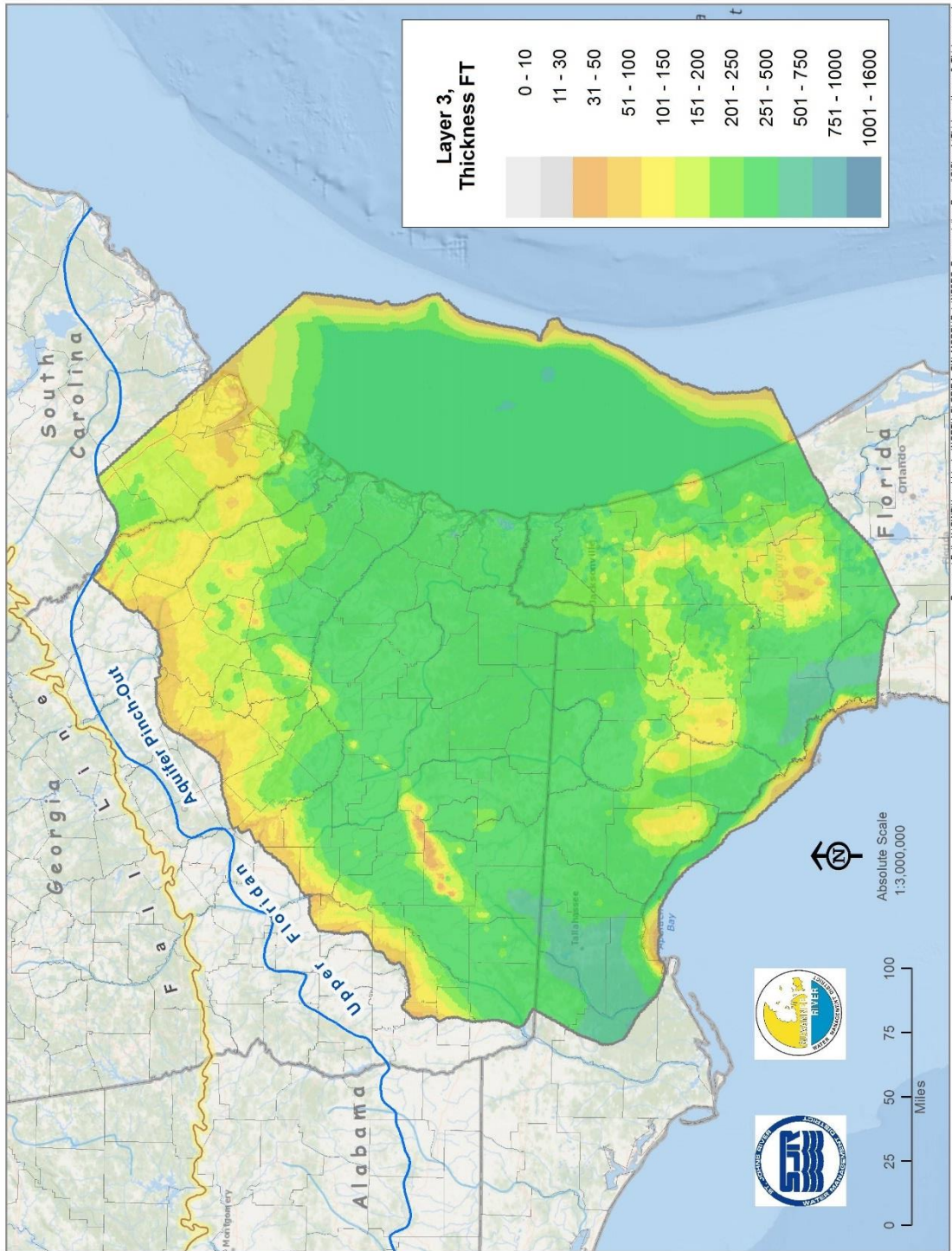


Figure 2-9. Thickness, Layer 3 (Feet)

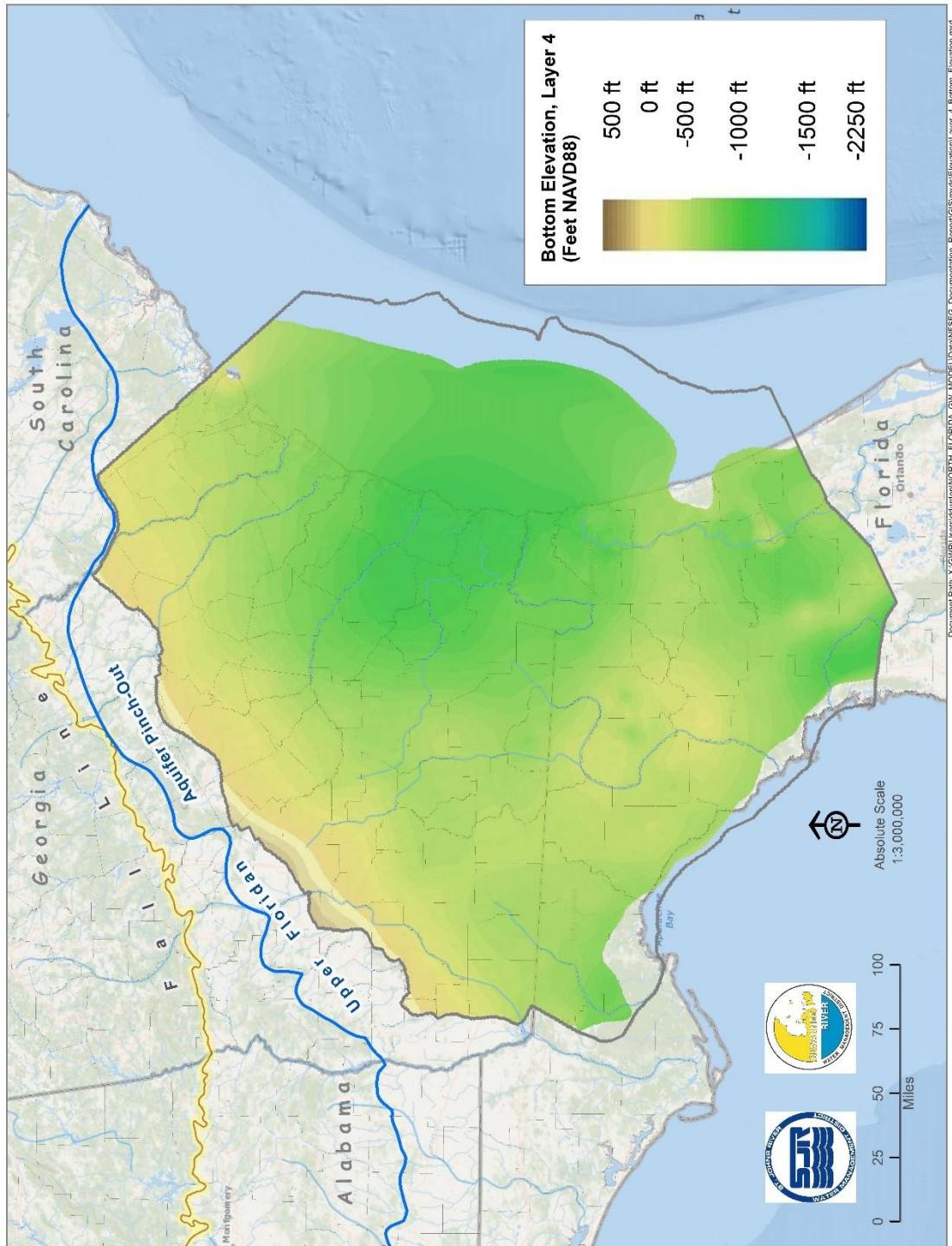


Figure 2-10. Bottom Elevation, Layer 4 (and Top Elevation, Layer 5; Feet NAVD88; after Boniol and Davis, digital communication)

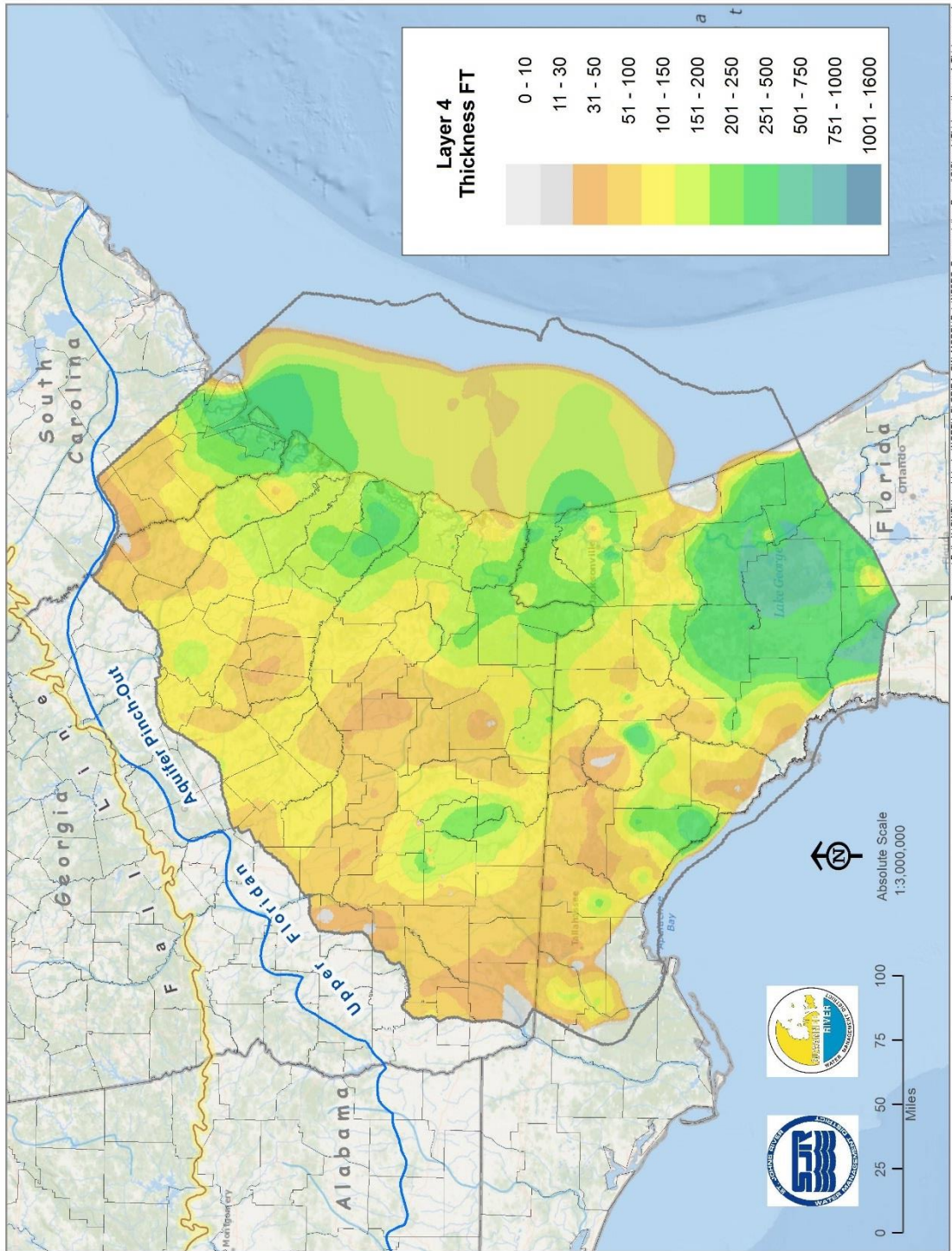


Figure 2-11. Thickness, Layer 4

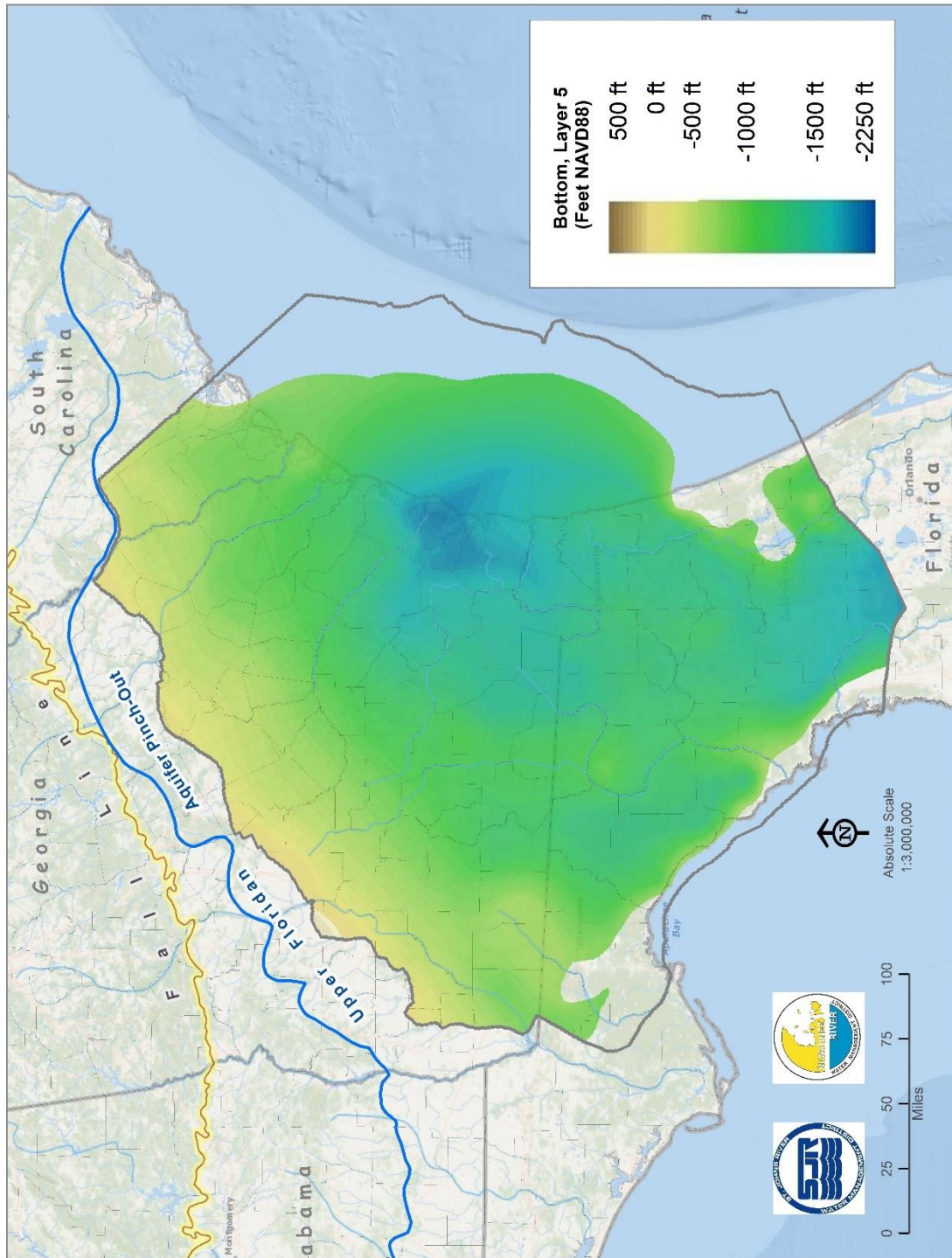


Figure 2-12. Bottom Elevation, Layer 5 (Feet NAVD88; after Miller, written communication, Williams, digital communication, and Miller 1986)

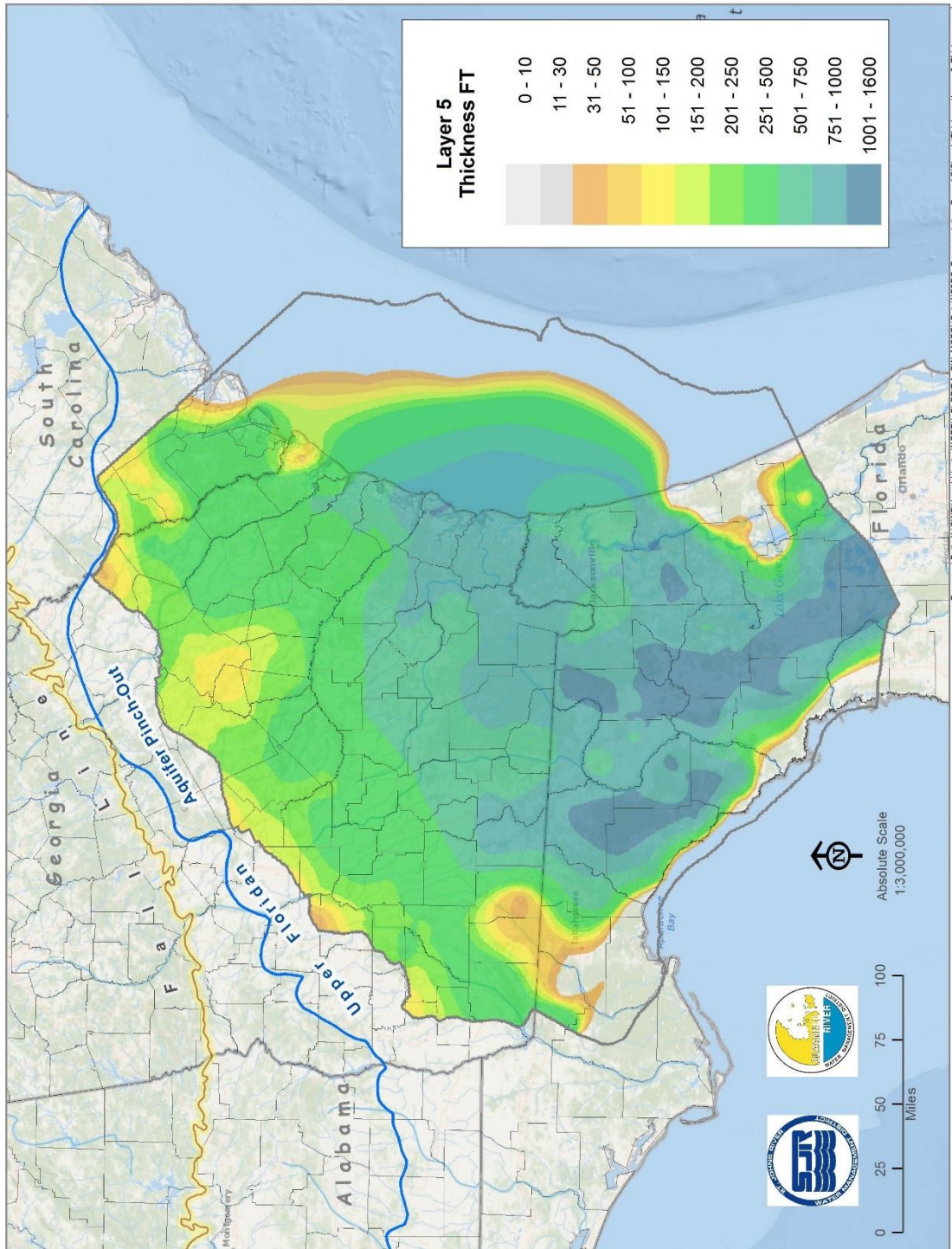


Figure 2-13. Thickness, Layer 5 (Feet)

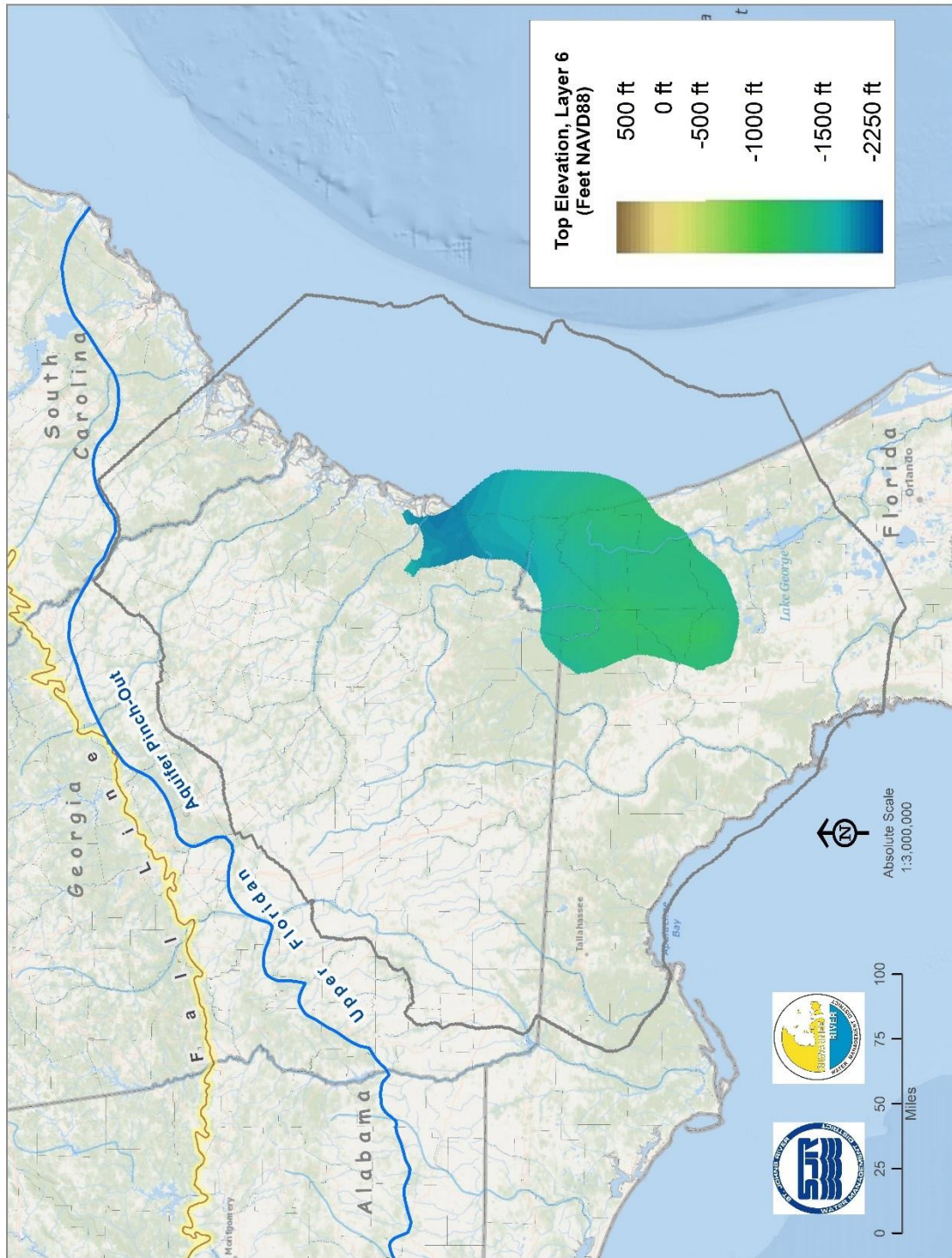


Figure 2-14. Top Elevation, Layer 6 (Feet NAVD88; after Miller, written communication)

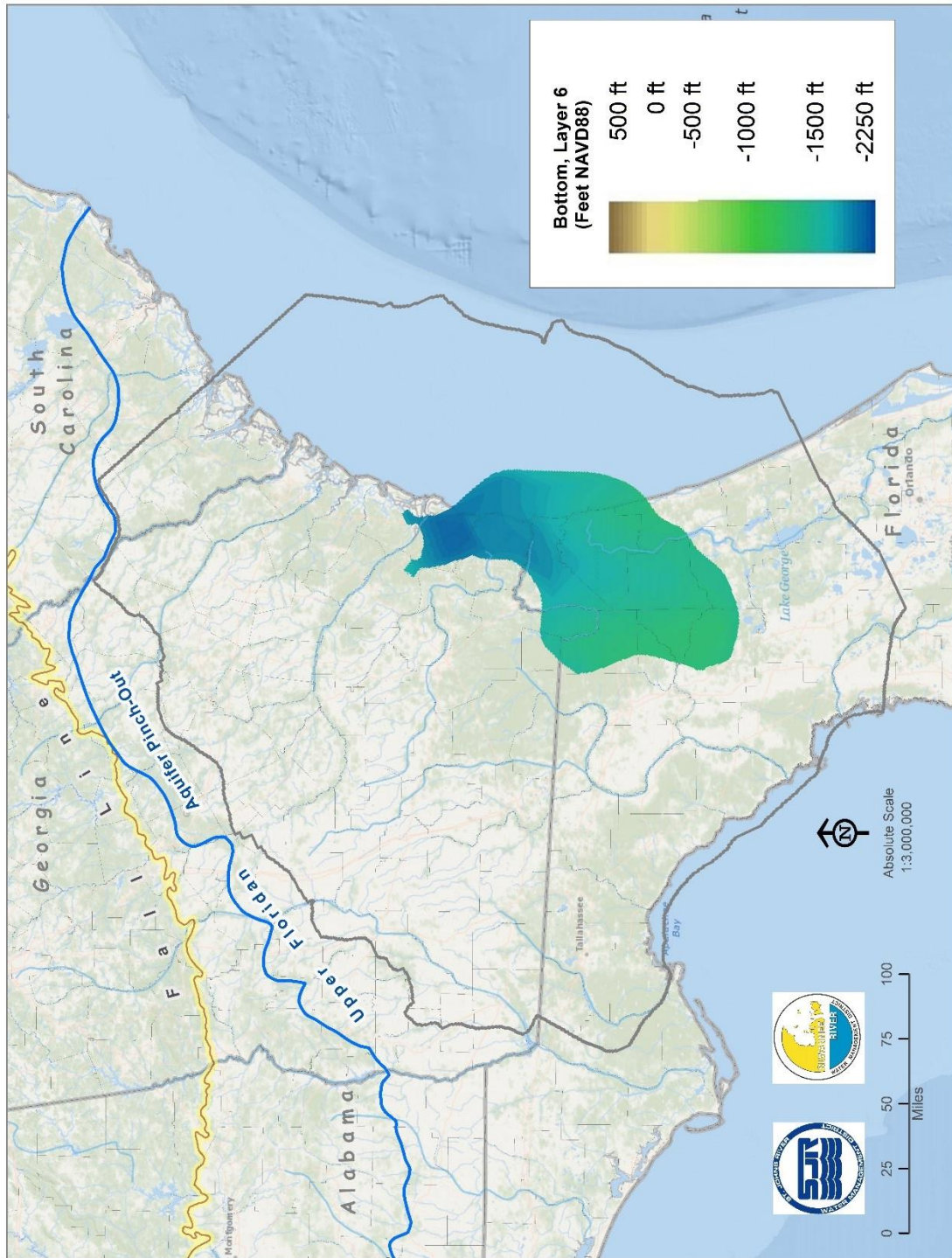


Figure 2-15. Bottom Elevation, Layer 6 (Feet NAVD88; after Miller, written communication)

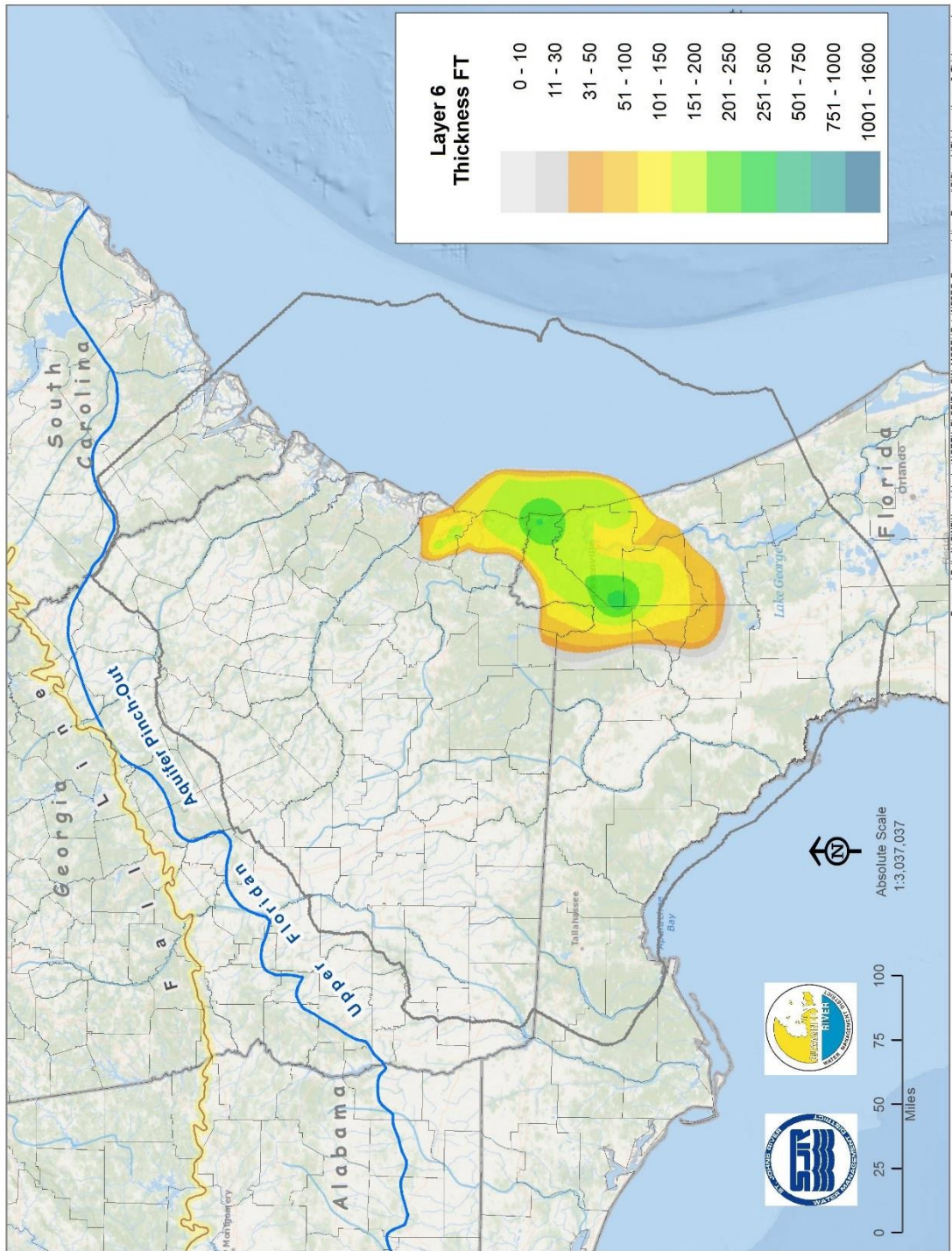


Figure 2-16. Thickness, Layer 6 (Feet)

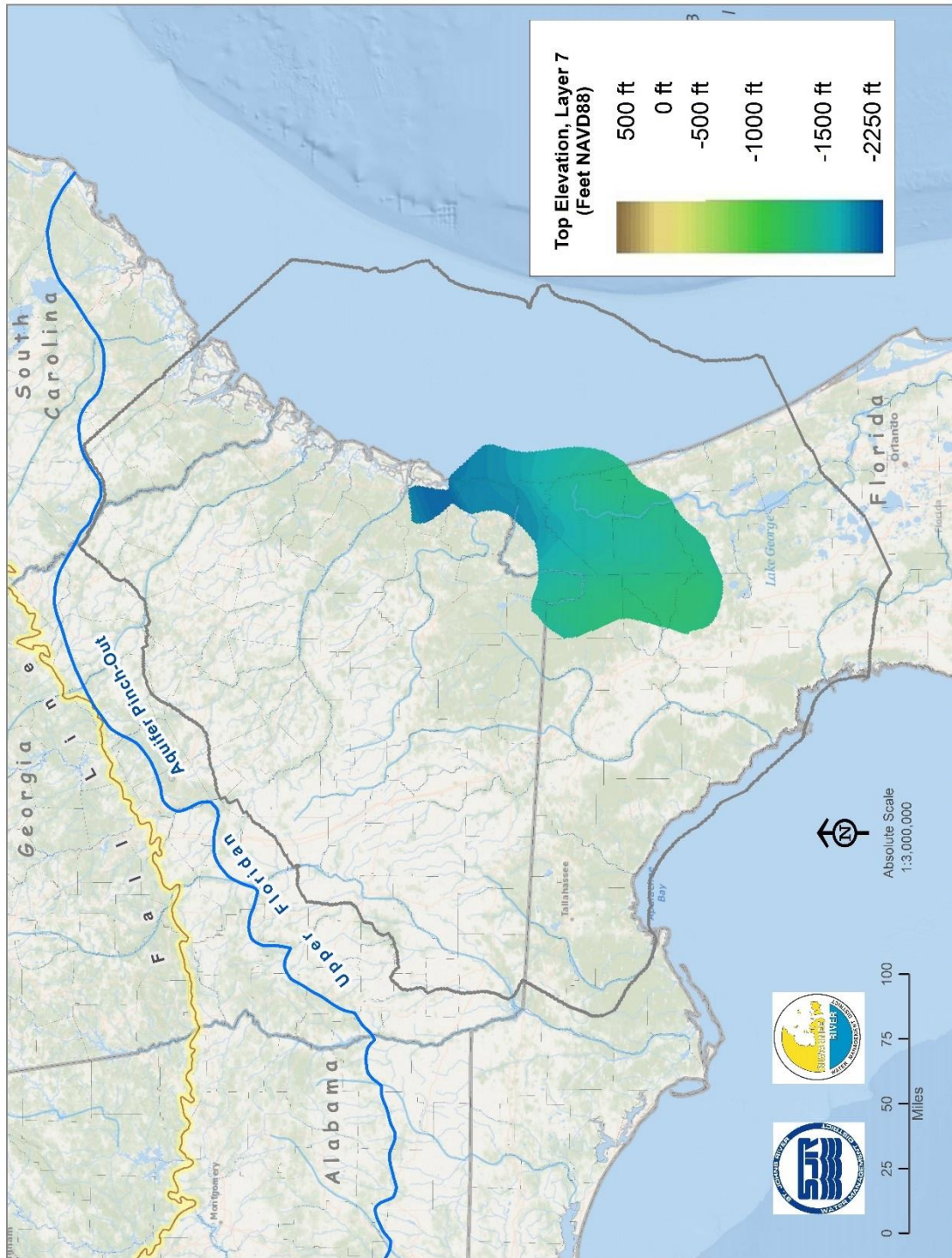


Figure 2-17. Top Elevation, Layer 7 (Feet NAVD88, after Miller, written communication, and Miller 1986)

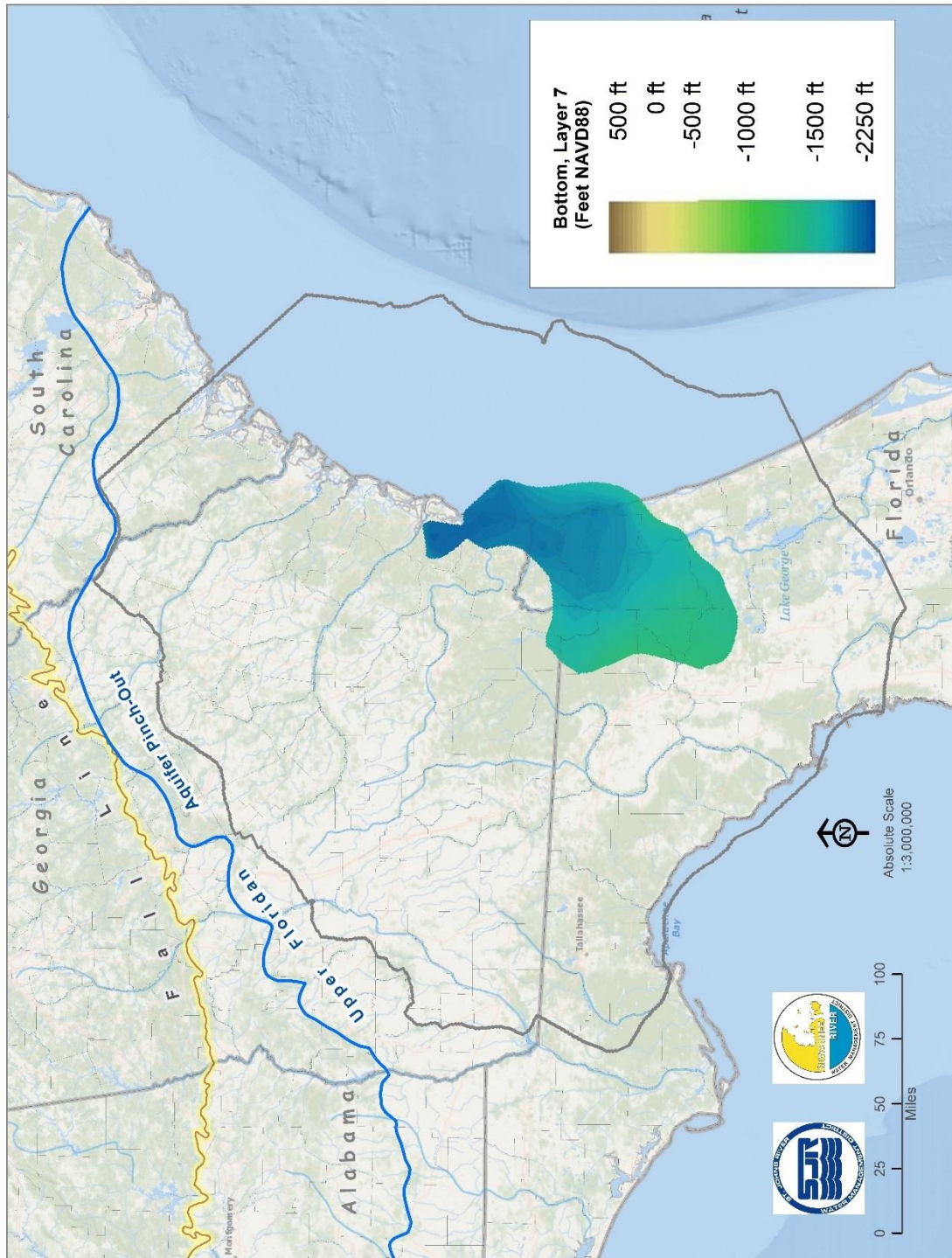


Figure 2-18. Bottom Elevation, Layer 7 (Feet NAVD88; after Williams, digital communication, and Miller, 1986)

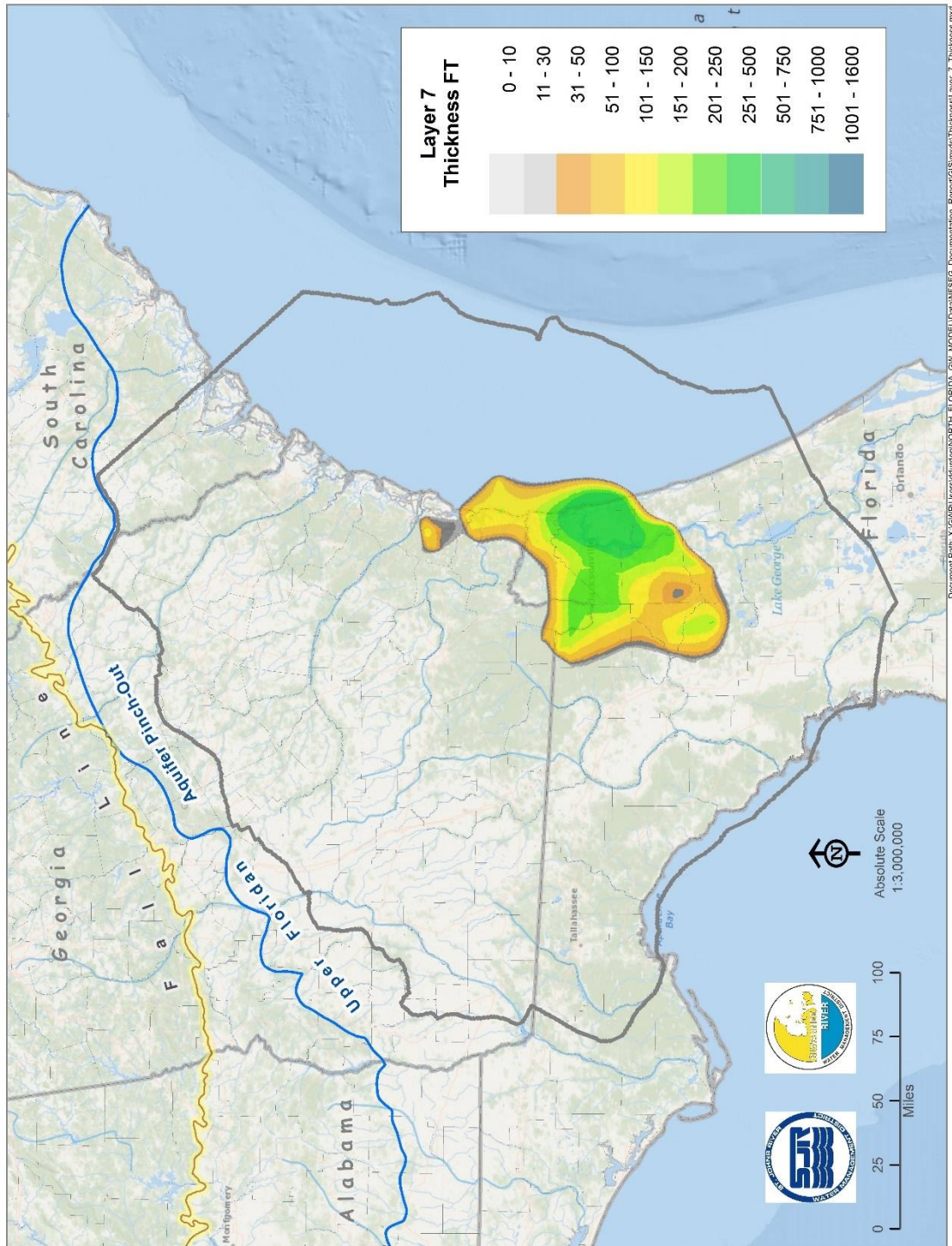


Figure 2-19. Thickness, Layer 7 (Feet)

MODEL LATERAL BOUNDARY CONDITIONS

The model lateral boundary conditions represent prevailing flow conditions at the model lateral boundaries. In some cases, lateral boundaries coincide approximately with the pinch-out of a hydrogeologic unit or the fresh-water flow system. In other cases, lateral boundaries are oriented parallel to the direction of groundwater flow, as inferred from the configuration of the potentiometric surface of the Upper Floridan aquifer. Conditions at lateral boundaries in these cases are specified as no-flow (i.e., no flux across model lateral boundaries). Where flux across lateral boundaries is inferred based on the configuration of the potentiometric surface of the Upper Floridan aquifer, general-head boundary (GHB) conditions are specified. To facilitate the following discussion of the model lateral boundary conditions, the lateral boundaries of model layers 3 through 5 are subdivided into northern, eastern, southern, and western segments and sub-segments. The lateral boundaries of model layers 6 and 7 are subdivided into two sub-segments, respectively, also for this purpose.

Prior to reading this section and others that follow concerning NFSEG model internal boundary conditions, the reader is encouraged to review the document “Description of NFSEG Model Input Files.” This is an existing report provided to the NFSEG Technical Team that describes in detail the application of various MODFLOW packages in the representation of the various NFSEG boundary conditions (see Appendix A).

Model Layers 1 and 2

Model layers 1 and 2 represent the surficial aquifer system and/or intermediate confining unit, where they are present. Flow in these hydrogeologic units is typically local in nature in the case of the surficial aquifer system or dominated by vertical gradients in the case of the intermediate confining unit and therefore generally absent of regionally significant lateral gradients. The lateral boundaries of model layers 1 and 2 were therefore specified as no-flow. Along the coasts of the Atlantic Ocean and Gulf of Mexico, the active domain of model layer 1 is bounded by constant-head grid cells used to represent the equivalent fresh-water head of the ocean.

Model Layer 3

Northern (N3)

Although the northern lateral boundary of model layer 3 was relocated somewhat to the south of the estimated line of pinch-out of the Upper Floridan aquifer as delineated by Williams and Kuniansky (2015, Figure 2-1), the resulting northern lateral boundary was assumed to approximate conditions of zero lateral flux. Hence, no-flow lateral boundary conditions were specified for the entire length of the northern lateral boundary of model layer 3, which is designated as “northern” (N3; Figure 2-20).

Eastern, Upper (EU3)

The eastern lateral boundary of model layer 3 is subdivided into three sub-segments, to facilitate the present discussion. The northernmost sub-segment is labeled the “eastern, upper” (EU3; Figure 2-20). This sub-segment is oriented parallel to the direction of groundwater flow, as inferred from the configuration of the 2010 potentiometric surface of the Upper Floridan aquifer (Kinnaman and Dixon 2011). Conditions along the EU3 sub-segment are accordingly represented as no-flow.

Eastern, Central (EC3)

The “eastern, central” (EC3; Figure 2-20) lateral boundary sub-segment passes through an area of induced lateral influx. The lateral influx is caused by a large cone of depression in the potentiometric surface of the Upper Floridan aquifer that results from groundwater withdrawals near Savannah, Georgia. The EC3 sub-segment is accordingly represented with GHB lateral boundary conditions along its length. The source heads of the GHB conditions were interpolated from the May-June 2010 map of the potentiometric surface of the Upper Floridan aquifer (Kinnaman and Dixon 2011).

Eastern, Lower (EL3)

The “eastern, lower” (EL3; Figure 2-20) lateral boundary sub-segment extends offshore beneath the Atlantic Ocean. Groundwater flow in this area is assumed to be unaffected by on-shore pumping and therefore in the same general direction as groundwater flow along the EU3 sub-segment. Conditions along the EL3 sub-segment are therefore designated as no-flow.

Eastern, Seaward (ES3)

The “eastern, seaward” (ES3; Figure 2-20) lateral boundary sub-segment represents the approximate line of pinch-out of fresh-water flow in the Upper Floridan aquifer beneath the Atlantic Ocean. Conditions along the ES3 sub-segment are therefore designated as no-flow.

Southern, East (SE3)

The southern lateral boundary of model layer 3 is subdivided into three sub-segments. The easternmost sub-segment is the “southern, east” (SE3; Figure 2-20) sub-segment. This sub-segment is oriented parallel to the general direction of groundwater flow. Conditions along the SE3 sub-segment are therefore designated as no-flow.

Southern, Central (SC3)

The Green Swamp potentiometric high, which occurs mainly to the south of the NFSEG model domain, intersects the NFSEG model domain along the “southern, central” (SC3; Figure 2-20) sub-segment of the southern lateral boundary. The SC3 sub-segment is accordingly represented with GHB conditions along its length. GHB source heads representing 2001 and 2009 average water levels were interpolated for use, respectively, in the 2001 and 2009 steady-state versions of

the NFSEG model. For 2001, a map representing the average of water levels observed in May and September of 2001 was derived from the maps of Knowles (2001) and Knowles and Kinnaman (2001) and was utilized for this purpose. A similar map of 2009 average water levels, based on the maps of Kinnaman and Dixon (2009) and Boniol (digital communication), was utilized for interpolation of 2009 source heads.

Southern, West (SW3)

The westernmost sub-segment of the southern lateral boundary of model layer 3 is the “southern, west” (SW3; Figure 2-20) sub-segment. This sub-segment is oriented parallel to the general direction of groundwater flow. Conditions along the SW3 sub-segment are therefore designated as no-flow.

Western, Seaward (WS3)

The western lateral boundary of model layer 3 is subdivided into two sub-segments. The more southerly is the “western, seaward” (WS3; Figure 2-20) sub-segment. This location of this sub-segment represents an approximation of the seaward limit of fresh-water flow in the Upper Floridan aquifer beneath the Gulf of Mexico. GHB conditions were specified along the WS3 sub-segment to allow for the possibility that fresh-water flow in the Upper Floridan aquifer might, in places, extend farther seaward than the location of the WS3 sub-segment. The source heads of all GHB conditions comprising sub-segment WS3 are equivalent fresh-water heads of the Gulf of Mexico.

Western, North (WN3)

The more northerly sub-segment of the western lateral boundary is the “western, north” (WN3; Figure 2-20) sub-segment. In Florida, this sub-segment is oriented parallel to the general direction of groundwater flow and is therefore designated as a no-flow condition. In Georgia, it is coincident with the path of Spring Creek, the smallest of three tributaries whose confluence forms the Apalachicola River. Spring Creek is in close hydraulic connection with the Upper Floridan aquifer, as evidenced by the configuration of the 2010 potentiometric surface of the Upper Floridan aquifer (Kinnaman and Dixon 2011) along its flow path, so groundwater flow is assumed to be converging on it from opposing directions. Spring Creek therefore approximates a line of stagnation within the Upper Floridan aquifer, a no-flow condition. Accordingly, conditions along the entire length of the WN3 sub-segment are designated as no-flow.

Model Layer 4

The corresponding lateral boundary sub-segments in model layer 4 are N4, EU4, EC4, ES4, SE4, SC4, SW4, WS4, and WN4 (Figure 2-21). Because of the manner in which the 10,000 mg/l TDS-concentration iso-surface (Figure 2-2) intersects the top of model layer 4, model layer 4 sub-segments differ in exact shape and/or length as compared to corresponding model layer 3 sub-segments. Also for this reason, a layer-4 sub-segment that corresponds to sub-segment EL3 of the eastern lateral boundary of model layer 3 does not exist.

Conditions at sub-segment WS4, which corresponds to the Gulf coastal region, are designated as no-flow, in contrast with those of WS3, which were designated as GHB to allow for the possibility of lateral flux to areas beyond the seaward limits of the layer-3 active model domain. WS4 is closer to shore and based on the intersection of the 10,000 mg/l TDS-concentration iso-surface (Figure 2-2) with the top of model layer 4. Therefore, it is considered a reasonable approximation of the seaward limit of fresh-water flow in model layer 4 in the region of the Gulf Coast.

Conditions at sub-segments EU4, EC4, ES4, SE4, SC4, SW4, and WN4 are assumed to be similar in nature to those of corresponding sub-segments of model layer 3. The source heads of GHB conditions assigned to sub-segment EC4 are identical to those of the corresponding GHB conditions of sub-segment EC3. The source heads of GHB conditions assigned to sub-segment SC4 are identical to those of the corresponding GHB conditions of sub-segment SC3.

Conditions along sub-segment N4 are designated as GHB, in contrast with the no-flow designation of sub-segment N3. No-flow conditions are specified along the N3 sub-segment because the northern lateral boundary approximates the line of pinch-out of the Upper Floridan aquifer. The lines of pinch-out of hydrogeologic units beneath the Upper Floridan aquifer are farther to the north, however. Use of GHB conditions to represent conditions along the N4 sub-segment enables lateral fluxes across N4 to be simulated without extending the domain of model layer 4 to the line of pinch-out of the hydrogeologic unit(s) being represented by it in this area. The source heads of GHB conditions specified along the N4 sub-segment are interpolated from the May-June 2010 map of the potentiometric surface of the Upper Floridan aquifer (Kinnaman and Dixon 2011).

Model Layer 5

The corresponding lateral boundary sub-segments in model layer 5 are N5, EU5, EC5, ES5, SE5, SC5, SW5, WS5, and WN5 (Figure 2-22). Because of the manner in which the 10,000 mg/l TDS-concentration iso-surface (Figure 2-2) intersects the top of model layer 5, model-layer 5 sub-segments differ in exact shape and/or length with respect to corresponding model-layer 3 and 4 sub-segments. Also for this reason, a corresponding layer-5 sub-segment to sub-segment EL3 of the eastern lateral boundary of model layer 3 does not exist.

Conditions along sub-segment WS5, which corresponds to the Gulf coastal region, are designated as no-flow, in contrast with those of WS3, which were designated as GHB to allow for the possibility of lateral flux beyond the seaward limits of the layer-3 active model domain. WS5 is closer to shore and based on the intersection of the 10,000 mg/l TDS-concentration iso-surface (Figure 2-2) with the top of model layer 5. Therefore, it is considered a reasonable approximation of the seaward boundary of fresh-water flow in model layer 5 along the Gulf Coast.

Conditions at sub-segments EU5, EC5, ES5, SE5, SC5, SW5, and WN5 are assumed to be the same as those of corresponding sub-segments of model layer 3. The source heads of GHB conditions assigned to sub-segment EC5 are identical to those of the corresponding GHB

conditions of sub-segment EC3. The source heads of GHB conditions assigned to sub-segment SC5 are identical to those of the corresponding GHB conditions of sub-segment SC3.

Conditions along sub-segment N5 are designated as GHB, in contrast with the no-flow designation of sub-segment N3. No-flow conditions are specified along the N3 sub-segment because the northern lateral boundary approximates the line of pinch-out of the Upper Floridan aquifer. The lines of pinch-out of the middle semi-confining unit and the Lower Floridan aquifer (or equivalent hydrogeologic units in this area) are farther north, however. Use of GHB conditions to represent conditions along the N5 sub-segment enables lateral fluxes across N5 to be simulated without extending the domain of model layer 5 to the line of pinch-out of the hydrogeologic unit(s) being represented by it. The source heads of GHB conditions specified along the N5 sub-segment are interpolated from the map of the May-June 2010 potentiometric surface of the Upper Floridan aquifer (Kinnaman and Dixon 2011).

Model Layer 6

The lateral boundary of model layer 6 is comprised of two sub-segments, one that is the result of the intersection of the 10,000 mg/l TDS-concentration iso-surface (Figure 2-2) with the top of model layer 6 (FWSW6; Figure 2-23) and another that approximates the line of pinch-out of the lower semi-confining unit (HGL6; Figure 2-23). Conditions along both sub-segments are designated as no-flow.

Model Layer 7

The lateral boundary of model layer 7 is comprised of two sub-segments, one that is the result of the intersection of the 10,000 mg/l TDS-concentration iso-surface (Figure 2-2) with the top of model layer 7 (FWSW7; Figure 2-24) and another that approximates the line of pinch-out of the lower semi-confining unit (HGL7; Figure 2-24). Conditions along both sub-segments are designated as no-flow.

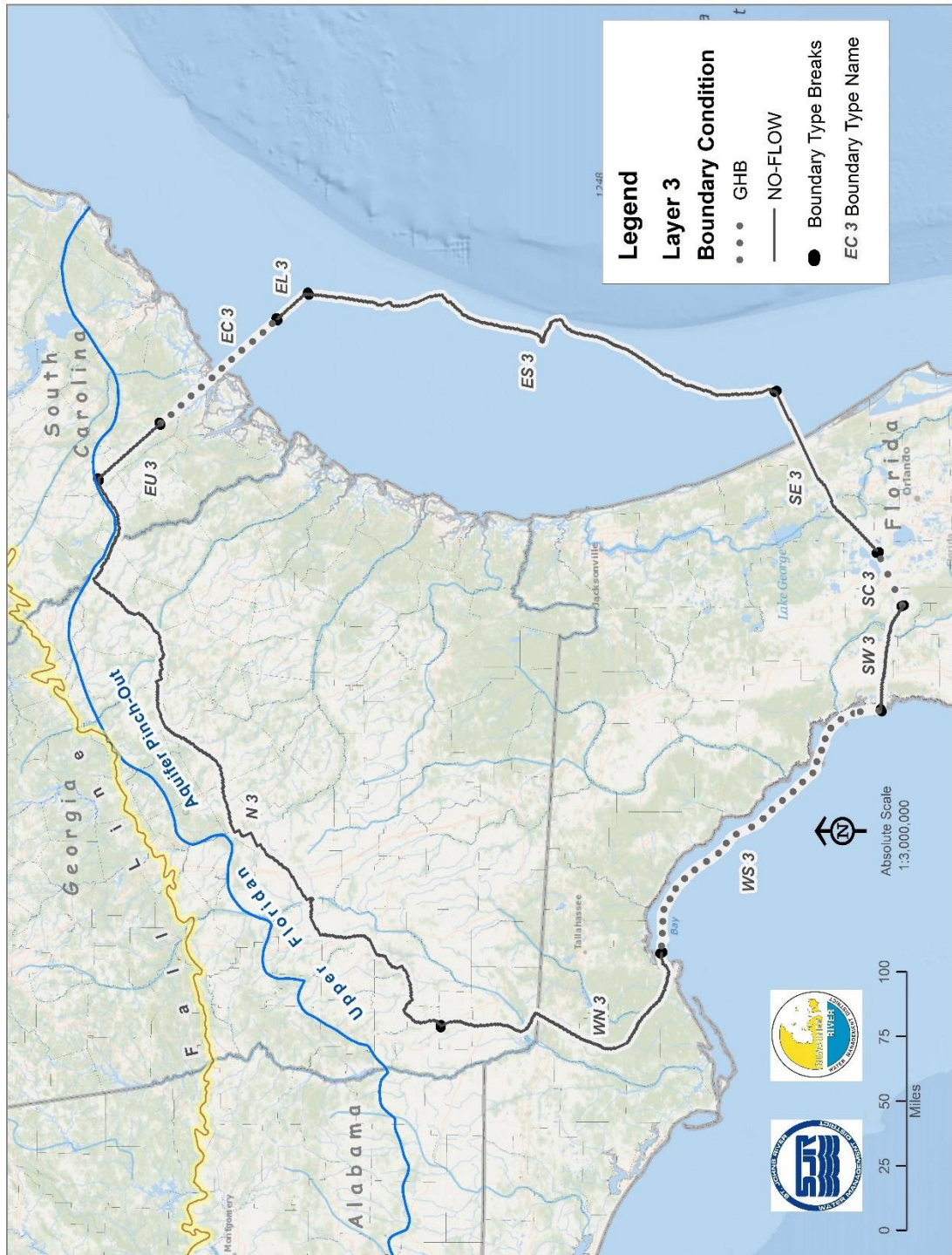


Figure 2-20. Model Lateral Boundaries, Layer 3

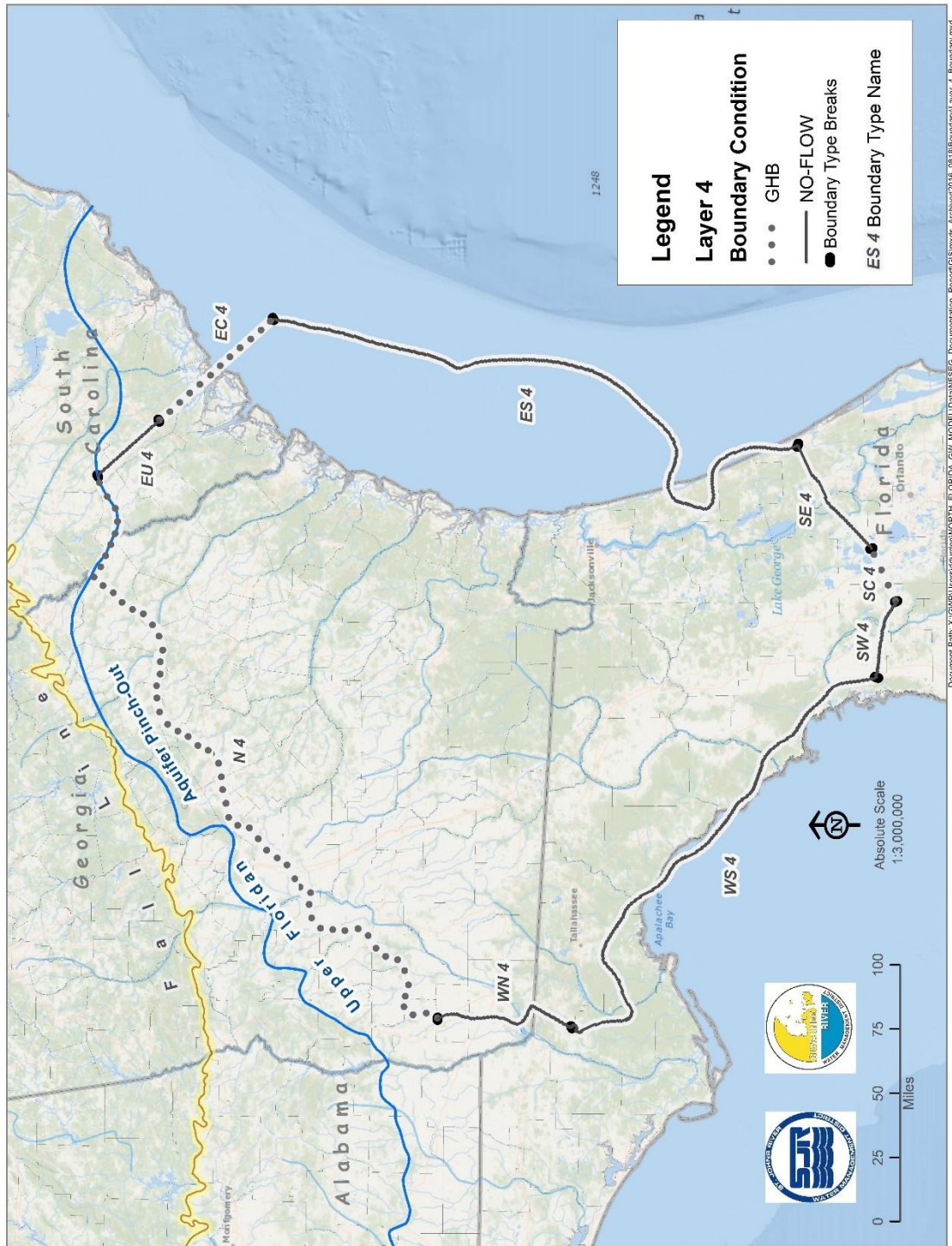


Figure 2-21. Model Lateral Boundaries, Layer 4



Figure 2-22. Model Lateral Boundaries, Layer 5

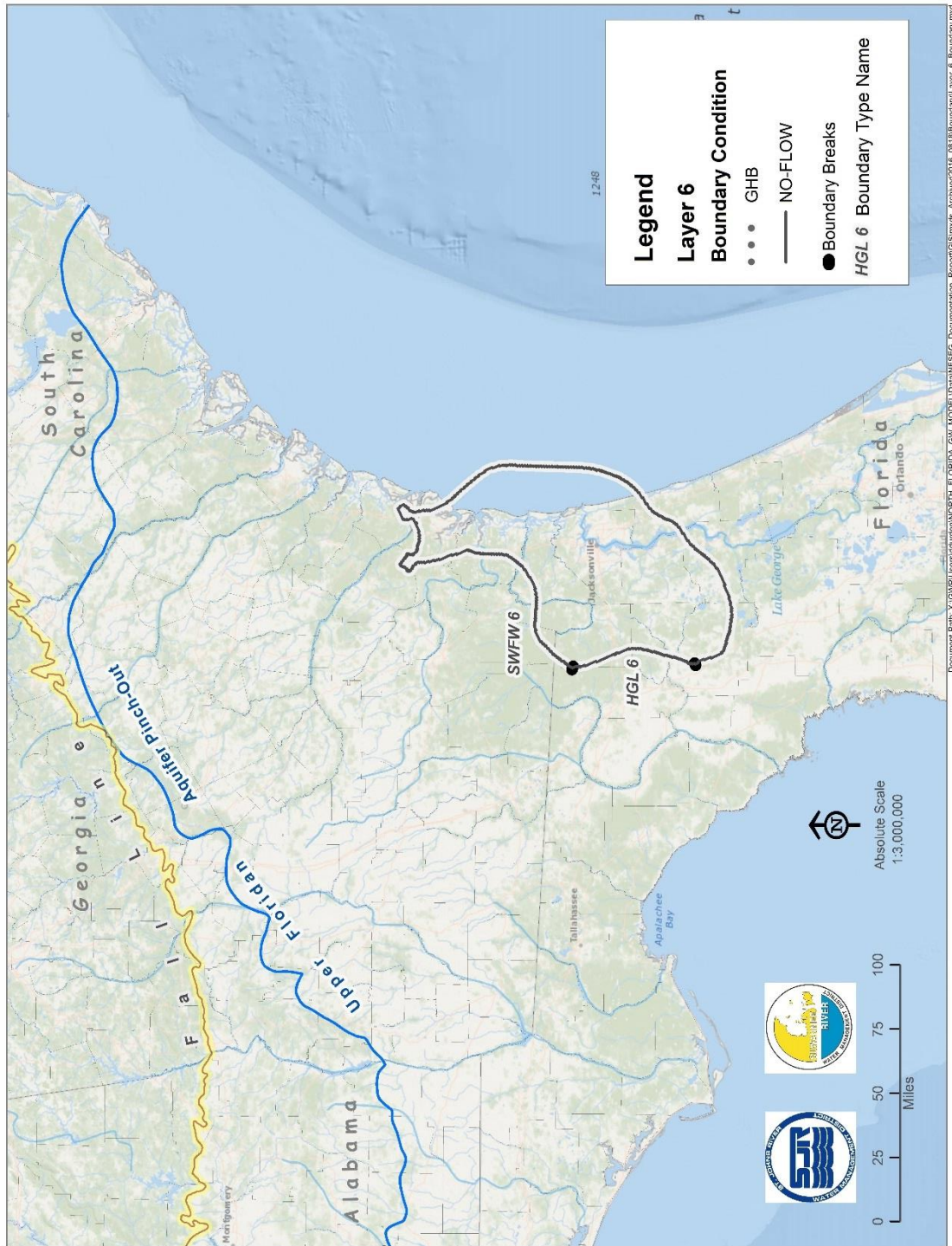


Figure 2-23. Model Lateral Boundaries, Layer 6

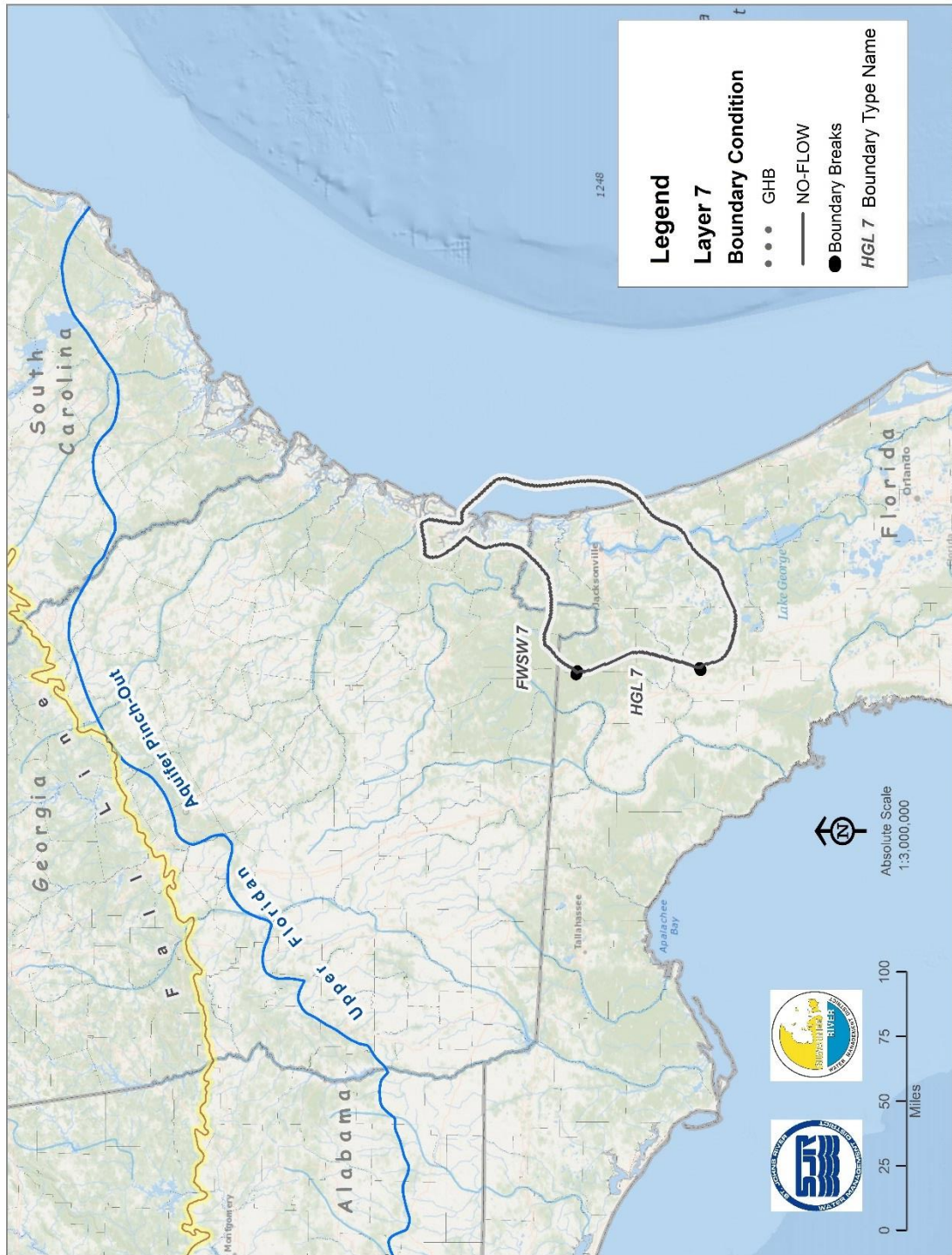


Figure 2-24. Model Lateral Boundaries, Layer 7

MODEL INTERNAL BOUNDARY CONDITIONS

Internal boundary conditions enable the representation of interaction with features, such as streams, springs, and the ocean, that are hydraulically connected to the groundwater flow system. In the NFSEG groundwater model, internal boundary conditions are utilized to represent the following flow phenomena: groundwater flux to and from perennial streams and lakes; groundwater discharge to ephemeral streams; discharge to springs; artesian discharge to land surface; discharge to single-zone wells; discharge to dual-zone wells; recharge to the groundwater system; discharge to the atmosphere via evapotranspiration, and discharge to oceans. These processes are represented through implementation of various MODFLOW packages, described as follows.

River-Package Implementation

Discharge between the groundwater flow system and perennial streams and lakes are represented in the NFSEG groundwater model by implementation of the MODFLOW river package. An estimate of stage, conductance, and bottom elevation is required for each river-package boundary condition.

River Stage and Bottom Elevation

The paths of streams were represented using flowlines of the National Hydrography Dataset Plus, Version 2 (NHDPlusV2; McKay et al. 2013; http://www.horizon-systems.com/NHDPlus/NHDPlusV2_documentation.php). This data set includes Strahler-order classifications for stream and river reaches. Stream reaches classified as Strahler-order 2 and above were included in the NFSEG implementation of the MODFLOW river package as perennial streams. Stream reaches classified as Strahler-order 1 were included in the NFSEG implementation of the MODFLOW drain package as ephemeral streams, to be discussed in the section on the drain-package implementation.

The estimation of stream stages involved first intersecting NHDPlusV2 flowlines with the NFSEG model grid in ArcGIS, thereby breaking the NHDPlusV2 flowlines into flowline sub-segments (Figure 2-25, Appendix B). NHDPlusV2 flowlines were broken at confluence points within grid cells as well. Within each grid cell, a bank elevation for each of the resulting sub-segments was computed by averaging the 3DEP DEM (<http://nationalmap.gov/3DEP/index.html>) elevation values over the length of each sub-segment.

The mean depth of the stream was calculated according to the following formula, obtained from Moore (2007):

$$Y_m = 0.28Q^{0.22}, \text{ where}$$

Y_m = mean channel depth (meter [m]), and

Q = mean channel discharge (m^3/second [s]).

The value of Q was approximated as the flow parameter Q0001E (m^3/s) of the NHDPlusV2 dataset (McKay et al. 2013).

The “incised” depth of the stream, i.e., the distance from bank to stream bottom, was assumed to be 1.25 times the mean depth, as suggested by Moore (2007). The incised depth was then subtracted from the 3DEP 10m DEM-derived elevation to yield an estimate of the stream bottom elevation. The depth was then added to the bottom elevation to obtain an estimate of the stream stage. Stages so derived were implemented throughout the model domain initially except in the cases of portions of the St. Johns River and Suwannee River for which stages derived from existing surface-water models were obtained. Later, many of the 3DEP 10m DEM-derived stages and corresponding bottom elevations were altered to address a tendency in the derived elevations to increase in the downstream direction along portions of some NHDPlusV2 flowlines, rather than decline consistently. These alterations were effected through use of an interpolation process carried out in ArcGIS. The interpolation process resulted in smooth, steady declines in stage from the uppermost flowline sub-segments to as far downstream as necessary.

Later still, additional adjustments were made to many river-package boundary stages and corresponding bottom elevations based on stage observations obtained at U.S. Geological Survey stream gaging stations. For a given sub-basin, the adjustments were applied in the form of a single sub-basin-wide adjustment to all NHDPlusV2 sub-segments. Separate adjustments were applied for the years 2001 and 2009.

Stages and river bottom elevations in portions of the Suwannee River and its tributaries and portions of the St. Johns River and its tributaries were, as stated previously, not extracted from the 3DEP 10m DEM. In the case of the Suwannee River, stages and corresponding bottom elevations were obtained from SRWMD HEC-RAS surface-water models. These stages were not subjected to the modification processes that were applied to the 3DEP 10m DEM-derived stages (Figure 2-26).

In the case of the St. Johns River, stages and bottom elevations were obtained from a hydrodynamic model of the St. Johns River created by the SJRWMD (Suscy et al. 2012). These stages were not subjected to the modification processes that were applied to the 3DEP 10m DEM-derived stages Figure 2-26).

Lake Stage and Bottom Elevation

Representations of lake areas were obtained from the National Land Cover Database (NLCD; <http://www.mrlc.gov>). The lake areas were converted to lake polygons in ArcGIS and then intersected with the NFSEG model grid, resulting in the formation of lake sub-polygons (Figure 2-26). A 10m DEM elevation was extracted at the centroid location of each sub-polygon for use as an approximate lake stage, unless actual stage data were available. Sources of actual lake-stage data included the SJRWMD, the Northwest Florida Water Management District, and the U.S. Geological Survey. Lake bottom elevations were based on an assumed average depth, usually 8 feet.

Where lake sub-polygons coincided with river-boundary sub-segments, river-boundary sub-segments were removed. Likewise, river-boundary sub-segments were also removed wherever constant-head boundary conditions were assigned to represent the ocean.

Initial Conductance Estimates

Initial river-package conductance values were estimated based on assumed horizontal and vertical hydraulic conductivities, corresponding hydraulic areas, and assumed lengths of flow. The bottom areas of stream sub-segments were determined as the products of sub-segment lengths and mean widths, with the length determined by ArcGIS and the mean width determined according to the following formula, obtained from Moore (2007), as follows

$$W = 11.95Q^{0.47}, \text{ where}$$

W = mean width (m), and

Q = mean channel discharge (m³/s).

As in the case of the mean depth, discussed previously, the value of Q was approximated as the flow parameter Q0001E (m³/s) of the NHDPlusV2 dataset (McKay et al. 2013).

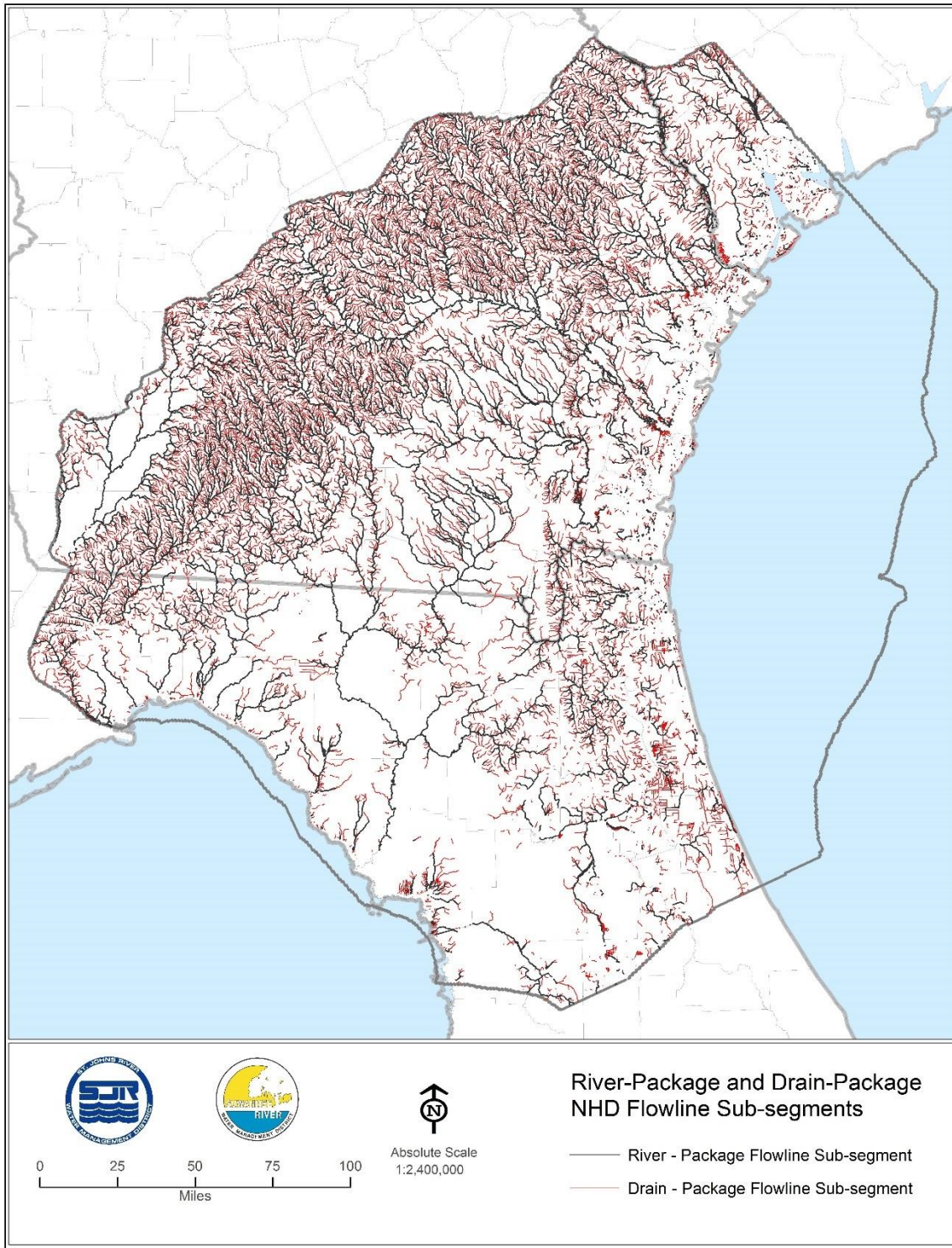


Figure 2-25. NHDPlusV2 Flow-Line Sub-Segments Used in River- and Drain-Package Implementations

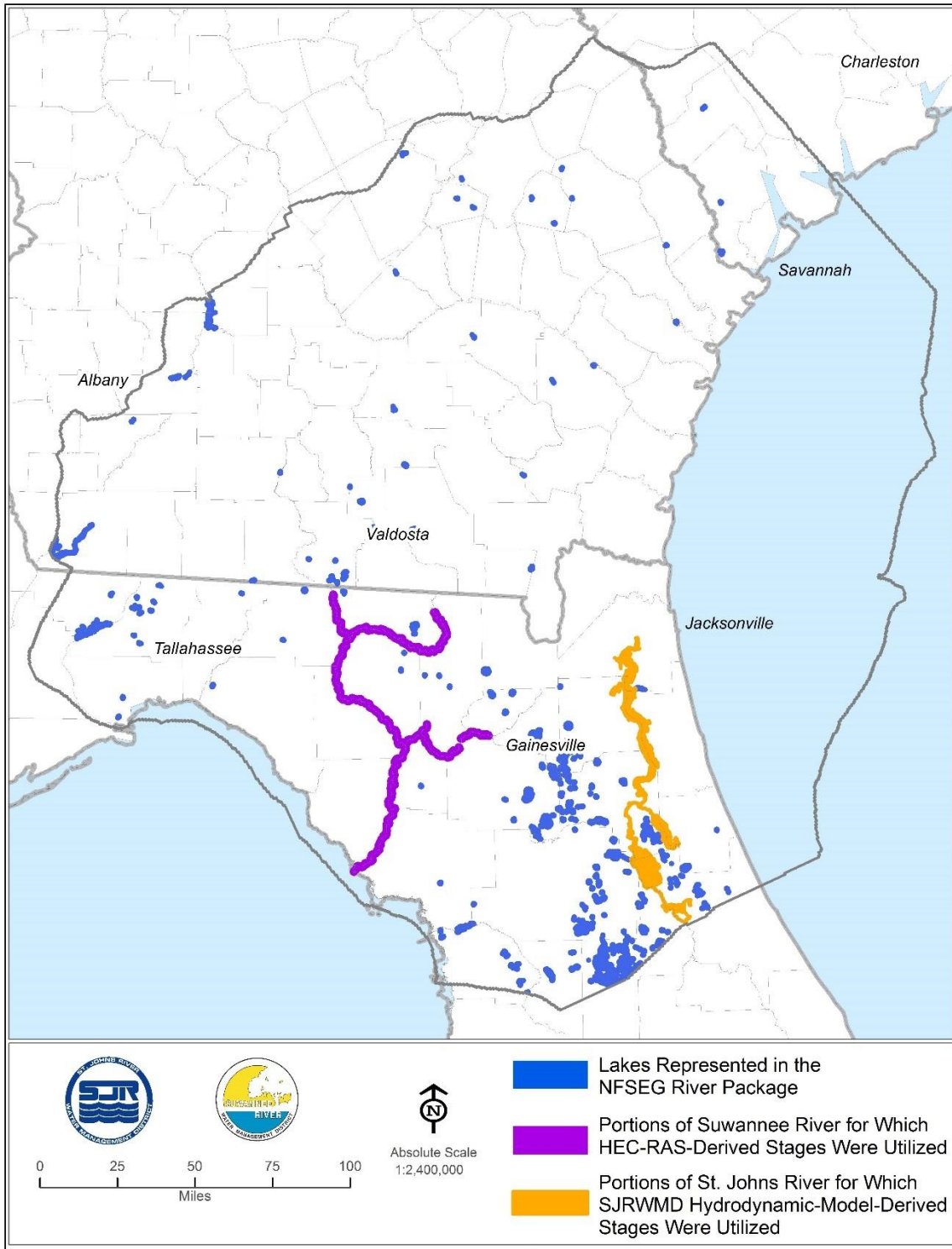


Figure 2-26. Portions of NHD Flowlines for Which River Stages Were Obtained from Existing Surface-Water Models and Lake Sub-Polygons Represented in the NFSEG River Package

GENERAL-HEAD-BOUNDARY-PACKAGE IMPLEMENTATION

In addition to representing lateral fluxes, GHB conditions were also used to enable the determination of spring discharge rates by the NFSEG model. In this application, the value of the GHB-condition source head represents the elevation of the surface of the receiving body of water into which a given spring discharges (i.e., the “spring-pool elevation”). Use of the GHB package as opposed to the drain package to represent springs enables the simulation of reverse spring flow. This phenomenon, which is typically the result of seasonally high surface water, occurs wherever a spring-pool elevation exceeds the aquifer head at the spring.

Most springs within the NFSEG model domain emanate from the Upper Floridan aquifer. A smaller number emanate from the intermediate aquifer system. Accordingly, most GHB conditions used to represent springs are assigned to model layer 3, used principally in the NFSEG model to represent the Upper Floridan aquifer (Table 1 and Appendix C). Some are assigned to aquifer layer 2 instead, which represents the intermediate aquifer system at the locations of such springs.

Drain-Package Implementation

Gulf-of-Mexico Coastal Swamps

The drain package is used in the NFSEG groundwater model to represent discharge from the Floridan aquifer to land surface in low-lying areas of the Gulf-of-Mexico coastal region. In this application, portions of wetlands in areas of the model domain that are unconfined and in which the elevation of the potentiometric surface of the Upper Floridan aquifer exceeds land-surface elevation were assumed to be areas of artesian discharge from the Upper Floridan aquifer to land surface. These drain boundaries were assigned to model-layer 1, as model-layers 1 and 2, in addition to model layer 3, represent the Upper Floridan aquifer in unconfined areas (Figure 2-27). The map of the May-June 2010 potentiometric surface of the Upper Floridan aquifer of Kinnaman and Dixon (2011) was used in this analysis.

Ephemeral Stream Reaches

The drain package was used also to represent ephemeral portions of streams. In the NFSEG implementation, the portion of a stream represented by a given drain boundary condition flows only when the elevation of the simulated water table of the grid cell to which it is assigned exceeds the elevation of the drain boundary. Ephemeral portions of streams were identified in this process as the portions of the NHDPlusV2 flowlines with a Strahler order designation of 1. The portions of streams with Strahler order in excess of 1 are represented using the NFSEG river-package implementation (Figure 2-25).

Recharge-Package Implementation

The MODFLOW recharge package processes arrays of specified recharge rates. In the NFSEG groundwater model, separate arrays are specified for representation of recharge rates in years 2001 and 2009 (Figures 2-28 and Figure 2-29).

The recharge arrays used in the NFSEG groundwater model are weighted averages of the sums of the “AGWI” (i.e., active groundwater inflow) and “IGWI” (i.e., inactive groundwater inflow) parameters obtained from all or portions of 46 different HSPF (Hydrological Simulation Program—FORTRAN; Bicknell et al., 1997) models. HSPF is a model code used primarily to represent surface-water hydrological processes, including the processes of interaction between the surface-water and the unsaturated and saturated groundwater hydrological systems. Separate 2001 and 2009 recharge arrays were derived from the HSPF output for use in the 2001 and 2009 versions of the NFSEG groundwater model, respectively.

The HSPF models of the present project were developed as part of the overall NFSEG groundwater-model development process for the specific purposes of estimating recharge rates, maximum saturated evapotranspiration rates, and base-flow rates within the NFSEG model domain. Each HSPF model corresponds to a separate U.S. Geological Survey HUC-8 basin area. The HSPF models can be used to simulate both naturally occurring and human-induced recharge. Examples of human-induced recharge simulated by the HSPF models include that due to spray fields, septic tanks, and agricultural and domestic lawn irrigation. Runoff to closed basins in the form of influx to features such as sinkholes and drainage wells and influx to rapid infiltration basins are represented using the well package rather than the recharge package.

During model simulations, a specified recharge rate is applied to the uppermost active grid cell of each vertical column of grid cells. In the usual situation, all NFSEG model layers are active. However, in some cases, the grid cells of layer 1 or layers 1 and 2 are simulated as being dry. Such grid cells are treated as inactive by the model in the application of recharge rates. Dry cells occur in areas of the model domain in which the water table is simulated as lying beneath the bottom of layer 1 or bottoms of layers 1 and 2. Areas in which layer 1 or layers 1 and 2 are dry correspond generally to those in which the surficial aquifer system and/or intermediate confining unit are thin to nonexistent. In cases in which layer 1 is active, recharge is applied to layer 1. For cases in which layer 1 is dry but layer 2 is not, recharge is applied to layer 2. For cases in which layers 1 and 2 are both dry, recharge is applied to layer 3.

Evapotranspiration-Package Implementation

The evapotranspiration (ET) package determines ET from the saturated groundwater flow system. To do this, arrays of the maximum rate of saturated evapotranspiration (MSET), the ET surface elevation (i.e., the water-table elevation at which the maximum rate of ET is realized—specified as land-surface elevation in the NFSEG model), and ET extinction depth (i.e., the depth at which the ET rate declines to zero) are specified.

In the NFSEG groundwater model, separate MSET-rate arrays were specified for the years 2001 and 2009 (Figure 2-30 and Figure 2-31). These arrays were estimated as the difference between estimated potential ET (PET) and sum of unsaturated ET components simulated in HSPF (i.e., “interception evaporation—CEPE,” “upper zone evaporation—UZET,” and “lower zone evaporation—LZET”). The PET rates used in this calculation were obtained from the NLDAS (<http://ldas.gsfc.nasa.gov/>) and U.S. Geological Survey ET databases (<http://fl.water.usgs.gov/et/>). The estimated ET extinction depths (Figure 2-32) were based on an adaptation of an approach utilized in Shah et al. (2007). This adaptation was developed by Freese (written communication; Appendix D) and implemented by Stokes and Finer (digital communication).

Well-Package and MNW2-Package Implementations

Well-Package versus. MNW2-Package Implementation

The well package was used to represent single-aquifer withdrawal wells. Single-aquifer withdrawals are withdrawals from wells that are open to only one aquifer (or model layer). The MNW2 package was used to represent so-called “multi-aquifer” withdrawal wells. Multi-aquifer wells are wells with open intervals that intersect the Upper Floridan aquifer, the middle semiconfining unit, and upper zone of the Lower Floridan aquifer and thus pull significant quantities of water from both the Upper and Lower Floridan aquifers.

The MNW2 package calculates the contributions to the total well withdrawal of the various aquifers intersected by the open interval of a multi-aquifer well. In the NFSEG-model implementation of MNW2, the distribution of the total discharge from a represented multi-aquifer well is based on the respective aquifer water levels and assigned horizontal hydraulic conductivities of the Upper Floridan aquifer, the middle semiconfining unit, and upper zone of the Lower Floridan aquifer at the location of the well.

The majority of wells represented in the NFSEG groundwater model are single-aquifer wells and are thus represented in the well package. Multi-aquifer wells, however, tend to be larger and deeper and therefore extract a disproportionate share total groundwater withdrawals (Figure 2-33).

Summary of Groundwater Withdrawals

Groundwater withdrawals in the NFSEG groundwater model represent all major types of water use within the model domain, including: (1) public-supply/commercial/industrial/institutional; (2) agricultural irrigation; (3) recreational irrigation [e.g., golf-course irrigation]; (4) and domestic self-supply. Most large withdrawals take place from the Upper Floridan aquifer, but significant amounts of water are also withdrawn from the upper zone of the Lower Floridan aquifer via multi-aquifer wells and, to a limited extent, the surficial aquifer system (Figure 2-34 to Figure 2-41).

Summary of Point Influxes

Significant influxes to the groundwater flow system, both human-induced and naturally occurring, are represented through use of the well package. Types of human-induced influxes include those due to RIBs, drainage wells, and injection wells. Naturally occurring influxes are those due to sinks. RIBs are used for wastewater disposal, and drainage wells are used for stormwater disposal (Figure 2-42). RIBs discharge to the land surface, so influx due to them is assigned to model layer 1. Influx due to drainage wells is assumed to be to the Upper Floridan aquifer, so influx due to them is assigned to model layer 3 (Figure 2-42). Influx due to injection wells is typically assigned to model layer 5, as these types of wells are generally open to the Lower Floridan aquifer or lower depths of the Upper Floridan aquifer within the model domain (Figure 2-42). Influx due to sinks is assumed to be to the Upper Floridan aquifer, i.e., model layer 3 (Figure 2-42). Rates of influx due to drainage wells and sinks were approximated as runoff to closed basins in HSPF.

Time-Variant Specified Head Package Implementation

The time-variant specified head package was used to implement the assignment of constant-head boundaries. Specified-head boundaries were used in the model primarily to represent water levels of the Atlantic Ocean and the Gulf of Mexico. These levels were represented as equivalent fresh-water heads. A separate set of specified heads were represented for the years 2001 and 2009, though the assigned values were constant (Figure 2-43).

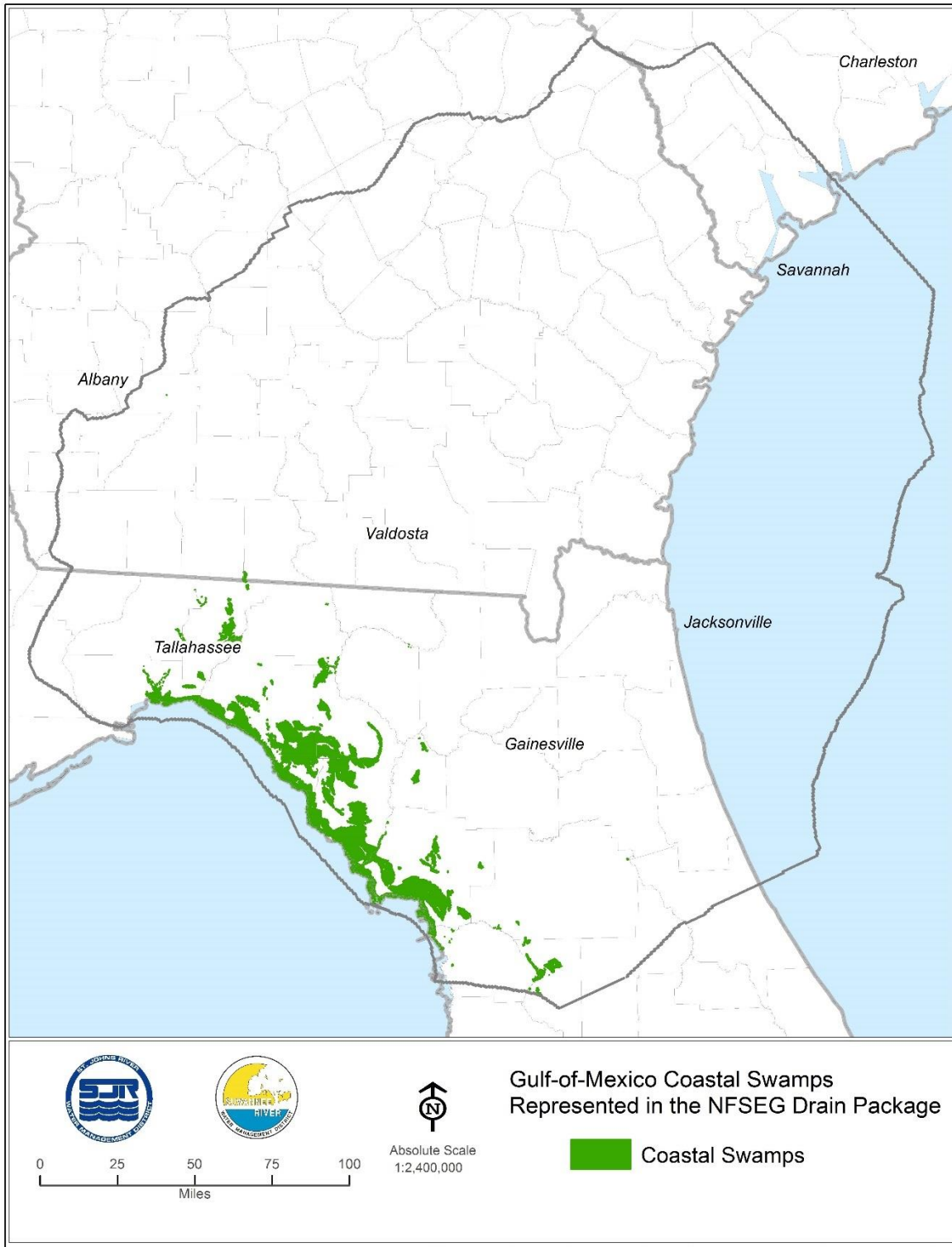


Figure 2-27. Gulf-of-Mexico Coastal Swamps Represented in the Drain Package

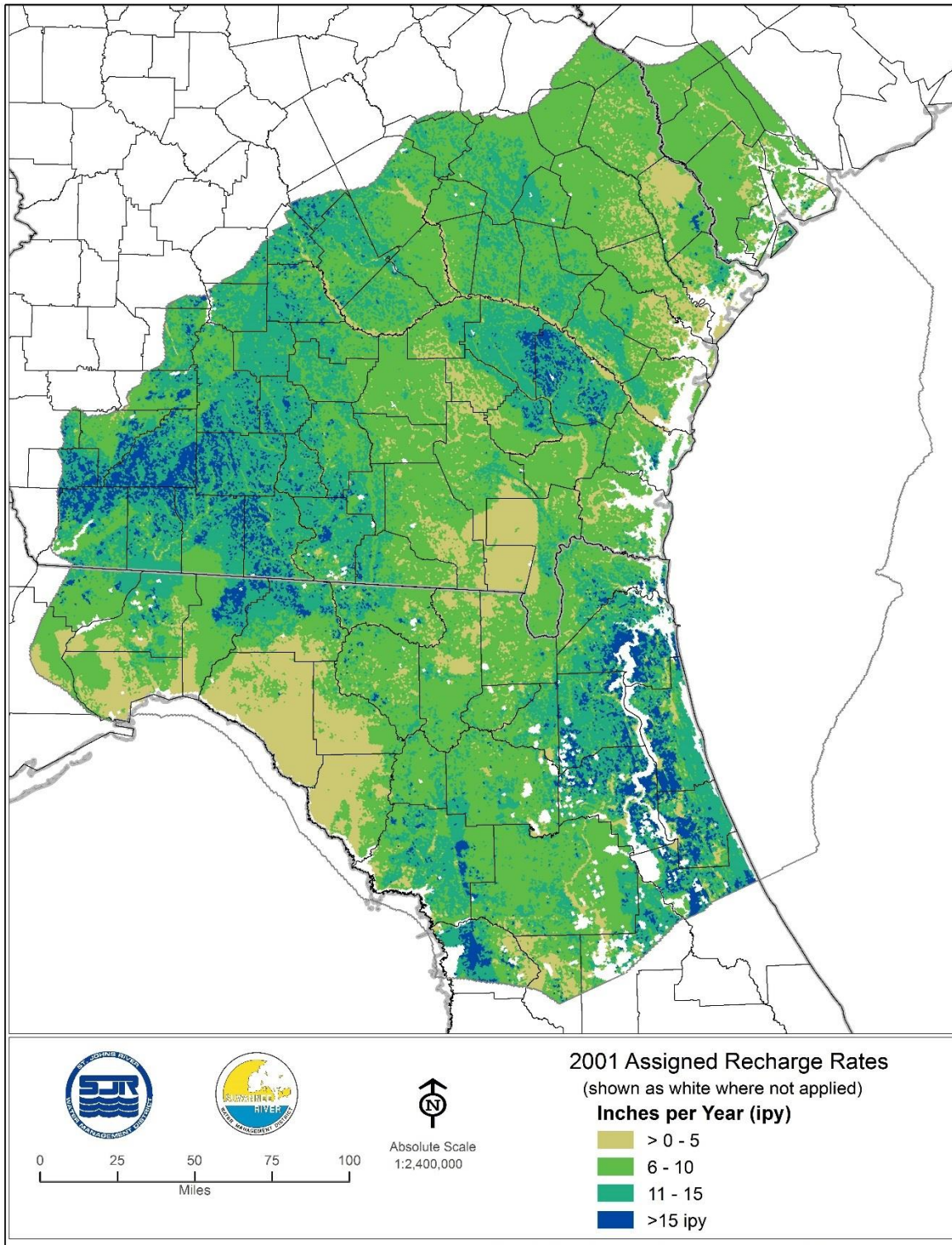


Figure 2-28. Assigned Recharge Rates, 2001

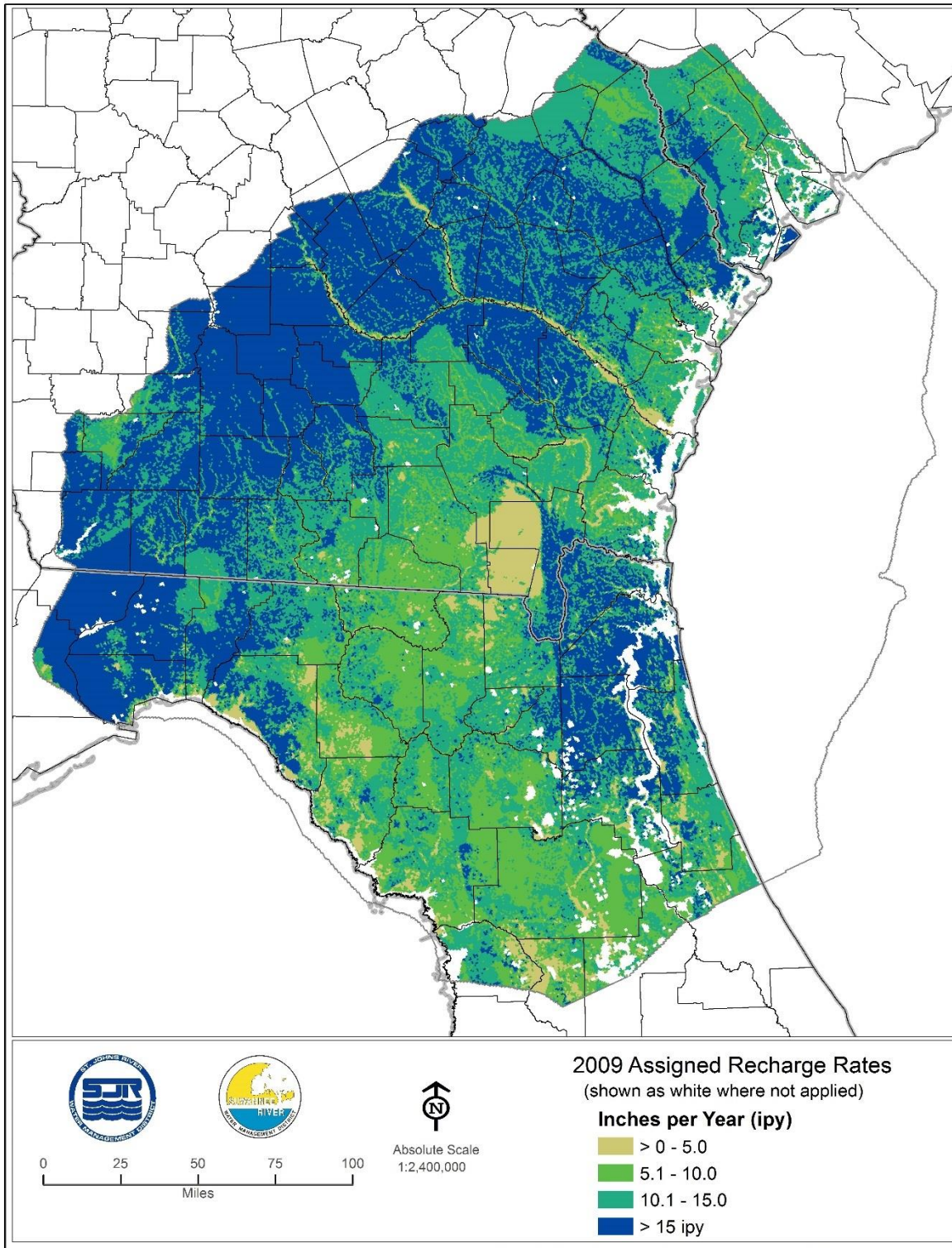


Figure 2-29. Assigned Recharge Rates, 2009

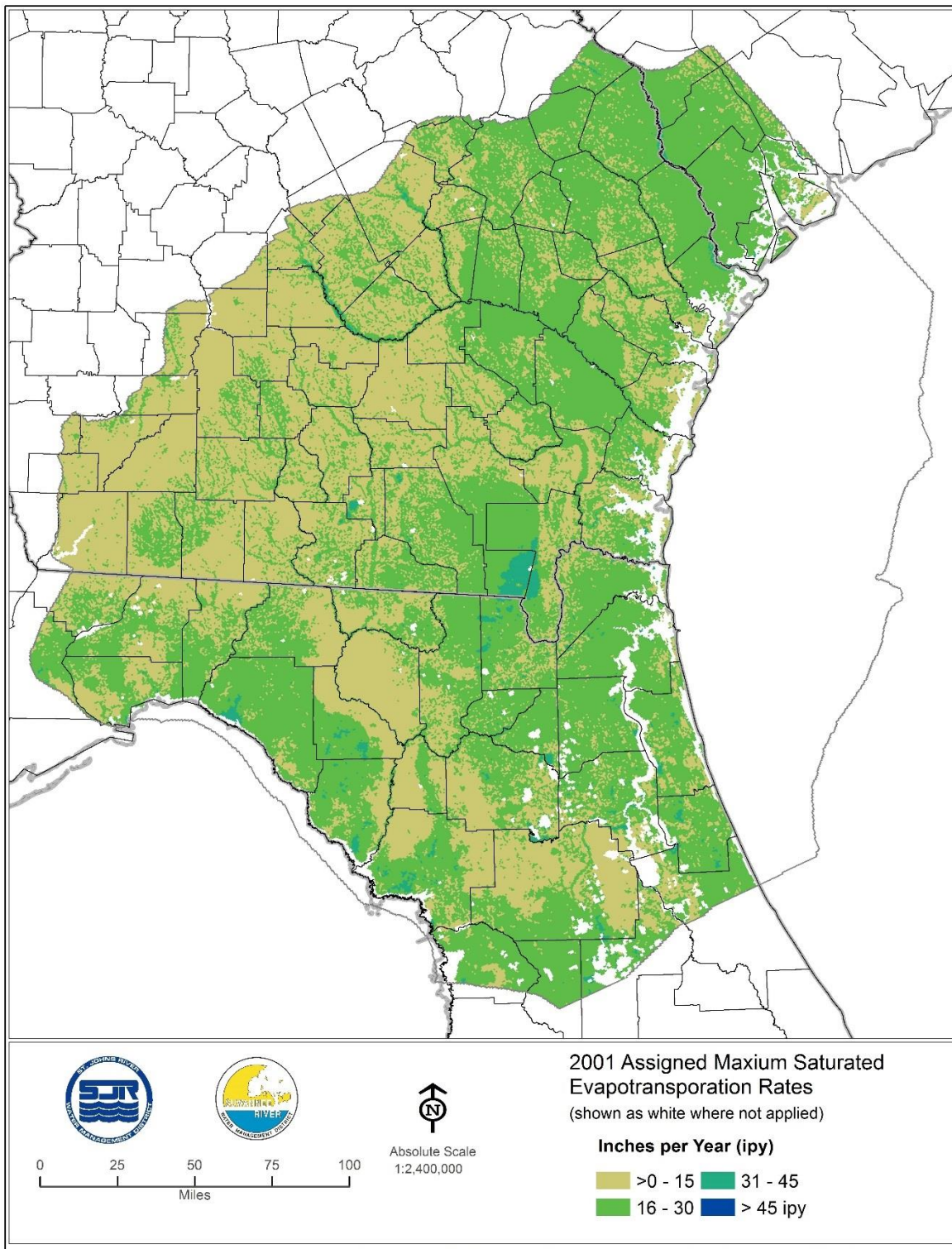


Figure 2-30. Assigned Maximum Saturated ET Rates, 2001

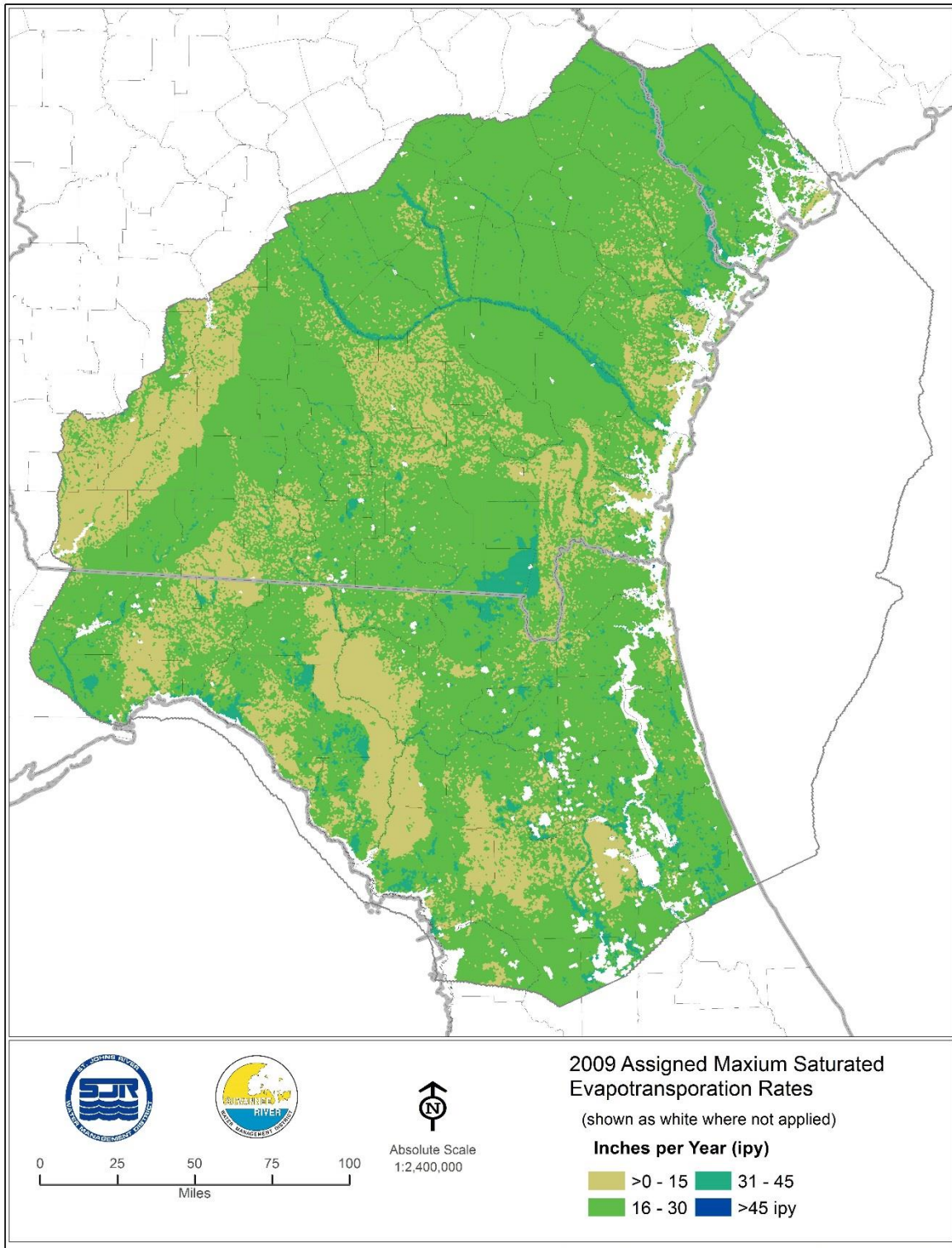


Figure 2-31. Assigned Maximum Saturated ET Rates, 2009

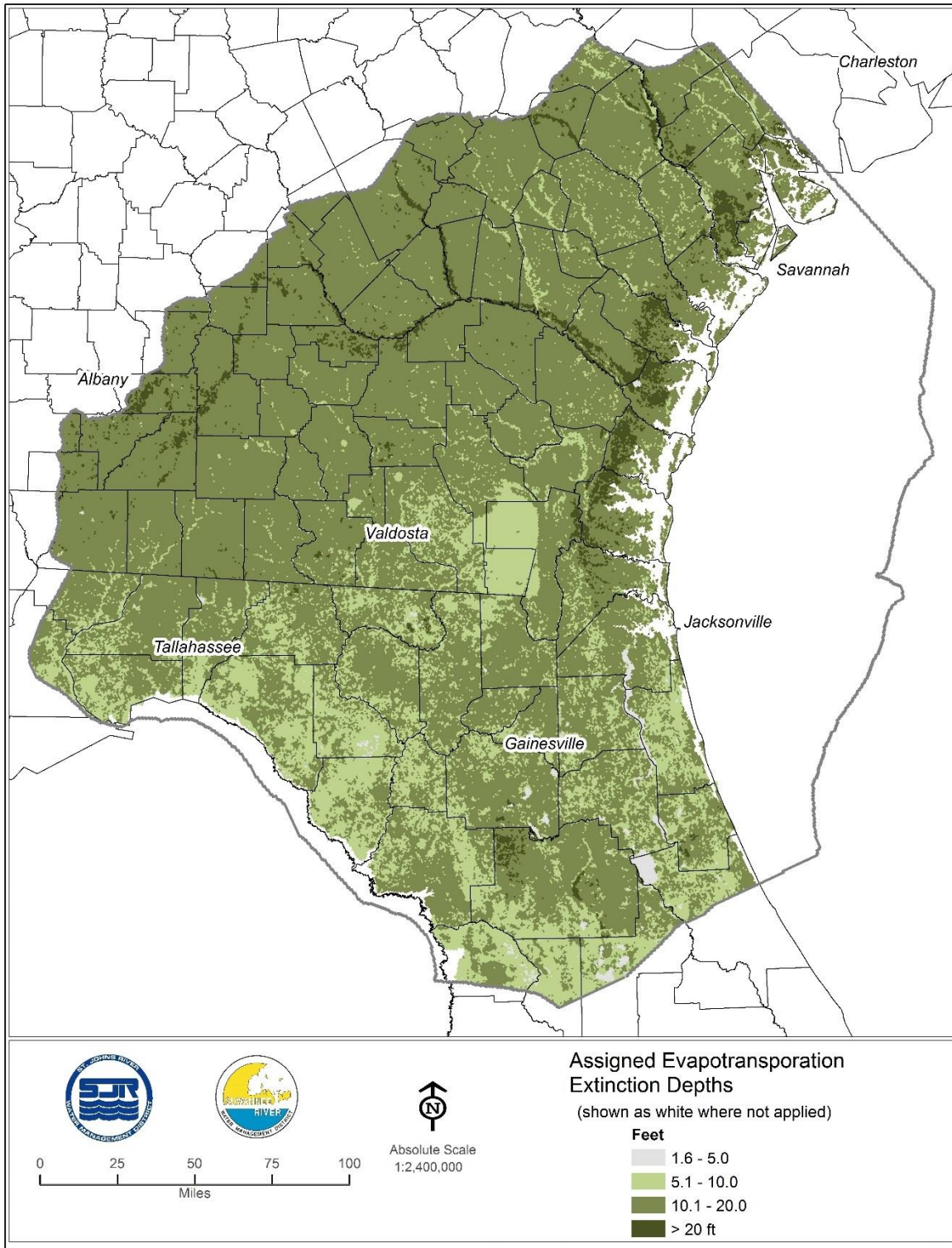


Figure 2-32. Assigned ET Extinction Depths

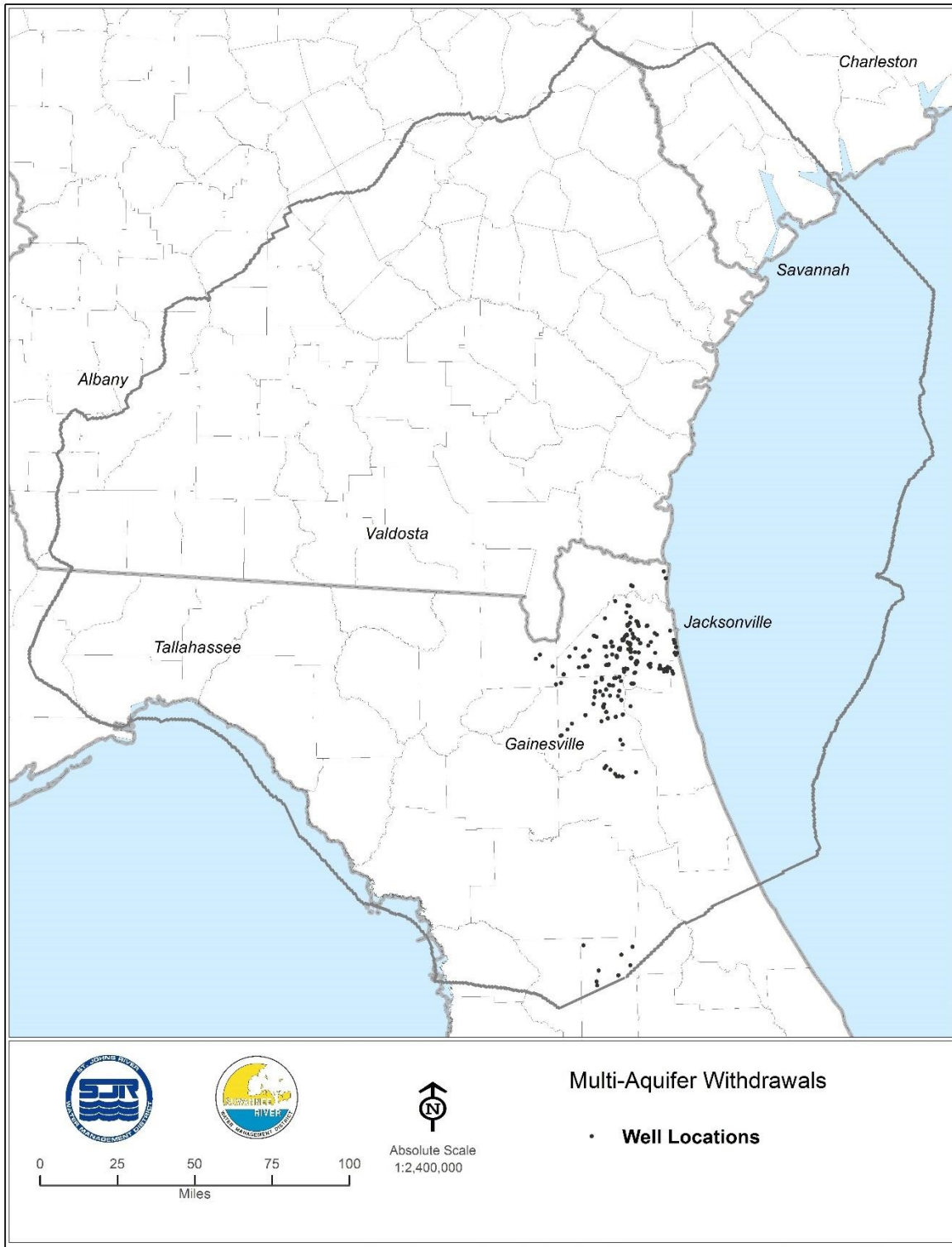


Figure 2-33. Distribution of Multi-Aquifer Wells

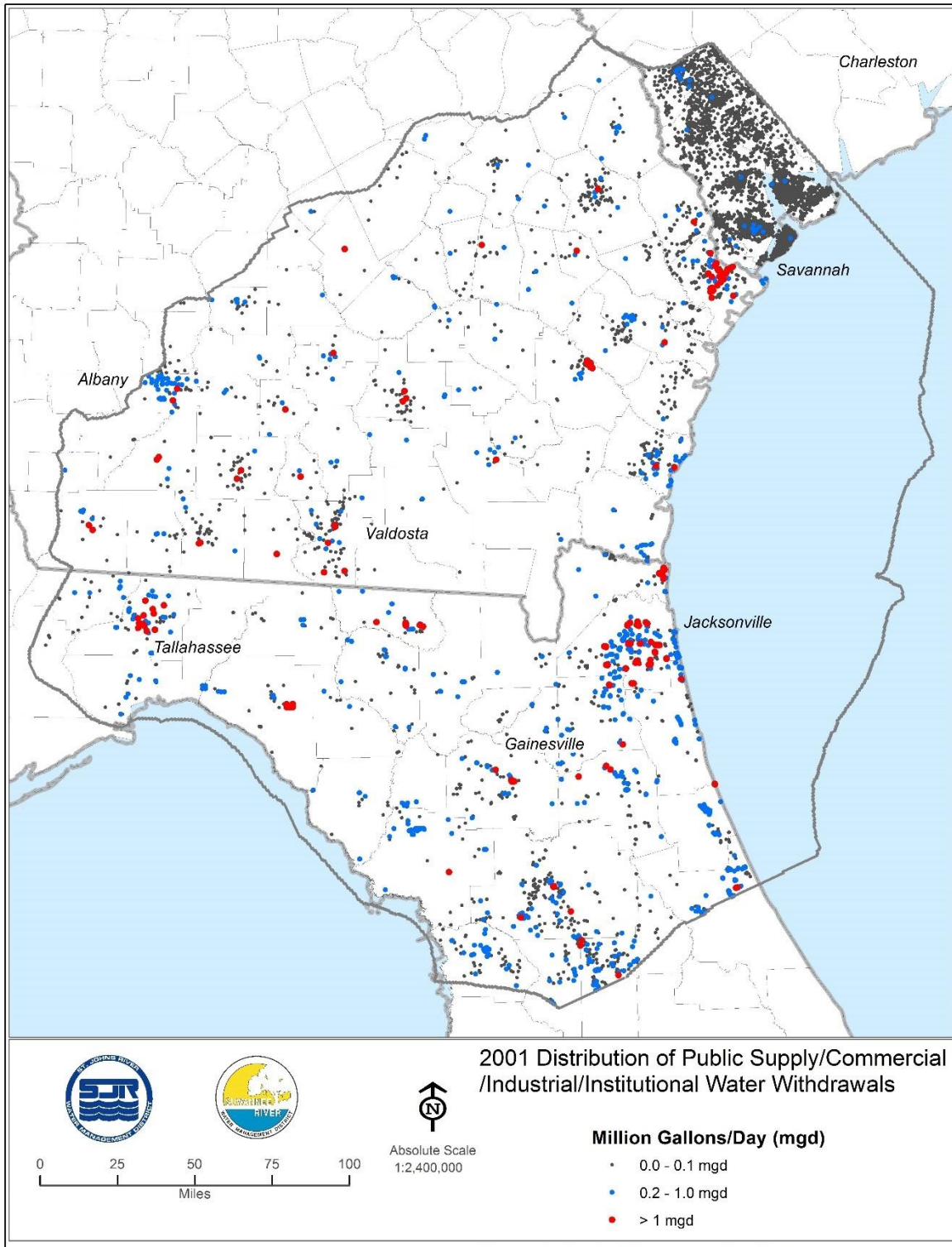


Figure 2-34. Distribution of Public-Supply, Commercial-Industrial, and Institutional Withdrawals, 2001

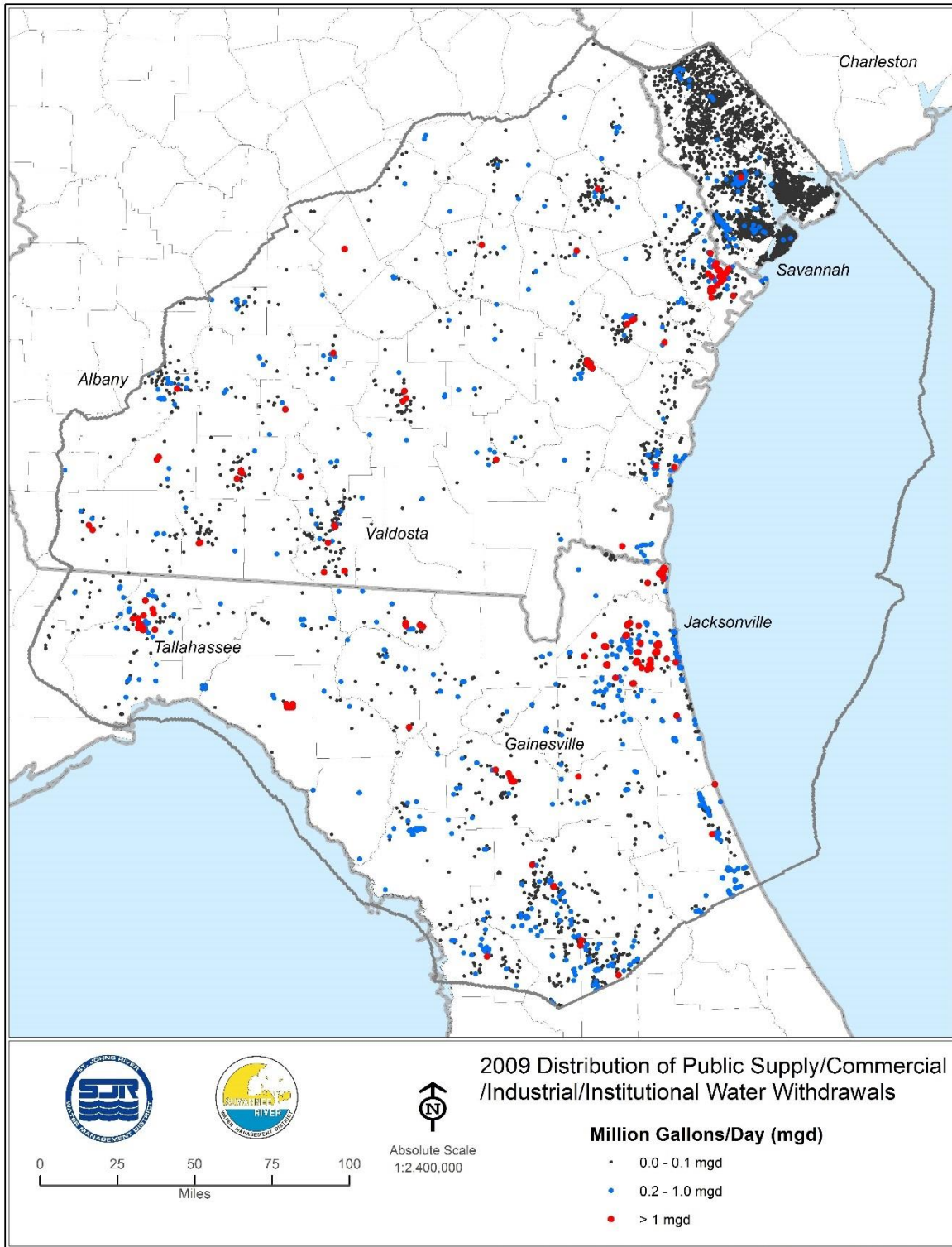


Figure 2-35. Distribution of Public-Supply, Commercial-Industrial, and Institutional Withdrawals, 2009

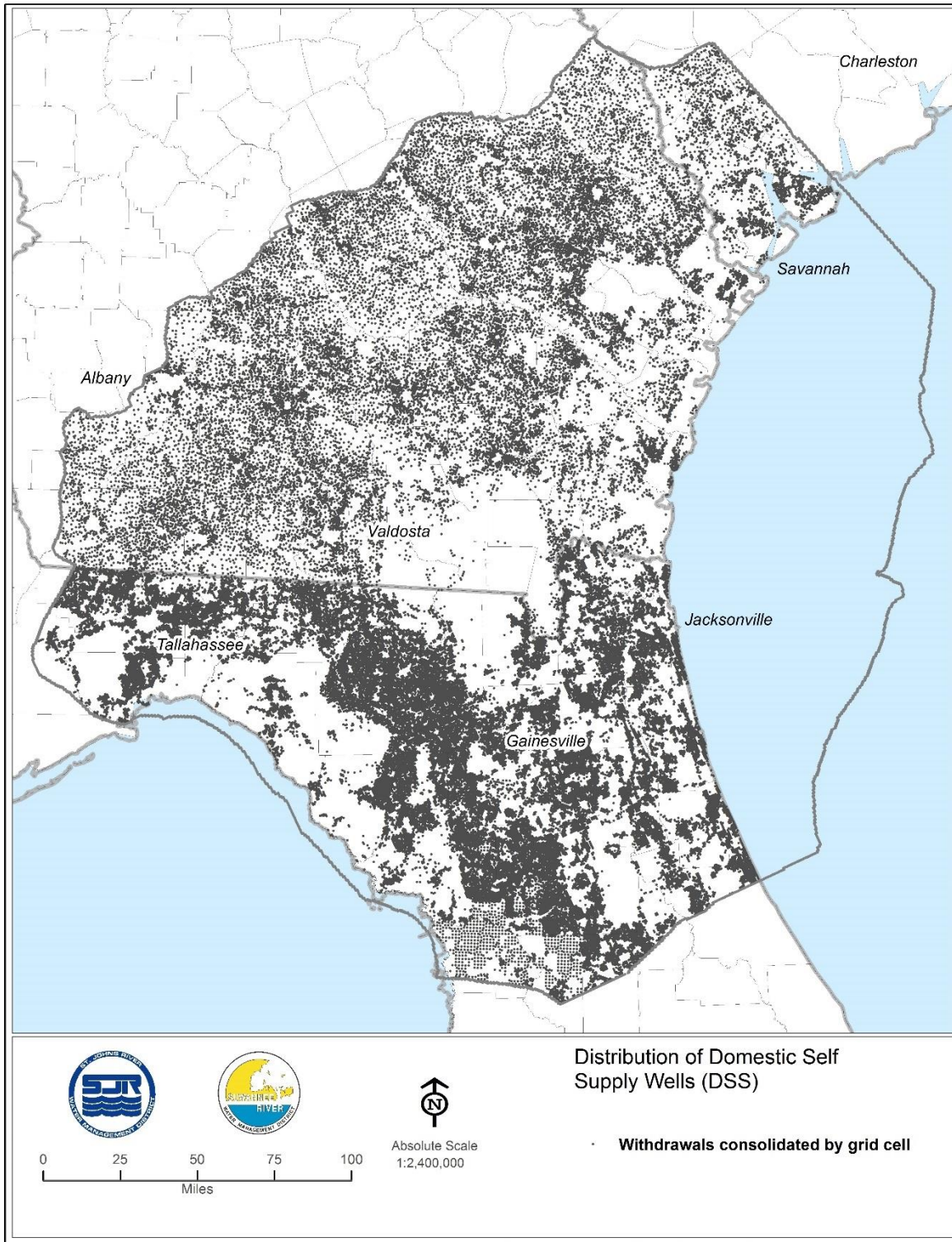


Figure 2-36. Distribution of DSS Withdrawals

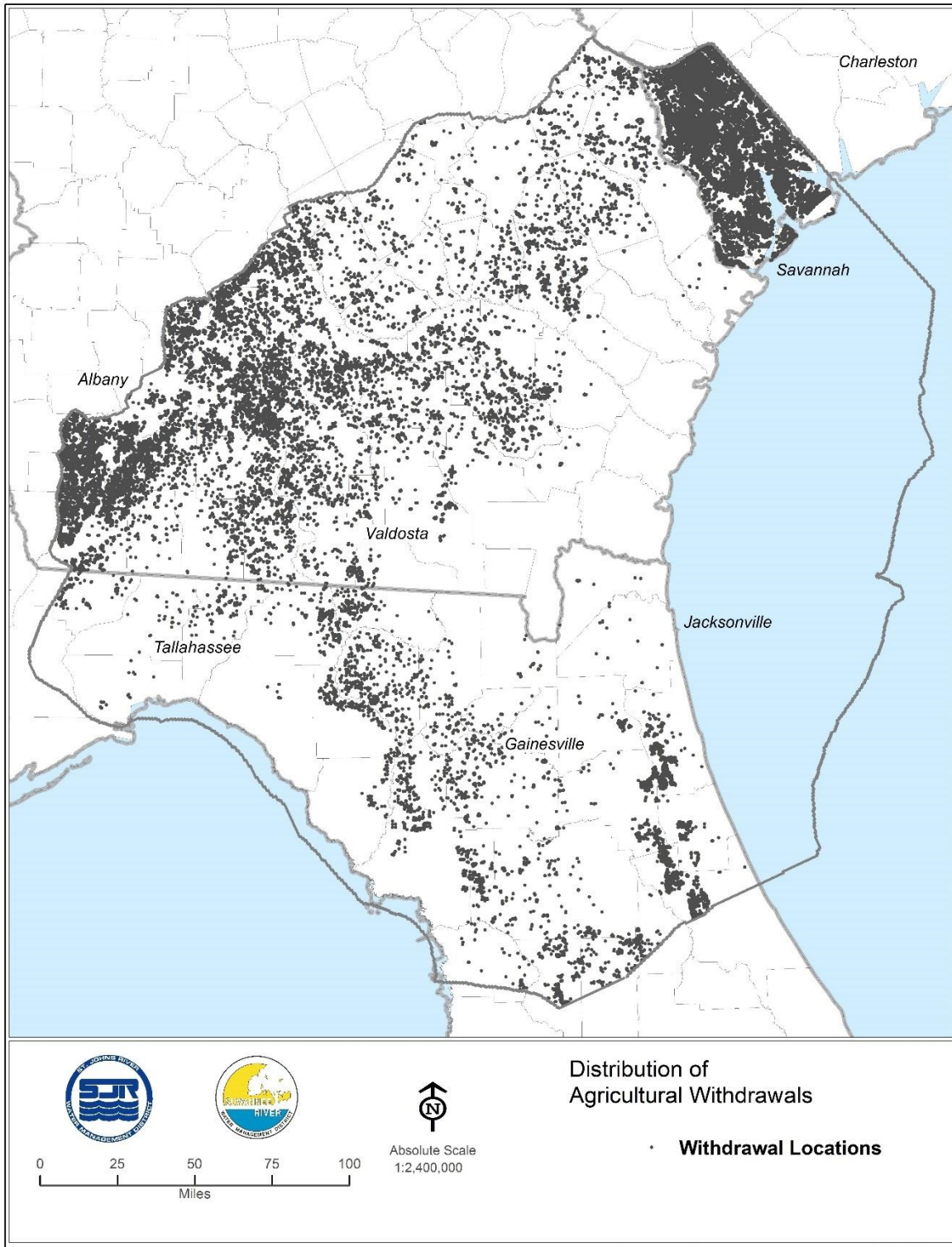


Figure 2-37. Distribution of Agricultural Withdrawals

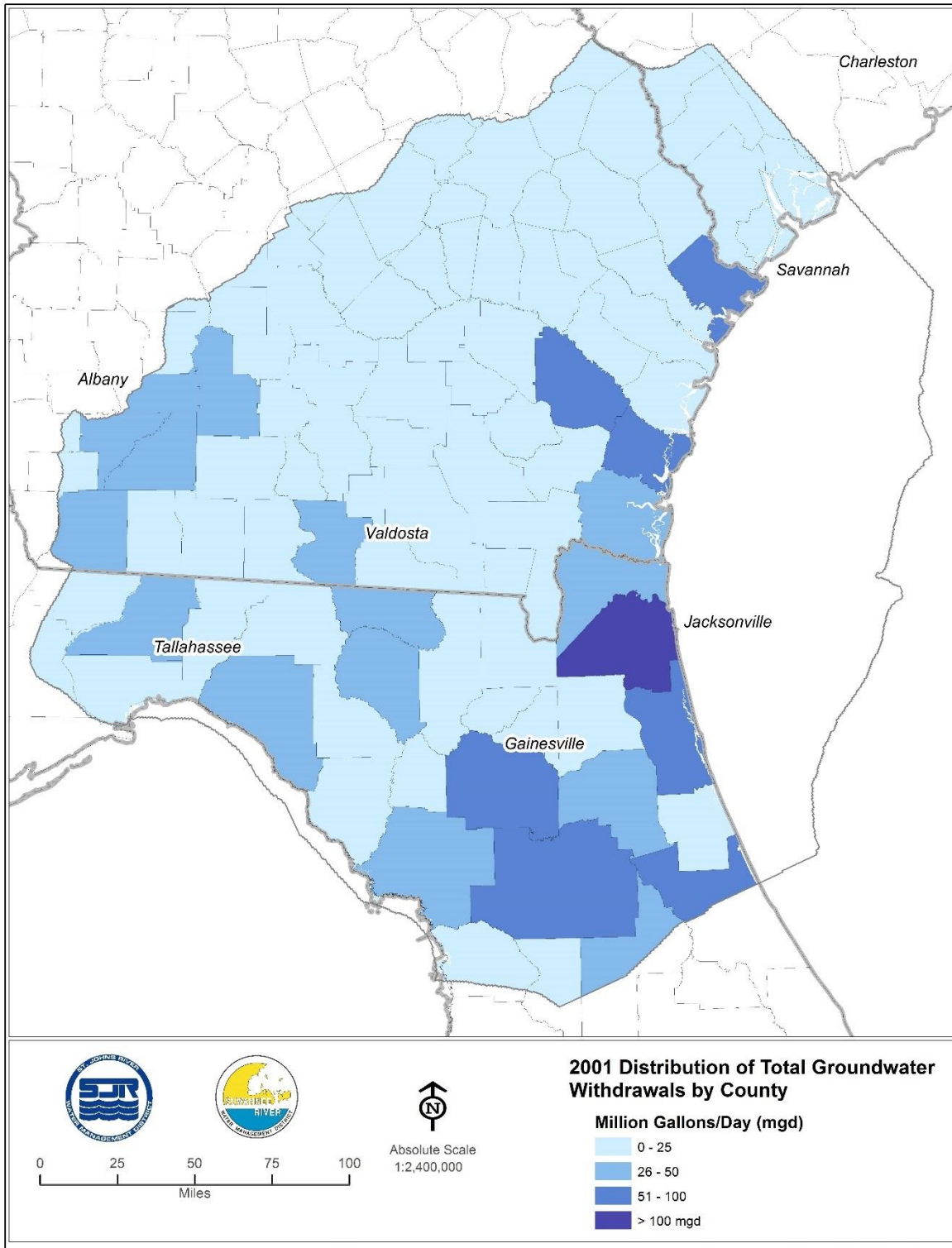


Figure 2-38. Distribution of Total Groundwater Withdrawals by County, 2001

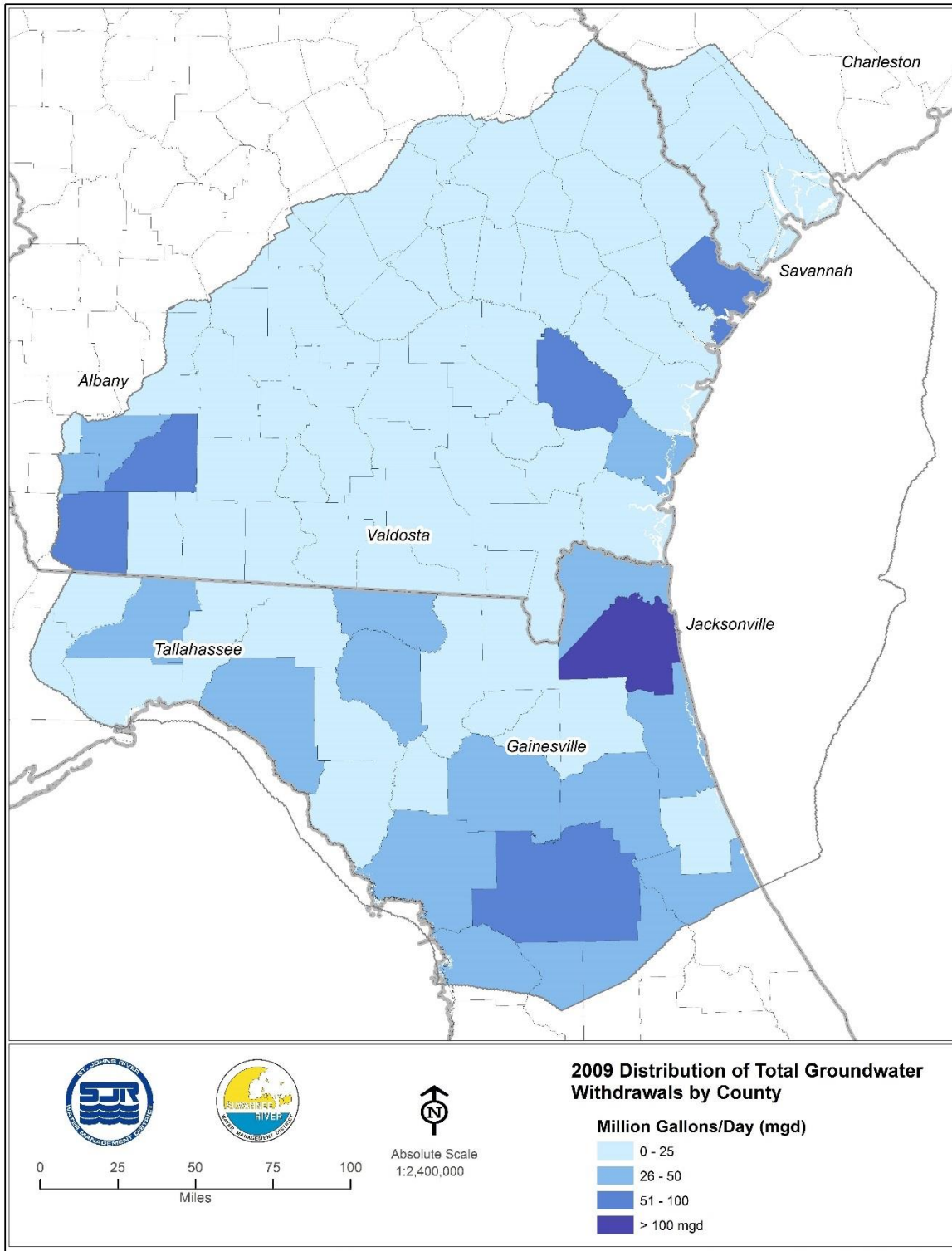


Figure 2-39. Distribution of Total Groundwater Withdrawals by County, 2009

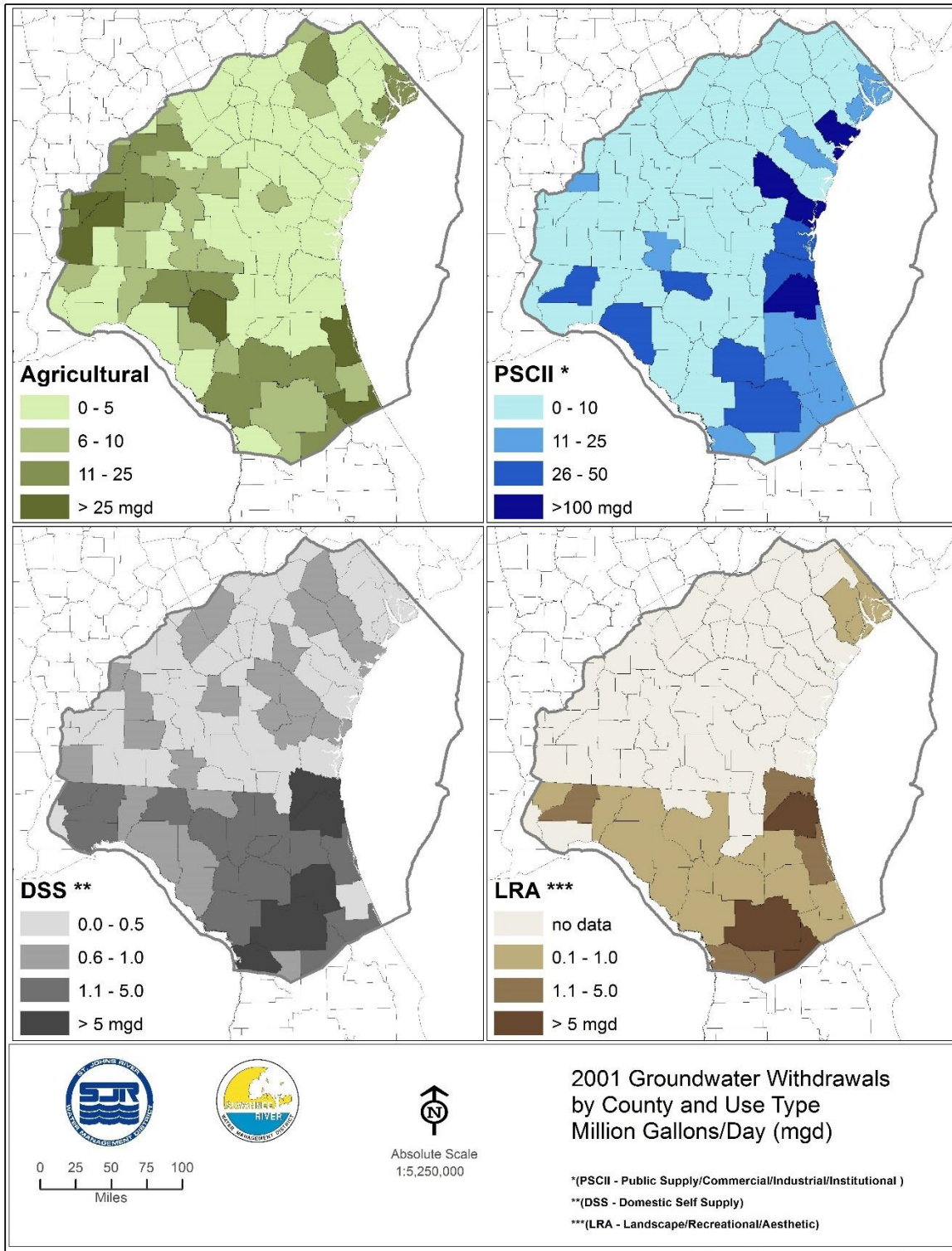


Figure 2-40. Groundwater Withdrawals by County and Use Type, 2001

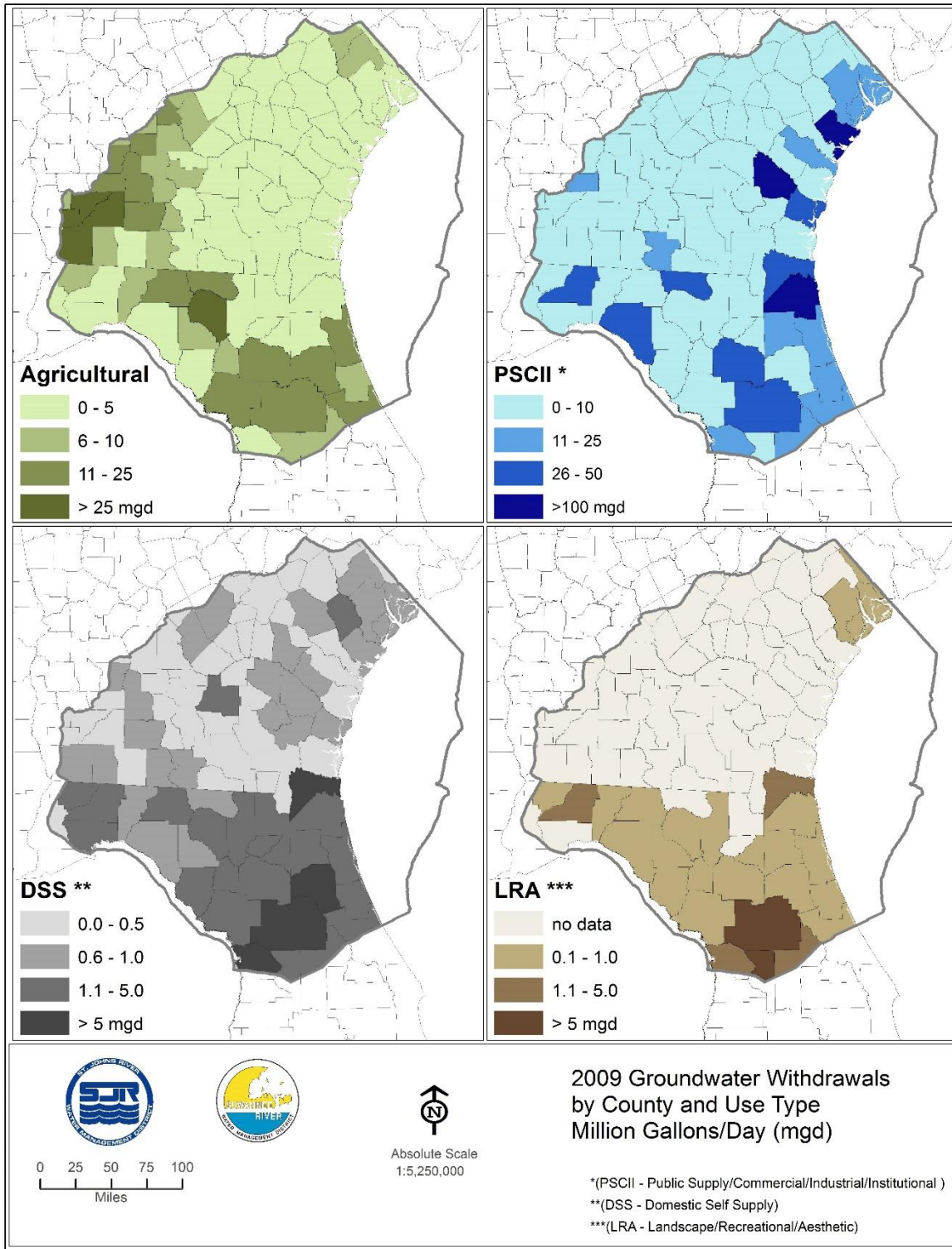


Figure 2-41. Groundwater Withdrawals by County and Use Type, 2009

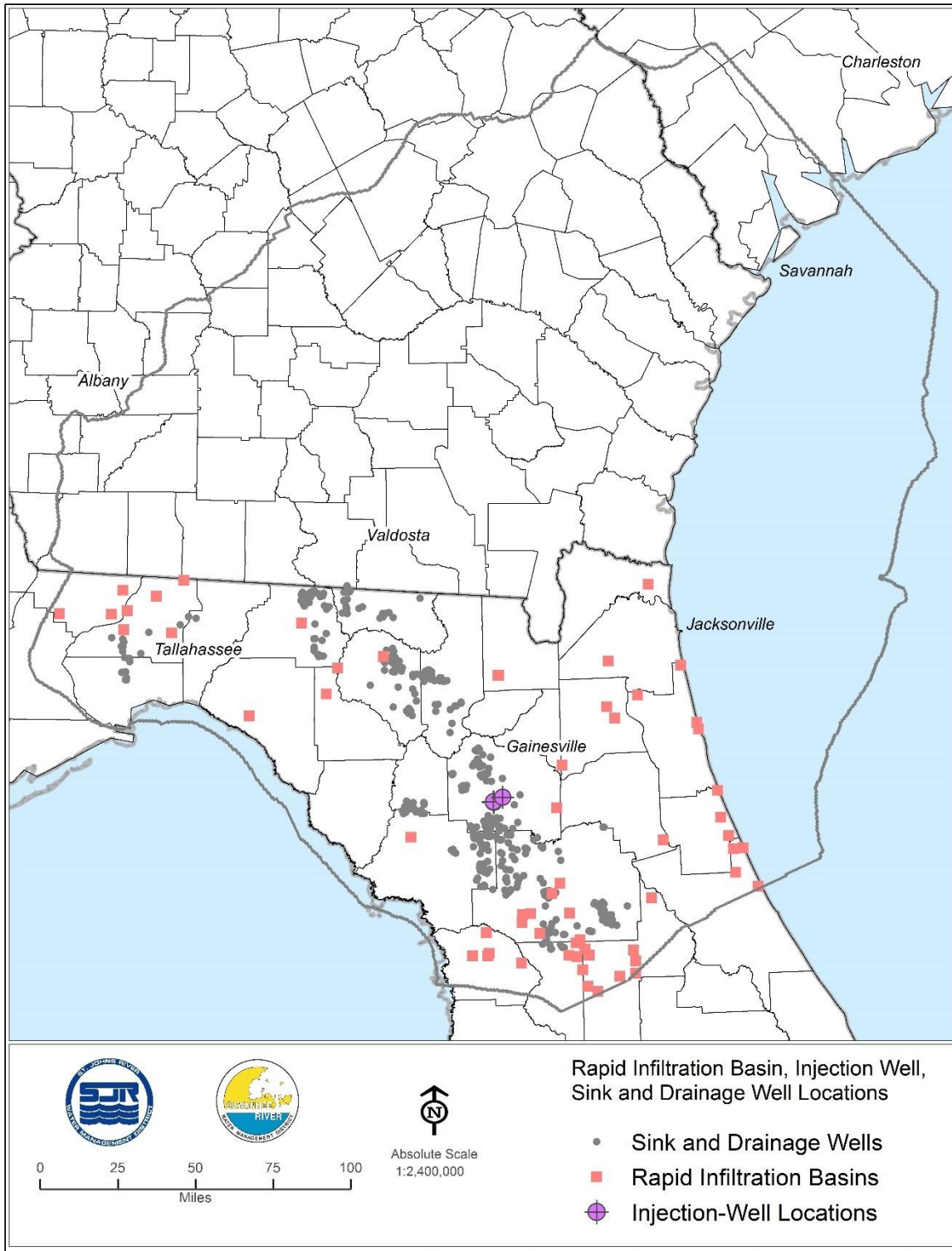


Figure 2-42. Location of Rapid Infiltration Basins, Injection Wells, and Sinks and Drainage Wells

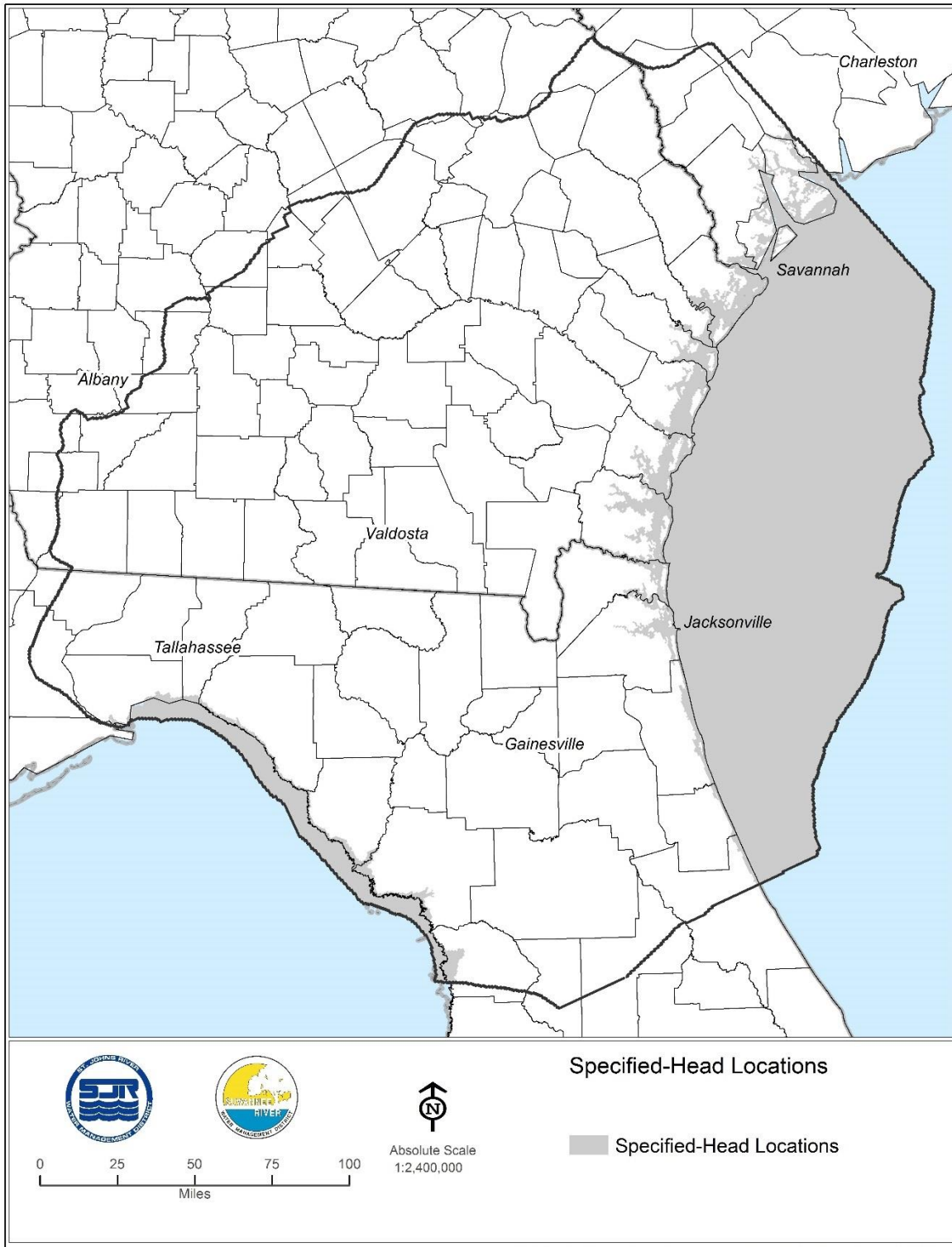


Figure 2-43. Distribution of Specified-Heads

3.0 NFSEG STEADY-STATE MODEL CALIBRATION

PRELIMINARY MODEL TESTING AND SENSITIVITY ANALYSIS

The NFSEG v1.0 model was calibrated using the model independent parameter estimation code (PEST) (Doherty 2015; Doherty 2016a; and Doherty 2016b). Prior to the PEST calibration, however, a process of extensive testing was undertaken to gauge the sensitivity of the NFSEG groundwater model to changes in hydraulic conductivity and other model parameters and to aid in the determination of reasonable ranges for these parameters. This process was used as well to assess the workability of the various lateral and internal boundary conditions and other model features and to affect necessary improvements or corrections. The following benefits were derived from the preliminary testing and sensitivity analysis:

1. Improved understanding of the hydrological system;
2. Improved knowledge of model sensitivity to changes in hydraulic conductivity and other parameters;
3. Improved understanding of potential ranges of horizontal and vertical hydraulic conductivity within model layers;
4. Improved understanding of model numerical requirements, resulting in improved numerical stability and performance through implementation of MODFLOW-NWT;
5. Corrections of and/or improvements in model features.

The analysis involved matching model-simulated water levels and spring discharges to corresponding observed or estimated values throughout the model domain. The groundwater flow system was approximated as steady-state in this analysis, and matching was carried out to 2001 and 2009 median observed conditions. The analysis culminated in a high level of consistency between simulated and observed water levels and spring discharges throughout the model domain for both 2001 and 2009. Insights and results obtained from the preliminary model testing and sensitivity analysis were lent to the PEST calibration process.

PEST CALIBRATION

PEST calibration is organized around two primary data groups: observation data groups and calibration-parameter data groups. The observation data groups are comprised of various water-level and/or flow-rate observations that PEST is tasked with enabling the model to simulate acceptably. PEST does this by adjusting systematically the various model parameters that constitute the calibration-parameter data groups. In the context of the NFSEG groundwater model, parameters are model representations of physical aspects of the hydrological system that control groundwater levels and flow rates. PEST adjusts these model parameters so that the weighted difference between the observed values and their model-simulated counterparts (model residuals) is minimized.

PEST runs a model many times through numerous iterations in this effort to minimize the weighted residuals. During each iteration, and prior to estimating a set of parameter values, PEST constructs a Jacobian matrix, which contains the sensitivity of each weighted observation to a unit change in the value of each model parameter. PEST uses this knowledge to arrive at an improved parameter data set, having been supplied with starting parameter values and their acceptable ranges by the PEST user. The quality of a particular parameter data set is encapsulated in the PEST objective function, a measure of the goodness of fit between observed and corresponding simulated values of the observations that comprise the observation data groups. In its simplest form, the PEST objective function is defined as follows:

$$\Phi = \sum (w_i r_i)^2,$$

$$(i = 1, n)$$

where

Φ = the value of the PEST objective function resulting from a given PEST iteration, equal to the summation of the squares of the products of w_i and corresponding value of r_i , summed over n observations;

w_i = the weight assigned to observation i ;

r_i = the difference between the value of observation i and its model-simulated counterpart (i.e., the residual of observation i); and

n = the number of all observations comprising the various observation data groups.

The primary objective of PEST is to reduce the value of the objective function to below a user-specified level while maintaining the values of the various calibration parameters within user-specified ranges.

OBSERVATION DATA GROUPS

Using PEST, the NFSEG groundwater model was calibrated simultaneously to median observed water levels and flow rates for the years 2001 and 2009, with conditions in both years being represented as steady-state. The observation data groups utilized in the 2001 and 2009 steady-state calibrations for the NFSEG groundwater model are as follows:

1. Groundwater levels;
2. Spring-discharge rates;
3. Baseflow rates (as a total baseflow accumulation for a given gage and as the difference in baseflow between gages);

4. Vertical head differences, i.e., between corresponding aquifer water levels in model layers 1 and 3 or 3 and 5;
5. Horizontal head differences within model layer 3;
6. Temporal water-level differences
7. Lake leakage estimates

In the earlier stages of the calibration process, a wetting penalty function that incorporated observations of maximum water table elevations was also implemented in limited areas to prevent excessive flooding. This function assumed a maximum height of the water table above land surface in wetlands and uplands.

Additional information concerning the observation data groups follows:

Groundwater Levels

The groundwater-level observation data group is a compilation of data obtained from various sources, including the U.S. Geological Survey, the SJRWMD, the SRWMD, the Southwest Florida Water Management District, and the Northwest Florida Water Management District. In a number of cases, statistical methods were used (Appendix E) to augment the number and quality of water-level observations in areas of limited water-level data availability (Appendix F).

Spring Discharge Rates

Spring discharge rates for the years 2001 and 2009 were based on direct observations (Figure 3-1, Figure 3-2 and Appendix C). Sources of data include the U.S. Geological Survey, the SJRWMD, the SRWMD, and the Southwest Florida Water Management District, and the Northwest Florida Water Management District.

Baseflow Rates

Stream base-flow rate was estimated using one of three different methods: (1) by equating it to the observed total stream flow rate at a given gage or the change in total stream flow between gages (Figure 3-3; Figure 3-4; and Appendix G); (2) by separation from the observed total stream flow rate as observed at a given gage using the U.S. Geological Survey program PART (Rutledge 1993); (3) by adjusting the observed, total stream flows with the ratio of HSPF-simulated baseflows and total flows. The observed total stream flow rate or changes in total stream flow along a given river reach were used for cases in which stream flow or stream-flow change was predominated by groundwater discharge. PART or the HSPF-ratio approach were used for cases in which stream flow was not predominated by spring flows. Where observed stream flow rates were deemed to be unreliable, HSPF-simulated baseflow rates were employed.

Two baseflow observation sub-groups are employed in the NFSEG calibration process: the “pick-up” group, which represents the change in the baseflow rate between adjacent stream

gages (or along a reach bounded by a downstream gage but no upstream gages), and the “cumulative” group, which represents the total baseflow rate at a given stream gage. Cumulative estimates were used in basins for which calibration to baseflow was considered to be more critical (such as in the Suwannee and Santa Fe River basins), or to provide a cumulative baseflow target for a larger area of the model domain. The number of pick-up estimates for 2001 was 85, and the number for 2009 was 92. The number of cumulative estimates for 2001 was 10, and number for 2009 was six.

Estimation of reliable baseflow rates proved difficult in many cases. Less reliable baseflow estimates were de-emphasized in or eliminated from the calibration process. Baseflow estimates are one of several NFSEG-model observation groups. Fortunately, some of the more important river reaches in the model domain (with respect to the NFRWSP area) were dominated by groundwater discharge, allowing the use of changes in total stream flow to estimate changes in baseflow. Use of the other observation groups also helped mitigate the effect that missing or less reliable baseflow estimates might have on the calibration.

Vertical Head Differences

Vertical head differences are based on observations obtained in the same year from two wells that are open to different aquifers at or near the same geographical location. Differences in water level between the surficial aquifer system and the Upper Floridan aquifer (model layers 1 and 3, respectively) and between the Upper Floridan aquifer and the upper zone of the Lower Floridan aquifer (model layers 3 and 5, respectively) were included in this observation data group (Figure 3-5; Figure 3-6; Figure 3-7; Figure 3-8; and Appendix H). The purpose of this group was to provide information for calibration of the vertical hydraulic conductivity of the confining layers between the surficial aquifer system and the Upper Floridan aquifer and between the Upper Floridan aquifer and the Lower Floridan aquifer.

Horizontal Head Differences

Horizontal head differences are based on observations obtained in the same year from two wells that are open to the same aquifer at different geographical locations. This observation data group was limited to water level differences in the Upper Floridan aquifer (Figure 3-9; Figure 3-10; and Appendix I). The purpose of this group was to aid in the calibration of areas of very high and low transmissivity and in areas with abrupt changes in transmissivity and to ensure that the lateral flow directions in the Upper Floridan aquifer were simulated reasonably well.

Lake Leakages

The purpose of this group was to limit the leakages from the lakes to acceptable rates so that the lakes do not become artificial sources or sinks of water in the model. Except for the lakes in Keystone Heights region in southeast Clay County, the leakage rates were roughly estimated as the difference between rainfall and potential evapotranspiration. The leakage rates for the lakes in Keystone Heights area were estimated based on the review of literature and measured surface

flow data. Because of the approximate nature of leakage-rate estimates, lake leakage was de-emphasized in the calibration process by assignment of lower weights

Temporal Head Differences

Temporal head differences are computed as the difference between the 2001 and 2009 groundwater levels at a given well. Due to the nature of steady-state model, the water levels in each year was estimated by averaging the observed water levels throughout year. Data quality or availability may vary from one year to another year so temporal differences were only employed at a subset of wells. Temporal differences were de-emphasized in the calibration process by assignment of lower weights.

Wetting Penalty

Wetting penalty is a special observation data group created for purposes of reducing the occurrence of excessive simulated flooding. In the wetting-penalty implementation, the NFSEG model grid is subdivided into grid-cell blocks of 10 rows by 10 columns. Each active grid cell of each grid-cell block is designated as wetland or upland, depending on prevailing conditions within the grid cell. A “wetting penalty” is then determined for each active grid, depending on its designation. The wetting penalty is a contribution to the objective function that depends on the grid-cell designation and the height of the simulated water table above land surface within the grid cell.

For each wetland-designated grid cell of a given grid-cell block, the wetting penalty is

$$\pi = w_p(m-1), \text{ where}$$

π = wetting-penalty contribution to the PEST objective function of the grid cell in question,

w_p = the weight assigned to all grid cells contained within grid-cell block p ; and

m = height of the simulated water table above the average land-surface elevation of the grid cell (feet).

The wetting penalty is not applied to wetland-designated grid cells if the simulated water table is less than 1 foot above land surface.

For each upland-designated grid cell of grid-cell block p , the wetting penalty is

$$\pi = w_p(m)$$

The wetting penalty can be emphasized to a lesser or greater degree over an entire grid-cell block through adjustment of the assigned wetting-penalty weight, as the same weight is used for all grid cells within a grid-cell block. By setting the weight to zero, the cumulative wetting penalty over an entire grid-cell block can be eliminated entirely from the objective function. As the calibration phase of the NFSEG model development progressed, flooding issues were

insignificant, so most of these observations were assigned zero-weights to reduce potential problems that occur because of nonlinearities introduced into the calibration process with wetting penalty observations.

CALIBRATION-PARAMETER DATA GROUPS

The calibration-parameter data groups utilized in the 2001 and 2009 steady-state calibrations of the NFSEG groundwater model are as follows:

1. Hydraulic conductivity (horizontal and vertical), horizontal- and vertical-hydraulic-conductivity multipliers, and anisotropy ratio;
2. GHB conductance for spring representation;
3. River-package-conductance multipliers for application to river-package-conductance determination in the representation of stream baseflows;
4. Drain-package-conductance multipliers for application to drain-package-conductance determination in the representation of ephemeral stream baseflows;
5. River-package conductance multipliers for lake representation;
6. Lake-zone multipliers for adjustment of model-layer-2 vertical hydraulic conductivity beneath lakes.
7. Recharge multipliers; and
8. Maximum-Saturated-ET multipliers

PEST requires specification of a preferred value and an upper and lower bound for each parameter member of the calibration-parameter data groups. The preferred value is the starting value in the PEST-calibration process. Additional information concerning the calibration-parameter data groups follows:

Hydraulic-Conductivity-Related Calibration Parameters

Horizontal Hydraulic Conductivity Determination of Model Layers 1, 3, and 7 and Vertical Hydraulic Conductivity Determination of Model Layer 6

Horizontal hydraulic conductivity is determined in the NFSEG PEST calibration process directly for model layers 1, 3, and 7 using “pilot points.” Vertical hydraulic conductivity is likewise determined directly for model layer 6 using pilot points. After determination of hydraulic conductivity at the pilot-point level, surface interpolation of calibrated values at pilot points using an advanced kriging method is performed by PEST for determination of hydraulic conductivities at the grid-cell level.

Pilot points are specified locations at which PEST calculates the value of a calibration parameter, the parameters of interest in this case being horizontal or vertical hydraulic conductivity. Pilot-point locations are user-specified. The creation of the pilot-point distributions used in the NFSEG calibration process was initialized through application of Groundwater Vistas, a program that facilitates the processing of input and output data for MODFLOW and for MODFLOW-related applications of PEST. This step resulted in the creation of pilot-point meshes comprised of triangular patterns formed around observation wells. Gaps in a mesh, which can occur due to localized sparseness in the observation-well network, were filled with pilot points spaced at regular intervals of 25,000 to 125,000 feet (varies by layer), resulting in localized, gridded patterns of pilot points interspersed within the overall mesh. As a final step, individual or small groups of pilot points were added at specific locations as deemed necessary or desirable. Typical locations for such points were where additional information was needed from the calibration process or where additional information was available for application to it. Examples of such places include areas of steep gradient in the potentiometric surface of the Upper Floridan aquifer and areas at and near springs (Figure 11; Figure 22; Figure 13; and Figure 14).

Vertical Hydraulic Conductivity of Model Layers 2 and 4, Horizontal Hydraulic Conductivity of Model Layer 5, and Vertical- and Horizontal-Hydraulic-Conductivity Multipliers

For model layer 2, vertical hydraulic conductivity is calibrated directly in the parts of the model domain that correspond to areas in which the intermediate confining unit is present (Figure 16). This approach involves the use of pilot points, as described above in regards to the determination of horizontal hydraulic conductivity in model layers 1, 3, and 7 and vertical hydraulic conductivity in model layer 6. After its determination at the pilot-point level, layer-2 vertical hydraulic conductivity is interpolated by PEST between pilot points at the grid-cell level.

For portions of the model domain that correspond to areas in which the intermediate confining unit is thin or non-existent, an indirect approach is used for determining the vertical hydraulic conductivity of model layer 2. In the indirect approach, the vertical hydraulic conductivity of a given layer-2 grid cell is equated to the product of the vertical hydraulic conductivity at the corresponding grid cell of model layer 3 and a PEST-derived vertical-hydraulic-conductivity multiplier. Vertical-hydraulic-conductivity multipliers are calibrated at the pilot-point level in parts of the model domain that correspond to areas in which the intermediate confining unit is thin or non-existent. PEST interpolates between these pilot points for determination of the vertical-hydraulic-conductivity multiplier at the grid-cell level (Figure 15).

This approach tends towards similarity between the distributions of layer-2 and layer-3 vertical hydraulic conductivity in areas in which the intermediate confining unit is generally absent. This is by design, because layer 2 is generally more representative of the Floridan aquifer system than the intermediate confining unit in this area, due to the general absence of the intermediate confining unit and thinness of the overburden above the top of the Floridan aquifer system. Nevertheless, the approach provides for the possibility of deviation, to a significant degree if needed to match observed data, between the vertical hydraulic conductivities of layers 2 and 3 in specific instances. This is also by design, the intent being the representation of outliers of the intermediate confining unit, which are distributed sporadically within the area. Outliers of the

intermediate confining unit encompass areas that correspond in size to a portion of only one to many model grid cells.

A similar approach is used for model layers 4 and 5 in regard to areas of presence and absence of the middle semiconfining unit. Vertical hydraulic-conductivity values of model layer 4 and horizontal hydraulic conductivity values of model layer 5 are calibrated directly in areas in which the middle semiconfining unit is present according to Miller (1986). These values are determined for respective arrays of layer-4 and layer-5 pilot points (Figure 3-16 and Figure 3-17). Values of vertical hydraulic conductivity of model layer 4 and horizontal hydraulic conductivity of model layer 5 are interpolated at the grid-cell level between the respective arrays of pilot points.

In the parts of the model domain that correspond to areas in which the middle semiconfining unit is not present according to Miller (1986), vertical-hydraulic-conductivity multipliers are calibrated for model layer 4, and horizontal-hydraulic-conductivity multipliers are calibrated for model layer 5. These values are estimated at the pilot-point level and interpolated at the grid-cell level between pilot points (Figure 3-16 and Figure 3-17).

Model-layer-4 vertical hydraulic conductivity of a particular grid cell in the area of no middle semiconfining unit is equated to the product of the vertical hydraulic conductivity of model layer 3 and the model-layer-4 vertical-hydraulic-conductivity multiplier as interpolated at the grid cell.

With respect to the grid cells of model layer 5 within this area, model-layer-5 horizontal hydraulic conductivity of a particular grid cell is equated to the product of the horizontal hydraulic conductivity of model layer 3 and the model-layer-5 horizontal-hydraulic-conductivity multiplier as interpolated at the grid cell.

Anisotropy Ratio. The ratio of anisotropy as applied in the NFSEG calibration process is defined as the ratio of horizontal hydraulic conductivity to vertical hydraulic conductivity. A single value of the anisotropy ratio is estimated through calibration for each NFSEG model layer (Table 3-1).

Table 3-1. NFSEG Layer-Wide Ratios of Modeled Anisotropy Ratios

Area of Application	Modeled Anisotropy
Model Layer 1	6.1
Model Layer 2, ICU Present	18.8
Model Layer 2, ICU Not Present	13.5
Model Layer 3	5.5
Model Layer 4, MSCU Present	7.3
Model Layer 4, MSCU Not Present	10.5

Model Layer 5, MSCU Present	100.0
Model Layer 5, MSCU Not Present	6.6
Model Layer 6	10.0
Model Layer 7	10.0

As described above, horizontal hydraulic conductivity was a calibration parameter under certain circumstances, while under others, vertical hydraulic conductivity was a calibration parameter. Under the circumstances where horizontal hydraulic conductivity was a calibration parameter, vertical hydraulic conductivity was calculated by dividing the value of horizontal hydraulic conductivity by the applicable layer-wide anisotropy ratio (Table 3-1). In similar fashion, where vertical hydraulic conductivity was a calibration parameter, horizontal hydraulic conductivity was calculated by multiplying the value of vertical hydraulic conductivity by the appropriate layer-wide value of the anisotropy ratio.

GHB Conductance for Representation of Spring Discharge

As stated previously, GHB conditions were used in the representation of springs (Appendix A; Appendix C; Figure 1; and Figure 2). GHB conductance is an important factor in the simulation of spring flows, the other factors being the specified pool elevation and the simulated groundwater level of the grid cell to which the GHB condition is assigned. GHB conductance cannot be measured readily and must therefore be determined through the calibration process. The set of GHB conductance values used in the representation of springs is therefore included in the calibration process as a calibration-parameter data group.

The primary objective of the calibration process in the determination of spring conductance is to enable the model to simulate spring flows adequately. In general, a greater emphasis is placed on matching the flows of larger springs and the total flows of spring complexes, as the estimates of such flows are generally more reliable due to better data availability. They are more significant in terms of their effects on the flow system as well and therefore more critical to the overall representation of the groundwater system. See Appendix C for simulated vs. observed or estimated spring discharge rates.

River-Package-Conductance Multipliers for Representation of Stream Baseflow

As stated previously, the river package was used in the representation of stream reaches of Strahler Order 2 and above. The primary objective of the calibration process in this regard is adequate simulation of stream baseflow rates. To this end, cumulative baseflow rates were estimated at a number of stream gages within the model domain (Figure 3-3 and Figure 3-4).

As with GHB conductance in the simulation of spring-discharge rates, river-package conductance is a primary factor in the simulation of stream baseflow rate, the others being the assigned stage and the simulated groundwater level of the grid cell to which the boundary is assigned. In the calibration process, the river-package conductance was calculated initially based

on calibration-derived values of hydraulic conductivity, calculated hydraulic areas, and assumed lengths of flow path (see “River-Package Implementation” under “Model Configuration” above). This approach has the advantage of relating conductance to local values of hydraulic conductivity and thereby providing a reasonable starting point, but the results are imprecise, as the approach does not account for local-scale conditions in the stream bottom.

Refinement of the initial conductance values is achieved through determination and application of river-package-conductance multipliers. The set of river-package-conductance multipliers is a calibration-parameter data group in the calibration process. River-package-conductance multipliers are updated in each PEST iteration and hence evolve as the calibration process advances. These parameters are determined on an HSPF sub-basin-wide basis for each river-package sub-segment contained within a given sub-basin. The river-package conductance values were updated by multiplying the current river-package conductance of each river-package boundary used for stream representation within a given HSPF sub-basin by the river-package-conductance multiplier estimated for the sub-basin.

Drain-Package-Conductance Multipliers for Representation of Stream Baseflow

As stated previously, the drain package was used in the representation of stream reaches of Strahler Order 1. As with the conductance values of river-package boundaries discussed in the previous section, values of drain-package conductance are also adjusted through the use of conductance multipliers. As in the river-package implementation of this approach, drain-package-conductance multipliers are estimated on an HSPF sub-basin-wide basis for each drain-package boundary. As with the river-package implementation, the drain-package conductance values were updated by multiplying the current drain-package conductance of each drain-package boundary used for stream representation within a given HSPF sub-basin by the drain-package-conductance multiplier estimated for the sub-basin.

Lake-Related Multipliers: River-Package-Conductance and Lake-Zone Multipliers

The approach to constraining lake leakage rates involved adjustments to the river-package conductance of the river-package boundaries used to represent the lakes. In regards to lakes, this value primarily controls exchanges of water between the lake and the aquifer that surrounds it, usually the surficial aquifer system. In addition, the rate of leakage between the lake and the underlying Floridan aquifer system is also constrained. This is accomplished in the calibration process with defined lake “zones” for which “lake-zone” multipliers are estimated for application to the vertical hydraulic conductivity of model layer 2, which is usually representative of the intermediate confining unit. A lake zone is merely a group of layer-2 model grid cells. A single lake-zone multiplier is estimated for each lake zone (i.e., one for each lake). Likewise, a single river-package-conductance multiplier is estimated for each lake.

Recharge and Maximum-Saturated ET Multipliers.

Multipliers for recharge and maximum-saturated ET were also included in the set of parameters available for calibration to adjust the HSPF-derived recharge and maximum-saturated ET by sub-

basins. The purpose of these multipliers was to allow for the adjustment of the HSPF-derived recharge and maximum-saturated ET rates during the calibration, if needed. To date, however, this feature of the calibration process has not been activated, as it has not yet been required.

DRAFT

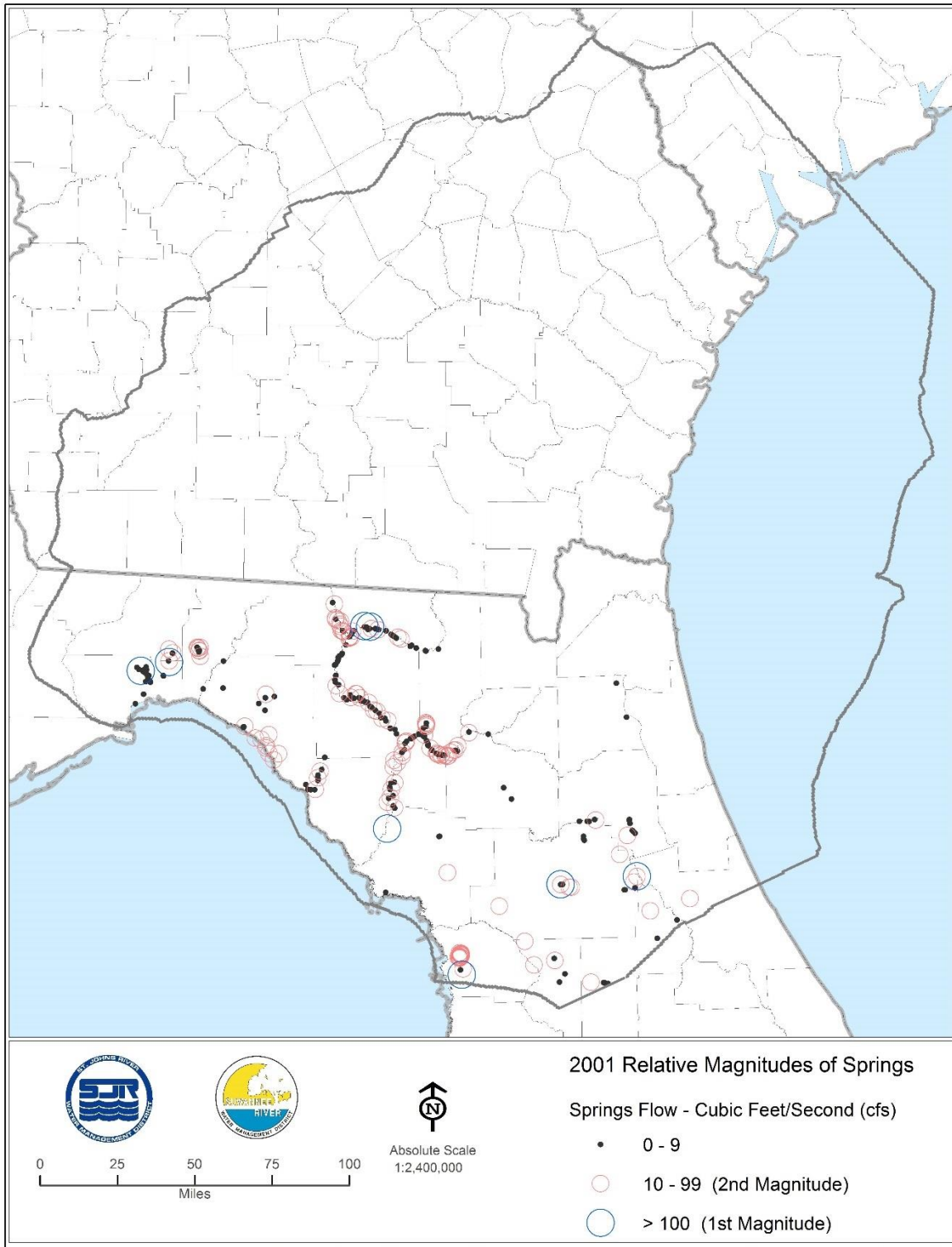


Figure 3-1. Location and Relative Magnitude of Springs 2001

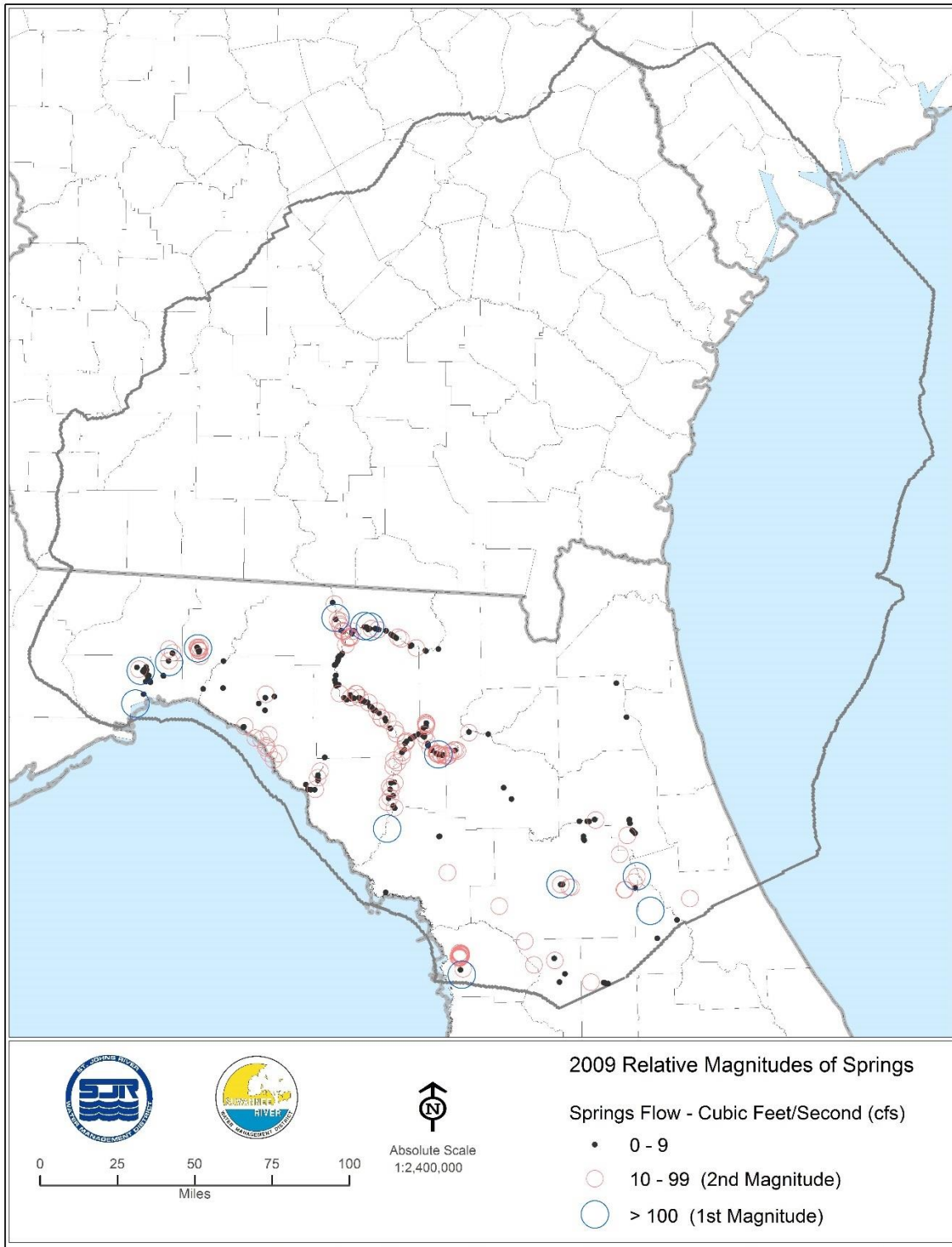


Figure 3-2. Location and Relative Magnitude of Springs 2009

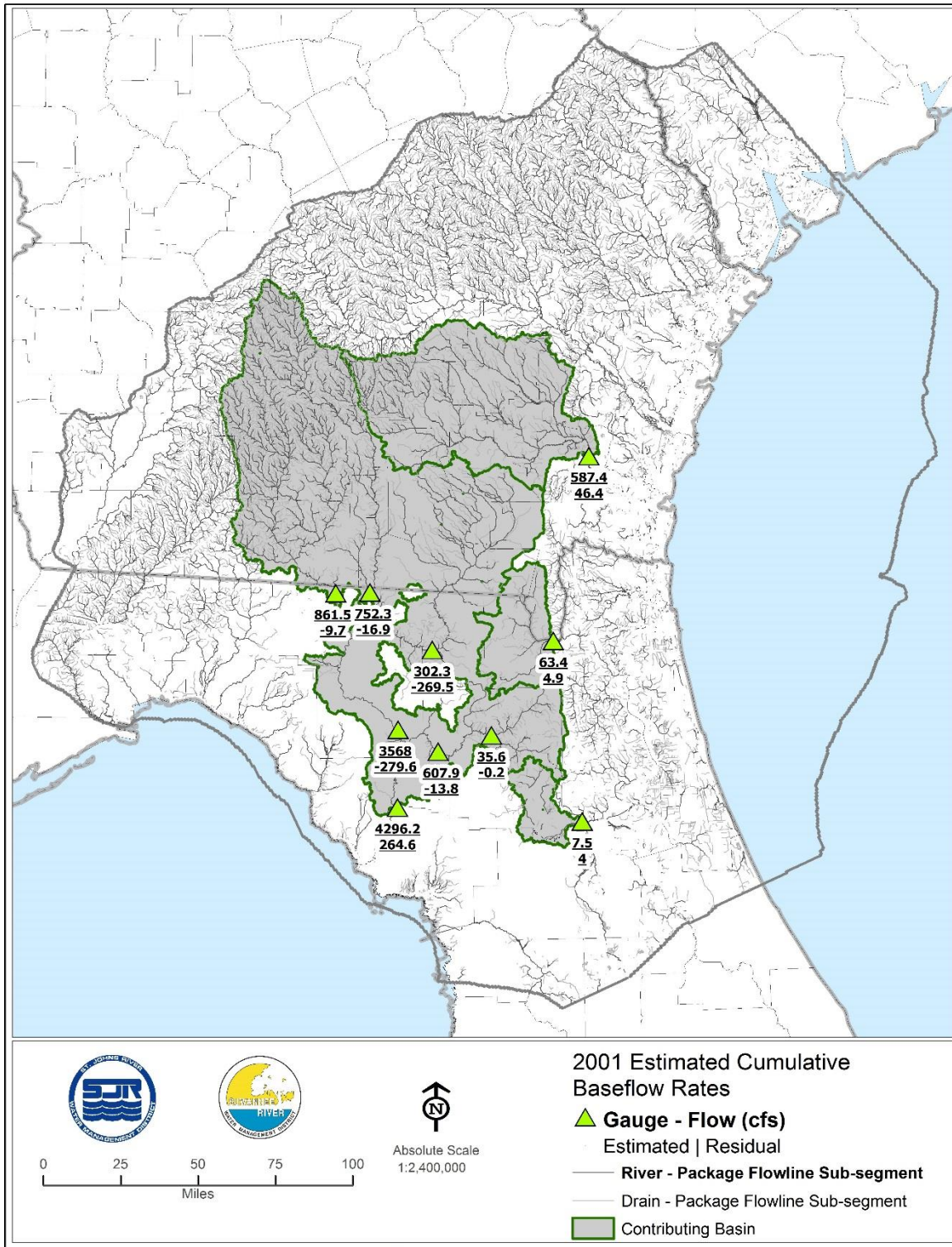


Figure 3-3. Estimated Cumulative Baseflows 2001

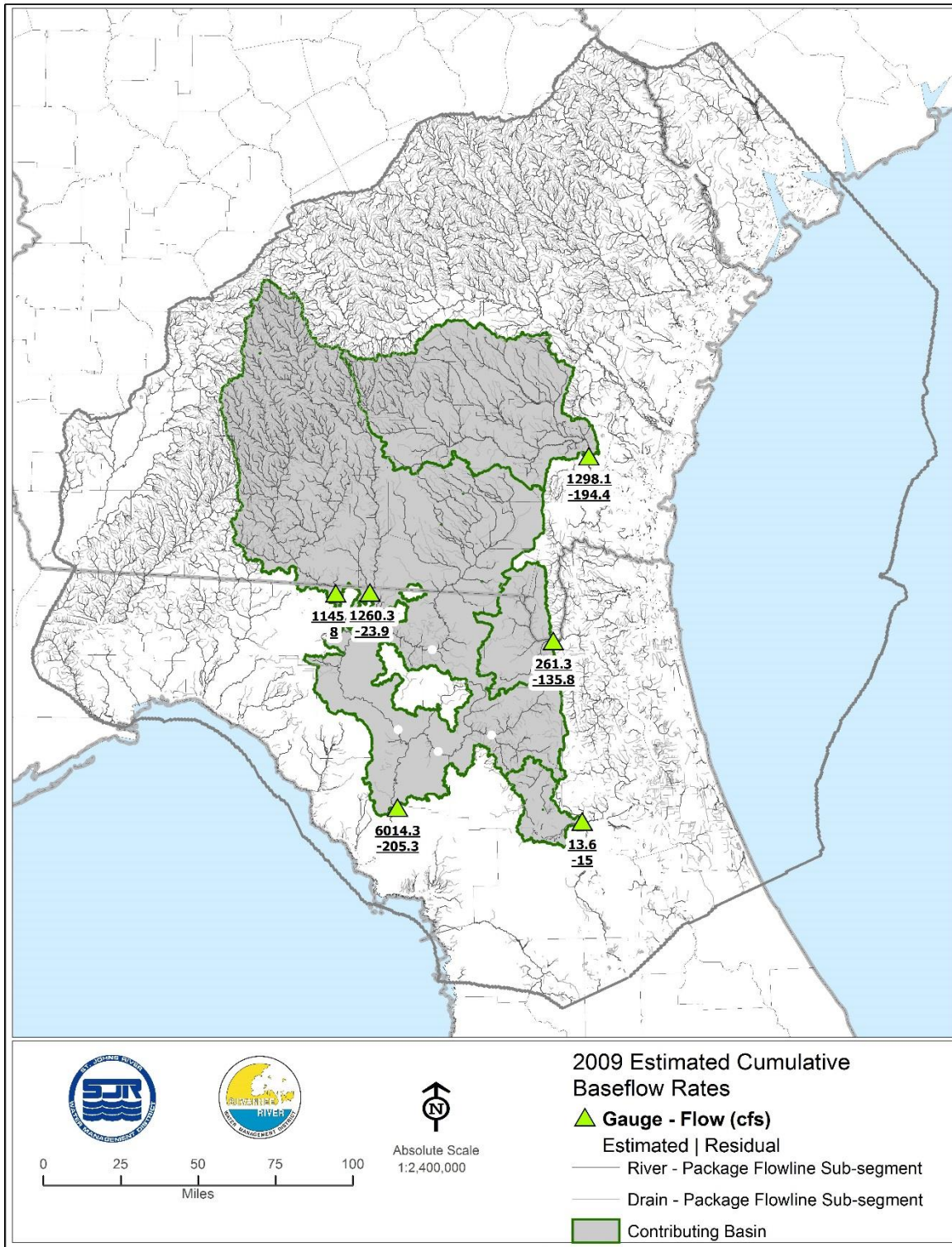


Figure 3-4. Estimated Cumulative Baseflows 2009

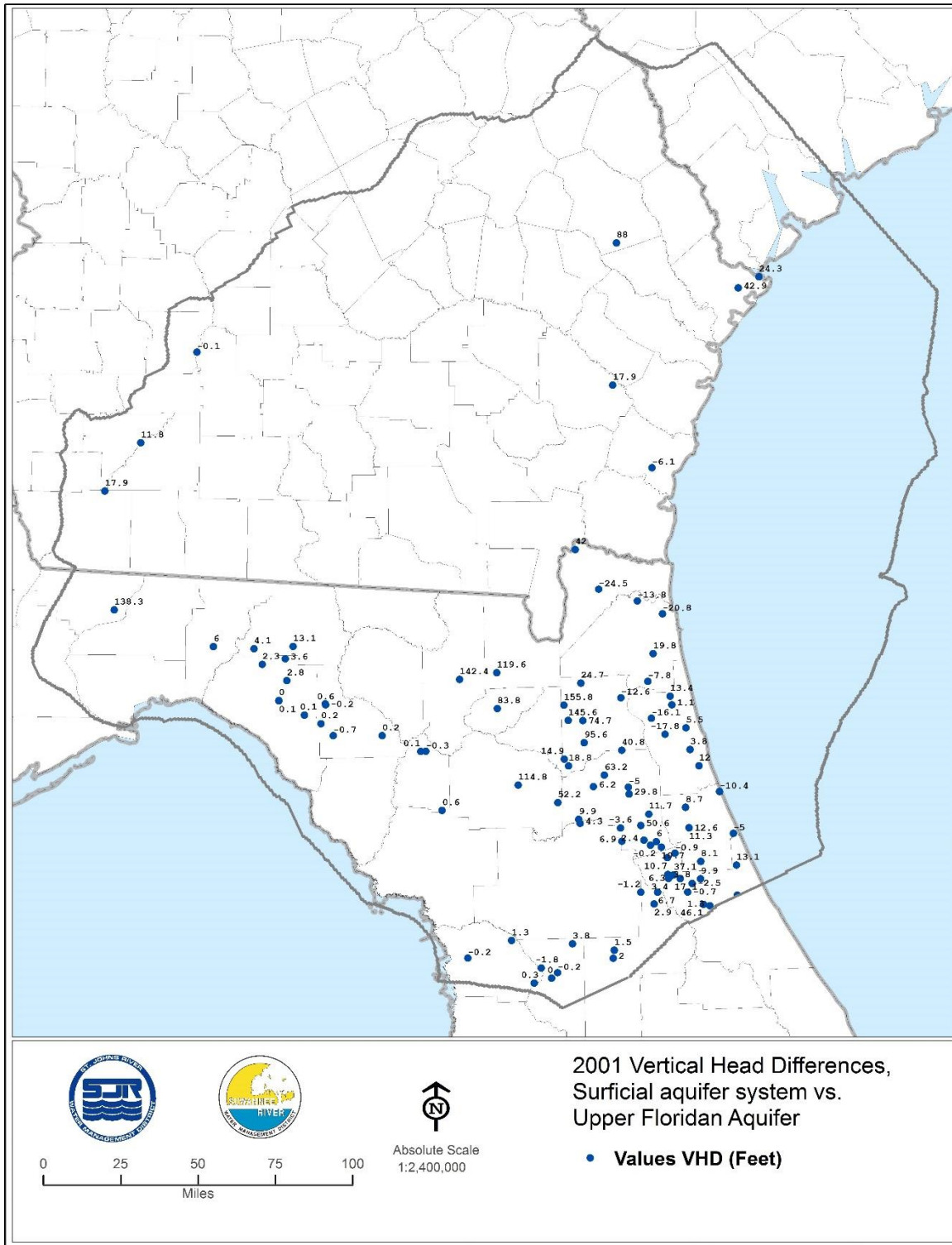


Figure 3-5. Vertical Head Differences, Surficial Aquifer vs. Upper Floridan 2001

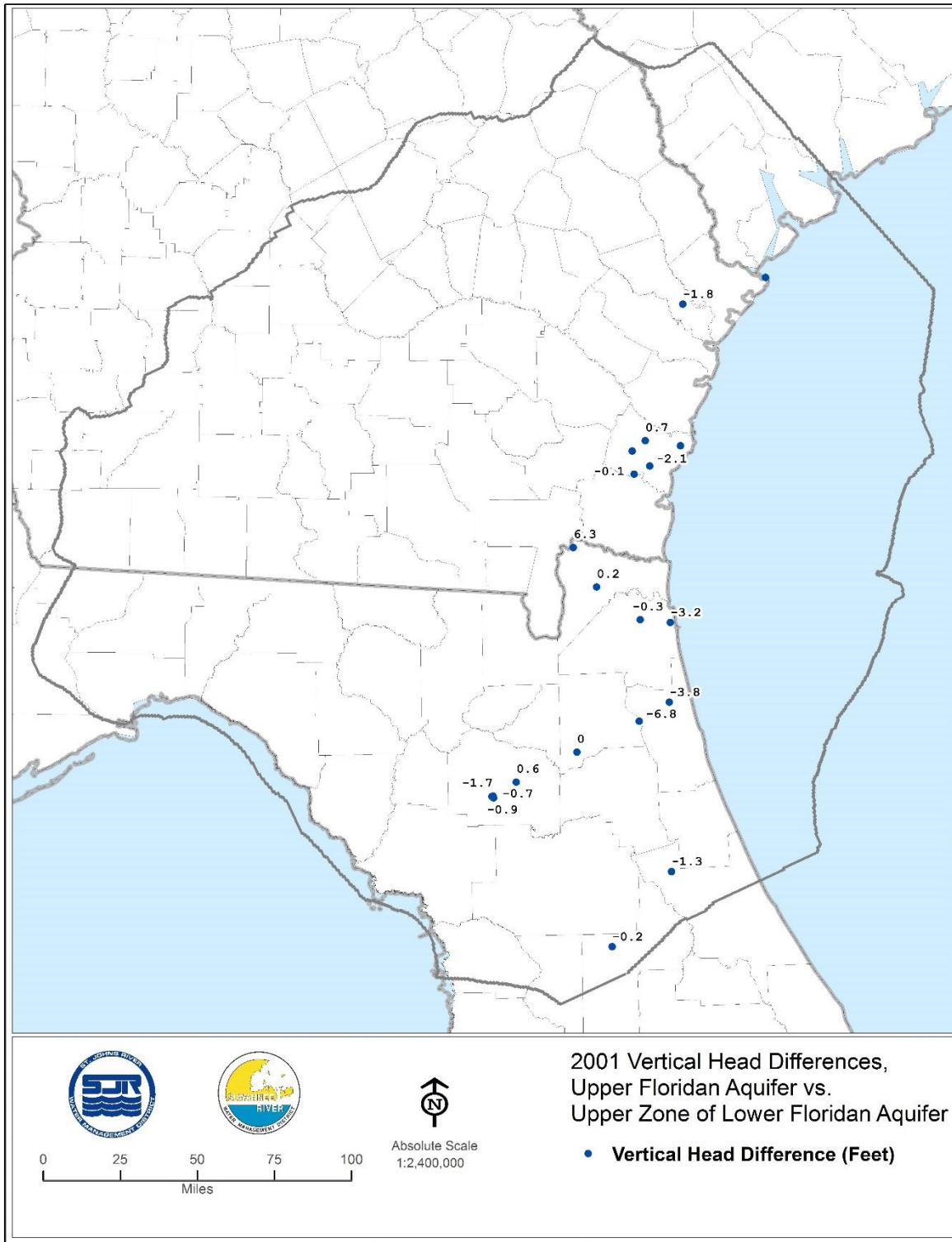


Figure 3-6. Vertical Head Differences, Upper Floridan vs. Upper Zone of Lower Floridan 2001

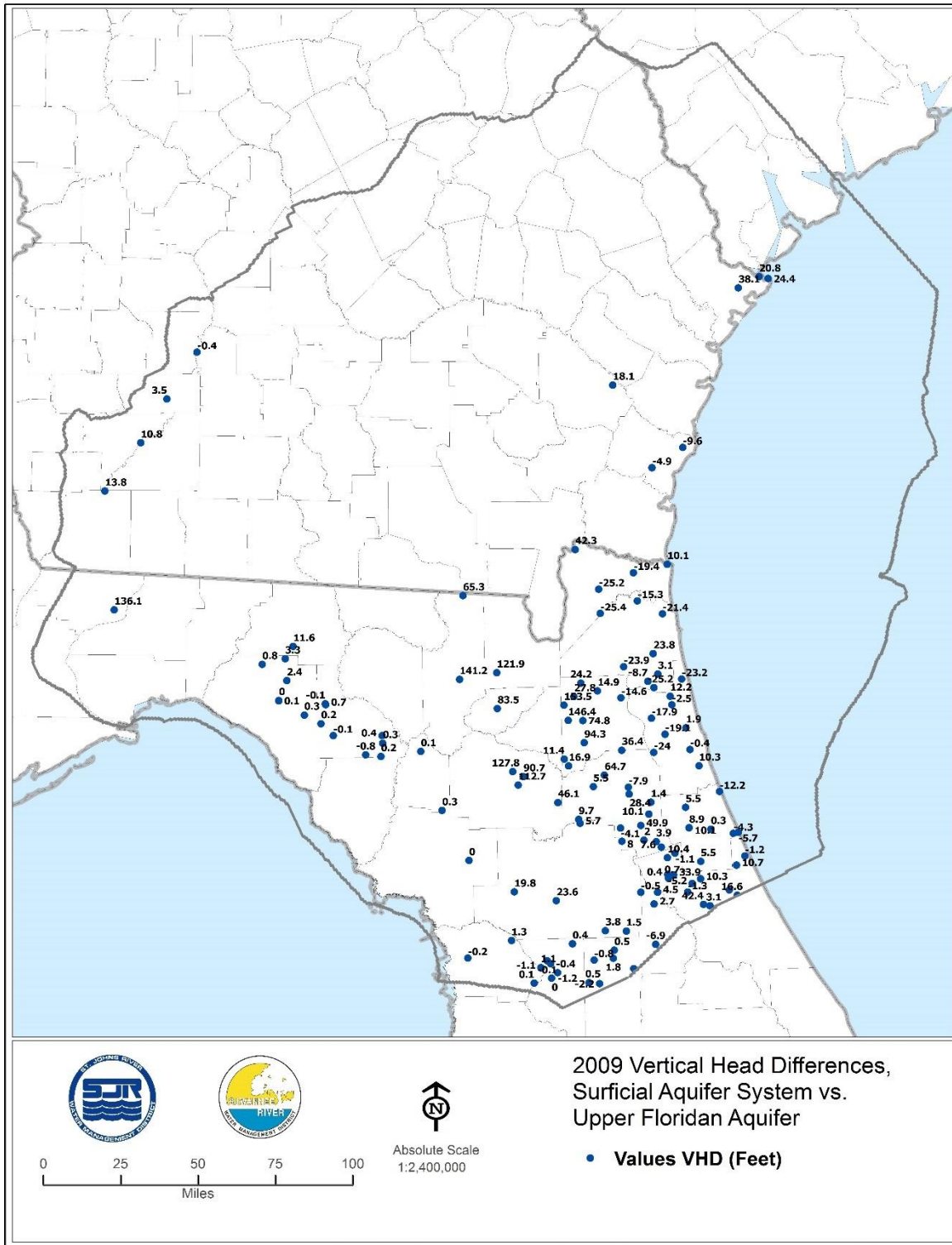


Figure 3-7. Vertical Head Differences, Surficial Aquifer vs. Upper Floridan 2009

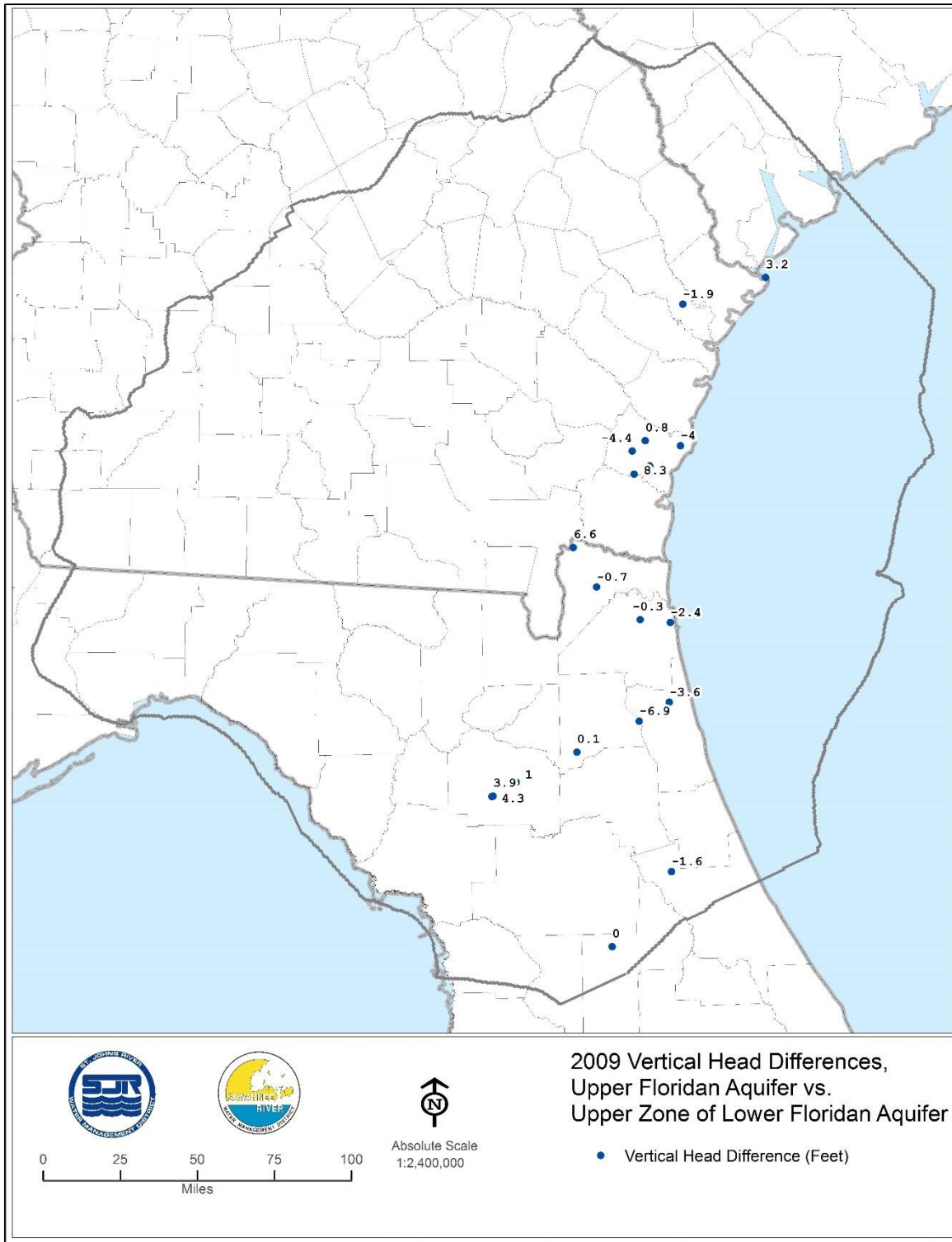


Figure 3-8. Vertical Head Differences, Upper Floridan vs. Upper Zone of Lower Floridan 2009

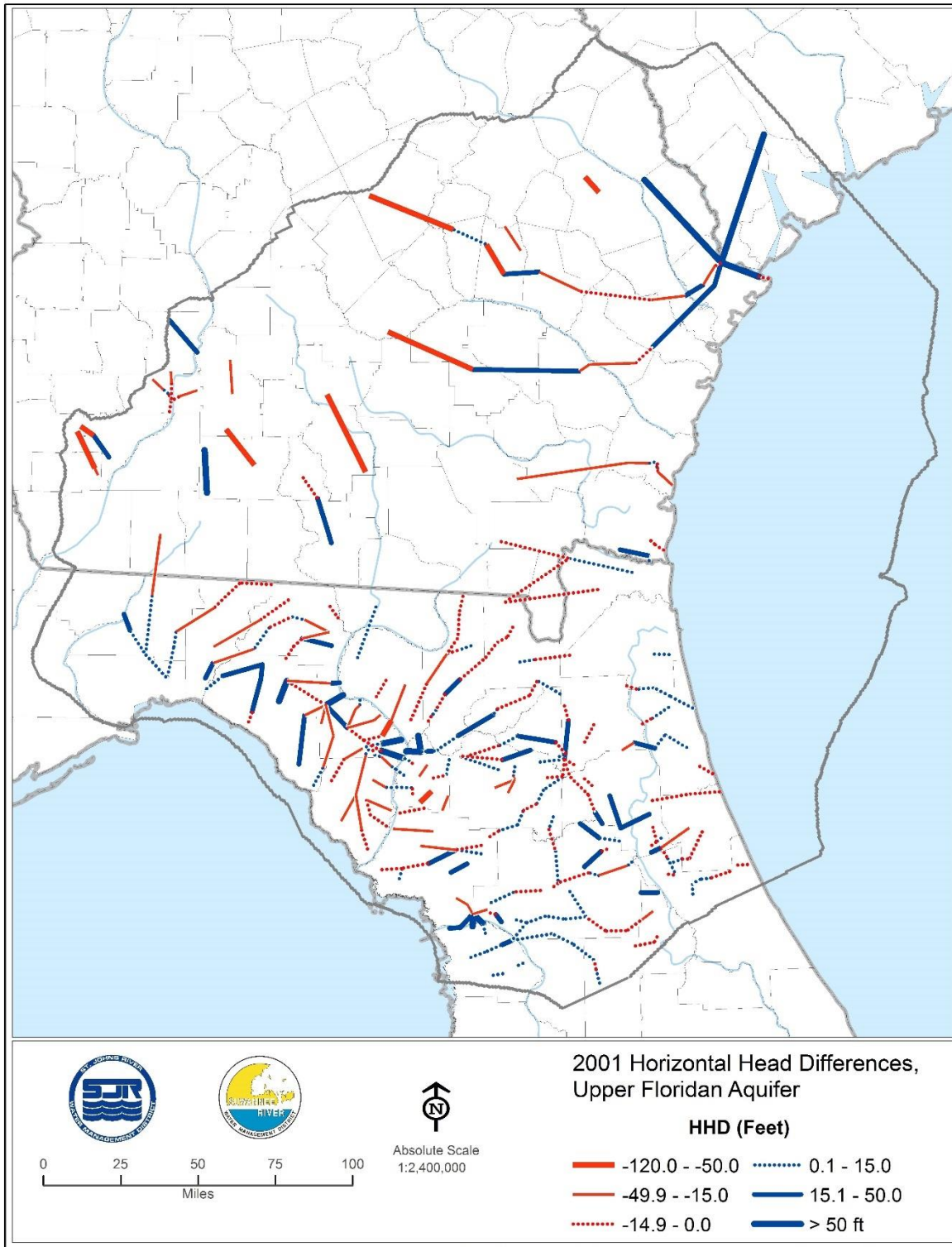


Figure 3-9. Horizontal Head Differences, Upper Floridan 2001

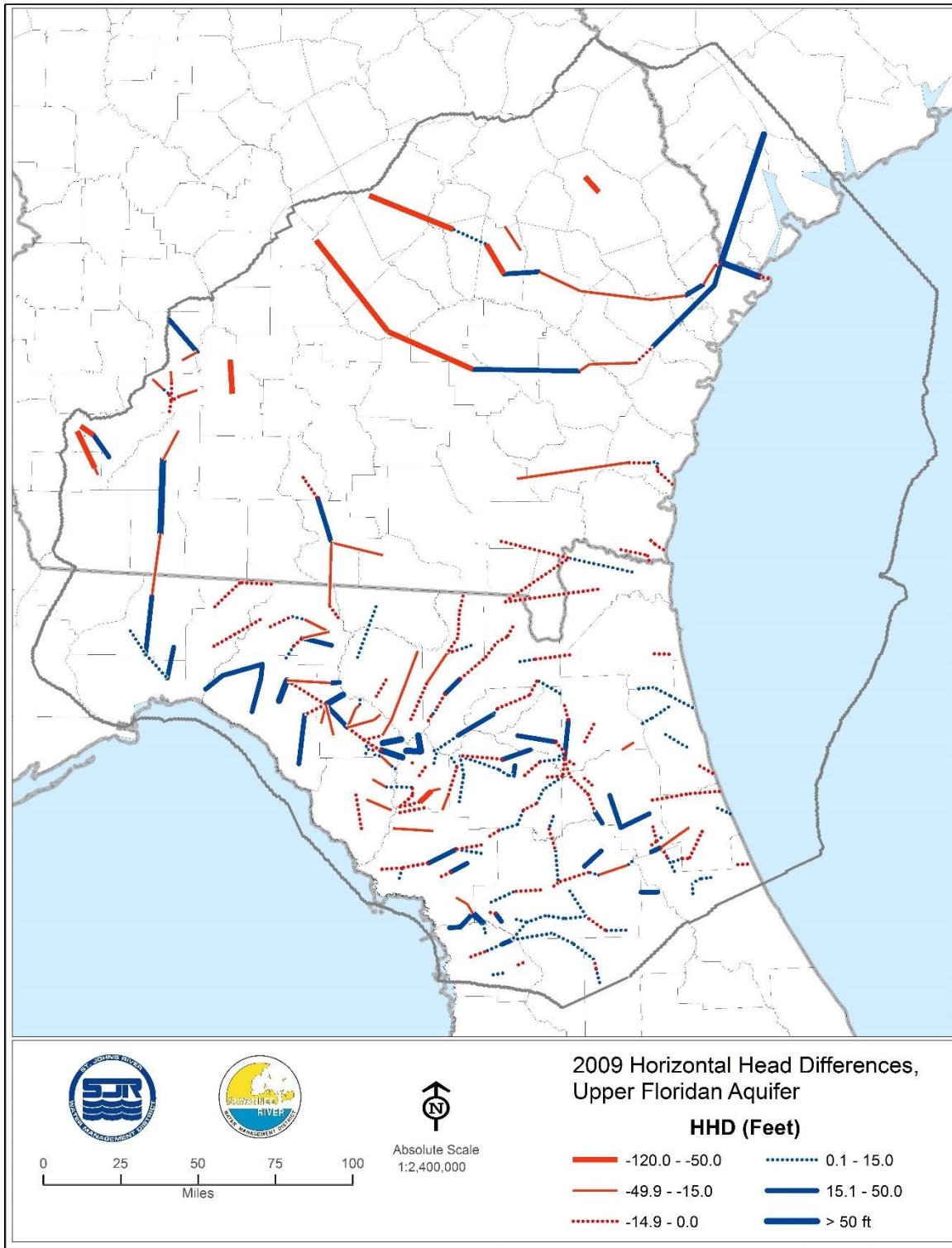


Figure 3-10. Horizontal Head Differences, Upper Floridan 2009

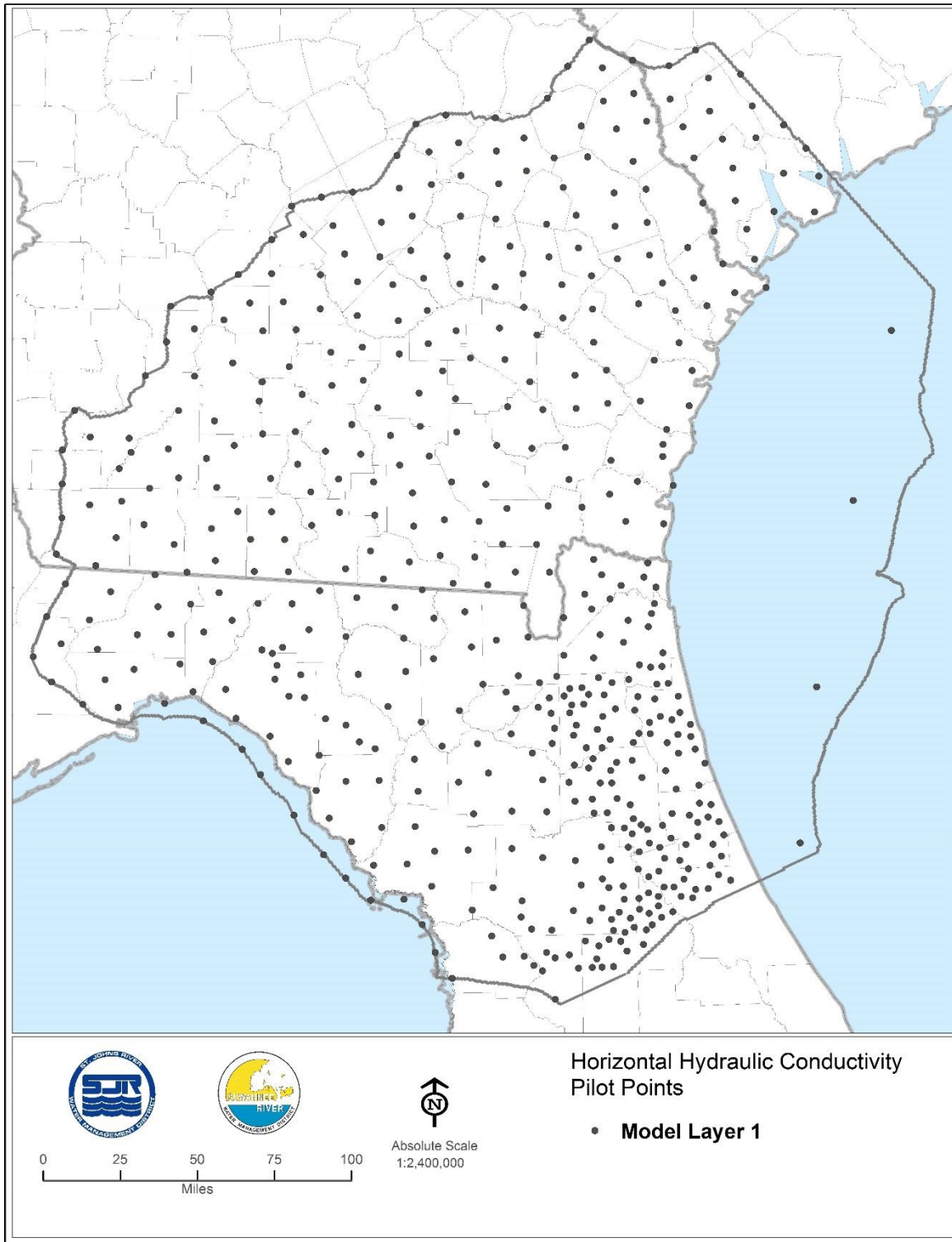


Figure 3-11. Distribution of Horizontal Hydraulic Conductivity Pilot Points, Model Layer 1

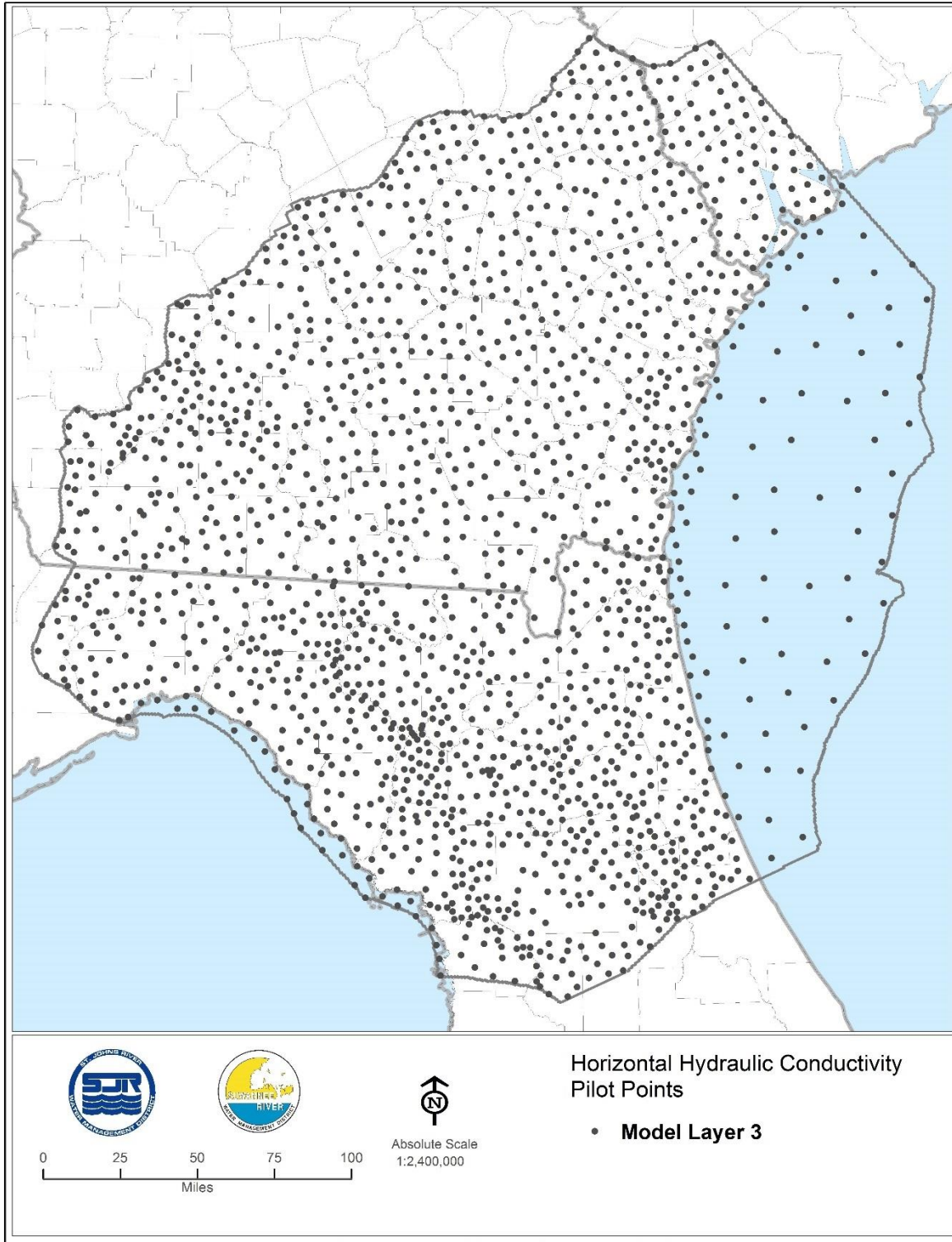


Figure 3-12. Distribution of Horizontal Hydraulic Conductivity Pilot Points, Model Layer 3

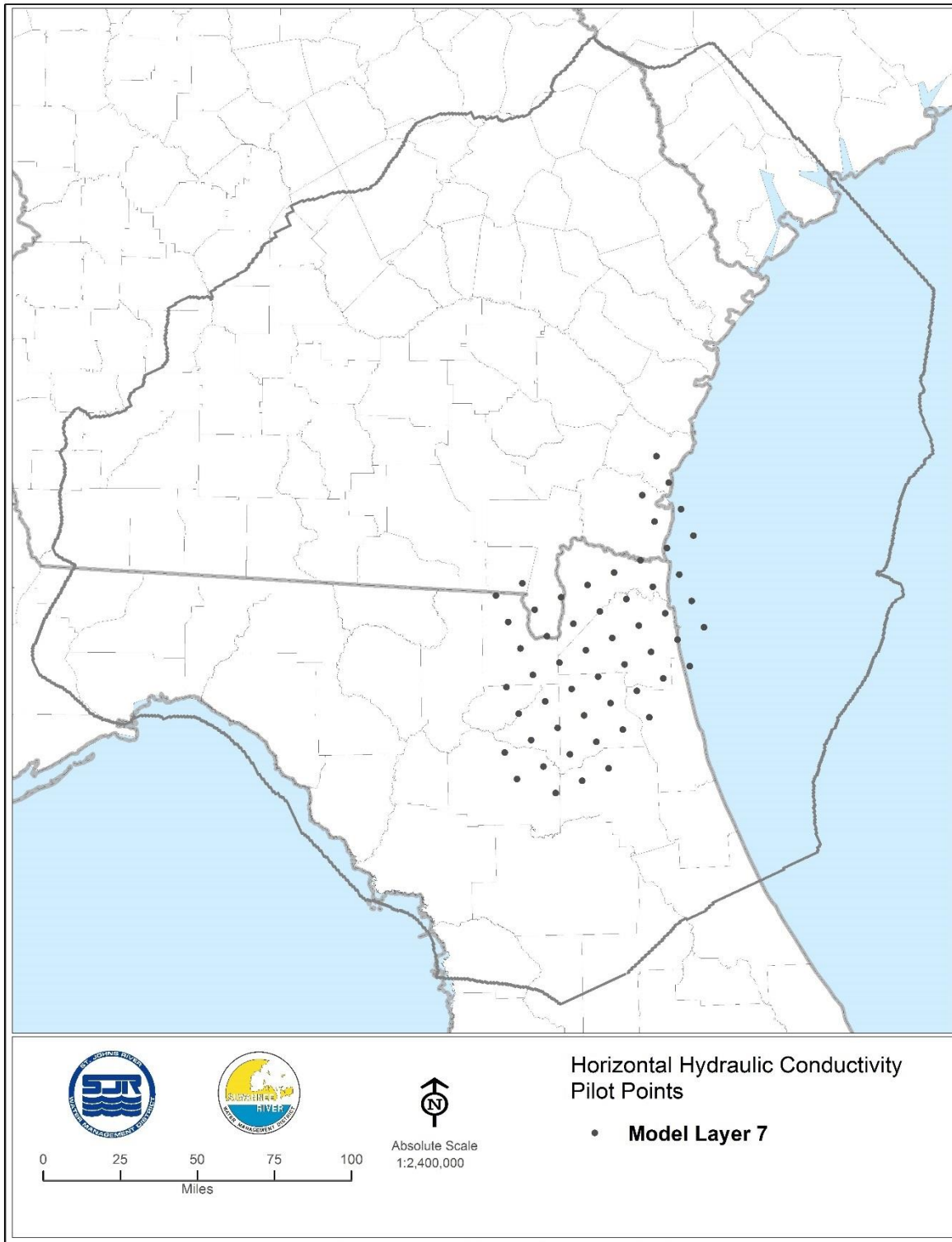


Figure 3-13. Distribution of Horizontal Hydraulic Conductivity Pilot Points, Model Layer 7

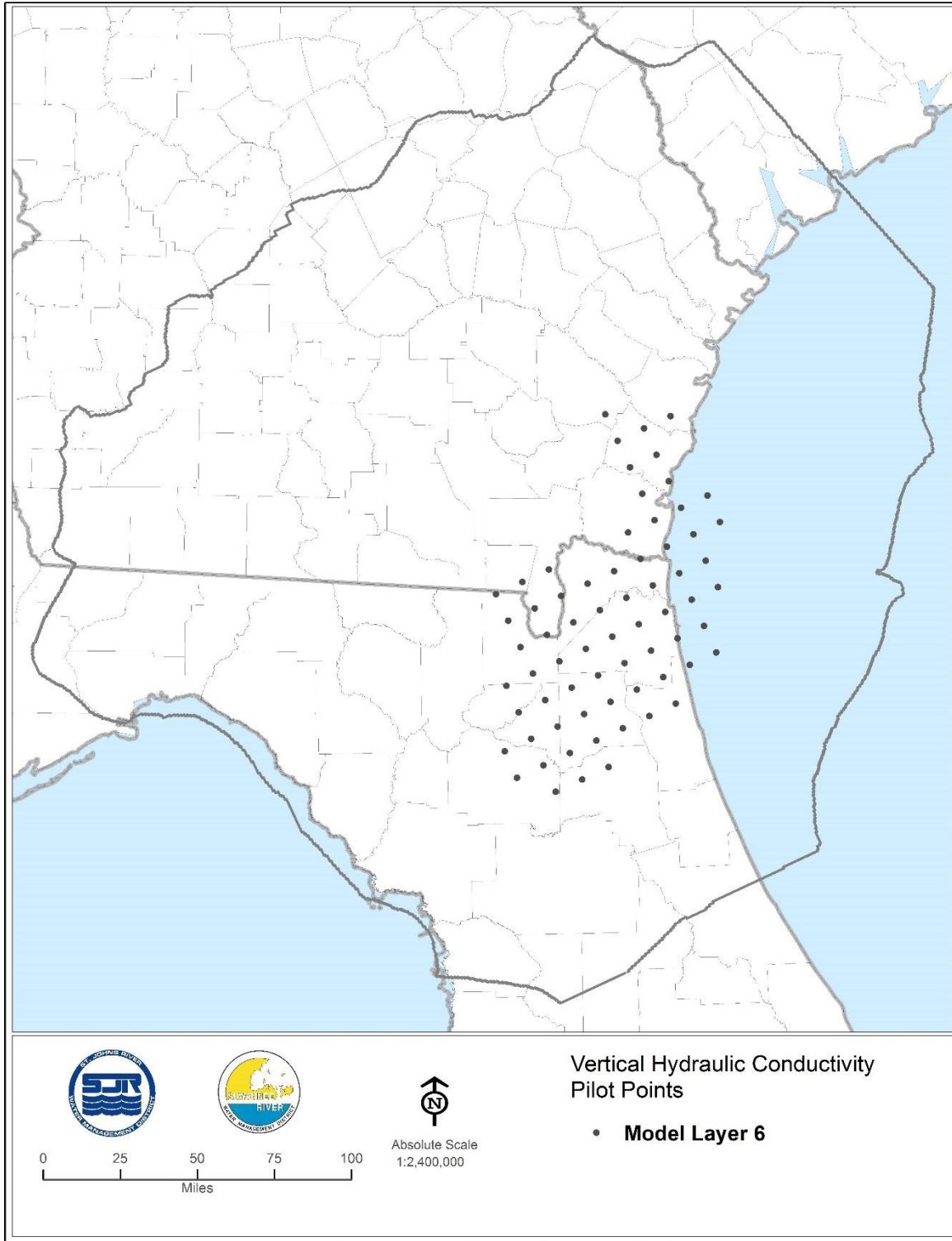


Figure 3-14. Distribution of Vertical Hydraulic Conductivity Pilot Points, Model Layer 6

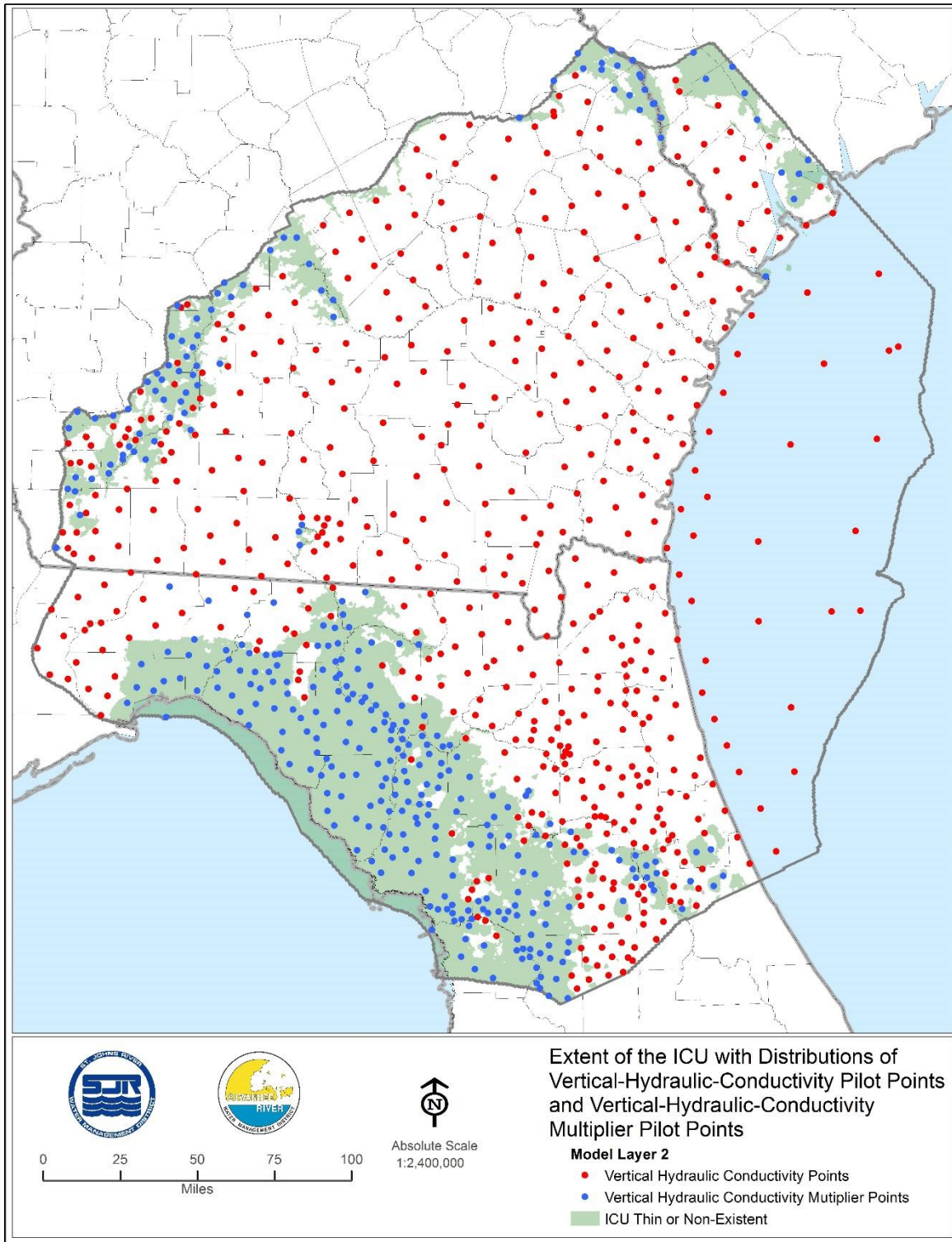


Figure 3-15. Distribution of Vertical Hydraulic Conductivity Pilot Points and Vertical Hydraulic Conductivity Multiplier Pilot Points, Model Layer 2

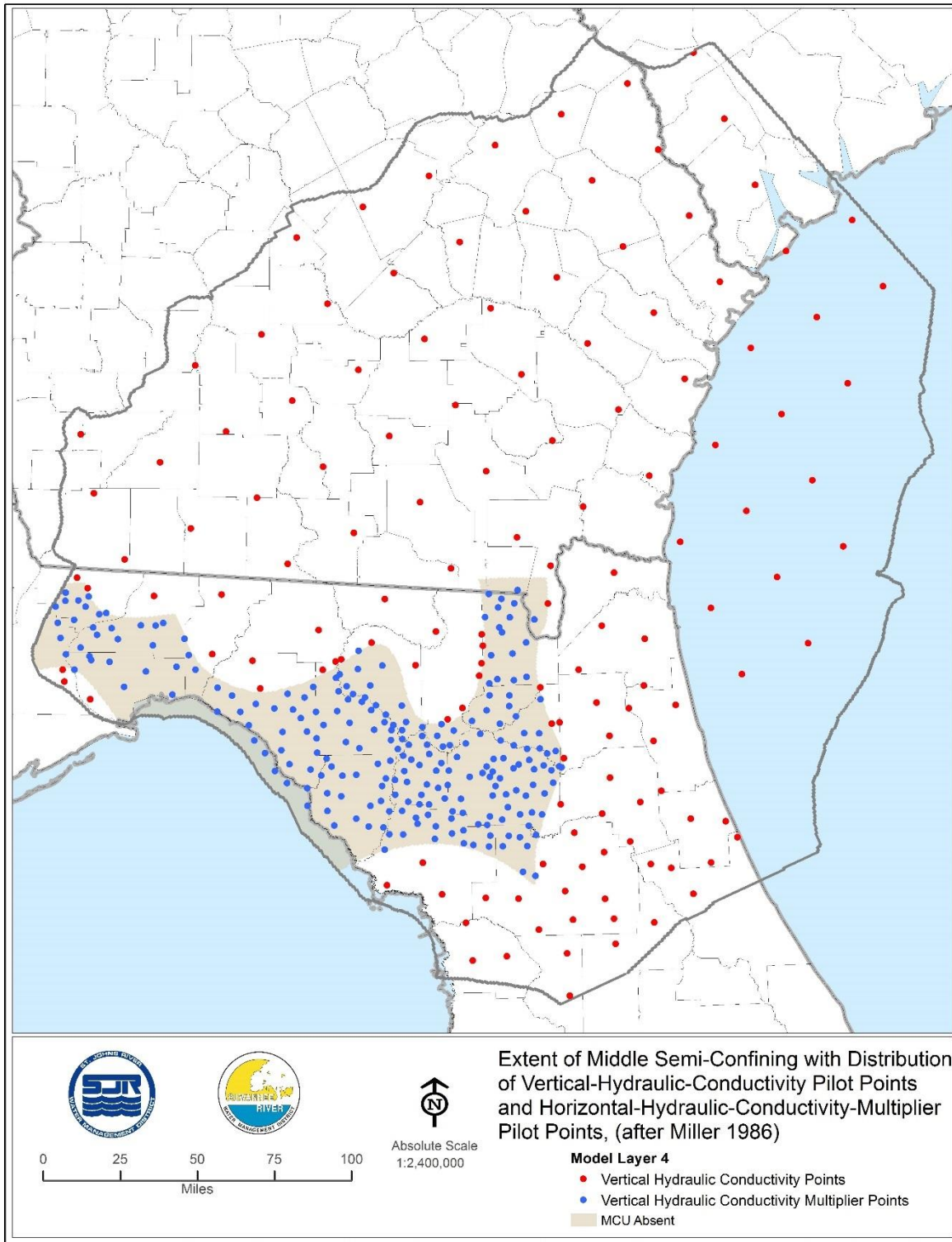


Figure 3-16. Distribution of Vertical Hydraulic Conductivity Pilot Points and Vertical Hydraulic Conductivity Multiplier Pilot Points, Model Layer 4

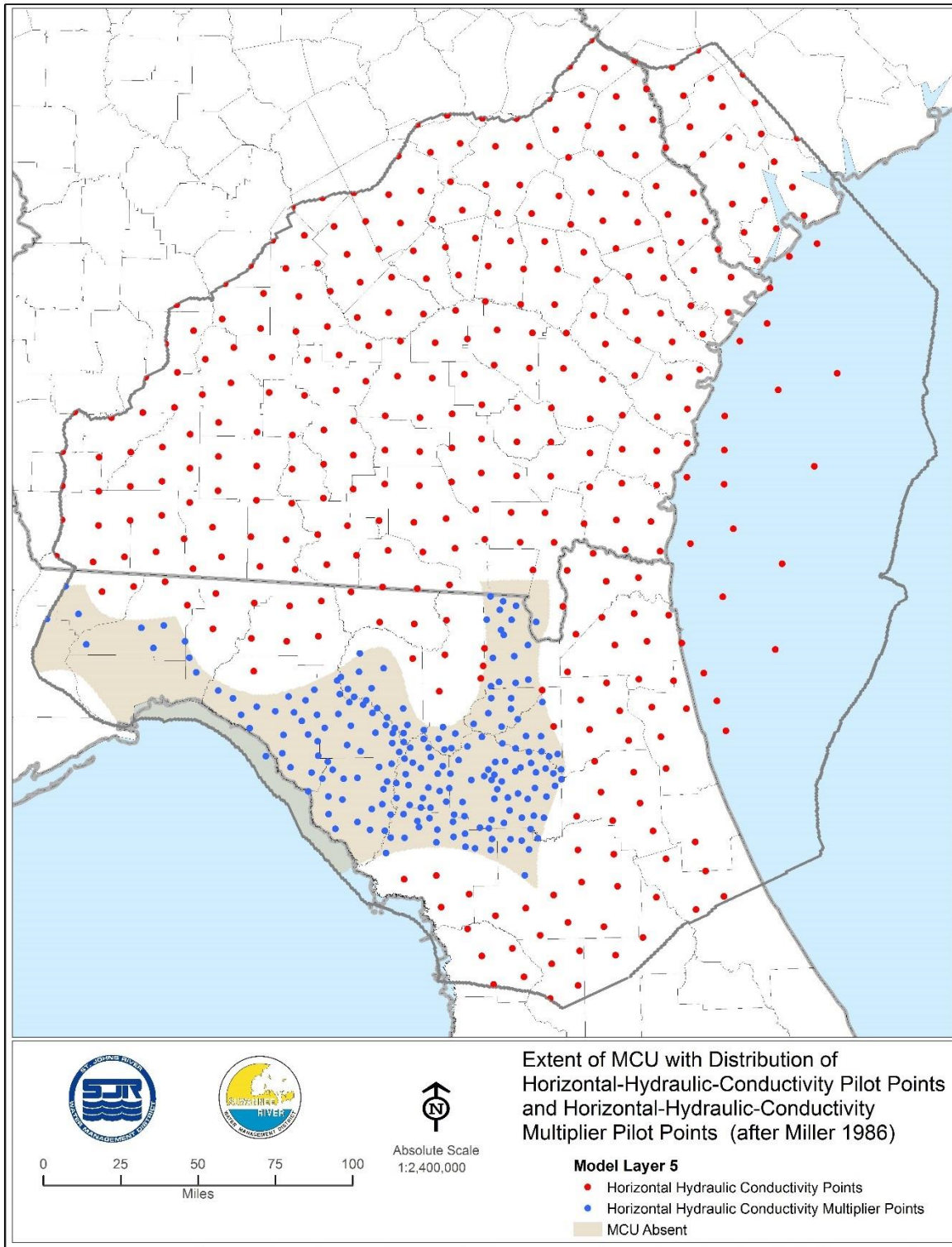


Figure 3-17. Distribution of Vertical Hydraulic Conductivity Pilot Points and Vertical Hydraulic Conductivity Multiplier Pilot Points, Model Layer 5

CALIBRATION RESULTS

Progress in the calibration process was measured by comparing the members of the observation data groups to corresponding observed or estimated values. Differences between simulated and observed or estimated values are referred to as residuals. The following review of the calibration results will be presented primarily in terms of residuals of members of the observation data groups—statistics, values, and distributions. In addition, resulting fields of horizontal hydraulic conductivity of model layers 1, 3, 5, and 7 and vertical hydraulic conductivity of model layers 2, 4, and 6 will be shown. Corresponding distributions of aquifer transmissivity of model layers 1, 3, 5, and 7 and distributions of semi-confining-unit leakance of model layers 2, 4, and 7 will be shown as well. Finally, maps of the simulated potentiometric surface of the Upper Floridan aquifer will be shown.

Calibration Statistics

Table 3.2 summarizes statistical goals for the NFSEG model calibration along with the corresponding actual values for the 2001 and 2009 calibration years as well as other pertinent statistics.

The goals were specified prior to construction and calibration of the NFSEG model in the NFSEG model-conceptualization report, which may be found on-line at http://northfloridawater.com/pdfs/NFSEG/NFSEG_modelconceptualization.pdf. As stated in the model-conceptualization report, the goals of Table 3-2 were guidelines, not intended as hard-and-fast requirements, and they were treated as such in the NFSEG model-calibration process.

Detailed calibration results are presented in the following figures and table, which are organized as follows.

- Spatial Distribution of Hydraulic Head Residuals, 2001 and 2009, Model Layers 1, 3, and 5 (Figures 3-18 to 3-23)
- Simulated vs. Observed Hydraulic Head, Model Layers 1, 3, and 5 (Figures 3-24 to 3-29)
- Spatial Distribution of Vertical Head Difference Residuals, Between Model Layers 1 and 3, 2001 and 2009 and Model Layers 3 and 5, 2001 and 2009 (Figures 3-30 to 3-33)
- Simulated vs. Observed Vertical Head Differences, 2001 and 2009 (Figures 3-34 to 3-35)
- Spatial Distribution of Horizontal Head Difference Residuals, within Model Layer 3, 2001 and 2009 (Figures 3-36 to 3-37)
- Simulated vs. Observed Horizontal Head Differences, 2001 and 2009 (Figures 3-38 to 3-39)
- Simulated vs. Observed Spring Discharges, 2001 and 2009 (Figures 3-40 to 3-43)
- Simulated vs. Observed Baseflows (Table 3-3 and Figures 3-44 to 3-45)
- Spatial Distribution of Horizontal Hydraulic Conductivity, Model Layers 1, 3, 5, and 7 (Figures 3-46 to 3-49)
- Spatial Distribution of Transmissivity, Model Layers 3, and 5 (Figures 3-50 to 3-51)

- Spatial Distribution of Vertical Hydraulic Conductivity, Model Layers 2, 4, and 6 (Figures 3-52 to 3-54)
- Spatial Distribution of Leakance, Model Layers 2 and 4 (Figures 3-55 to 3-56)
- Simulated Potentiometric Surfaces of Model Layer 3, 2001 and 2009 (Figures 3-57 to 3-58)

Table 3-2. Calibration Statistics

Statistical Criterion	Proposed Target	All Target Wells		Target Wells (Number of Observed Data > 1)		North Florida WSP Area	
		2001	2009	2001	2009	2001	2009
-5 feet < Residual < 5 feet	80%	80%	81%	83%	82%	86%	87%
-2.5 feet < Residual < 2.5 feet	50%	53%	55%	55%	57%	63%	67%
Mean Error		0.2	-0.1	0.0	-0.1	-0.4	-0.1
Absolute Mean Error		3.2	3.0	2.9	3.0	2.6	2.5
Root Mean Square of Error		4.4	4.3	4.0	4.2	3.7	3.7
Nash–Sutcliffe Efficiency		0.99	0.99	0.99	0.99	0.99	0.99
No of Targets		1242	1260	1115	1114	446	447

Parameter Sensitivity and Predictive Uncertainty Analysis

SJRWMD contracted John Doherty, the developer of PEST, to conduct a predictive uncertainty analysis including evaluation of parameter sensitivities. This section of the report provides a brief summary of that work. A full description of the analysis is presented in Appendix I.

The predictive uncertainty analysis included the calculation of the uncertainties associated with some of the most important predictions made by the NFSEG model. These predictions included both the values of water levels and river and spring flows, as well as changes in these water levels and flows resulted from changes in pumping. To make these predictions, pumping within the North Florida water supply planning region was set to rates projected to occur 2035, while in the rest of the model domain pumping was assumed to be the same as in 2009. Recharge was assumed to be the same in both 2009 and 2035. The first step in this uncertainty evaluation was to conduct a linear uncertainty analysis, which is based on the assumption that the uncertainty estimates are independent of model parameter values. The results of this step were then used to generate two sets of parameters ($k-\delta k$ and $k+\delta k$) for each prediction of interest, such that the two parameter sets are expected to produce predictions that are one standard deviation above (for parameter set, $k+\delta k$) or below (for parameter set, $k-\delta k$) the value predicted using the parameter values from the calibrated model. The intent of this two-step, semi-linear process was to produce uncertainty estimates that were less subject to issues associated with the calculation of finite-difference derivatives. The predictions used in the analysis are listed in Table 4-1.

Table 4-1. List of predictions used in the uncertainty analysis

Prediction name	Description
w00202_09	UFA observation well near Lake Brooklyn
w00878_09	UFA observation well near Putnam County MFL lakes
qr09_iche_sprgrp	Ichetucknee Springs Group
qs09_2320500	Baseflow to the Suwannee River near Branford, Florida
qs09_2321500	Baseflow to the Santa Fe River near Worthington Springs
qs09_2322500	Baseflow to the Santa Fe River near Fort White

The results of the predictive uncertainty analysis are presented in Table 4-2.

Table 4-2. The results of predictive uncertainty analysis

Prediction	Value of prediction calculated using \underline{k}	Value of predictive change from 2009 to 2035 calculated using \underline{k}	Value of predictive change from 2009 to 2035 calculated using $\underline{k}-\delta k$	Value of predictive change from 2009 to 2035 calculated using $\underline{k}+\delta k$
w00202_09 ¹	78.37	1.3383	1.2311	1.4223
w00878_09 ¹	27.16	-1.2176	-1.4508	-0.9865
qr09_iche_sprgrp ²	-255.54	-12.8240	-13.1784	-12.4925
qs09_2320500 ²	-4067.08	-65.3840	-65.4740	-63.9390
qs09_2321500 ²	-36.00	-0.1455	-0.1453	-0.1440
qs09_2322500 ²	-676.95	-23.6933	-24.3685	-22.9294

¹Values are in feet. Positive predictive changes mean drawdown.

²Values are in cubic feet per second. Negative predictive changes mean reduction in flows.

Table 6.3 in Appendix J shows the results of predictive model runs undertaken to assess predictive difference uncertainty intervals. The third column of Table 4-2 shows the predicted drawdown or flow reduction due to pumping in 2035 using the NFSEG model with some preliminarily calibrated parameter estimates (the NFSEG v1.0 values were not available at the time of the analysis). The last two columns of Table 4-2 show the range of predicted values generated using the ‘bounding’ parameter sets ($\underline{k}-\delta k$ and $\underline{k}+\delta k$) for each prediction of interest.

The initial results shown in Table 6.3 in Appendix J indicate that the uncertainties associated with these predictive differences may be very small. The results are consistent with the findings of the uncertainty analysis performed for East-Central Florida Transient model (Sepulveda and Doherty, 2014).

Estimating uncertainties in predictions generated by groundwater models, especially large models like NFSEG, is a very challenging task. The uncertainty intervals that are quantified in this analysis using linear and semi-linear methods are reflective of parameter uncertainty only. No predictive noise term has been included in these analyses.

As stated previously, the predictions presented in Table 6.3 in Appendix J were not generated using the final version of NFSEG v1.0. Despite this, these results should provide a useful initial assessment of the magnitude of the predictive uncertainty, and represent a much more meaningful assessment of predictive uncertainty than that provided by a traditional sensitivity analyses. The uncertainty analysis also indicated the need to account for nonlinear relation between predictive uncertainty and parameter values in some instances. In addition, no return water due to increase in irrigation was simulated in 2035 simulations. Therefore, the predicted drawdown and flow reductions may be considered conservative in this regard. The details of the analysis is presented in Appendix J.

Model Capabilities and Limitations

The NFSEG model was designed to be a tool that can be used to evaluate inter-district and interstate groundwater pumping impacts. A primary function of the NFSEG model is to simulate the regional effects of pumping on groundwater levels, stream base flows, and spring flows. It has been calibrated and configured in a manner that is consistent with generally accepted standards to enable reliable fulfillment of this objective. In particular, a wide variety of observation types were employed in the development of the model, including observations that are directly and indirectly related to the head and flow predictions of interest. The differences between groundwater levels and their model-simulated equivalents were consistent with the goals specified at the outset of the project. In addition, predictive uncertainty analyses indicate that model may be capable of simulating changes in flows and heads with an accuracy that is comparable to or better than models currently used for planning or regulatory purposes. These and other analyses also indicate that the uncertainty in predicting changes in water levels and flows is generally less than the uncertainty in predicting the absolute value of water levels and flows.

Notwithstanding the above capabilities, a number of important model limitations should be noted. Like any model, the uncertainty in model predictions of changes in water levels and flows is generally lower in areas where observed data is abundant (i.e., North Florida Water Supply Planning Region), and greater in areas where observed data is limited, such as in Georgia. The same holds for hydrostratigraphic units with abundant head, spring flow, and baseflow data, such as the Upper Floridan aquifer. In units where these data are sparse or nonexistent, such as the deeper zones of the Upper or Lower Floridan aquifers, predictions will most likely have larger levels of uncertainty. The ability of the model to estimate drawdown is limited by the model grid-cell size and availability of observation data (as described above), which is true of any numerical regional model. For example, the ability of the model to calculate drawdown over areas completely contained in one or a few grid cells is limited due to grid-cell averaging.

The primary use of the model is for simulation of groundwater- levels of Floridan aquifer system, and exchanges of water between the Floridan aquifer system and contiguous surface water features. Representation of groundwater flows and levels in the surficial aquifer system is more difficult because of the relative lack of data for representation of the surficial aquifer system. Therefore, simulations of flow exchanges with, and water levels within, the Floridan aquifer system are expected to have a lower predictive uncertainty than those of the surficial aquifer system. Simulated flows and changes in flows at individual springs are also likely to be more uncertain than corresponding simulated values for collections of springs or for river reaches that contain such collections.

The NFSEG groundwater model represents a major advancement over existing groundwater models that cover parts or all of the North Florida Regional Planning Area. These improvements are summarized as follows:

- A. Ability to evaluate inter-district and inter-state groundwater pumping impacts by positioning model lateral boundaries at great distances from the NFRWSP planning area, in many instances at the approximate physical limits of the system;
- B. Improved methodology for determining rates of recharge and maximum saturated ET through the use of HSPF surface-water modeling;
- C. Improved calibration process and representation of aquifer heterogeneity through use of PEST;
- D. Enhanced calibration rigor obtained by matching water levels and flows to two calibration periods (calendar years 2001 and 2009) that represent significantly different hydrologic conditions;
- E. Improved estimates of agricultural and domestic-self-supply water use;
- F. Improved rigor in representation of dual-zone pumping wells through representation with the USGS MNW2 Package;
- G. Expanded availability of water-level data (used in the model calibration) in areas of limited data availability through implementation of sophisticated statistical estimation techniques;
- H. Improved representation of ET extinction depth that takes account of soil type and land cover;
- I. Inclusion of additional calibration constraints not used in the development of many of the models currently used in Florida, including: vertical head differences between adjacent aquifers, horizontal-head differences between corresponding adjacent points in the same aquifer, and a more extensive set of stream baseflow 'pickup' and spring-group observations.
- J. Collaboration with stakeholders by way of the NFSEG Technical Team throughout the development process.

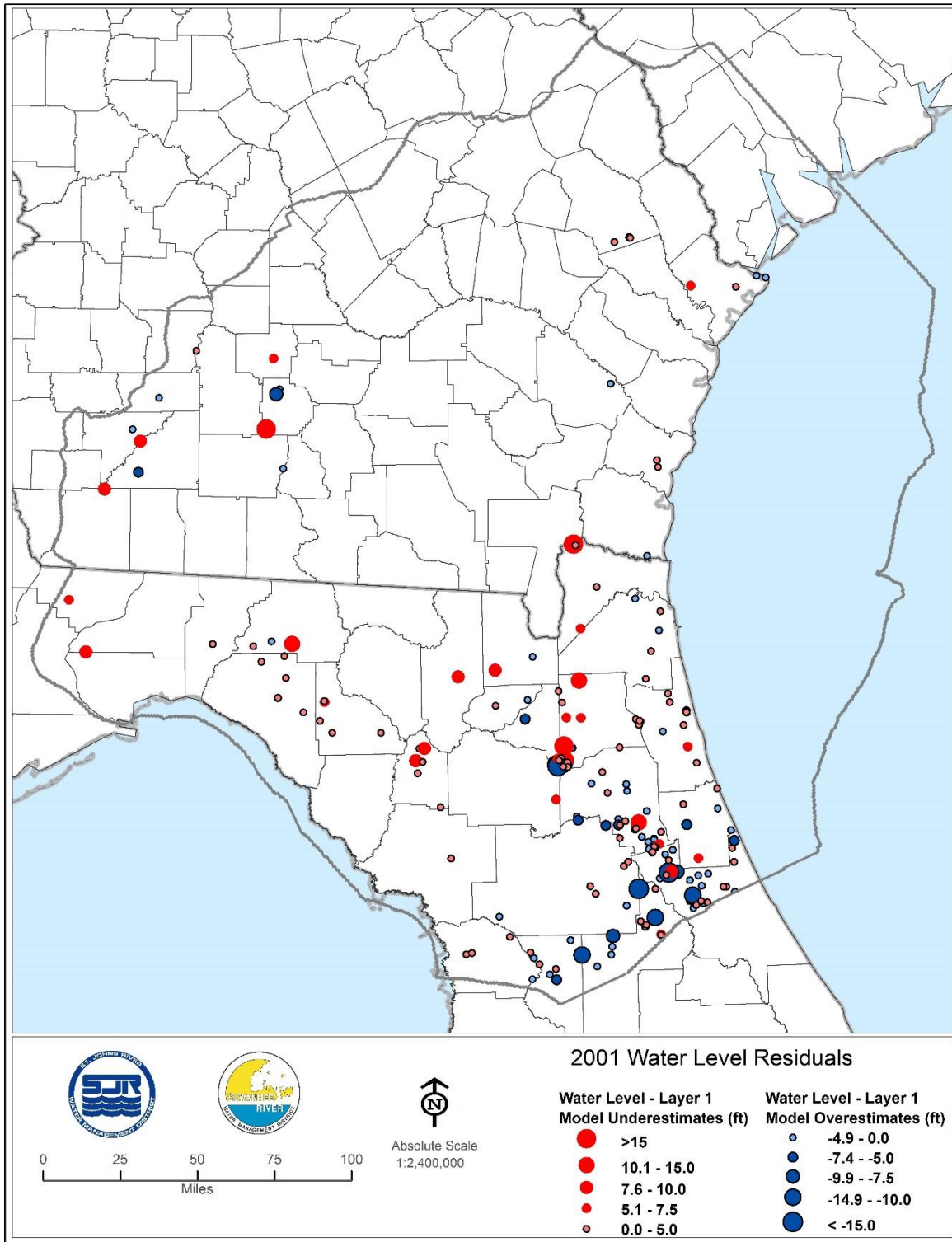


Figure 3-18. Residuals of Hydraulic Head, Model Layer 1, 2001

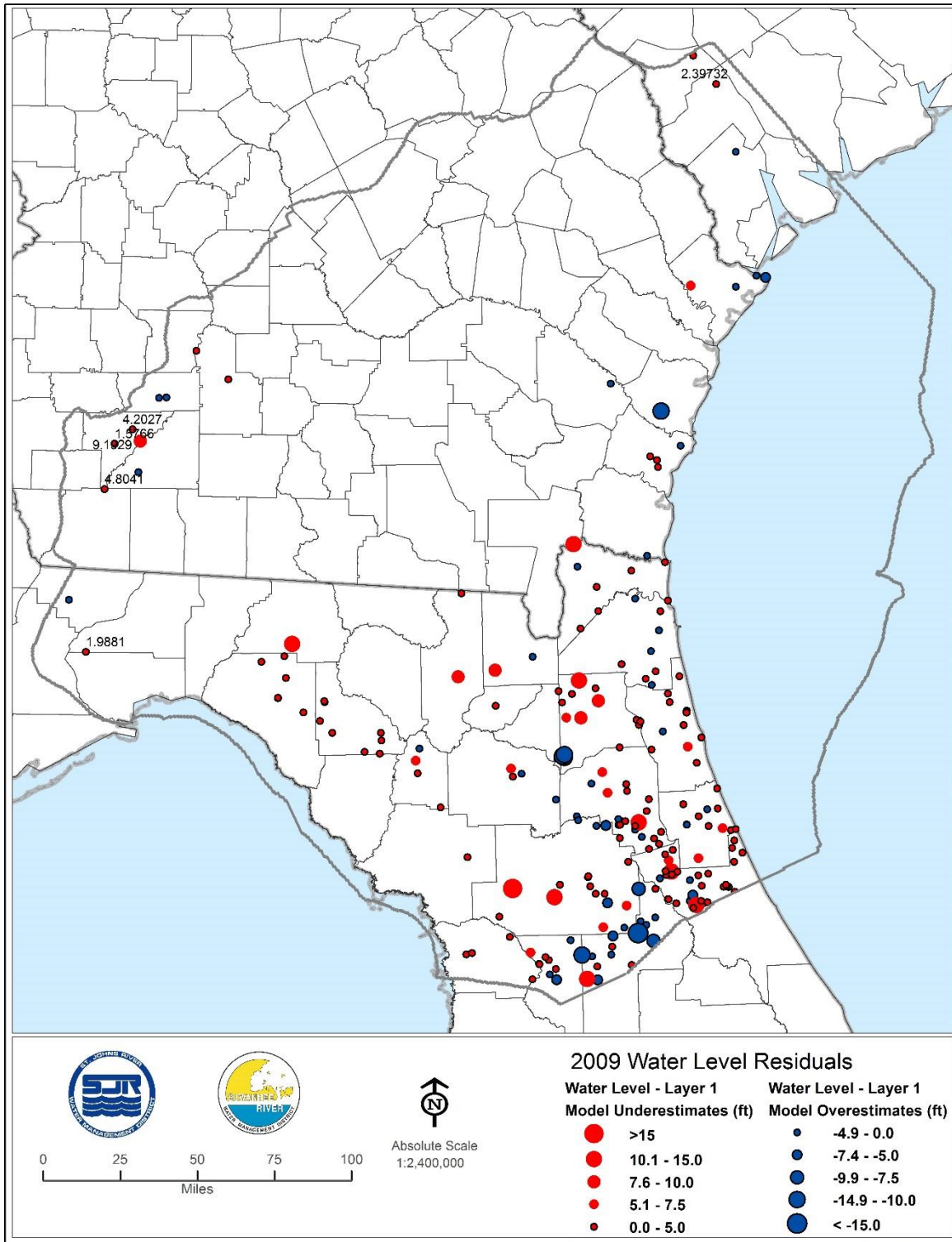


Figure 3-19. Residuals of Hydraulic Head, Model Layer 1, 2009

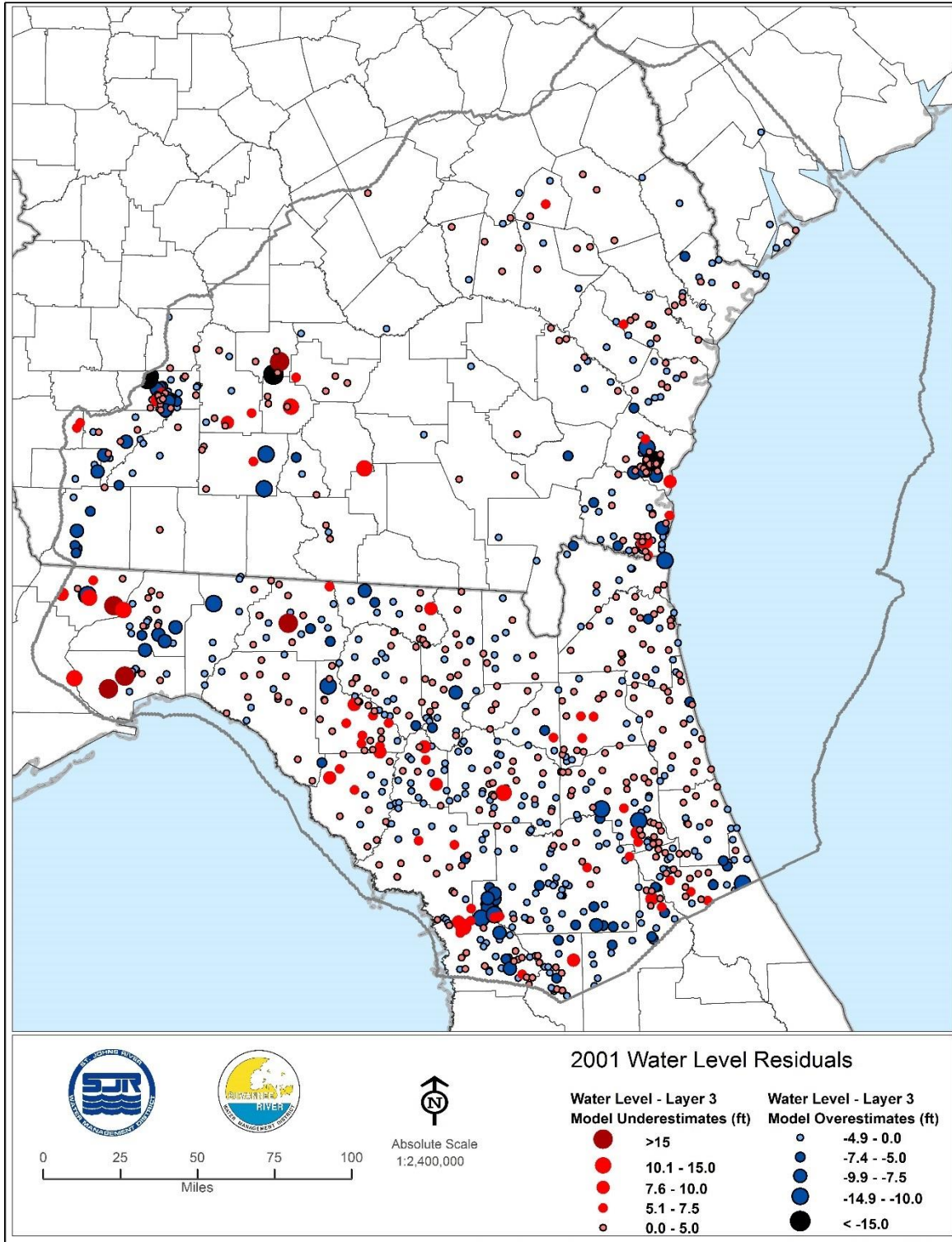


Figure 3-20. Residuals of Hydraulic Head, Model Layer 3, 2001

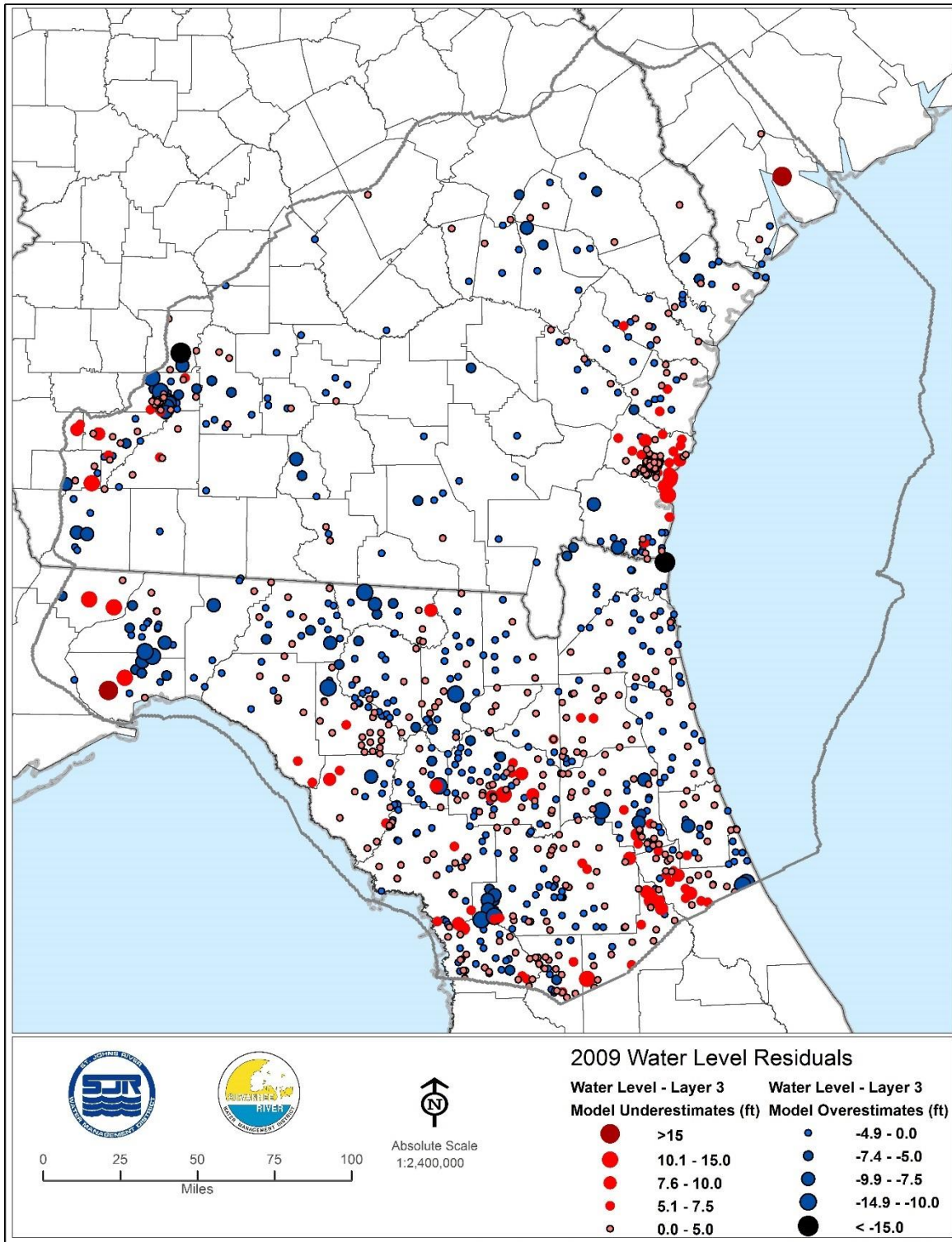


Figure 3-21. Residuals of Hydraulic Head, Model Layer 3, 2009

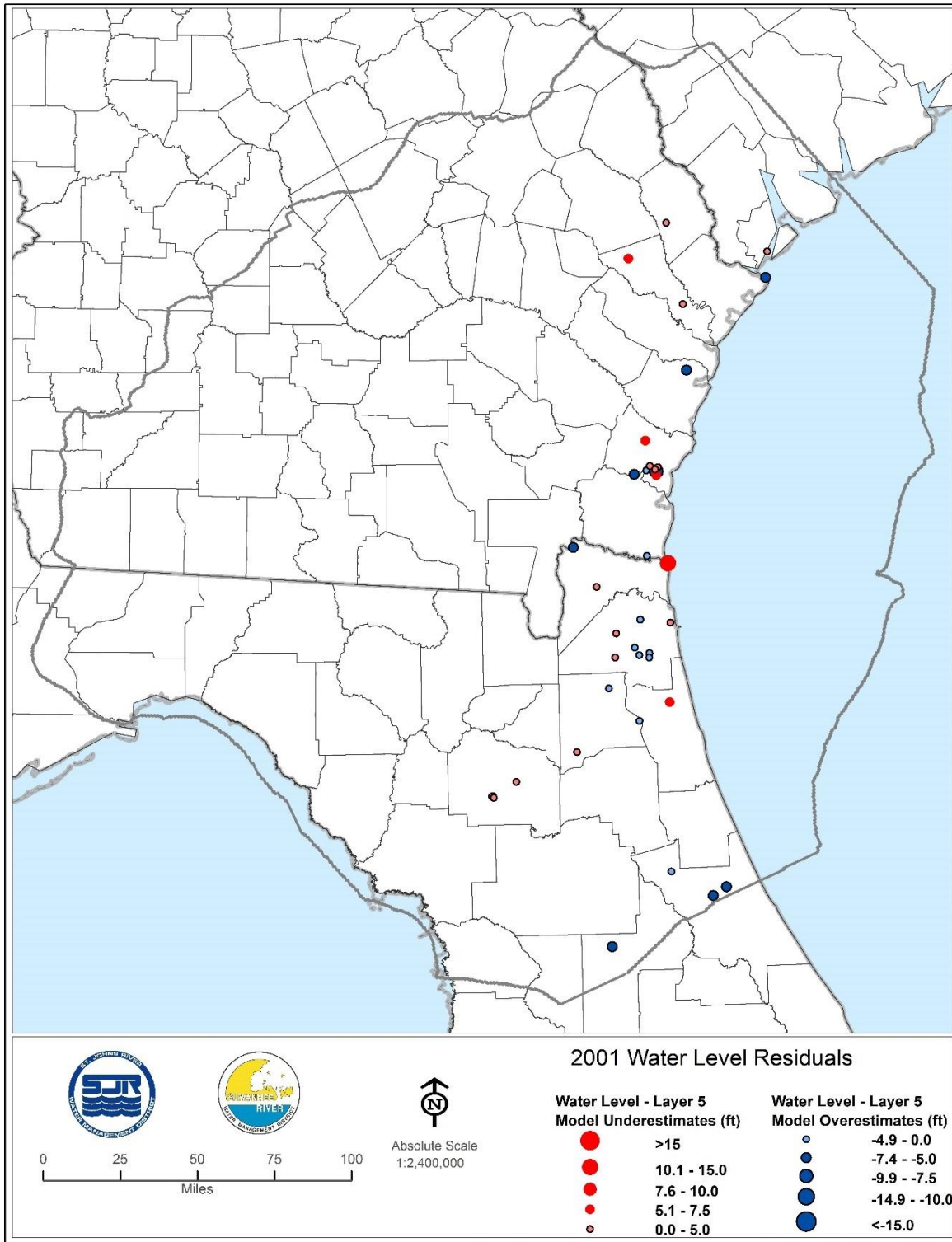


Figure 3-22. Residuals of Hydraulic Head, Model Layer 5, 2001

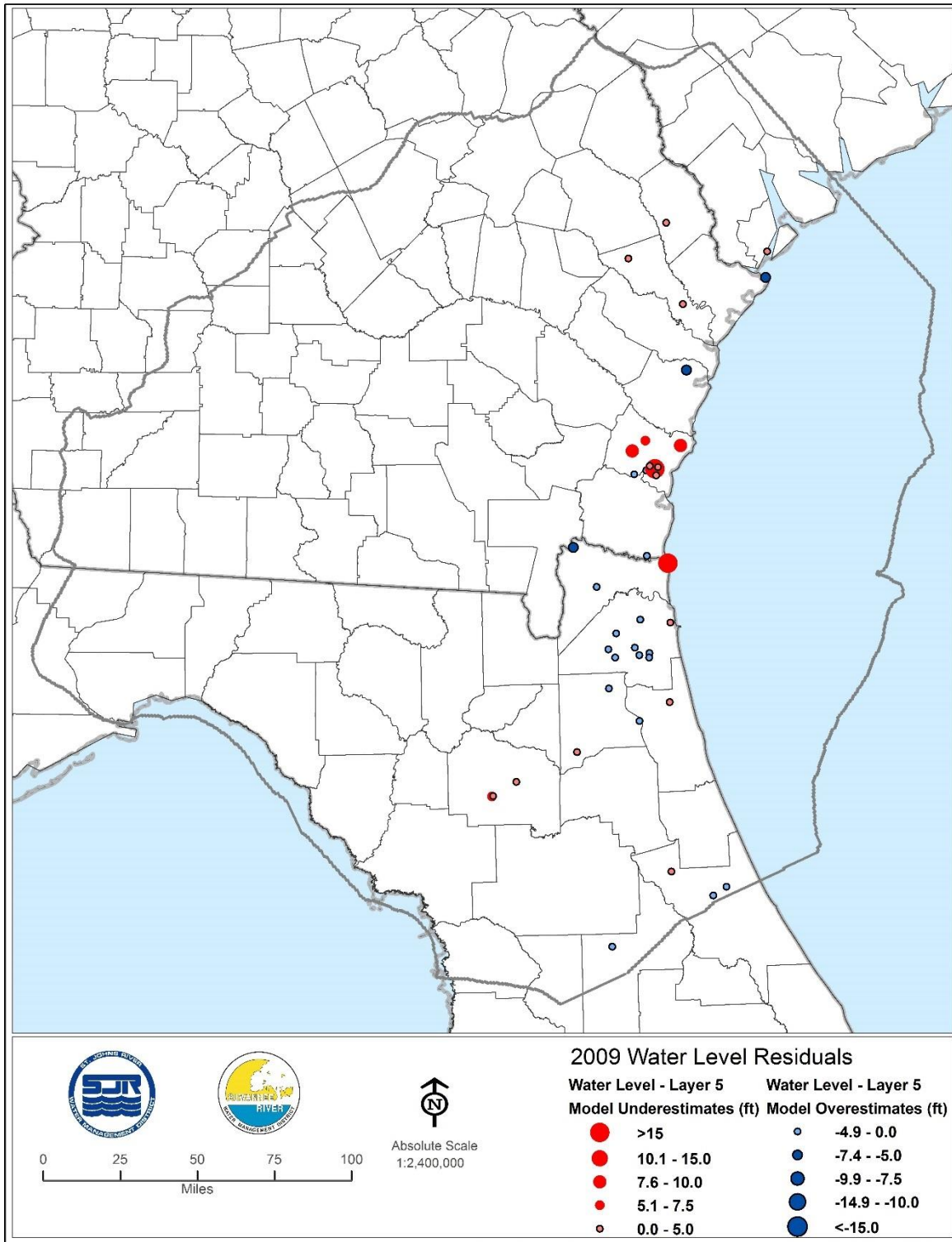


Figure 3-23. Residuals of Hydraulic Head, Model Layer 5, 2009

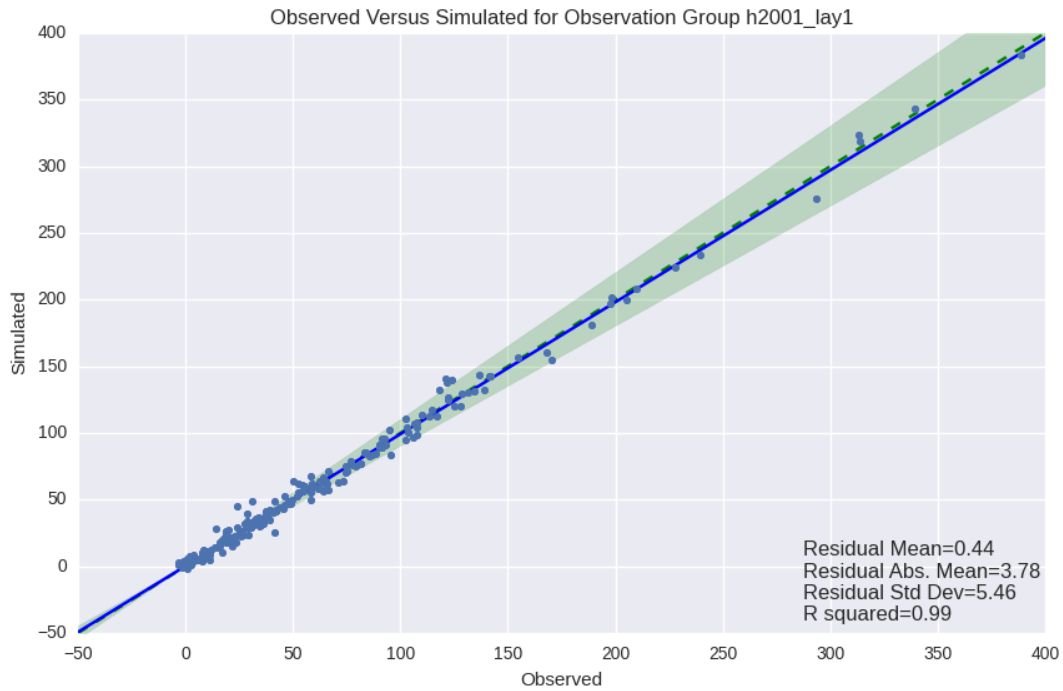


Figure 3-24. Simulated vs. Observed Hydraulic Head (feet), Model Layer 1, 2001

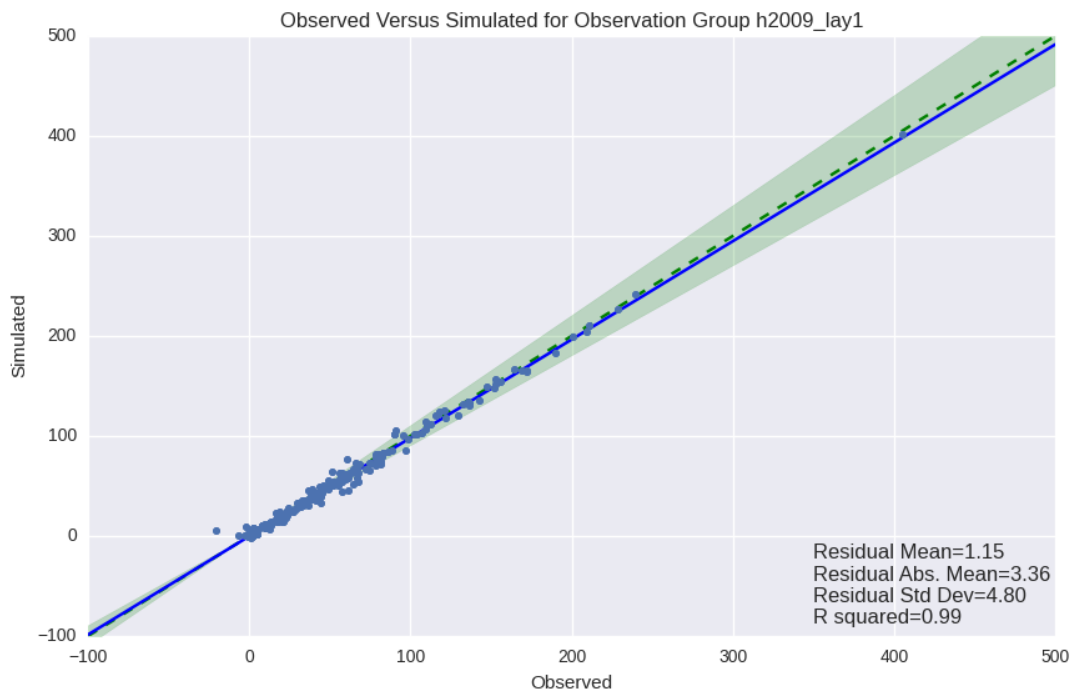


Figure 3-25. Simulated vs. Observed Hydraulic Head (feet), Model Layer 1, 2009

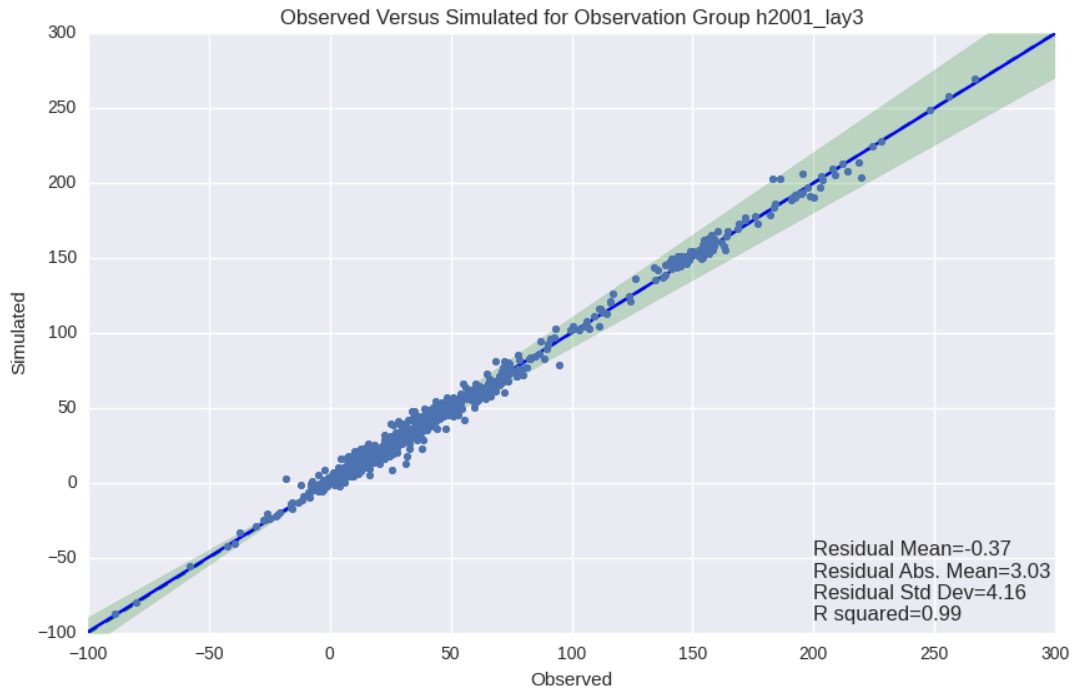


Figure 3-26. Simulated vs. Observed Hydraulic Head (feet), Model Layer 3, 2001

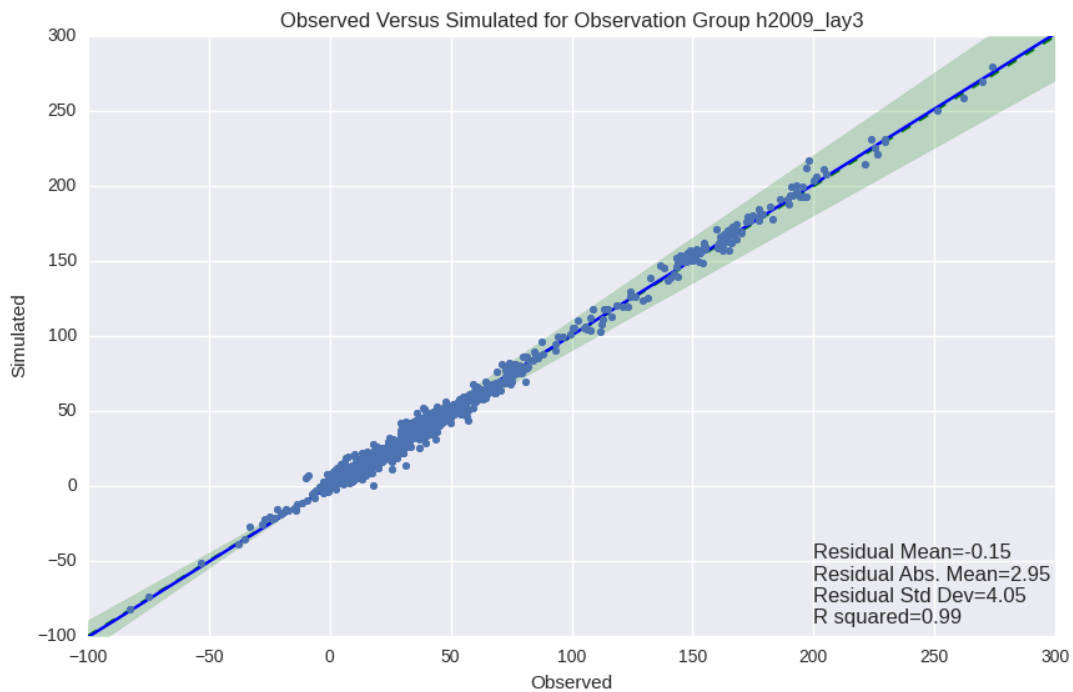


Figure 3-27. Simulated vs. Observed Hydraulic Head (feet), Model Layer 3, 2009

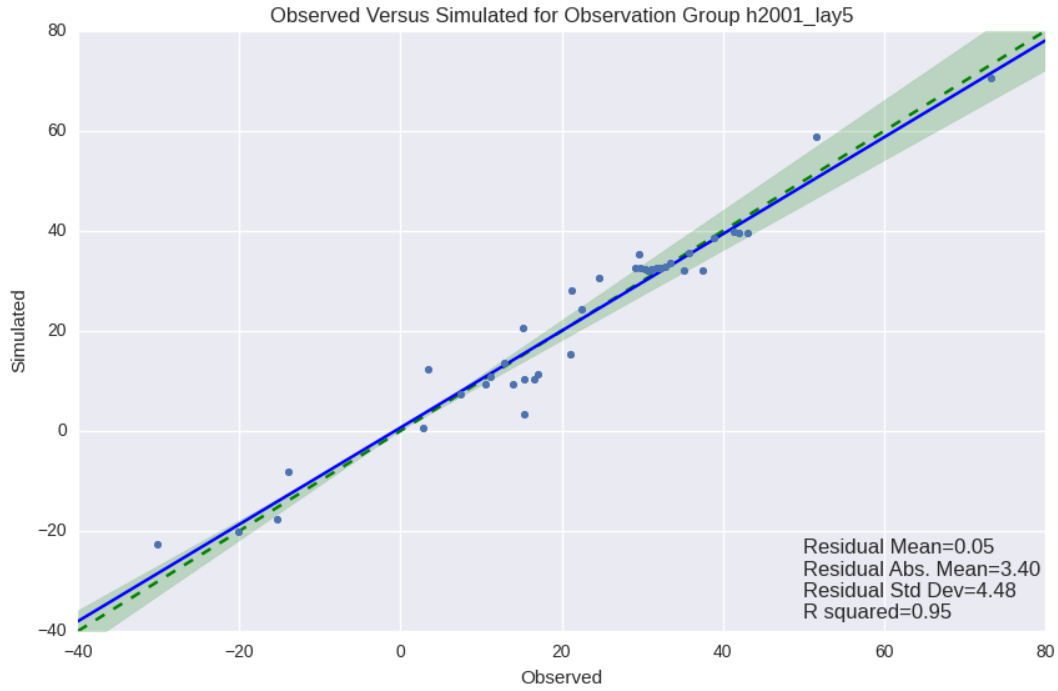


Figure 3-28. Simulated vs. Observed Hydraulic Head (feet), Model Layer 5, 2001

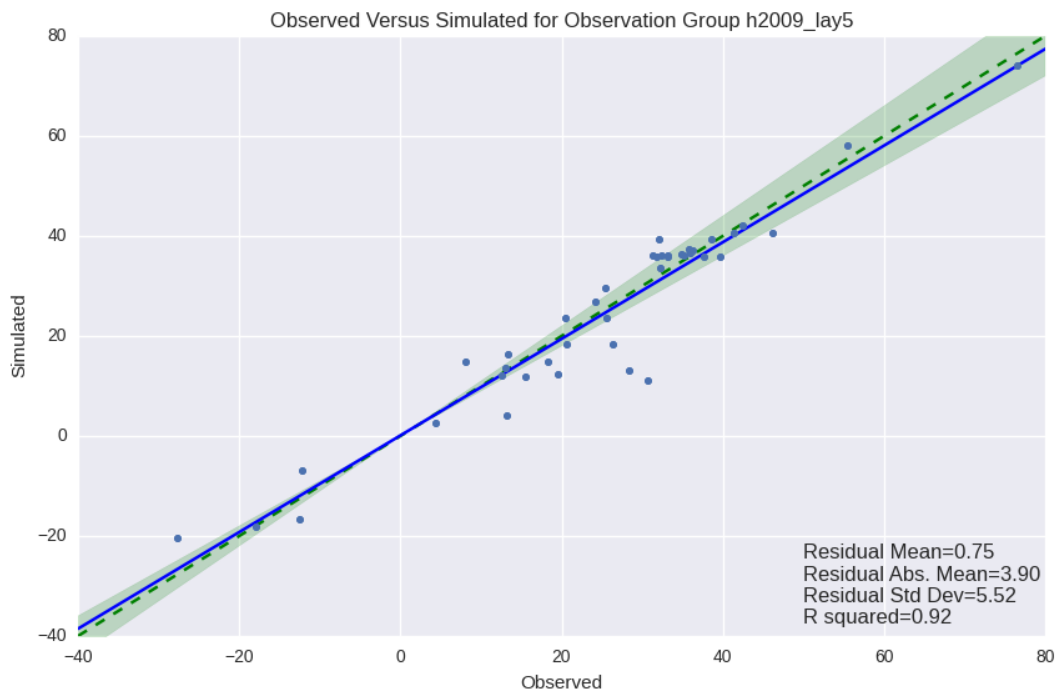


Figure 3-29. Simulated vs. Observed Hydraulic Head (feet), Model Layer 5, 2009

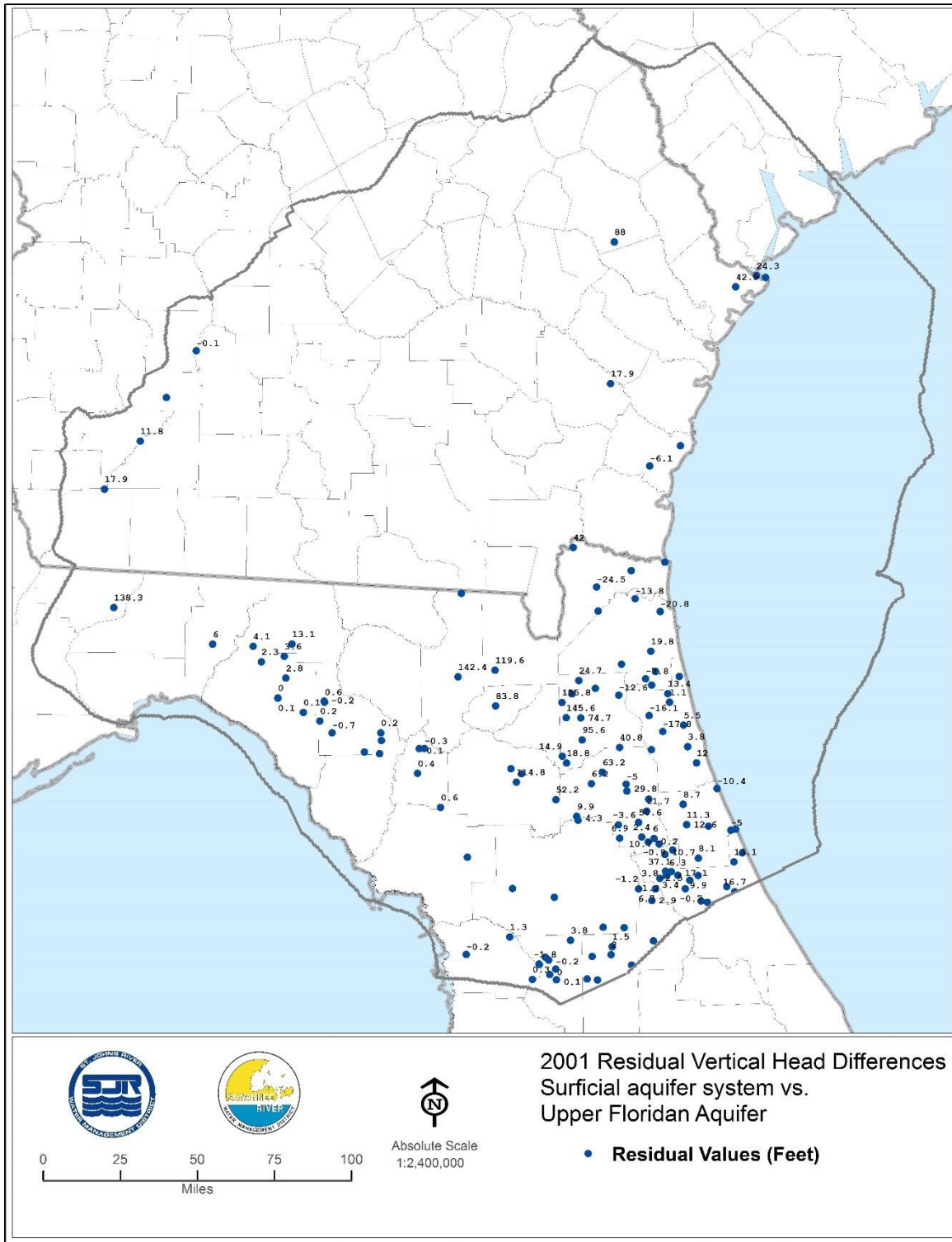


Figure 3-30. Residuals of Vertical Head Differences Between Model Layers 1 and 3, 2001

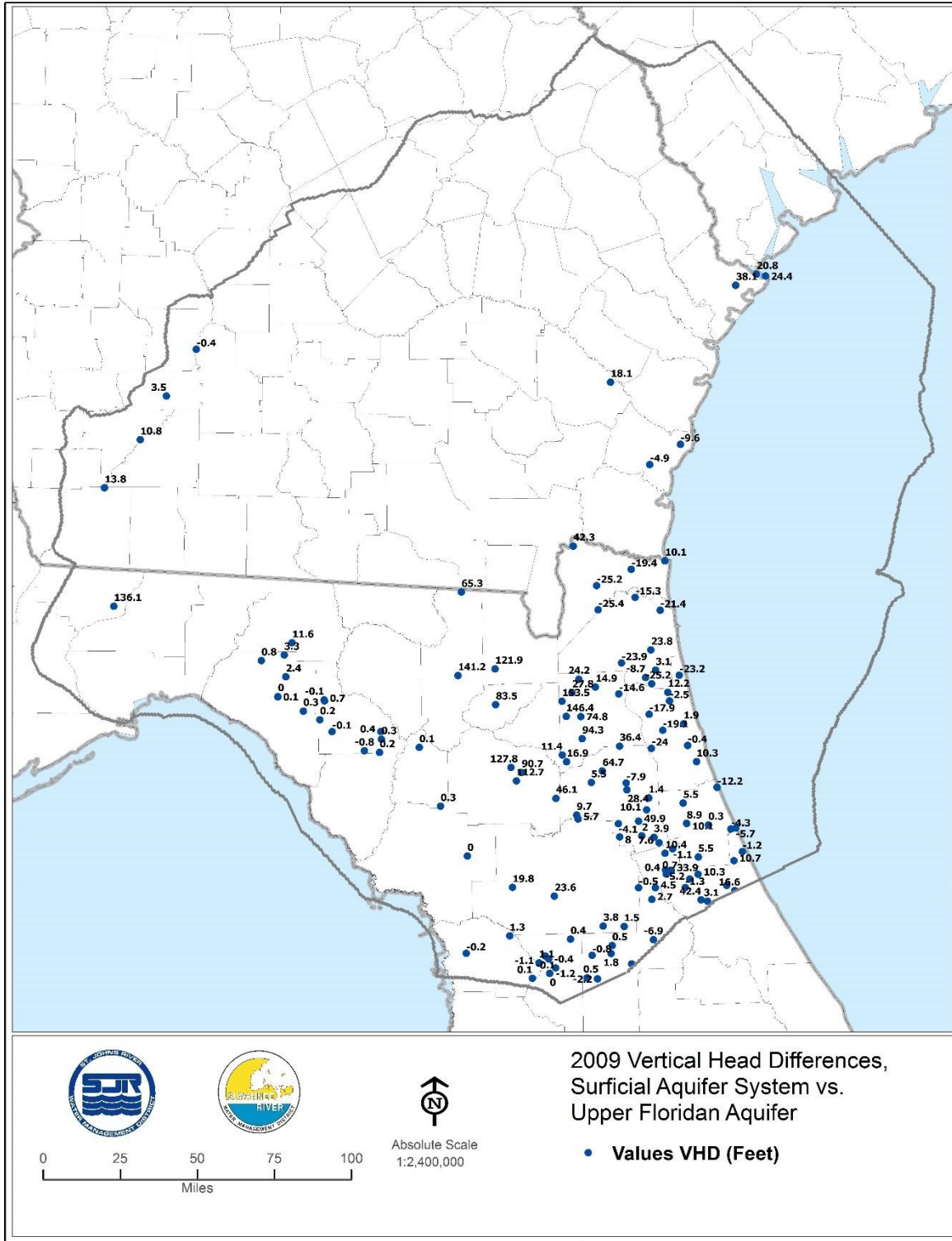


Figure 3-31. Residuals of Vertical Head Differences Between Model Layers 1 and 3, 2009

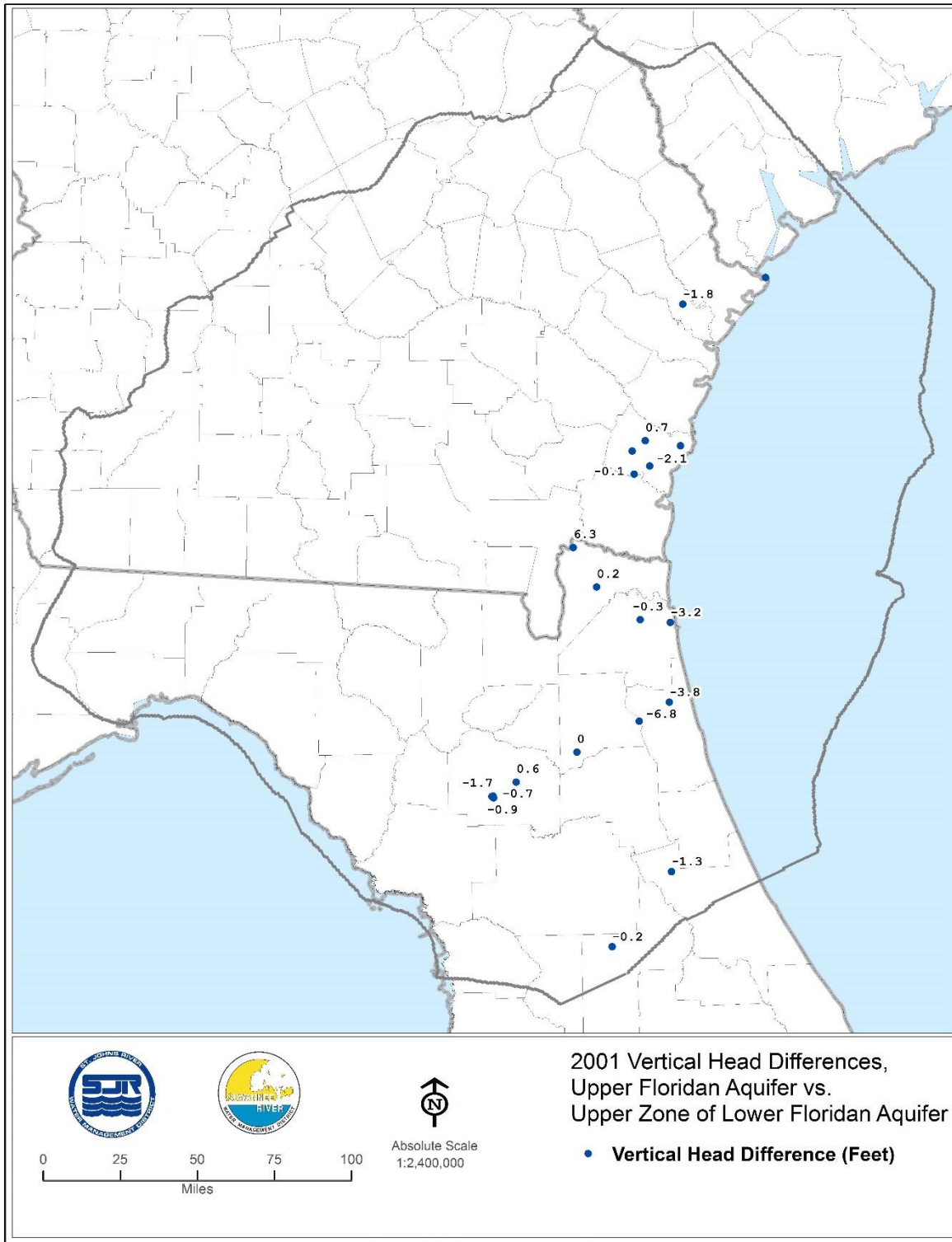


Figure 3-32. Residuals of Vertical Head Differences Between Model Layers 3 and 5, 2001

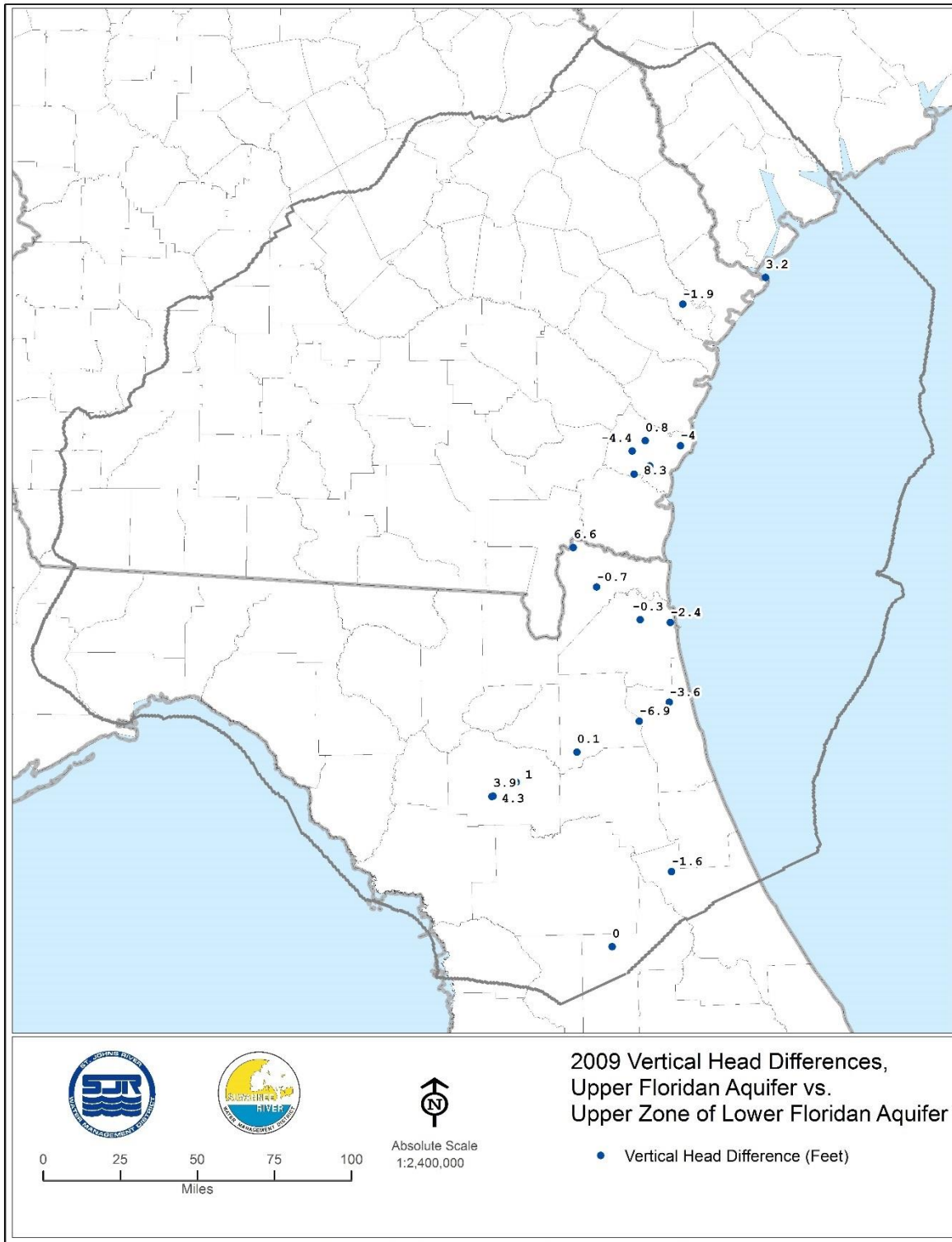


Figure 3-33. Residuals of Vertical Head Differences Between Model Layers 3 and 5, 2009

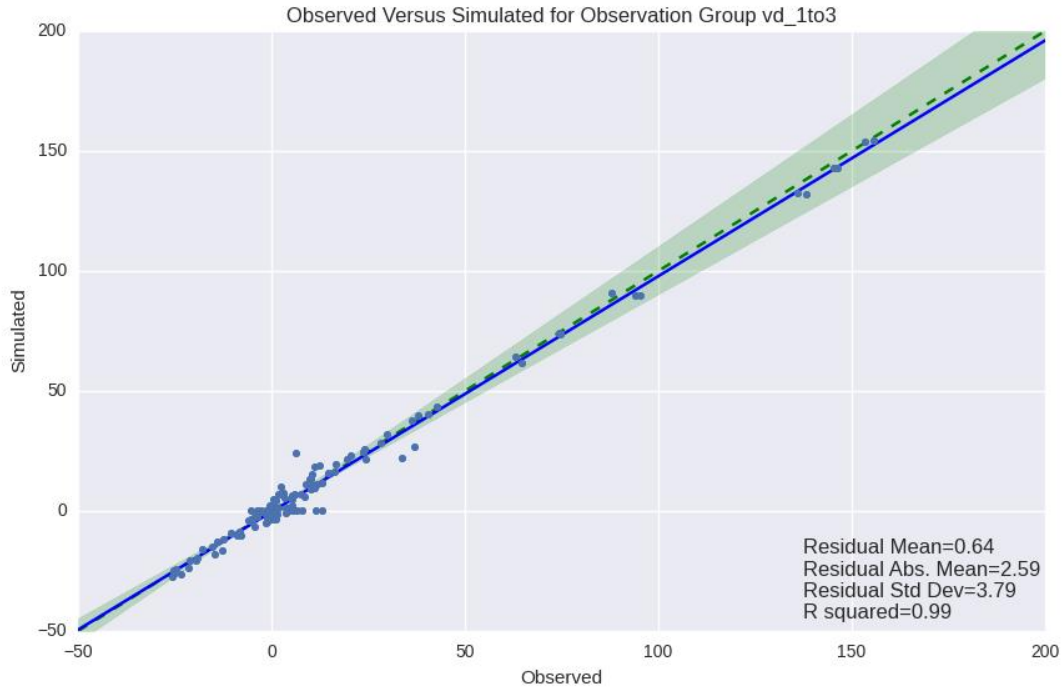


Figure 3-34. Simulated vs. Observed Vertical Head Differences (feet), Model Layers 1 to 3

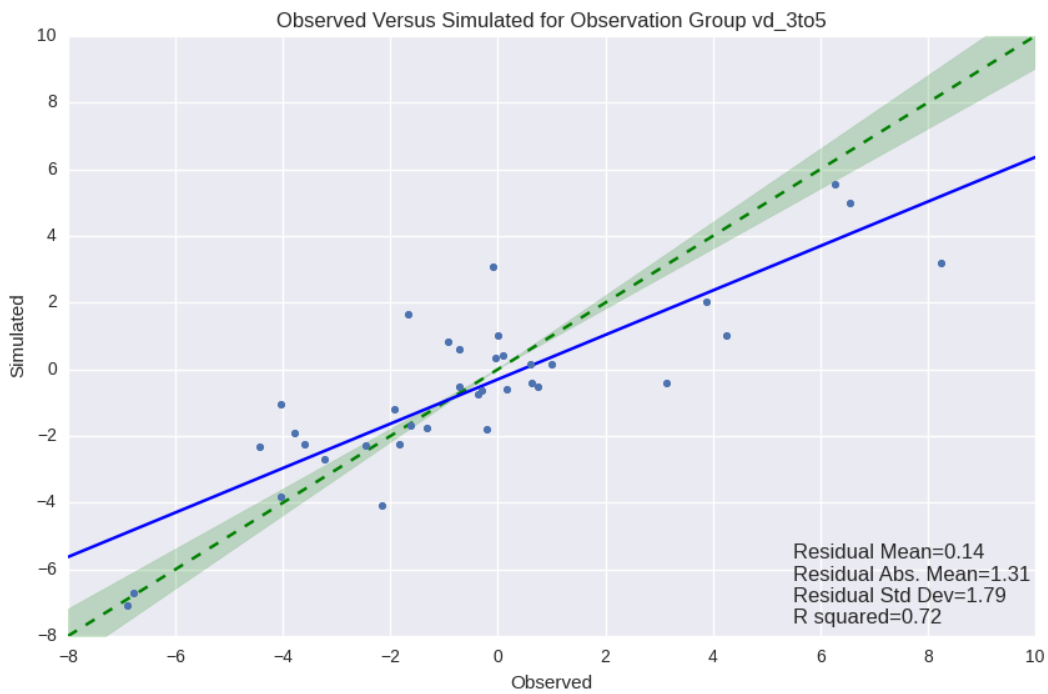


Figure 3-35. Simulated vs. Observed Vertical Head Differences (feet), Model Layers 3 to 5

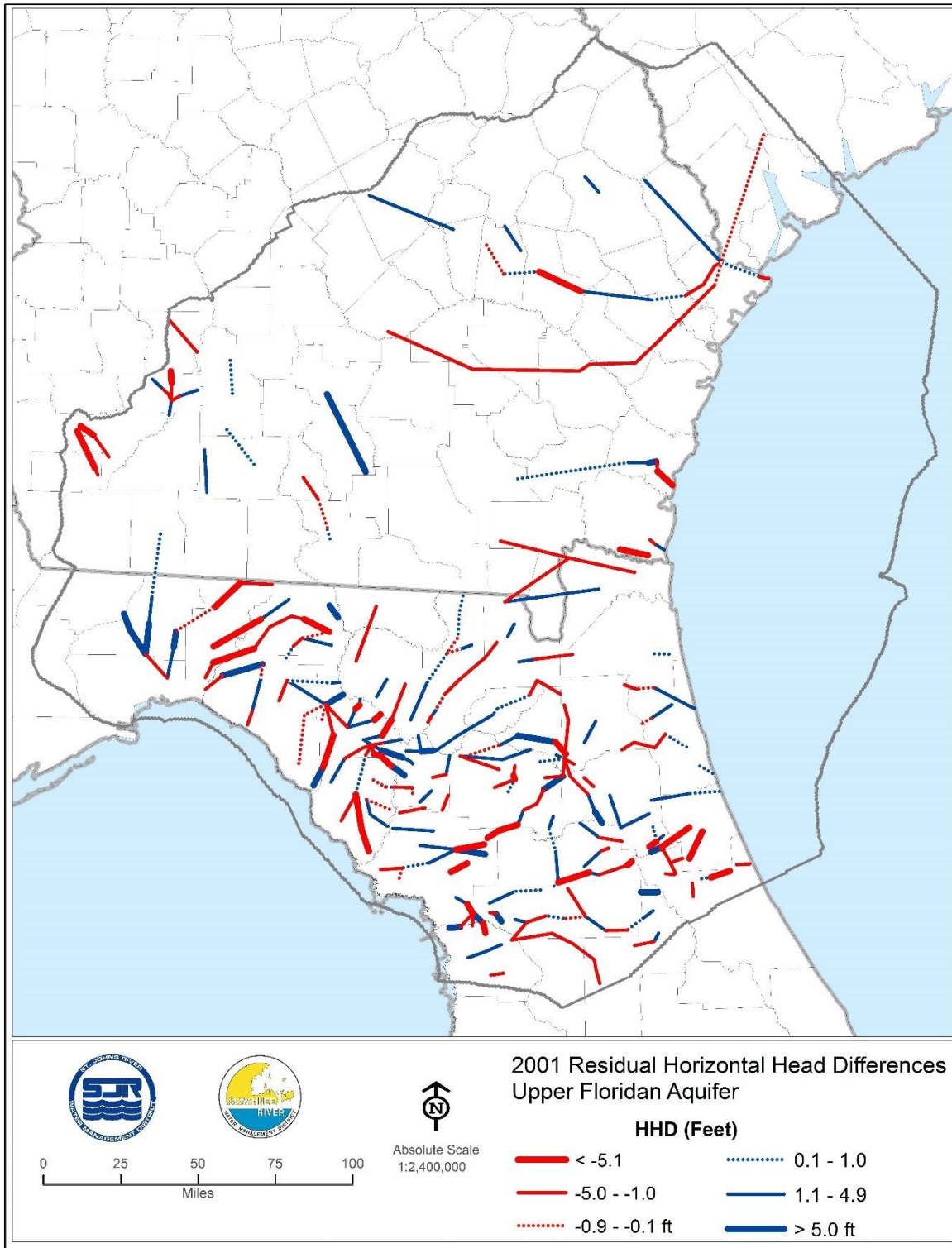


Figure 3-36. Residuals of Horizontal Head Differences, Model Layer 3, 2001

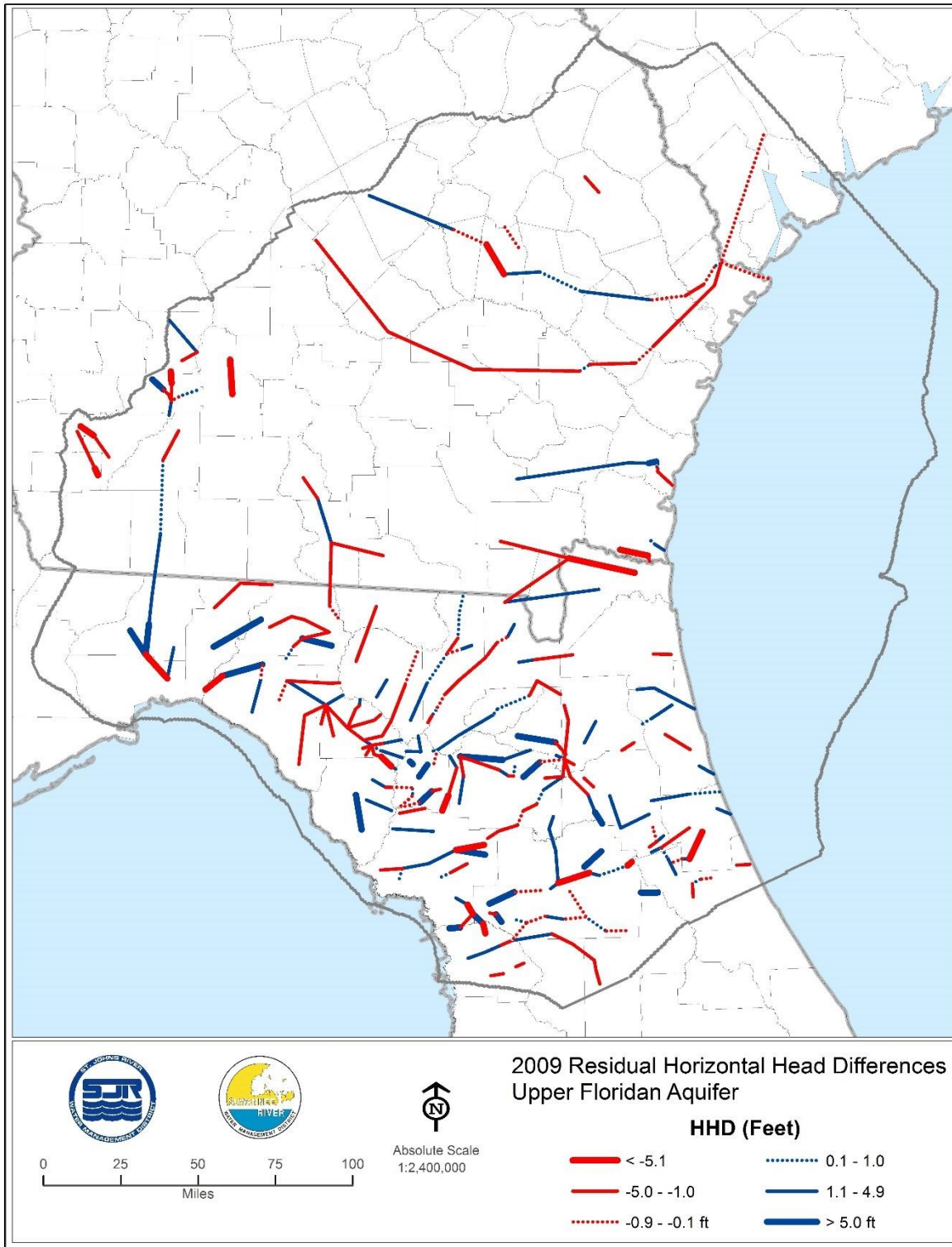


Figure 3-37. Residuals of Horizontal Head Differences, Model Layer 3, 2009

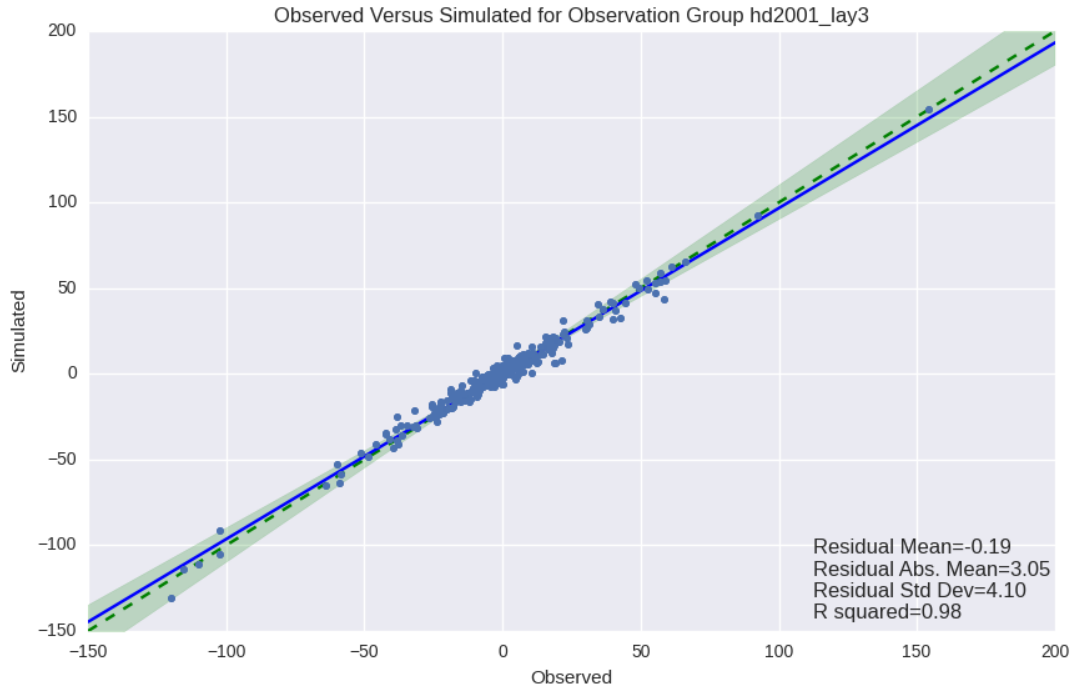


Figure 3-38. Simulated vs. Observed Horizontal Head Differences (feet), 2001

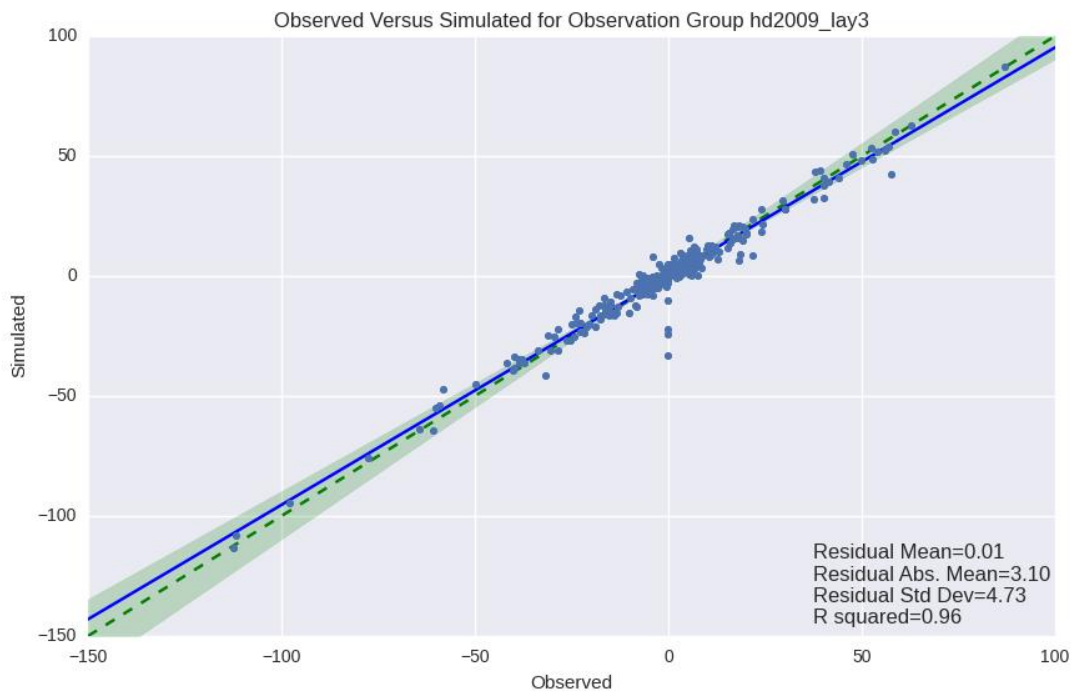


Figure 3-39. Simulated vs. Observed Horizontal Head Differences (feet), 2009

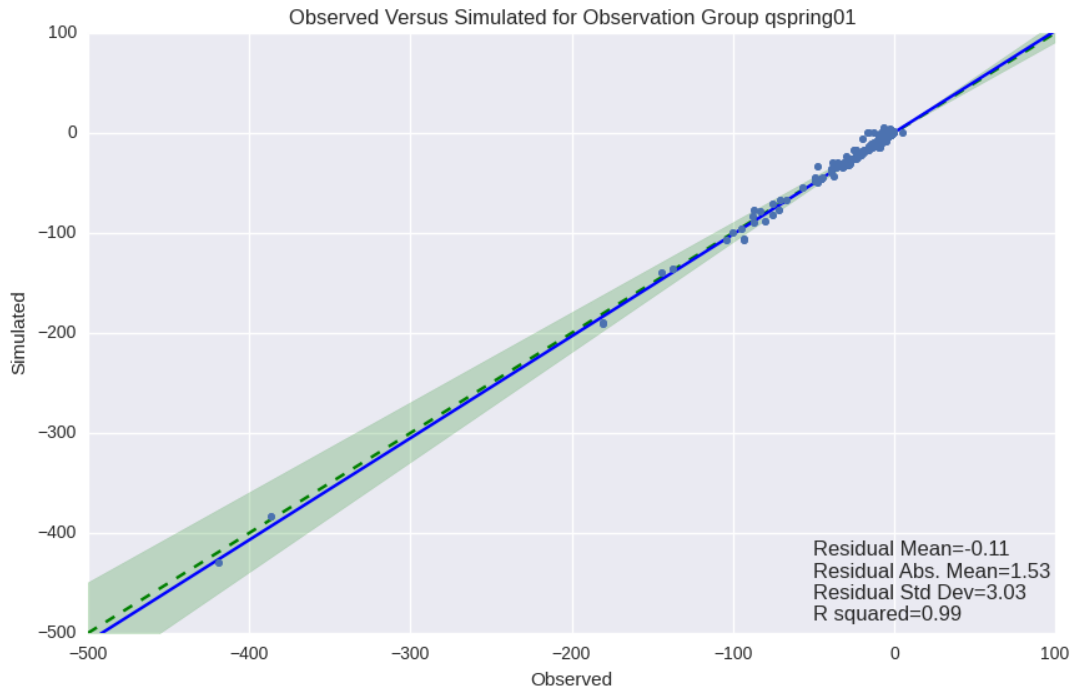


Figure 3-40. Simulated vs. Observed Spring Discharges (cfs), 2001

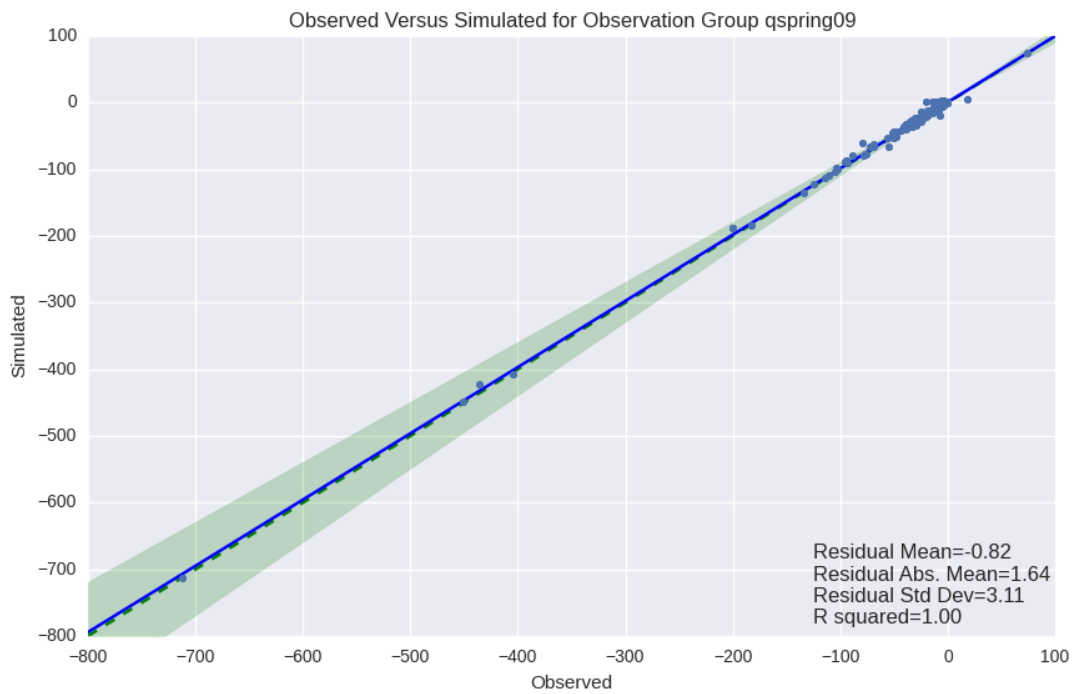


Figure 3-41. Simulated vs. Observed Spring Discharges (cfs), 2009

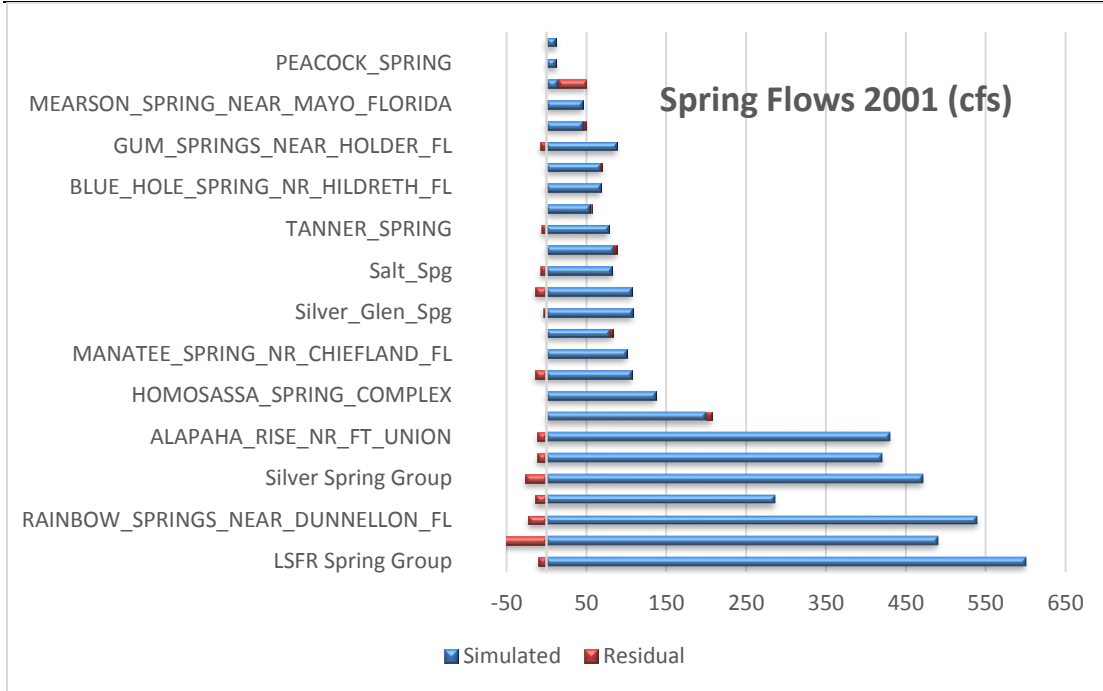


Figure 3-42. Simulated Spring Discharge for Selected Springs with Flow Residuals, 2001

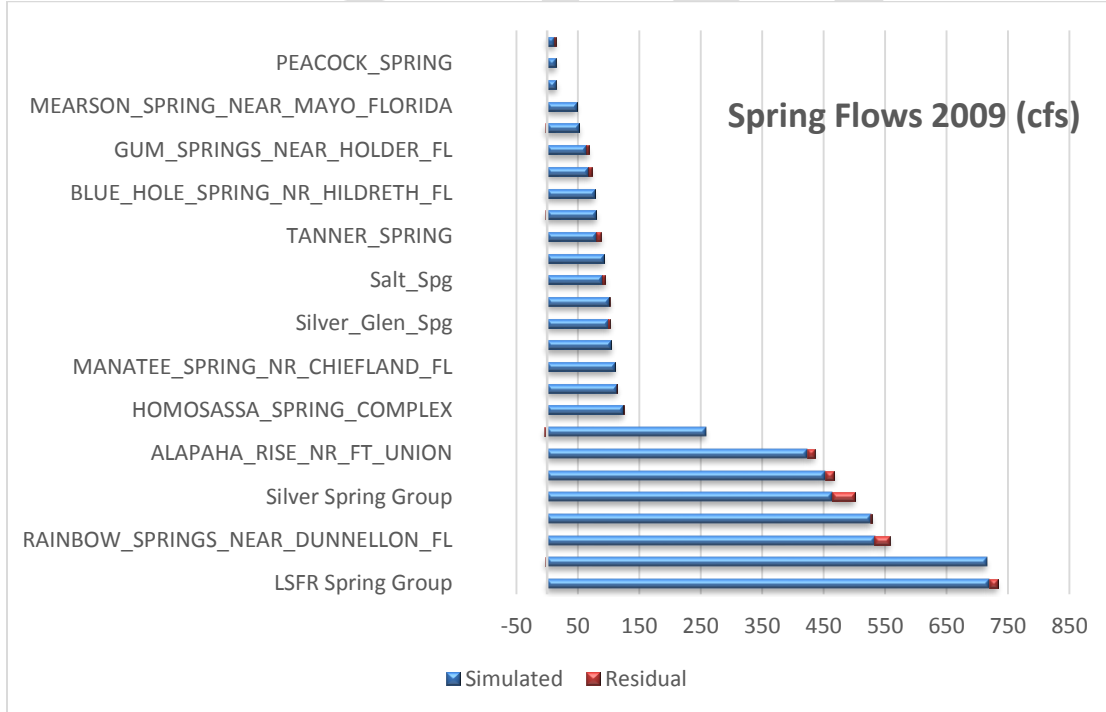


Figure 3-43. Simulated Spring Discharge for Selected Springs with Flow Residuals, 2009

Table 3-3. Simulated vs. Estimated Cumulative Baseflows, 2001 and 2009

Name	Year	Estimated Baseflow (cfs)	Simulated Baseflow (cfs)	Base Flow Residual (cfs)
qs01_2228000	2001	-587.4	-635.0	47.5
qs01_2231000	2001	-63.4	-68.3	4.9
qs01_2243000	2001	-7.5	-10.8	3.3
qs01_2315500	2001	-302.3	-32.6	-269.8
qs01_2317620	2001	-752.3	-736.2	-16.1
qs01_2319000	2001	-861.5	-849.4	-12.1
qs01_2320500	2001	-3568.0	-3317.9	-250.1
qs01_2321500	2001	-35.6	-34.8	-0.8
qs01_2322500	2001	-607.9	-608.0	0.1
qs01_2323500	2001	-4296.2	-4609.8	313.6
qs09_2228000	2009	-1298.1	-1104.8	-193.3
qs09_2231000	2009	-261.3	-125.6	-135.7
qs09_2243000	2009	-13.6	1.6	-15.3
qs09_2317620	2009	-1260.3	-1238.7	-21.6
qs09_2319000	2009	-1145.6	-1151.8	6.2
qs09_2323500	2009	-6014.3	-5860.4	-153.9

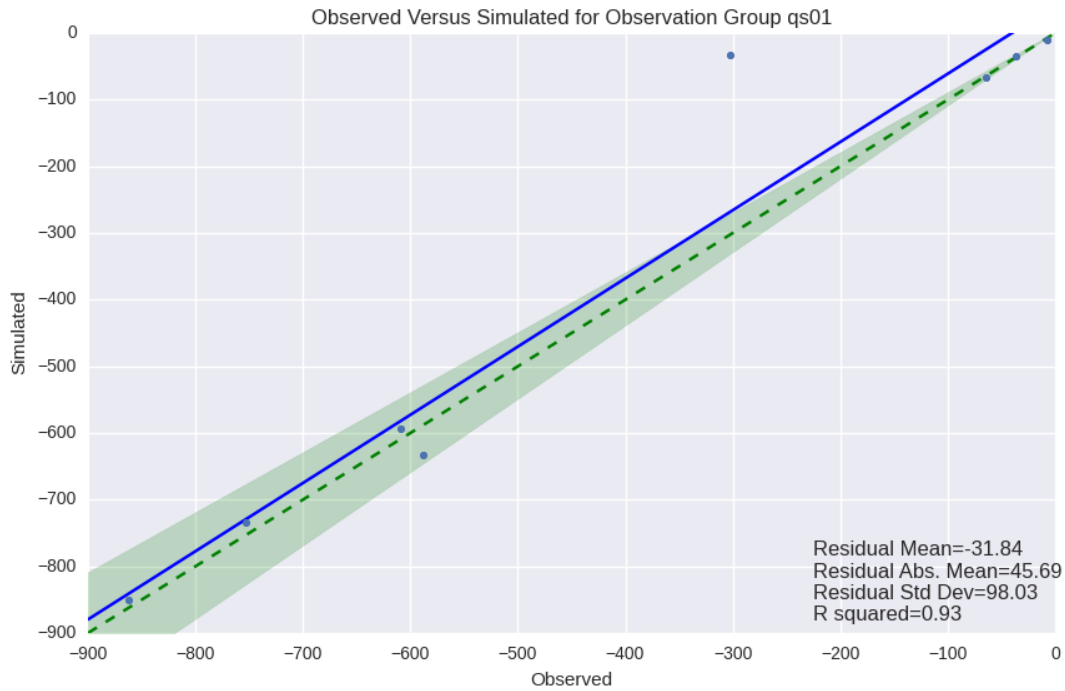


Figure 3-44. Simulated vs. Estimated Baseflows (cfs), 2001

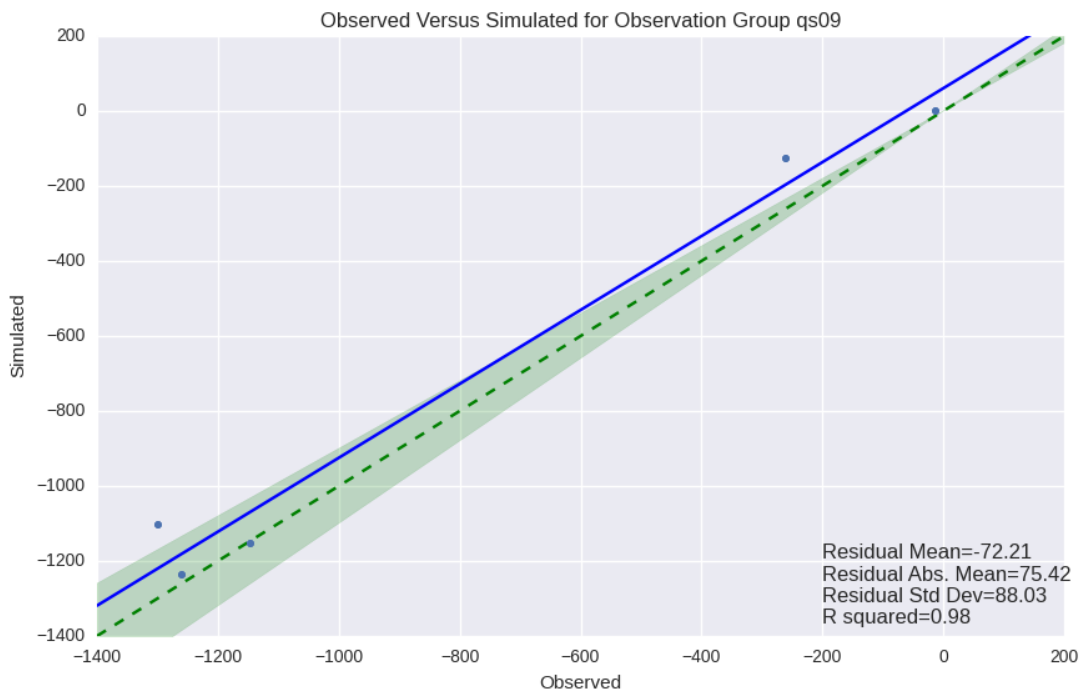


Figure 3-45. Simulated vs. Estimated Baseflows (cfs), 2009

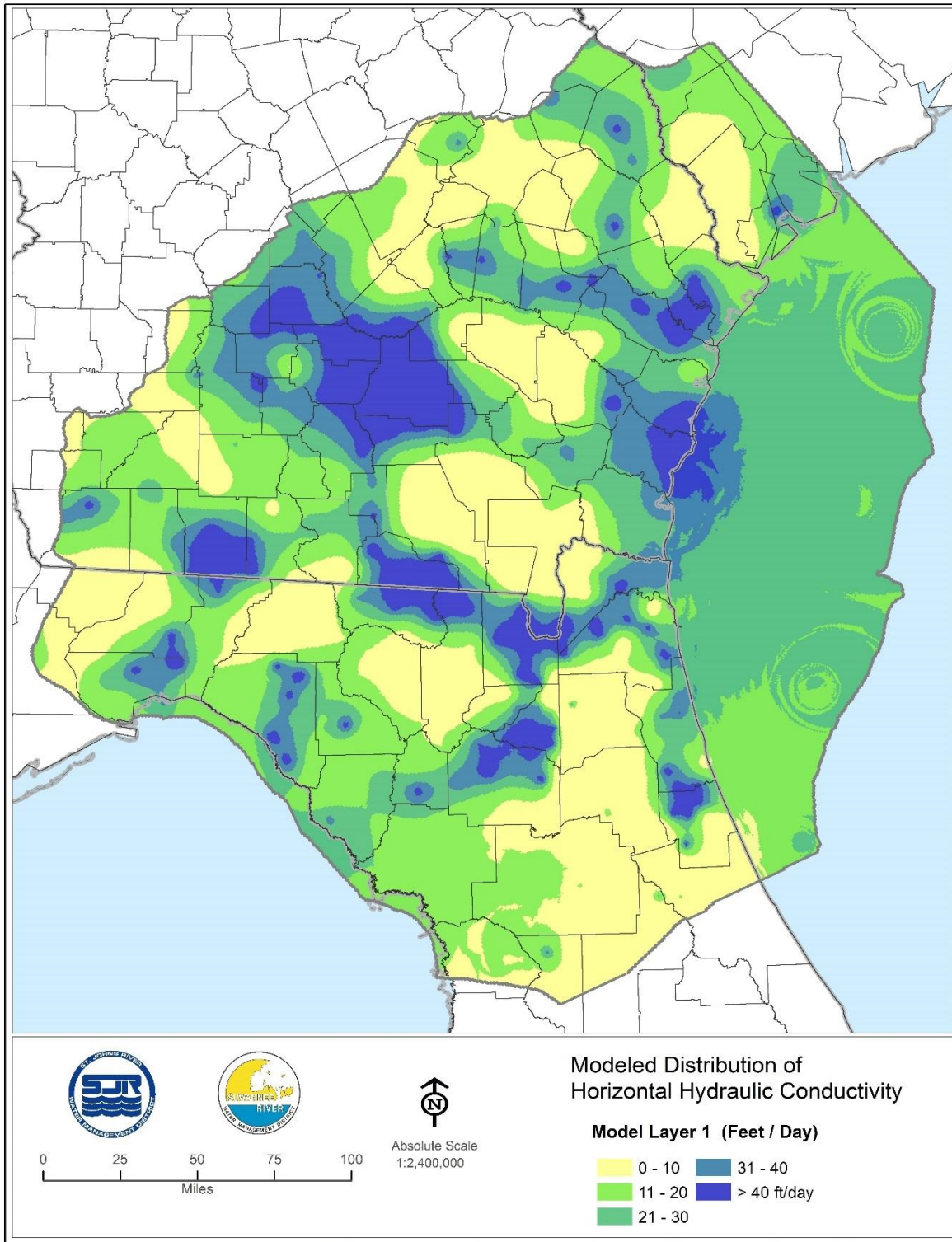


Figure 3-46. Modeled Distribution of Horizontal Hydraulic Conductivity, Model Layer 1

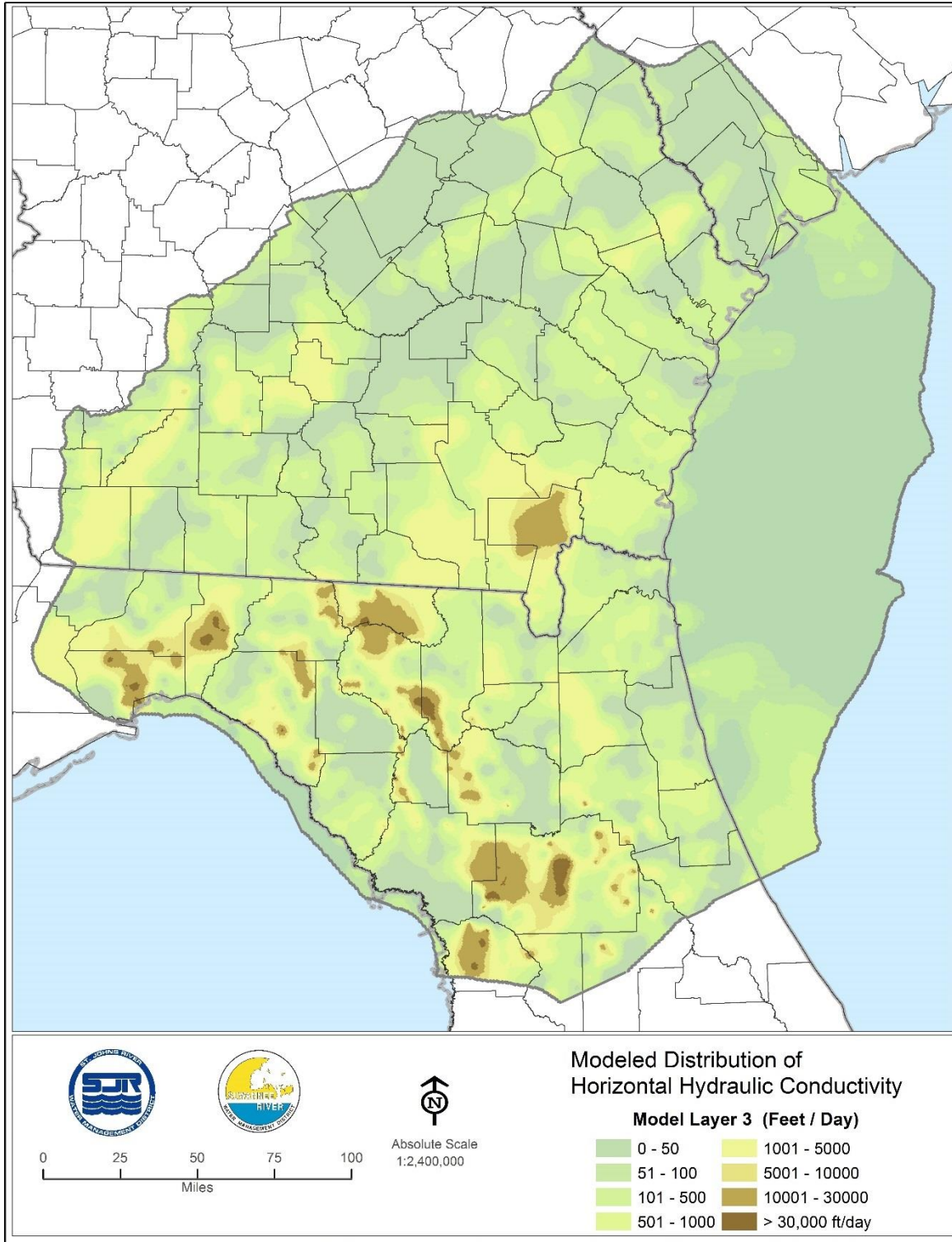


Figure 3-47. Modeled Distribution of Horizontal Hydraulic Conductivity, Model Layer 3

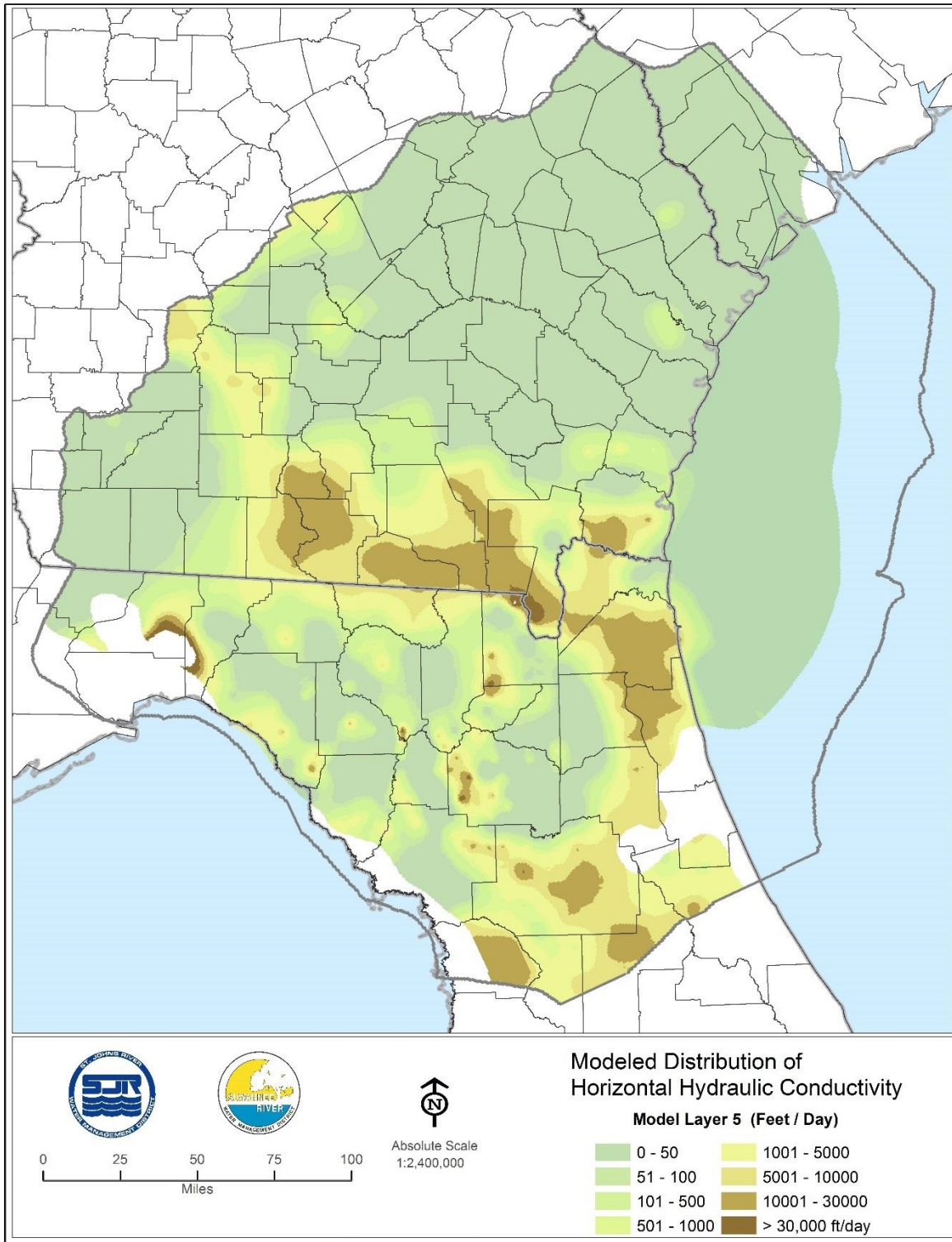


Figure 3-48. Modeled Distribution of Horizontal Hydraulic Conductivity, Model Layer 5

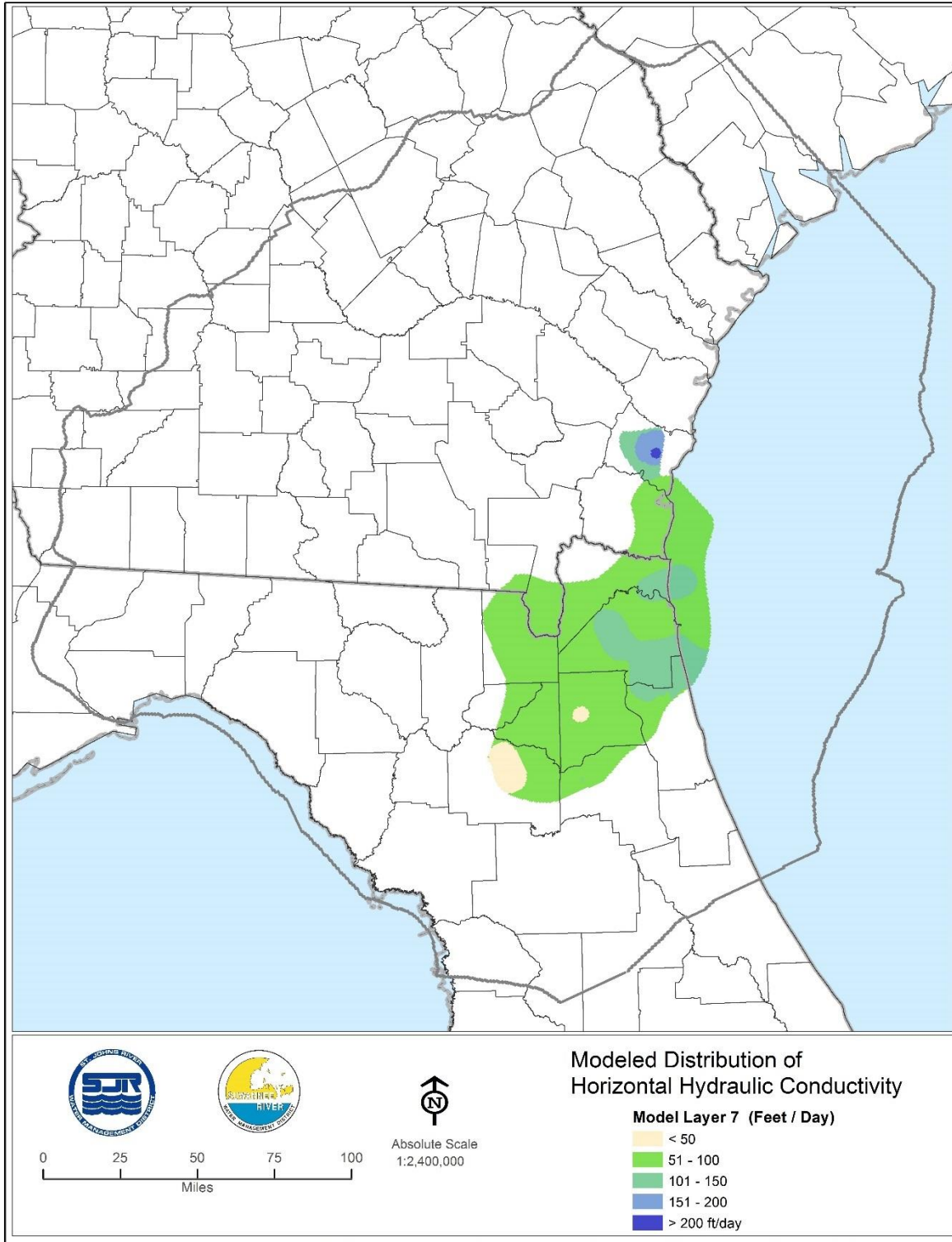


Figure 3-49. Modeled Distribution of Horizontal Hydraulic Conductivity, Model Layer 7

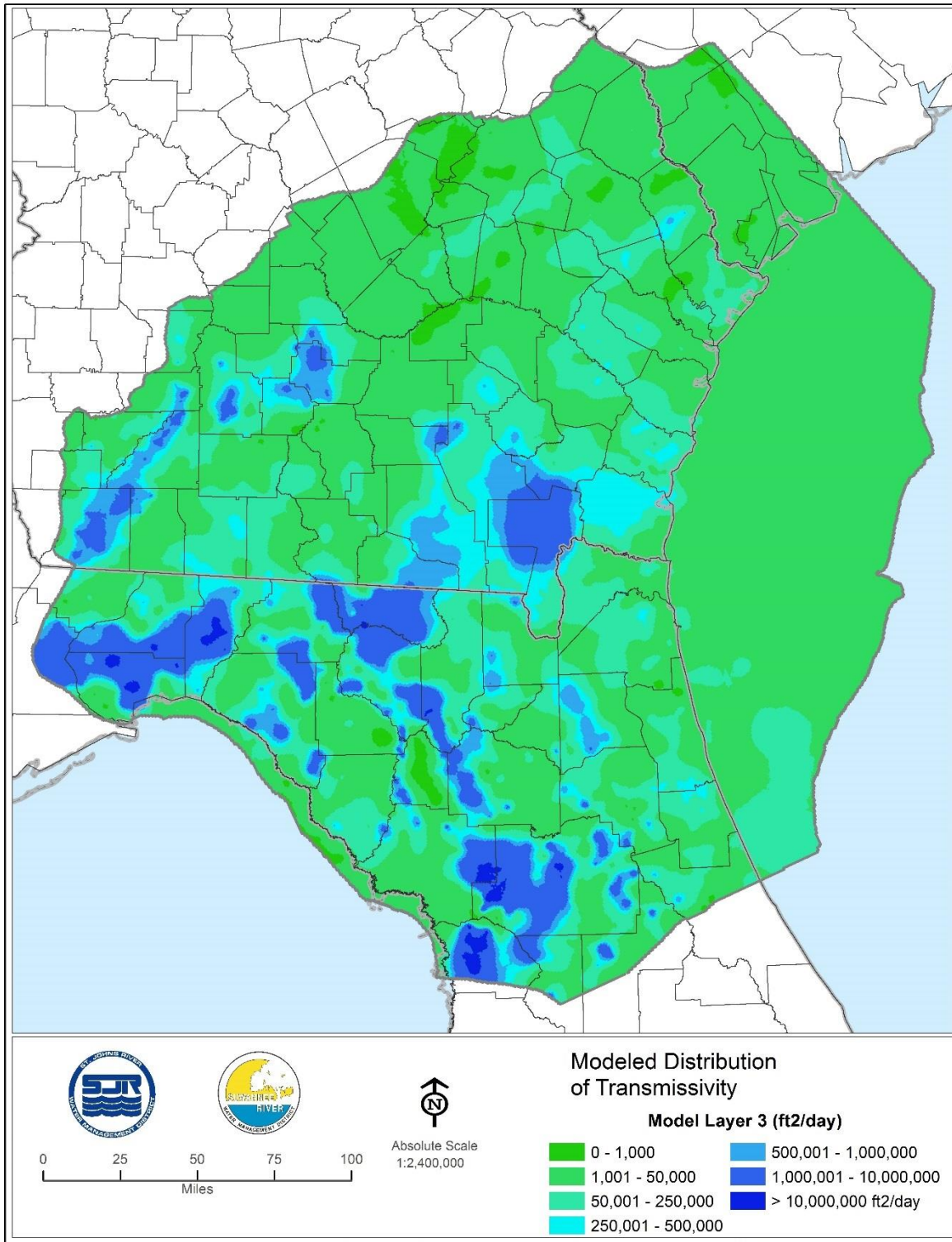


Figure 3-50. Spatial Distribution of Transmissivity, Model Layer 3

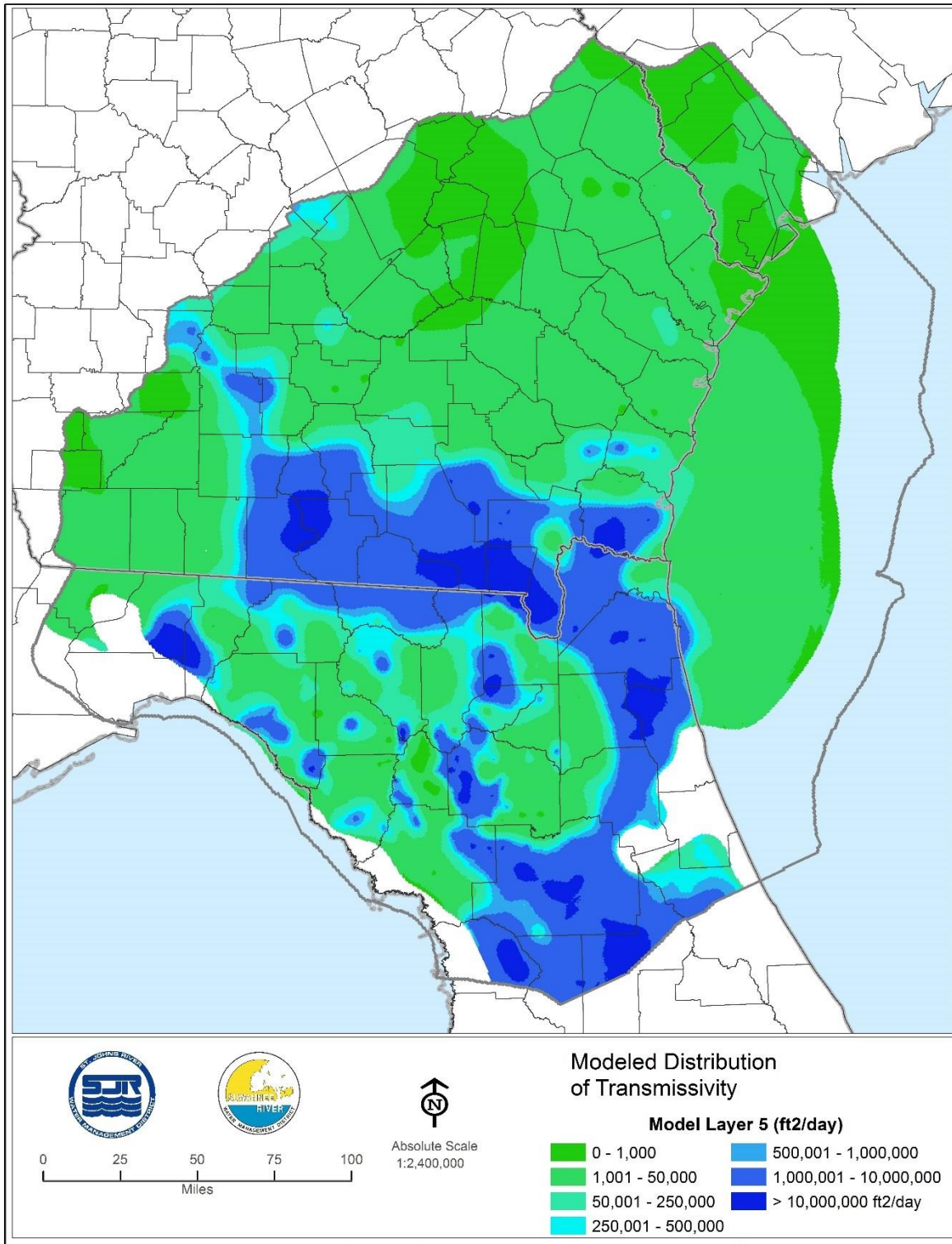


Figure 3-51. Spatial Distribution of Transmissivity, Model Layer 5

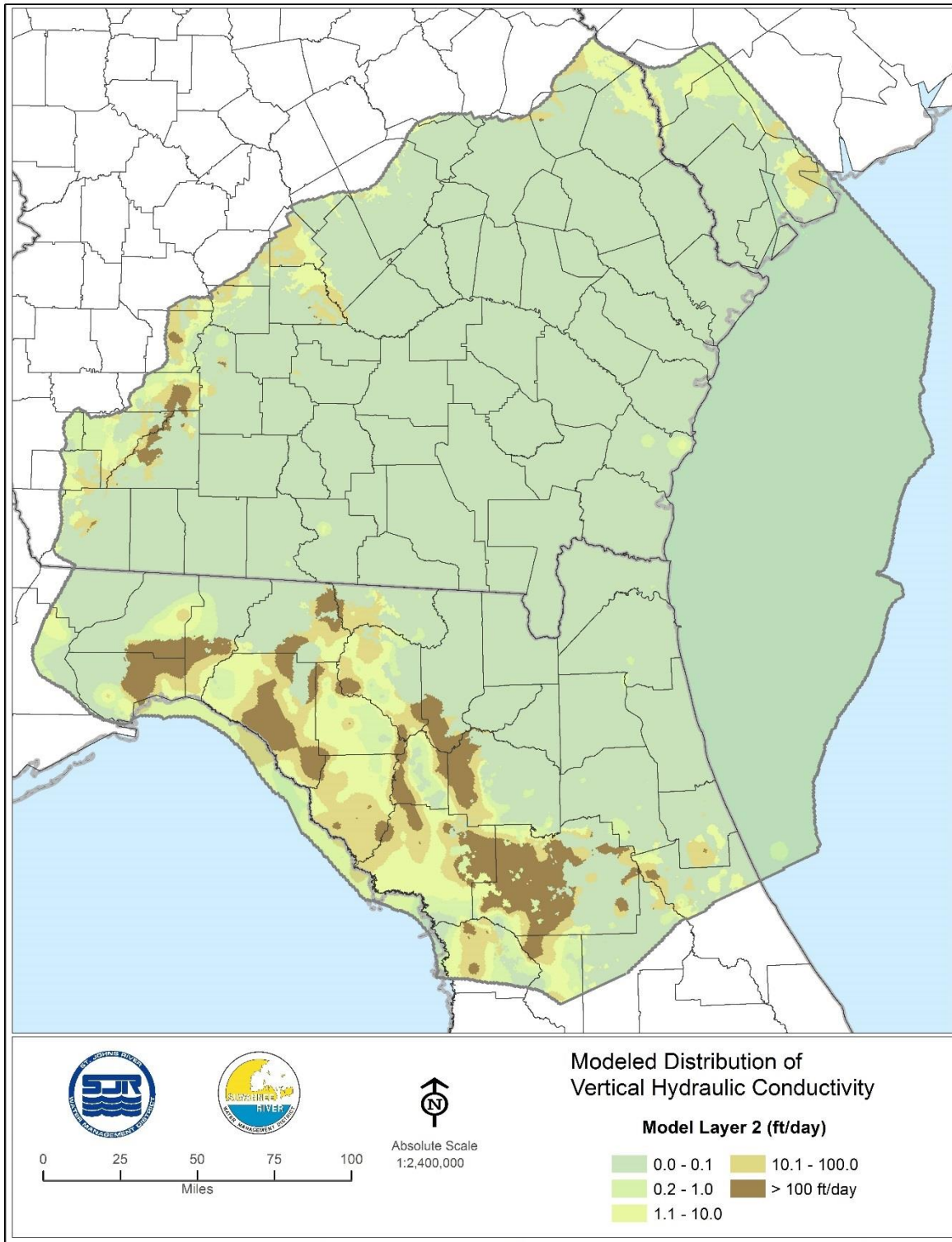


Figure 3-52. Modeled Distribution of Vertical Hydraulic Conductivity, Model Layer 2

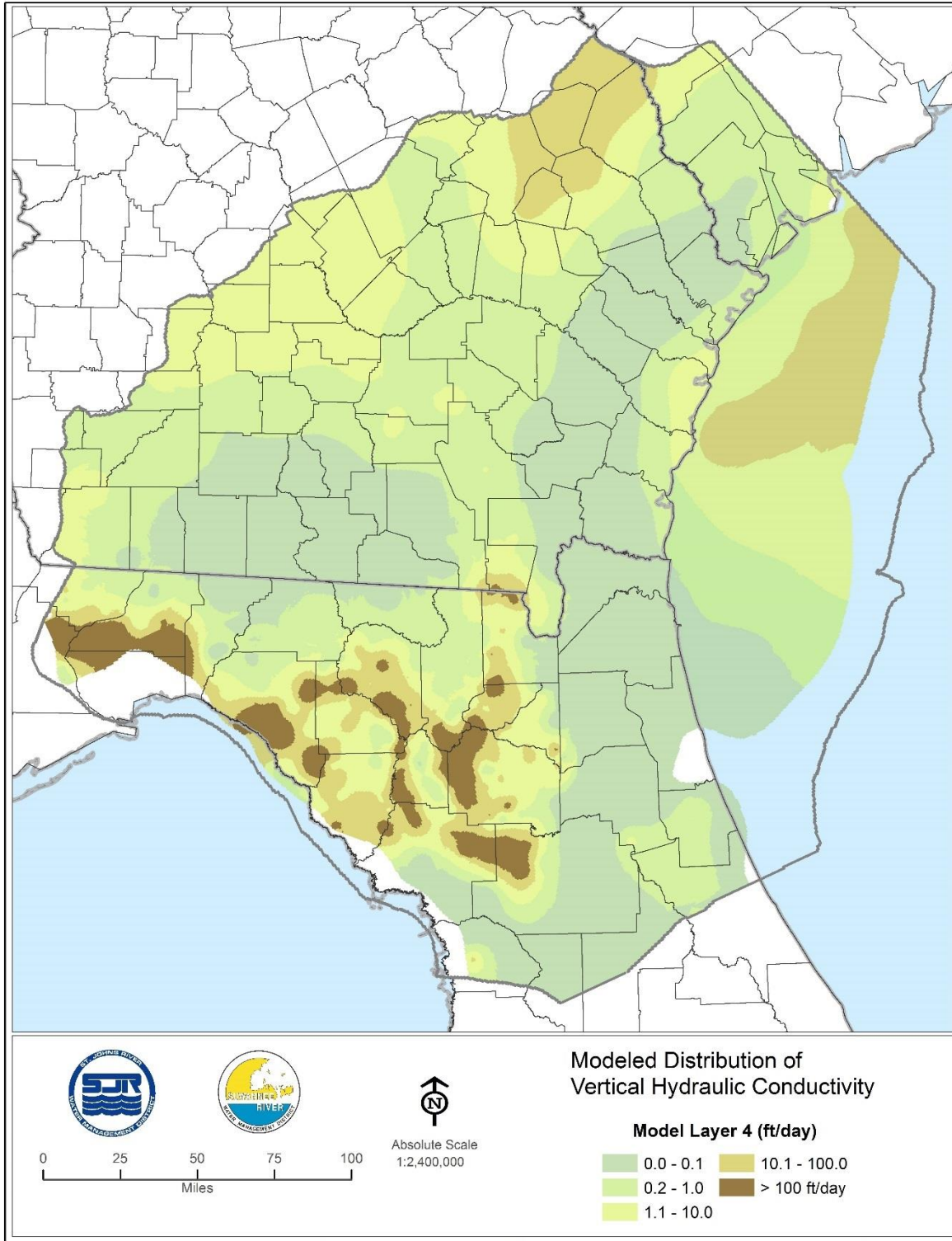


Figure 3-53. Modeled Distribution of Vertical Hydraulic Conductivity, Model Layer 4

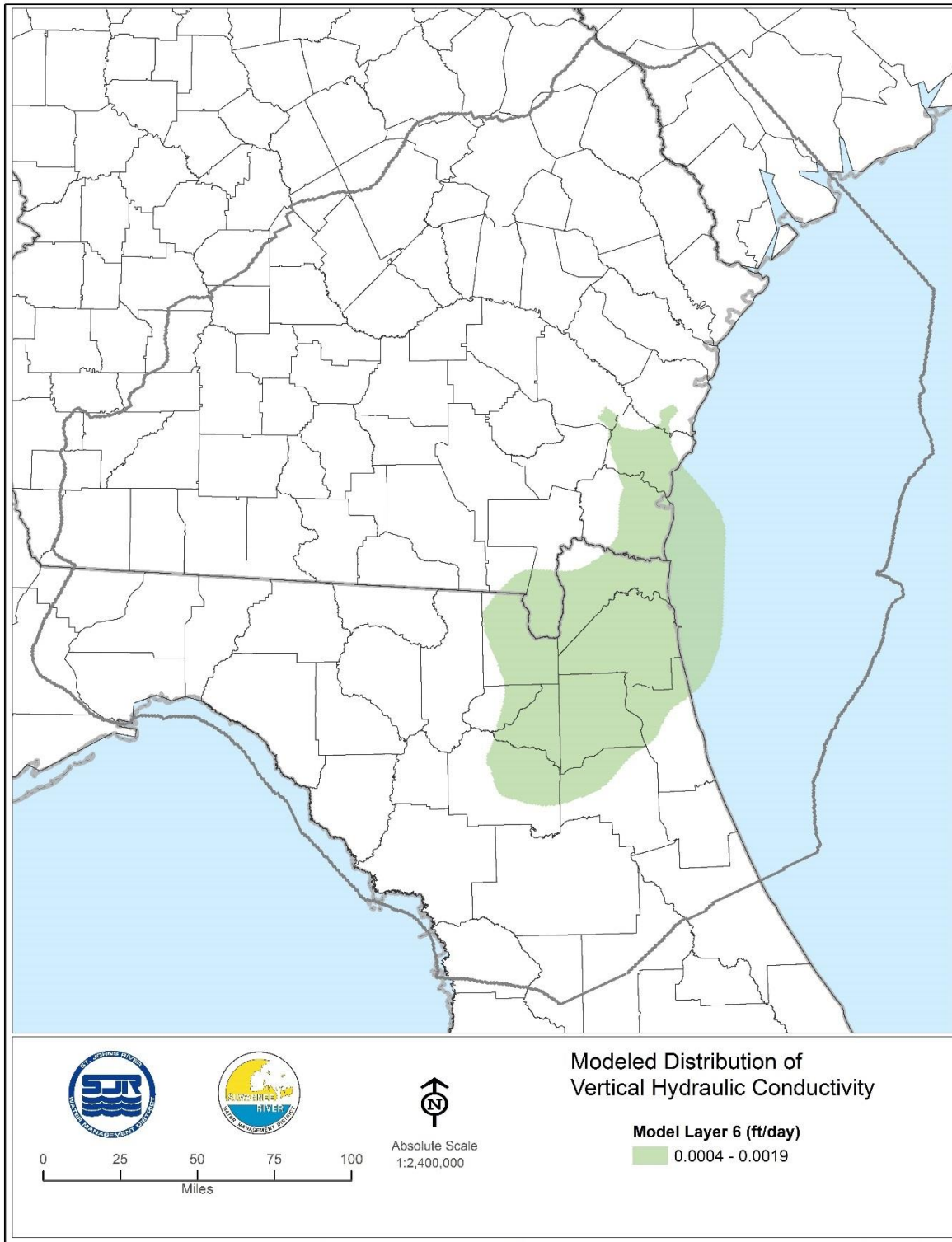


Figure 3-54. Modeled Distribution of Vertical Hydraulic Conductivity, Model Layer 6

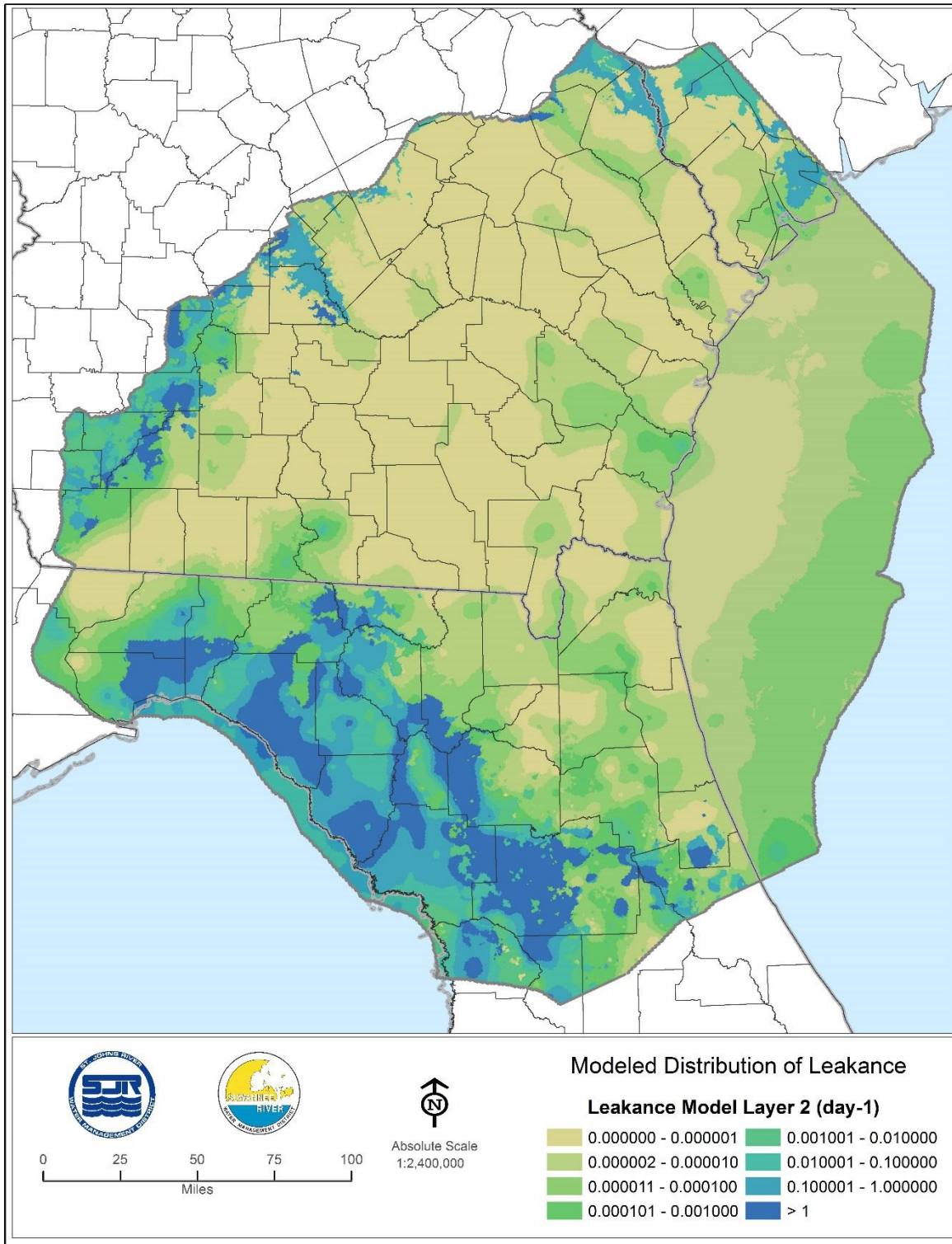


Figure 3-55. Modeled Distribution of Leakance, Model Layer 2

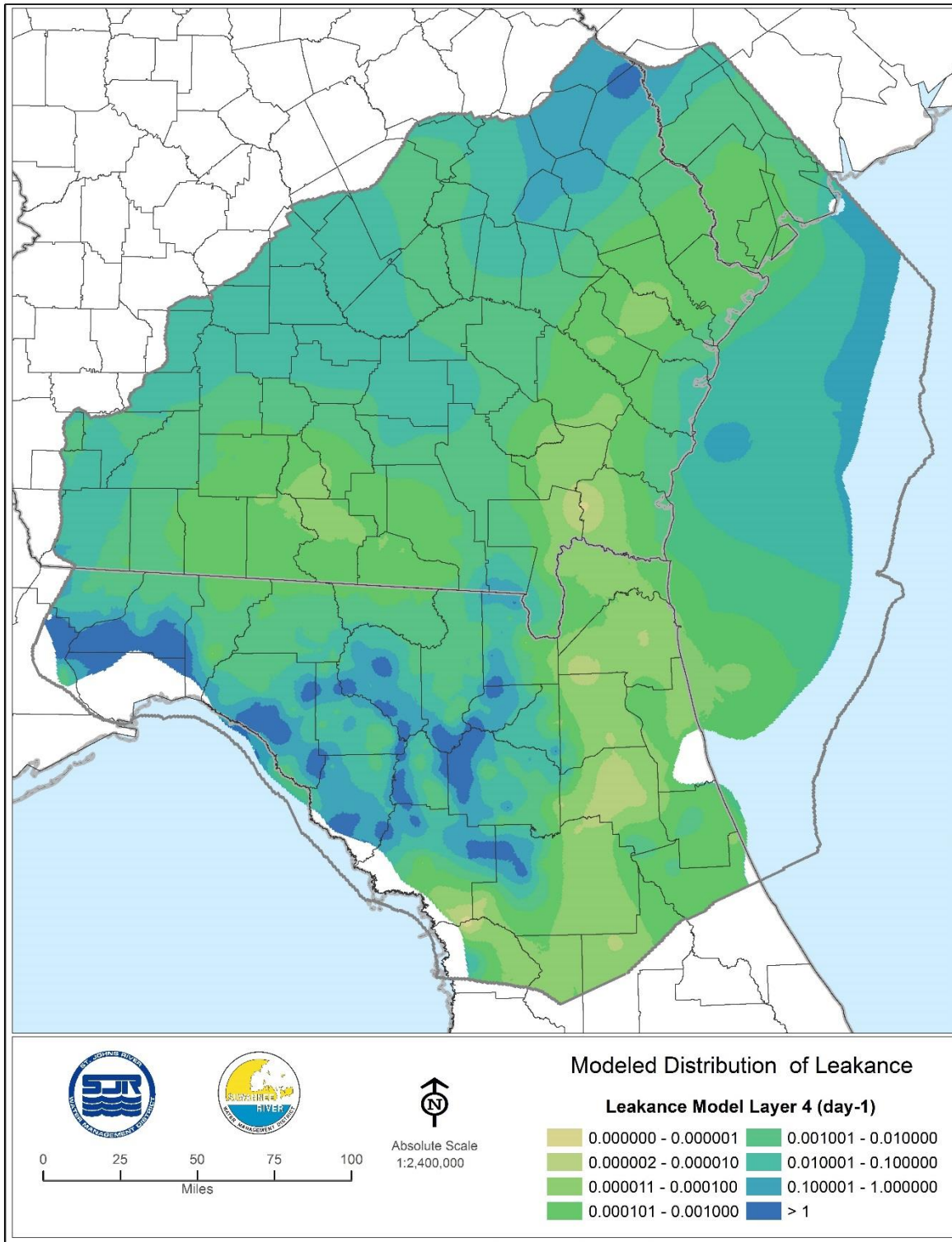


Figure 3-56. Modeled Distribution of Leakance, Model Layer 4

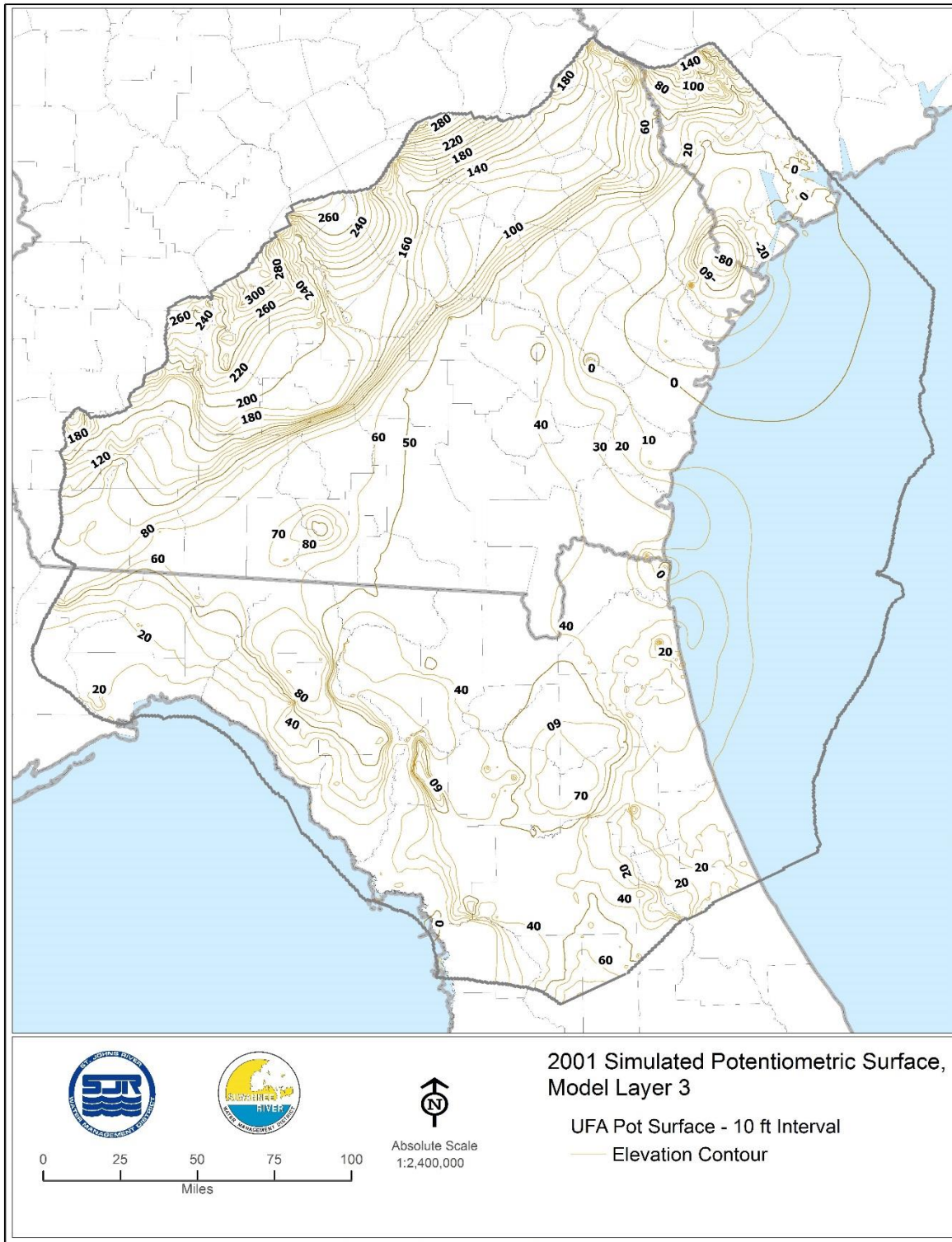


Figure 3-57. Simulated Potentiometric Surface of Model Layer 3, 2001

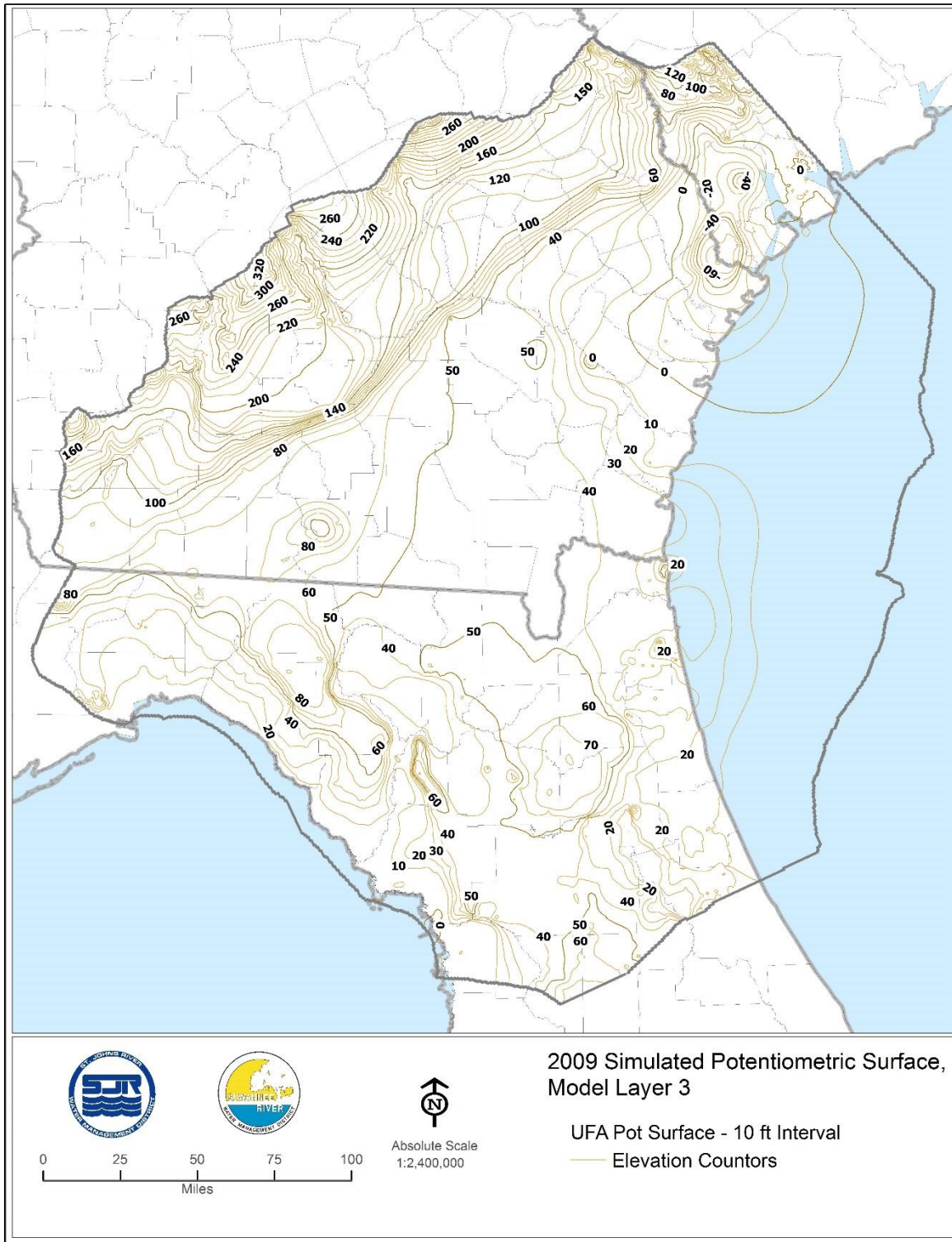


Figure 3-58. Simulated Potentiometric Surface of Model Layer 3, 2009

4.0 REFERENCES

- Bicknell, Brian R., John C. Imhoff, John L. Kittle, Anthony S. Donigian, and Robert C. Johanson. 1997. "Hydrological Simulation Program—FORTRAN User's Manual for Version 11." U.S. Environmental Protection Agency Project Summary. Research Triangle Park, NC: U.S. Environmental Protection Agency.
<http://nepis.epa.gov/Exe/ZyPDF.cgi/30006FIO.PDF?Dockey=30006FIO.PDF>.
- Doherty, John. 2015. *Calibration and Uncertainty Analysis for Complex Environmental Models; PEST: Complete Theory and What It Means for Modelling the Real World*. Brisbane, Australia: Watermark Numerical Computing. http://www.pesthomepage.org/PEST-The_Book.php.
- . 2016a. "PEST: Model-Independent Parameter Estimation; User Manual Part I: PEST, SENSAN and Global Optimisers (6th Edition)." Watermark Numerical Computing. <http://www.pesthomepage.org/Downloads.php>.
- . 2016b. "PEST: Model-Independent Parameter Estimation; User Manual Part II: PEST Utility Support Software (6th Edition)." Watermark Numerical Computing. <http://www.pesthomepage.org/Downloads.php>.
- Faulkner, Glen L. 1973. "Geohydrology of the Cross-Florida Barge Canal Area, with Special Reference to the Ocala Vicinity." WRI-73-1. U.S. Geological Survey. http://fl.water.usgs.gov/PDF_files/wri_1_73_faulkner.pdf.
- Harbaugh, Arlen W. 2005. "MODFLOW-2005, The U.S. Geological Survey Modular Ground-Water Model—the Ground-Water Flow Process." U.S. Geological Survey Techniques and Methods Report 6-A16. Reston, VA: U.S. Geological Survey. <http://pubs.usgs.gov/tm/2005/tm6A16/PDF/TM6A16.pdf>.
- Kinnaman, Sandra L., and J.F. Dixon. 2011. "Potentiometric Surface of the Upper Floridan Aquifer in Florida and Parts of Georgia, South Carolina, and Alabama, May-June 2010." Scientific Investigations Map. U.S. Geological Survey. <http://pubs.usgs.gov/sim/3182/>.
- Kinnaman, Sandra L., and Joann F. Dixon. 2009. "Potentiometric Surface of the Upper Floridan Aquifer in the St. Johns River Water Management District and Vicinity, Florida, May 2009." Scientific Investigations Map 3091. Scientific Investigations Map. U.S. Geological Survey. <http://fl.water.usgs.gov/PotMap/>.
- Knowles, Leel, and Sandra L. Kinnaman. 2001. "Potentiometric Surface of the Upper Floridan Aquifer in the St. Johns River Water Management District and Vicinity, Florida, September 2001." Open File Report. U.S. Geological Survey. <http://fl.water.usgs.gov/PotMap/>.
- Knowles, Jr., Leel. 1996. "Estimation of Evapotranspiration in the Rainbow Springs and Silver Springs Basins in North-Central Florida." U.S. Geological Survey Water-Resources Investigations 96-4024. Tallahassee, FL. <http://pubs.usgs.gov/wri/1996/4024/report.pdf>.

- . 2001. “Potentiometric Surface of the Upper Floridan Aquifer in the St. Johns River Water Management District and Vicinity, Florida, May 2001.” Open File Report. U.S. Geological Survey. <http://fl.water.usgs.gov/PotMap/>.
- McKay, L., T. Bondelid, T Dewald, Alan Rea, Craig Johnston, and Richard Moore. 2013. “NHDPlus Version 2: User Guide (Data Model Version 2.1).” United States Department of Environmental Protection and United States Geological Survey. http://www.horizon-systems.com/NHDPlus/NHDPlusV2_documentation.php.
- Miller, James A. 1986. “Hydrogeologic Framework of the Floridan Aquifer System in Florida and in Parts of Georgia, South Carolina, and Alabama.” U.S. Geological Survey Professional Paper 1403–B. Washington D.C.: U.S. Geological Survey. <http://pubs.er.usgs.gov/publication/pp1403B>.
- Moore, Keara. 2007. “BASINS Technical Note 2: Two Automated Methods for Creating Hydraulic Function Tables (FTABLES).” EPA BASINS Technical Note 2. United States Environmental Protection Agency. https://www.epa.gov/sites/production/files/2015-08/documents/2009_04_13_basinss_tecnote2.pdf.
- Niswonger, Richard G., Sorab Panday, Geomatrix, Inc., and Motomu Ibaraki. 2011. “MODFLOW-NWT, A Newton Formulation for MODFLOW-2005.” U.S. Geological Survey Techniques and Methods Report 6-A37. Reston, VA: U.S. Geological Survey. <http://pubs.usgs.gov/tm/tm6a37/pdf/tm6a37.pdf>.
- Rutledge, A.T. 1993. “Computer Programs for Describing the Recession of Ground-Water Discharge and for Estimating Mean Ground-Water Recharge and Discharge from Streamflow Records.” U.S. Geological Survey Water-Resources Investigations Report 93–4121. Richmond, VA: U.S. Geological Survey. <http://pubs.usgs.gov/wri/1993/4121/report.pdf>.
- Shah, Nirjhar, Mahmood Nachabe, and Mark Ross. 2007. “Extinction Depth and Evapotranspiration from Ground Water under Selected Land Covers.” *Ground Water* 40, No. 3 (May-June 2007): 329–38.
- Sepulveda, N., and Doherty, J., 2014. Uncertainty analysis of a groundwater flow model in East-Central Florida. *Groundwater*: 53 (3), 464-474.
- Suscy, Peter, Ed Carter, David Christian, Michael Cullum, Kijin Park, Joseph Stewart, and Yanfeng Zhang. 2012. “St. Johns River Water Supply Impact Study; Chapter 5, River Hydrodynamics Calibration.” St. Johns River Water Management District Technical Publication SJ2012-1. Palatka, FL: St. Johns River Water Management District. http://www.sjrwmd.com/technicalreports/pdfs/TP/SJ2012-1_Chapter05.pdf.
- Williams, Lester J., and Eve L. Kuniansky. 2015. “Revised Hydrogeologic Framework of the Floridan Aquifer System in Florida and Parts of Georgia, Alabama, and South Carolina.” U.S.

Geological Survey Professional Paper 1807. Reston, VA: U.S. Geological Survey.
<https://pubs.er.usgs.gov/publication/pp1807>.

Hydrological Simulation Program—FORTRAN User’s Manual for Version 11.” U.S. Environmental Protection Agency Project Summary. Research Triangle Park, NC: U.S. Environmental Protection Agency.
<http://nepis.epa.gov/Exe/ZyPDF.cgi/30006FIO.PDF?Dockey=30006FIO.PDF>.

Doherty, John. 2015. Calibration and Uncertainty Analysis for Complex Environmental Models; PEST: Complete Theory and What It Means for Modelling the Real World. Brisbane, Australia: Watermark Numerical Computing. http://www.pesthomepage.org/PEST-The_Book.php.

———. 2016a. “PEST: Model-Independent Parameter Estimation; User Manual Part I: PEST, SENSAN and Global Optimisers (6th Edition).” Watermark Numerical Computing. <http://www.pesthomepage.org/Downloads.php>.

———. 2016b. “PEST: Model-Independent Parameter Estimation; User Manual Part II: PEST Utility Support Software (6th Edition).” Watermark Numerical Computing. <http://www.pesthomepage.org/Downloads.php>.

Faulkner, Glen L. 1973. “Geohydrology of the Cross-Florida Barge Canal Area, with Special Reference to the Ocala Vicinity.” WRI-73-1. U.S. Geological Survey. http://fl.water.usgs.gov/PDF_files/wri_1_73_faulkner.pdf.

Harbaugh, Arlen W. 2005. “MODFLOW-2005, The U.S. Geological Survey Modular Ground-Water Model—the Ground-Water Flow Process.” U.S. Geological Survey Techniques and Methods Report 6-A16. Reston, VA: U.S. Geological Survey. <http://pubs.usgs.gov/tm/2005/tm6A16/PDF/TM6A16.pdf>.

Kinnaman, Sandra L., and J.F. Dixon. 2011. “Potentiometric Surface of the Upper Floridan Aquifer in Florida and Parts of Georgia, South Carolina, and Alabama, May-June 2010.” Scientific Investigations Map. U.S. Geological Survey. <http://pubs.usgs.gov/sim/3182/>.

Kinnaman, Sandra L., and Joann F. Dixon. 2009. “Potentiometric Surface of the Upper Floridan Aquifer in the St. Johns River Water Management District and Vicinity, Florida, May 2009.” Scientific Investigations Map 3091. Scientific Investigations Map. U.S. Geological Survey. <http://fl.water.usgs.gov/PotMap/>.

Knowles, Leel, and Sandra L. Kinnaman. 2001. “Potentiometric Surface of the Upper Floridan Aquifer in the St. Johns River Water Management District and Vicinity, Florida, September 2001.” Open File Report. U.S. Geological Survey. <http://fl.water.usgs.gov/PotMap/>.

Knowles, Jr., Leel. 1996. “Estimation of Evapotranspiration in the Rainbow Springs and Silver Springs Basins in North-Central Florida.” U.S. Geological Survey Water-Resources Investigations 96-4024. Tallahassee, FL. <http://pubs.usgs.gov/wri/1996/4024/report.pdf>.

———. 2001. “Potentiometric Surface of the Upper Floridan Aquifer in the St. Johns River Water Management District and Vicinity, Florida, May 2001.” Open File Report. U.S. Geological Survey. <http://fl.water.usgs.gov/PotMap/>.

McKay, L., T. Bondelid, T Dewald, Alan Rea, Craig Johnston, and Richard Moore. 2013. “NHDPlus Version 2: User Guide (Data Model Version 2.1).” United States Department of Environmental Protection and United States Geological Survey. http://www.horizon-systems.com/NHDPlus/NHDPlusV2_documentation.php.

Miller, James A. 1986. “Hydrogeologic Framework of the Floridan Aquifer System in Florida and in Parts of Georgia, South Carolina, and Alabama.” U.S. Geological Survey Professional Paper 1403–B. Washington D.C.: U.S. Geological Survey. <http://pubs.er.usgs.gov/publication/pp1403B>.

Moore, Keara. 2007. “BASINS Technical Note 2: Two Automated Methods for Creating Hydraulic Function Tables (FTABLES).” EPA BASINS Technical Note 2. United States Environmental Protection Agency. https://www.epa.gov/sites/production/files/2015-08/documents/2009_04_13_basinss_tecnote2.pdf.

Niswonger, Richard G., Sorab Panday, Geomatrix, Inc., and Motomu Ibaraki. 2011. “MODFLOW-NWT, A Newton Formulation for MODFLOW-2005.” U.S. Geological Survey Techniques and Methods Report 6-A37. Reston, VA: U.S. Geological Survey. <http://pubs.usgs.gov/tm/tm6a37/pdf/tm6a37.pdf>.

Rutledge, A.T. 1993. “Computer Programs for Describing the Recession of Ground-Water Discharge and for Estimating Mean Ground-Water Recharge and Discharge from Streamflow Records.” U.S. Geological Survey Water-Resources Investigations Report 93–4121. Richmond, VA: U.S. Geological Survey. <http://pubs.usgs.gov/wri/1993/4121/report.pdf>.

Shah, Nirjhar, Mahmood Nachabe, and Mark Ross. 2007. “Extinction Depth and Evapotranspiration from Ground Water under Selected Land Covers.” *Ground Water* 40, No. 3 (May-June 2007): 329–38.

Suscy, Peter, Ed Carter, David Christian, Michael Cullum, Kijin Park, Joseph Stewart, and Yanfeng Zhang. 2012. “St. Johns River Water Supply Impact Study; Chapter 5, River Hydrodynamics Calibration.” St. Johns River Water Management District Technical Publication SJ2012-1. Palatka, FL: St. Johns River Water Management District. http://www.sjrwmd.com/technicalreports/pdfs/TP/SJ2012-1_Chapter05.pdf.

Williams, Lester J., and Eve L. Kuniandy. 2015. “Revised Hydrogeologic Framework of the Floridan Aquifer System in Florida and Parts of Georgia, Alabama, and South Carolina.” U.S. Geological Survey Professional Paper 1807. Reston, VA: U.S. Geological Survey. <https://pubs.er.usgs.gov/publication/pp1807>.